

21 JANUARY 2022

**Report of the Inquiry
Committee for the accident
at Stars Engrg Pte Ltd on
24 February 2021**

(PART II – ANNEXES)

TABLE OF CONTENTS

Part II – Annexes

ANNEX A – STOP WORK ORDER	A-1
ANNEX B – BIOGRAPHIES OF IC MEMBERS	B-1
ANNEX C – LETTERS OF APPOINTMENT	C-1
ANNEX D – TERMS OF REFERENCE OF THE IC	D-1
ANNEX E – OPENING STATEMENT	E-1
ANNEX F – LIST OF WITNESSES	F-1
ANNEX G – LIST OF EXHIBITS	G-1
ANNEX H – LIST OF WITNESS STATEMENTS AND SUBMISSIONS	H-1
ANNEX I – EXPERT REPORTS	I-1
ANNEX J – WRITTEN REPRESENTATIONS	J-1
ANNEX K – CLOSING SUBMISSIONS	K-1
ANNEX L – EXTRACTS FROM THE WORKPLACE SAFETY AND HEALTH ACT	L-1
ANNEX M – EXTRACTS FROM THE WORKPLACE SAFETY AND HEALTH (RISK MANAGEMENT) REGULATIONS	M-1
ANNEX N - EXTRACTS FROM THE WORKPLACE SAFETY AND HEALTH (GENERAL PROVISIONS) REGULATIONS.....	N-1
ANNEX O – EXTRACTS OF COMBUSTIBLE DUST-RELATED LEGISLATION	O-1

ANNEX I – EXPERT REPORTS



ACCIDENT INVESTIGATION REPORT

FIRE AND EXPLOSION AT STARS ENGRG PTE LTD (32E, TUAS AVENUE 11)

Prepared by

Shaik Mohamed Salim PhD, P.Eng.
Principal Specialist
Institute of Chemical and Engineering Sciences, A*STAR

A handwritten signature in black ink, appearing to read 'Shaik Mohamed Salim'.

Prepared for



13 September 2021

CONFIDENTIAL

This Page is Left Blank

Contents

List of Tables.....	4
List of Figures.....	5
Abbreviations	6
Symbols and Units	6
Executive Summary	7
1 Background and Introduction.....	9
1.1 Initial Observations.....	9
2 Data Collection and Analysis	11
3 Review of CCTV Video	12
4 Primary Deflagration Analysis	13
4.1 Mixer Description	13
4.2 Finite Element Analysis (FEA)	15
4.2.1 FEA modelling – temperature profiles	17
4.2.2 FEA modelling - high convection at mixer’s inner surface (h=500 W/m ² K)	19
4.2.3 FEA modelling - moderate convection at mixer’s inner surface (h=50 W/m ² K)	20
4.2.4 FEA modelling - low convection at mixer’s inner surface (h=5 W/m ² K)	21
4.2.5 FEA modelling - analysis with 45 kW heat source	22
4.2.6 FEA modelling - effect of partially filled mixing chamber, insulation and very low HTF volumes	24
4.3 Analysis of heat transfer fluid.....	26
4.3.1 Differential scanning calorimetry of heat transfer fluid.....	27
4.3.2 Simultaneous DSC-TGA (SDT) testing of heat transfer fluid.....	28
4.3.3 Pressure-temperature analysis (closed system) of heat transfer fluid	29
4.4 Explosion Evaluation – Deflagration Overpressures	33
4.4.1 Physical explosion – estimation of overpressures.....	35
4.4.2 Chemical explosion – estimation of overpressures.....	36
5 Secondary Flash Fire Analysis.....	44
5.1 Materials sampling and analysis.....	46
5.2 Materials testing and analysis results	48
6 Discussion	53
7 Conclusion	61
References.....	63
Appendices	65

List of Tables

Table 1. Summary list of events observed from CCTV video clips	12
Table 2. Estimated heat transfer coefficients corresponding to a water fill volume of 176L.....	25
Table 3. Property comparison among various heat transfer fluids	27
Table 4. Results from SDT tests conducted on heat transfer fluid	28
Table 5. Damage produced by blast, overpressures	34
Table 6. Comparison between calculated physical overpressure and accident site damage.....	36
Table 7. Comparison between calculated chemical explosion overpressure and incident site damage	43
Table 8. Flammability and dust combustibility data for process materials used in mixer.....	45
Table 9. Types of analysis conducted on dust layer samples obtained from accident site (Stars Engrg factory unit).	47
Table 10. Overview of analytical test results for powder samples taken from the Stars Engrg factory unit ...	49
Table 11. Overview of analytical test results of raw material samples taken from Stars Engrg storage (level 2).	50
Table 12. Characteristic colour – temperature relationship of the surface oxide film on steel	56

List of Figures

Figure 1. Photograph of the rear, right edge of the mixer from the accident site taken by MOM	10
Figure 2. Schematic views of the mixer	15
Figure 3. Bottom view of damaged mixer taken by MOM.....	16
Figure 4. Overview of FEA heat transfer conditions for mixer.....	16
Figure 5. Temperature profiles (contour plots) of the mixer surfaces generated from FEA simulations where $k_{eff} = 200 \text{ W/mK}$	18
Figure 6. Maximum temperatures (average of HTF and mixer surface) obtained under high convective heat transfer conditions ($h=500 \text{ W/m}^2\text{K}$) with a 7.2 kW heating source input.....	19
Figure 7. Maximum temperatures (average of HTF and mixer surface) obtained under moderate convective heat transfer conditions ($h=50 \text{ W/m}^2\text{K}$) with a 7.2 kW heating source input.....	20
Figure 8. Maximum temperatures (average of HTF and mixer surface) obtained under low convective heat transfer conditions ($h=5 \text{ W/m}^2\text{K}$) with a 7.2 kW heating source input.....	21
Figure 9. Effect of increased heat source power on the mixer’s temperature profile	23
Figure 10. Illustration of mixing chamber with a water fill of 176 litres of water	24
Figure 11. Consolidated graph of pressure against temperature for experimental Runs 3, 4 and 5	30
Figure 12. Consolidated graph of pressure against temperature for experimental Runs 1 and 2	31
Figure 13. Consolidated graph of pressure logarithm against reciprocal temperature for experimental Runs 3, 4 and 5.....	32
Figure 14. Consolidated graph of pressure logarithm against reciprocal temperature for experimental Runs 1 and 2.....	32
Figure 15. Schematic representation of the damage caused by the accident.....	33
Figure 16. Graph of overpressure against distance for heating jacket failure at pressure $P = 2, 3$ and 4 barg	35
Figure 17. Breakdown of aerosol related fires and explosions according to fuel type.....	38
Figure 18. Breakdown of aerosol related incidents according to ignition sources.....	39
Figure 19. Graph of overpressure against distance for HTF volume = 300L	40
Figure 20. Graph of overpressure against distance for HTF volume = 200L	40
Figure 21. Graph of overpressure against distance for HTF volume = 160L	41
Figure 22. Graph of overpressure against distance for HTF volume = 120L	41
Figure 23. Graph of overpressure against distance for HTF volume = 80L	42
Figure 24. Graph of overpressure against distance for HTF volume = 40L	42
Figure 25. Images from CCTV Camera 6 showing the translation of large metal and cardboard sheets	54
Figure 26. Image showing glowing flange connection of one of the mixer’s heating element	56
Figure 27. Overview of the likely sequence of events that resulted in the primary and secondary deflagrations at Stars Engrg.....	60

Abbreviations

AIT: Auto Ignition Temperature	LCS/MCS: low/medium carbon steel
CAD: computer aided design	MIE: minimum ignition energy
CCTV: Closed Circuit Television	MIT: minimum ignition temperature
CFD: computational fluid dynamics	MOM: Ministry of Manpower
CHNS: carbon, hydrogen, nitrogen, sulphur analyser	NFPA: National Fire Protection Association
DSC: Differential Scanning Calorimetry	RTD: Resistance Temperature Detector
EDX: Energy-dispersive X-ray spectroscopy	SCDF: Singapore Civil Defence Force
FTIR: Fourier-transform infra-red spectroscopy	SDS: Safety Data Sheet
HTF: heat transfer fluid	SDT: Simultaneous DSC-TGA
IEC: International Electrotechnical Commission	SEM: scanning electron microscopy
ISO: International Organization for Standardization	St: Dust explosibility class
K_{st}: Deflagration Index, normalised maximum rate of pressure rise	TGA: Thermogravimetric analysis
	UV/Vis/NIR: ultraviolet/visible/near infra-red spectroscopy

Symbols and Units

°C: degree Celsius	kg: kilograms
BZ: burning number defined in EN 17077	kJ: kilojoules
cal: calories	kPa: kilopascals
h: convective heat transfer coefficient	kW: kilowatts
H_c: heat of combustion	L: litres
K: Kelvin	min: minutes
k: thermal conductivity	ml: millilitres
	wt%: weight percent

Executive Summary

2

An incident occurred at about 11.22 am on 24 February 2021 at Stars Engrg Pte Ltd's factory unit located on the first level of 32E Tuas Avenue 11. A visit of the site was conducted together with officers from the MOM and SCDF on 9 March 2021 to inspect the accident site, its immediate surrounds, and the equipment and materials used in the factory unit. Samples of residues found on the factory floor and materials used in the manufacturing process were collected by MOM officers for further analysis. A mixer machine ("**mixer**") was also retrieved from the factory by Matcor Technology & Services Pte Ltd ("**Matcor**") for analysis.

10

This technical investigation into the incident at Stars Engrg used the following methods to determine the cause of the fires and explosion that occurred:

12

- i. Review of CCTV video clips provided by MOM to ascertain chain of events.
- 14 ii. Finite Element Analysis to ascertain the heat transfer behavioural trends of the mixer's heating jacket's surface and the heat transfer fluid within the heating jacket.
- 16 iii. Analysis of the heat transfer fluid behaviour under elevated temperatures via DSC, SDT and Pressure-Temperature tests.
- 18 iv. Estimation of explosion overpressure and comparison with actual damage at the accident site to ascertain the likely mechanism (physical or chemical) of the primary deflagration event.
- 20 v. Analytical testing (CHNS, SEM/EDX, SDT, FTIR and UV/Vis) of samples collected from the immediate vicinity of the accident site to determine the presence of potato starch as a potential combustible dust hazard that could have caused the secondary deflagration event or flash fire.

22

24

Based on the modelling and analytical testing conducted, it was concluded that the accident comprised of a primary deflagration with overpressures that was followed by up to three secondary deflagrations in the form of flash fires occurring over an approximately three minute period.

28

CONFIDENTIAL

2 The root-cause of the incident on 24 February 2021 at Stars Engrg was likely due to the low amounts
of heat transfer fluid used in the mixer. This then led to the heat transfer fluid to be excessively
4 heated resulting in a pressure build-up in the mixer's heating jacket. This caused the heating jacket
to rupture and release hot, pressurised heat transfer fluid into the environment. This pressurised
6 release likely atomised the heat transfer fluid to form a liquid aerosol that was then probably ignited
by a hot surface. The ignited aerosol cloud resulted in the primary deflagration with estimated
overpressures in the range of 2.1 kPa to 58 kPa.

8

The secondary deflagrations which manifested as flash fires were likely the result of potato starch
10 accumulations in the workplace that were initially agitated and suspended by the overpressure from
the primary deflagration to form a combustible dust cloud. This combustible dust cloud was probably
12 ignited by the fires that were also initiated by the primary deflagration.

1 Background and Introduction

2

4 An incident occurred at about 11.22 am on 24 February 2021 at Stars Engrg's factory unit located on
6 the first floor of 32E Tuas Avenue 11. The SCDF responded to the incident and extinguished the fires
8 at the location. A total of ten workers were reported to have been injured in the accident with three
10 of them from Stars Engrg succumbing to their burn injuries. Of the remaining seven injured workers,
12 five of them were workers from Stars Engrg whilst the other two workers were from another
14 company that occupied Unit 38A which was located directly opposite the factory unit occupied by
16 Stars Engrg. The factory unit (32E) occupied by Stars Engrg was involved in the manufacture of fire
insulation wrapping.

12 An inspection of the site was carried out together with officers from MOM and SCDF on 9 March
14 2021. The inspection covered the accident site and its immediate surrounds, the adjacent factory
16 unit (32F), equipment involved and materials used in the factory. Samples of residues found on the
factory floor and materials used in the manufacturing process were collected by MOM officers for
analysis. Matcor also retrieved the mixer from the factory for analysis.

18 1.1 Initial Observations

20 The surfaces of the walls and ceiling of the factory unit were observed to be covered with black soot.
22 The floors were covered with a dried up, powdery paste that was yellowish-brown in colour. The rear
24 wall of the factory unit had almost entirely collapsed with the steel framework seen to be buckled
26 and dislodged from its fastenings. The front roller shutter which was partially opened was seen to
have been damaged and dislodged from its original fixtures. A number of gas cylinders containing
carbon dioxide, acetylene and oxygen were also seen to have partially toppled but were intact. Burn
marks or soot can also be seen on the columns and surfaces around the parking area, immediately
outside of the factory unit (32E).

28

CONFIDENTIAL

2 The two assembly tables used in the manufacture of fire insulation wrapping seemed to be intact and
had not been dislodged from their fastenings. The raised metal platform close to the rear portion of
the factory unit also seemed to be intact with no observable deformations or significant damage. A
4 mixer was located on top of this raised platform. The mixer was seen to be badly damaged with its
bottom half being split at the welding seams as shown in **Figure 1**.

6



8 **Figure 1.** Photograph of the rear, right edge of the mixer from the accident site taken by MOM

10 There was also damage seen on the wall closest to the mixer. A large hole was seen in the wall that
opened up into the adjacent factory unit (i.e. 32F). In addition, large cracks and semi-collapsed wall
12 sections were also seen on that same wall. An inspection of the adjacent unit (i.e. 32F) showed that
there were debris from the hole and damaged wall lying on the floor of this factory unit. Relatively
14 large chunks (brick-sized) of wall material could be seen scattered on the floor of unit 32F.

2 Data Collection and Analysis

2

The approach used for this technical investigation into the incident at Stars Engrg used several
4 different methods to scientifically collect and analyse data to determine the cause of the fires and
explosion that occurred:

6

i. Review of CCTV video clips furnished by MOM to ascertain chain of events.

8

ii. Primary Deflagration Analysis

10

a. Finite Element Analysis (FEA) modelling conducted by the Institute of High
Performance Computing (IHPC, A*STAR) to ascertain the heat transfer behavioural
trends of the mixer's heating jacket's surface and the HTF within the heating jacket.

12

b. Analysis of the HTF behaviour under elevated temperatures via DSC, SDT and
Pressure-Temperature tests by the Institute of Chemical and Engineering Sciences
(ICES, A*STAR).

14

c. Estimation of explosion overpressure and comparison with actual damage at the
accident site to ascertain the likely mechanism (physical or chemical) of the primary
deflagration event.

16

18

iii. Secondary Deflagration Analysis

20

a. Analytical testing (CHNS, SEM/EDX, SDT, FTIR, UV/Vis/NIR, MIE and MIT) conducted
by ICES on samples collected from the immediate vicinity of the accident site to
determine the presence of potato starch as a potential combustible dust hazard.

22

3 Review of CCTV Video

2

A total of eight video clips from eight different CCTV cameras which were located in and around the factory unit adjacent to the scene of the accident (unit 32F) were obtained from MOM. The locations of the CCTV cameras were provided by MOM. MOM’s instructions were that the timestamps reflected on the video clips were inaccurate and that, according to MOM’s investigations, a total of 1 day, 12 hours, 6 minutes and 48 seconds should be added to the original timestamps to arrive at the accurate timings.

The eight video clips were closely reviewed with significant observations and their corresponding timestamps (as adjusted) recorded. These observations are tabulated in **Appendix A**. The main observations from the CCTV video clips indicated the following:

Table 1. Summary list of events observed from CCTV video clips

Timestamp			Event
	Original	Adjusted	
i	22-2-21 Mon 23:15:40/41	24 Feb 2021 Wed 11:22:28/29	A large flash with a pressure wave and vibration (cameras 3, 5, 6, 7 and 8)
ii	22-2-21 Mon 23:17:05	24 Feb 2021 Wed 11:23:53	Flash (camera 8)
iii	22-2-21 Mon 23:17:45	24 Feb 2021 Wed 11:24:33	Flash (camera 8)
iv	22-2-21 Mon 23:18:15	24 Feb 2021 Wed 11:25:03	Flash (camera 7)

These observations from the CCTV videos indicated that there was likely a large primary event followed by up to three smaller events. The primary event that was captured by several cameras was likely to be a deflagration indicated by the bright flash and accompanied by a significant overpressure and vibrations within the workplace as evidenced by the movement of the dustbin and ladders in the neighbouring unit (32F). There were also three other events as evidenced by the bright flashes that

occurred at about 85 seconds, 125 seconds and 155 seconds after the primary deflagration as captured by Cameras 7 and 8. These events however did not seem to be accompanied by any observable vibrations.

Based on the CCTV observations, it is likely that a deflagration with a significant overpressure was the primary event that occurred within the factory unit 32E. This was then followed by three flash fires without significant overpressures. The primary deflagration is likely to be centred around the mixer based on the damage sustained by the mixer in addition to the proximity of the hole in the wall and the collapsed rear wall of the factory unit. On the other hand, the three subsequent flash fires are likely to be caused by potato starch powder which is the only known combustible material present in significant quantities within the factory unit other than the heat transfer fluid.

This scenario will be the focus of the scientific and technical analysis within this report.

4 Primary Deflagration Analysis

The epicentre of the explosion was seen to be located in the vicinity of the mixer based on the extent of damage sustained by the mixer. Specifically, the mixer was found to have suffered damage to its outer heating jacket with the heating jacket being spilt open at the welding seams. Hence, the primary deflagration analysis will focus on the mixer and its contents.

4.1 Mixer Description

The mixer is called the Sigma Kneader which was supplied to Stars Engrg by Laizhou Keda Chemical Machinery Co., Ltd, a manufacturer based in China. Based on the information furnished by MOM (including the Sigma Kneader User Guide published by Laizhou Keda Chemical Machinery Co., Ltd):

CONFIDENTIAL

- 2 i. The mixer is designed for use as a mixer and kneader of high viscosity materials via the use of
two rotary blades. Its mixing chamber has a capacity of 1000L and it is equipped with a heating
jacket to control the temperature of the materials being processed.
- 4 ii. The bottom of the mixing chamber is composed of two semi-cylindrical chambers with a
horizontal dividing ridge in the middle.
- 6 iii. The heating jacket is heated using nine electrical heaters which are rated to deliver 5 kW of
power each.
- 8 iv. Heat transfer from the electrical heaters to the process materials within the mixing chamber
is achieved via the use of a heat transfer fluid (Idemitsu Daphne Thermic 32-S oil) within the
10 heating jacket.
- 12 v. There are two openings on the mixer's heating jacket, one on its front (i.e. access port) and
the other on its back (i.e. vent port).
- 14 vi. The mixer's design temperature is 200 °C, with an operating temperature range of 70-160 °C,
a working pressure of up to 2 barg¹ and the material of construction is carbon steel².
- 16 A schematic diagram of the mixer is shown in **Figure 2** below.

¹ Equipment specifications obtained from Sigma Kneader User Guide published by Laizhou Keda Chemical Machinery Co., Ltd.

² Material of construction information obtained via MOM

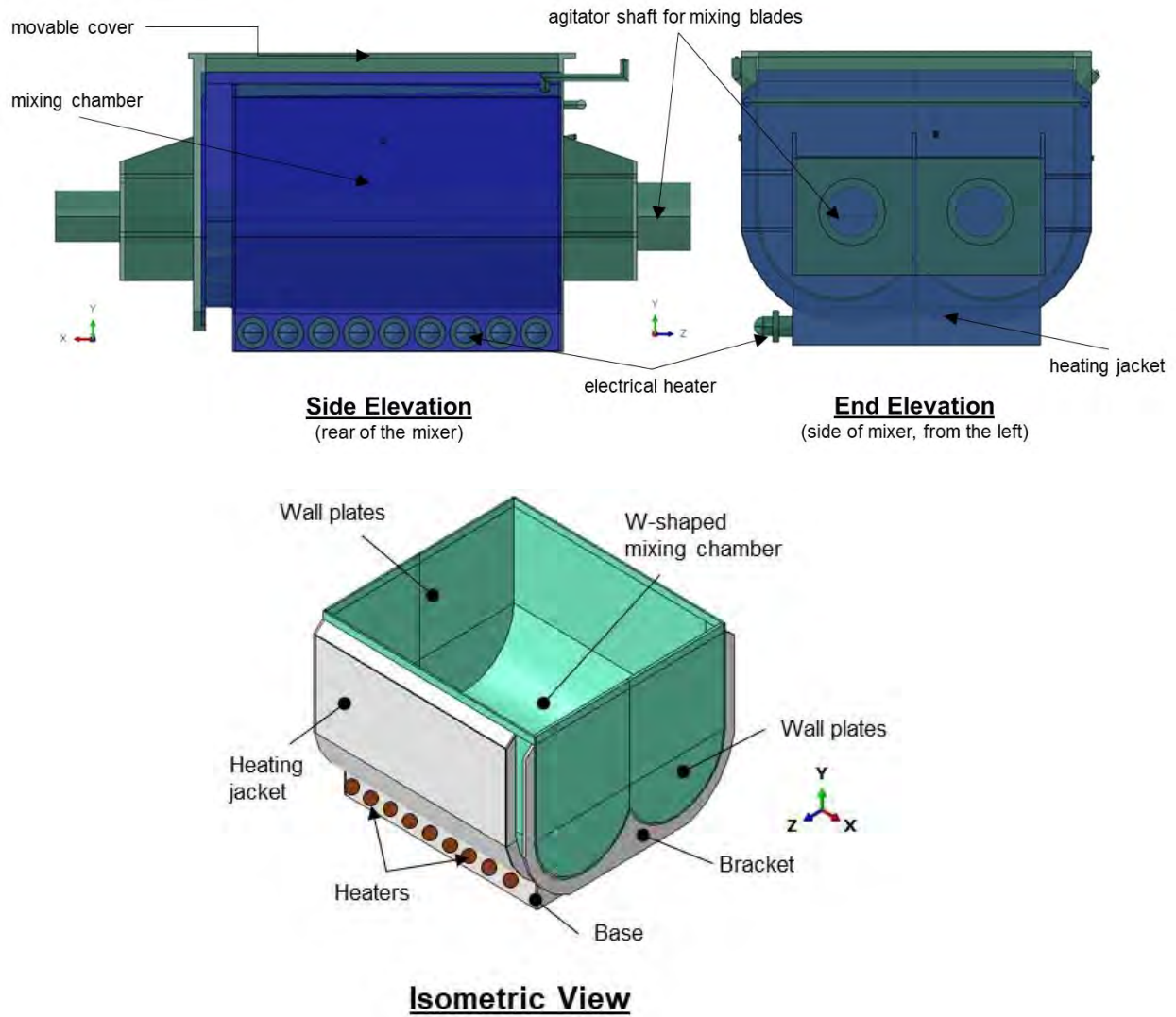


Figure 2. Schematic views of the mixer

4.2 Finite Element Analysis (FEA)

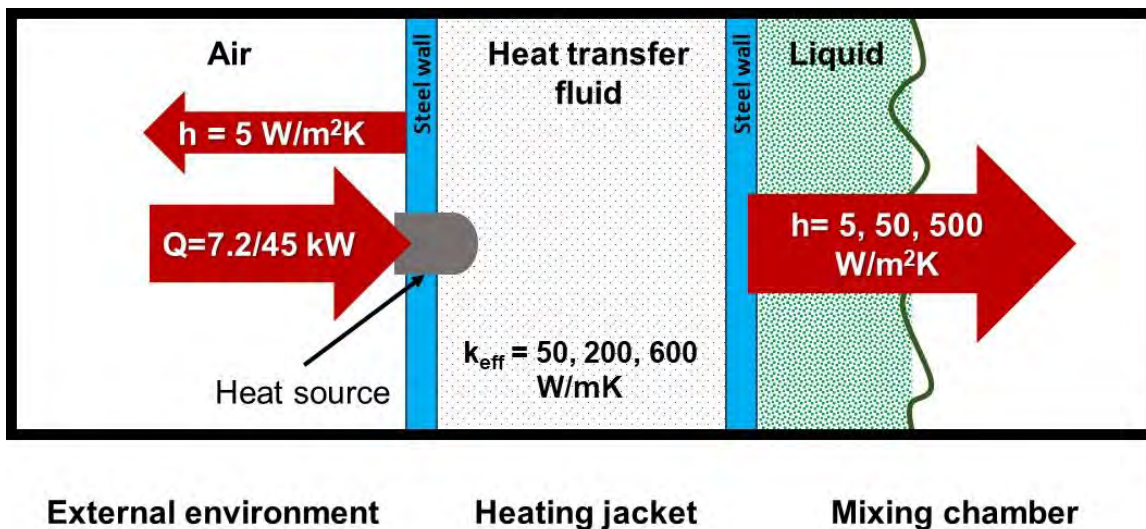
The mixer was found to have suffered catastrophic damage to its heating jacket. The bottom portion of the mixer could be seen to have been split open along its welding seams as shown in **Figure 3**.



2 **Figure 3.** Bottom view of damaged mixer taken by MOM

4 In order to better understand the heating behaviour of the mixer, an FEA was carried out by IHPC
 6 using the Abacus™ software. The geometric CAD model of the mixer (prepared by Matcor) was
 8 obtained from MOM. The modelling methods and details of the FEA are provided in **Appendix B**. The
 overview of the FEA heat transfer, boundary and load conditions are shown in **Figure 4** below. For
 the purposes of this study, the FEA heat transfer analysis was conducted under steady-state
 conditions with the heating jacket treated as a closed system (i.e. access and vent ports closed).

10



12

Figure 4. Overview of FEA heat transfer conditions for mixer

14

2 4.2.1 FEA modelling – temperature profiles

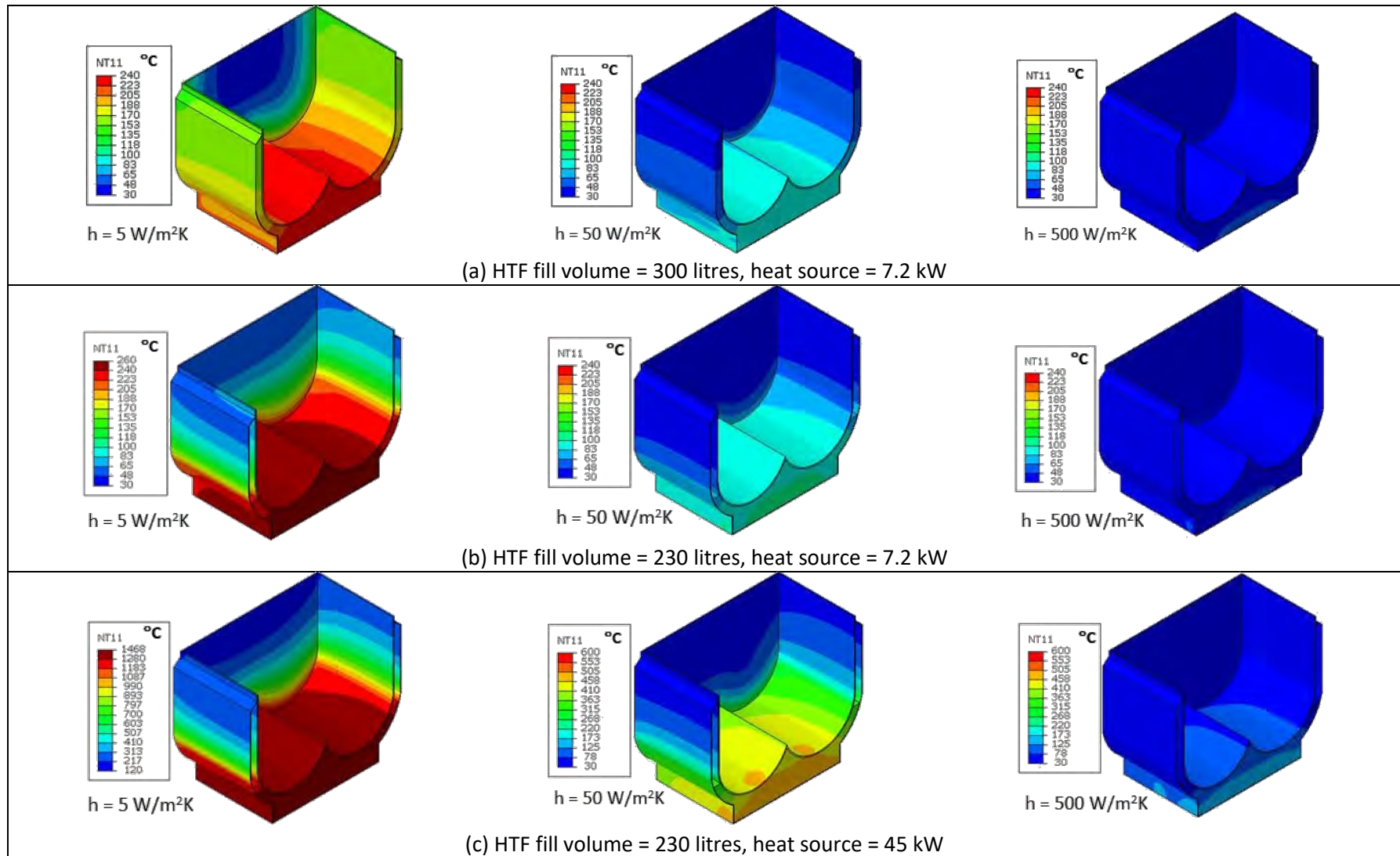
4 For a visual representation of the heat transfer trends, temperature profiles from the FEA simulations were extracted and shown in **Figure 5** below.

6 From these profiles, we can see that qualitatively, the maximum HTF temperatures and hotspots can be found near the heating elements at the heating jacket’s base. At the same time, for the inner mixer surface that faces the mixing chamber, the semi-circular region closest to the base is hottest. We also find that the temperature along the sides of the heating jacket decreases with increasing height along the sides of the heating jacket.

12 At a HTF fill volume of 230 litres, the HTF in the heating jacket will be in full contact with the surface of the mixing chamber as shown in **Appendix B, Figure B.4**. When comparing this low HTF fill volume (230 L) and that of a full HTF volume (300 L) within the heating jacket, we find that the temperatures along the sides are higher for the lower HTF level. Under moderate convection conditions of the mixer’s inner surface (i.e. $h=50 \text{ W/m}^2\text{K}$ – where the mixing chamber is filled with liquid but not agitated), HTF=230 L and heat source = 45 kW, the temperatures around the middle region of the mixer’s heating jacket sides range between 125 °C to 220 °C. The RTD sensor for the heating jacket, which should be fixed around this region, should therefore be able to adequately register the high temperature. This should then be able trigger the necessary signals for the control loop³ to take effect and prevent the HTF from being heated to excessively high temperatures.

24 A closer examination of the mixer structure also reveals minimal temperature gradients across the thickness of the metal wall. This is due to the good thermal conduction properties of steel along with a relatively thin wall thickness of approximately 10 mm.

³ Based on the ‘Electrical Report on Local Electric Panel’ dated 25 July 2021, prepared by Yong Chun Hao, a licensed electrical worker with Yogo Engineering, and Vincent Char Poh Fang, a Switchboard Manufacturer of One Electric Pte Ltd (annexed to Matcor’s report dated 10 Sep 2021, which we reviewed), the RTD sensor for the heating jacket operates on an interlock system where, once the heating jacket temperature exceeds the value preset at the control panel, the interlock system will switch off power supply to the electrical heaters for safety.



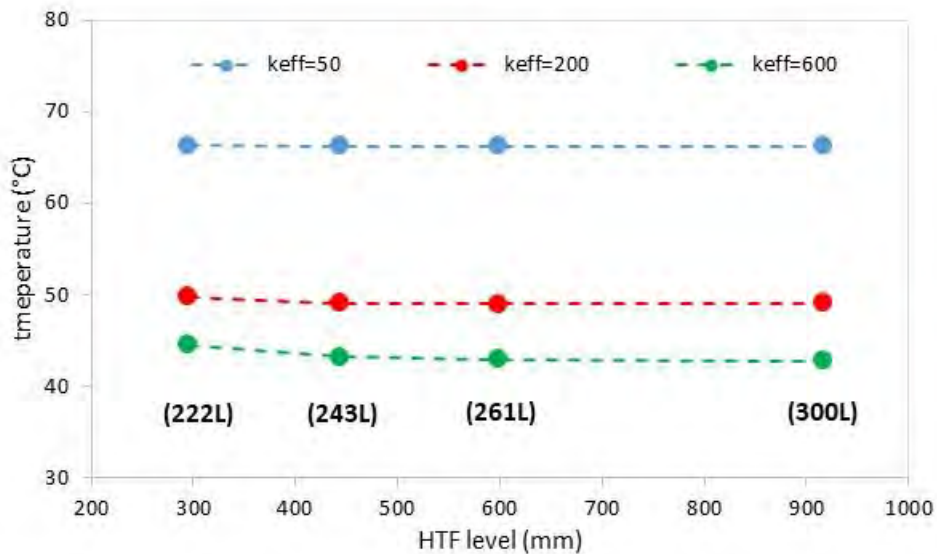
2

Figure 5. Temperature profiles (contour plots) of the mixer surfaces generated from FEA simulations where $k_{eff} = 200 \text{ W/mK}$

2 4.2.2 FEA modelling - high convection at mixer's inner surface ($h=500 \text{ W/m}^2\text{K}$)

4 For the case of high convection over the entire mixer's inner surface, which represents the mixer in
 6 operation with rotating/agitated contents, the maximum temperatures found from the FEA for a heat
 source totalling 7.2 kW of are shown graphically in **Figure 6** with the detailed tabulated data provided
 in **Appendix B, Table B.2**.

8



10 **Figure 6.** Maximum temperatures (average of HTF and mixer surface) obtained under high convective heat
 12 transfer conditions ($h=500 \text{ W/m}^2\text{K}$) with a 7.2 kW heating source input

12

14 Under high convective heat transfer conditions within the mixing chamber, it was found that the
 height of the HTF within the heating jacket did not significantly affect the HTF's temperature even at
 16 differing values of k_{eff} . The highest temperature for the HTF was approximately 80 °C while the
 highest mixer internal surface temperature was about 55 °C. The temperature difference between
 18 mixer's inner surface and HTF ranged between 2 °C to 26 °C depending on the k_{eff} for HTF. It should
 be noted that these results were based on a HTF fill volume of at least 222 litres which translates to
 a HTF level of 295 mm.

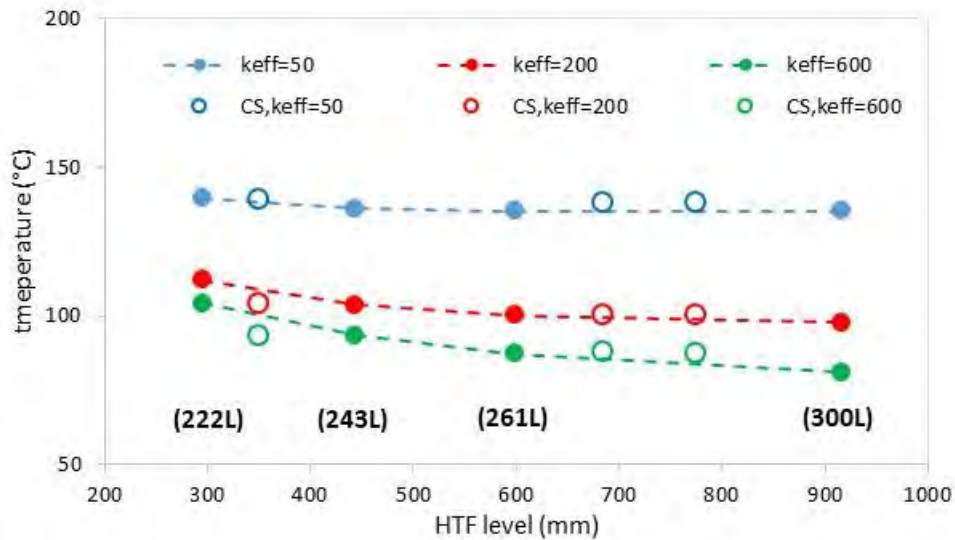
20

4.2.3 FEA modelling - moderate convection at mixer's inner surface ($h=50 \text{ W/m}^2\text{K}$)

2

For moderate convection over the entire mixer's inner surface, it represents the mixer with static liquid contents (natural convection) within the mixing chamber, i.e. non-rotating. The maximum temperatures found from the FEA for a heat source totalling 7.2 kW of are shown graphically in **Figure 7** with the detailed tabulated data provided in **Appendix B, Table B.3**.

6



8

Figure 7. Maximum temperatures (average of HTF and mixer surface) obtained under moderate convective heat transfer conditions ($h=50 \text{ W/m}^2\text{K}$) with a 7.2 kW heating source input

10

Note: “ k_{eff} ” indicates simulations conducted using stainless steel as the material of construction for the mixer whilst “CS, k_{eff} ” indicates simulations conducted using carbon steel as the material of construction.

12

Each plotted data point in **Figure 7** represents the averaged maximum temperatures obtained for the HTF and the inner mixer surface. Although the temperature of the HTF was found to be higher than that of the inner walls, this difference is relatively small with the difference in values ranging from 0.2% to 7.9%. In absolute terms the temperature difference between inner mixer surface and HTF ranges between 2 °C to 21 °C.

18

From the graph shown in **Figure 7**, it can be seen that for a given effective thermal conductivity (k_{eff}) of the HTF, variations in the HTF level within the heating jacket did not affect the fluid or the mixer's inner surface temperature much. However, it can be noted that where the HTF level drops below 450

22

mm (ca. 243 L), the fluid and the mixer’s internal surface temperature begins to show a significant increase.

Under these simulated conditions (i.e. $h = 50 \text{ W/m}^2\text{K}$, $k_{\text{eff}} = 50 \text{ W/mK}$, heat source = 7.2 kW), the highest temperature attained by the HTF (222 L) is about 150 °C.

4.2.4 FEA modelling - low convection at mixer’s inner surface ($h=5 \text{ W/m}^2\text{K}$)

The low convection condition at mixer’s inner surface represents an empty mixer, i.e. no contents within the mixing chamber. In addition, it is also assumed that the top hatch⁴ of the mixer is left open to atmosphere. Under these conditions, the maximum temperatures found from the FEA for a heat source totalling 7.2 kW are shown graphically in **Figure 8** with the detailed tabulated data provided in **Appendix B, Table B.4**. Each plotted data point in **Figure 8** represents the averaged maximum temperatures obtained for the HTF and the inner mixer surface.

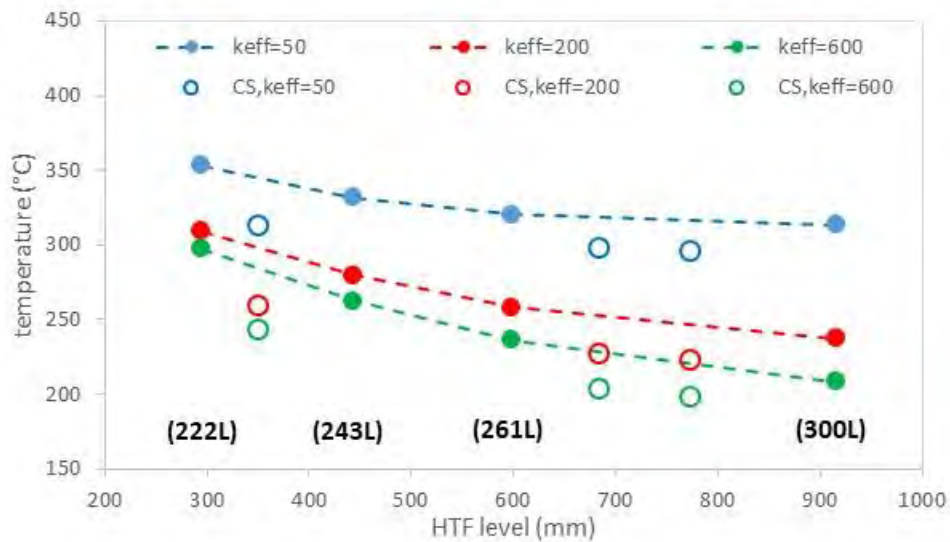


Figure 8. Maximum temperatures (average of HTF and mixer surface) obtained under low convective heat transfer conditions ($h=5 \text{ W/m}^2\text{K}$) with a 7.2 kW heating source input

⁴ If the hatch is partially closed, the temperatures attained will be higher due to heat build-up.

Under the low convection conditions (i.e. $h=5 \text{ W/m}^2\text{K}$), we can observe that the system temperatures (HTF and mixer inner surface) increase significantly once the HTF level drops below 450 mm (ca. 243 L). A similar trend was also observed for the moderate convection scenario previously.

The temperatures attained by the HTF and the mixer's inner surface generally exceeds the mixer's design temperature of $200 \text{ }^\circ\text{C}$ with temperatures rising up to $353 \text{ }^\circ\text{C}$ when HTF levels are low (less than ca. 222L). It should also be noted that under these conditions (i.e. $h = 5 \text{ W/m}^2\text{K}$, $k_{\text{eff}} = 50 \text{ W/mK}$, heat source = 7.2 kW), the temperature of the HTF is above its flash point ($220 \text{ }^\circ\text{C}$) and maximum recommended operating temperature ($300 \text{ }^\circ\text{C}$)⁵.

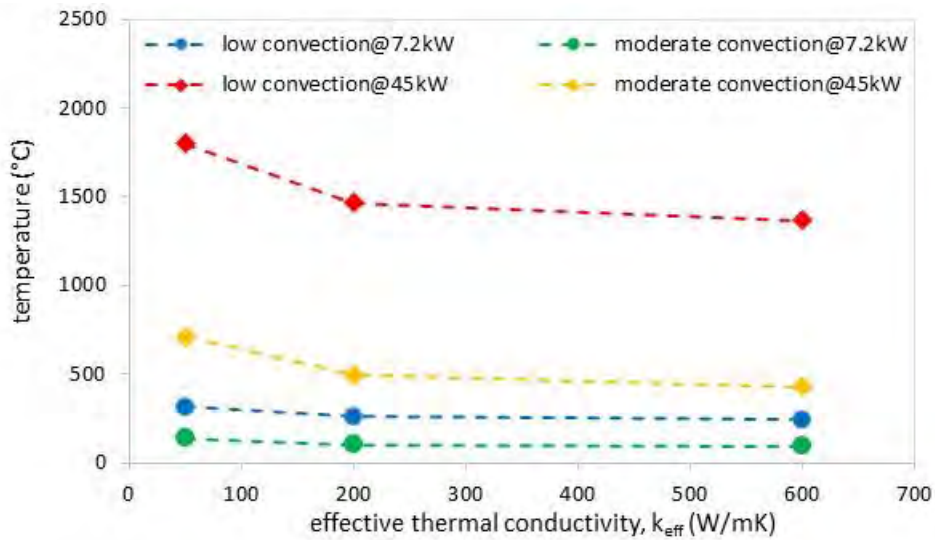
4.2.5 FEA modelling - analysis with 45 kW heat source

The preceding simulations were all carried out using a 7.2 kW heat source as it was initially assumed that the heat source for the mixer was 7.2 kW in total⁶. However, as noted in Section 4.1 (iii), investigations subsequently revealed that each of the heating elements used in the mixer was actually rated at 5 kW⁷. This results in a total heating power input of 45 kW for nine heating elements. Due to this additional information, several additional FEA simulation runs were conducted to study the effects of the increased power input on the heat transfer of the system. The results obtained are shown in **Figure 9** below with the data tabulated in **Appendix B, Table B.5**.

⁵ Flash point and maximum operating temperature information obtained from Idemitsu Daphne Thermic 32-S oil product information sheets (see Section 4.3 below).

⁶ See **Appendix B**, p3.

⁷ See **Appendix B**, Figure B.3.



2 **Figure 9.** Effect of increased heat source power on the mixer’s temperature profile

Note: low convection, $h = 5 \text{ W/m}^2\text{K}$ whilst moderate convection, $h = 50 \text{ W/m}^2\text{K}$.

4

The FEA results shown in **Figure 9** are based on a single HTF level (350 mm) corresponding to a liquid volume of 230 litres within the heating jacket. The increased heat source input, as expected, raised the maximum temperatures of both the HTF and the mixer’s inner surface.

8

Under the low convection conditions of an empty mixer, the temperatures were raised to levels exceeding 1000 °C. In reality, this would have caused phase changes, bubbling, cavitation and even cracking/decomposition reactions within the HTF. These phenomena have not been taken into account by the simplified FEA modelling that was conducted.

14 On the other hand, under moderate convection conditions where the mixing chamber is filled with liquid but not agitated, the simulated temperatures for the HTF in the heating jacket and the mixer’s inner surface ranged from 427 °C to 714 °C. At the higher end of this temperature range some degree of HTF phase change could also be expected to occur.

18

4.2.6 FEA modelling - effect of partially filled mixing chamber, insulation and very low HTF volumes

2

Based on further details provided by MOM, it was indicated that the internal mixing chamber was likely filled with approximately 176 litres of water just prior to the incident (based on the usual production process). This translates to the water level being about 175 mm from the base of the mixing chamber. This volume of water will only partially fill the mixing chamber as shown in **Figure 10** below.

8

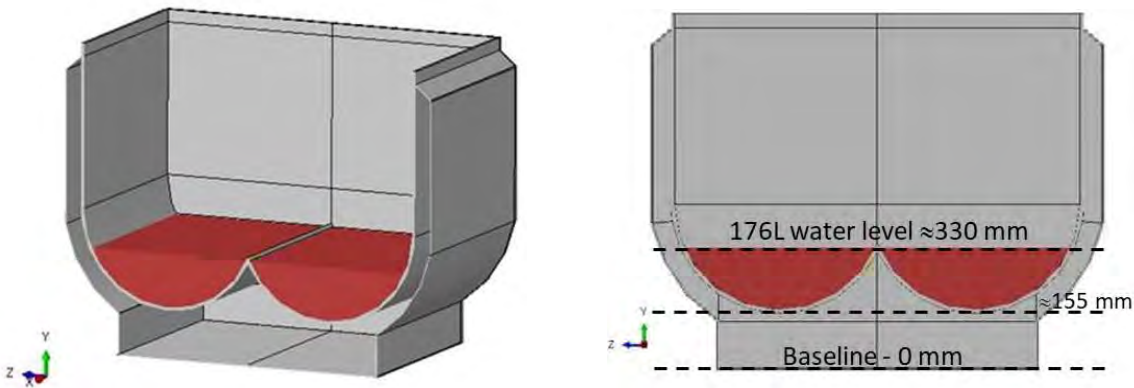


Figure 10. Illustration of mixing chamber with a water fill of 176 litres of water

10

The heat transfer coefficient for water under natural convection conditions can be between 50 to 1000 W/m²K depending on the temperature of the water and geometry profiles etc.

12

Based on Matcor’s CAD drawing of the mixer provided by MOM, the internal surface areas within the mixing chamber are as follows:

14

- 16 i. Total inner surface area available within the mixing chamber = 5,113,712 mm²
- ii. Surface area in contact with 176 L of water within the mixing chamber = 2,029,932 mm²
- 18 iii. Surface area in contact with air = 3,083,780 mm²

18

The nett heat transfer coefficient (h_{nett}) that corresponds to a partial (176 L) water fill within the mixing chamber can be estimated by taking the weighted-average heat transfer coefficient of water

20

and air together with their respective surface contact area within the mixing chamber. The estimated values of h_{nett} are shown in **Table 2** below.

Table 2. Estimated heat transfer coefficients corresponding to a water fill volume of 176L

h_{water} (W/m ² K)	50	100	1000
h_{nett} (W/m ² K)	23	43	400

As shown in **Table 2**, the weighted-average heat transfer coefficient (h_{nett}) within the mixing chamber with a partial water fill (176 L) lies well within the FEA modelling range of 5 to 500 W/m²K. Hence, the moderate heat transfer scenario ($h=50$ W/m²K) presented in Section 4.2.3 can be seen to be a fair representation of conditions within the mixing chamber prior to the incident. It follows therefore that the FEA results from **Figure 9** which shows that the HTF in the jacket and the mixer's inner surface temperatures ranging from 427 °C to 714 °C (moderate convection at 45 kW) could be taken as a reasonable base-case representation.

These FEA results were obtained based on an assumption that the external surfaces of the mixer were exposed to ambient air with convective heat losses corresponding to $h = 5$ W/m²K. However, as seen in **Figure 1**, it is known that the external surfaces of the mixer were actually covered with insulating material (i.e. white coloured material). In the presence of insulation, it is expected that the heat loss from the mixer's external surfaces would be reduced. In such a situation, the temperatures of the HTF and the mixer's internal surfaces would also increase above that obtained in the base-case FEA simulations (i.e. 427 °C to 714 °C).

Furthermore, it has been shown in **Figure 7** and **Figure 8** that lower amounts of HTF within the heating jacket would lead to higher temperatures. In our FEA simulations, the lowest HTF volume modelled was 222 litres. This level was chosen to ensure that the HTF was in contact with the inner (lower) surface of the mixing chamber. HTF volumes less than 222 litres (i.e. 40 to 200 litres) would result in the formation of a void space above the HTF's surface as shown in **Appendix B, Figure B.6**. This then results in a two-phase situation in the heating jacket that will further reduce the heat

transfer efficiency to the liquid contents within the mixing chamber. In such a situation, the
2 temperature of the HTF within the heating jacket is expected to be higher than the base-case (427 °C
to 714 °C). This could also result in phase changes and potential decomposition of the HTF with gases
4 and vapours accumulating in the void space above the liquid level.

6 Based on Matcor's report dated 10 Sep 2021, which we reviewed, at very low HTF volumes (i.e. 40 to
80 litres), at least one of the heater's metal tubes would not be in contact with the HTF. Compounding
8 this will be the lack of contact between the HTF and the mixer's inner surface (mixing chamber) which
would result in very low heat transfer to the contents within the mixing chamber. In such a scenario,
10 the heating rods are likely to overheat.

12 4.3 Analysis of heat transfer fluid

14 Under certain conditions, as shown by the FEA analysis, the HTF could be subjected to high
temperatures that exceed its flash point (220 °C) and its recommended operating temperature (300
16 °C). Although the HTF is classified as a non-combustible liquid, it could still undergo cracking or
decomposition reactions when exposed to sufficiently high temperatures. Under such conditions, the
18 HTF could vaporise and release smaller, lighter hydrocarbon fragments that are flammable.

20 The publicly available information on the HTF used in the mixer (Idemitsu Daphne Thermic 32-S oil)
is limited and does not provide any information relating to its potential decomposition or autoignition
22 temperatures as shown in **Table 3**.

Table 3. Property comparison among various heat transfer fluids

Heat Transfer Fluids	Density* (kg/m ³)	Specific heat* (kJ/kgK)	Thermal conductivity* (W/mK)	Viscosity* (mPa-s)	Vapour pressure* (bar)	Heat of combustion (kJ/kg)	Flash point (°C)	AIT (°C)
Dowtherm A	991	1.8	0.125	0.91	0.0100	36053	113	599
Dowtherm J	800	2.1	0.128	0.42	0.1700	41400	57	420
Dowtherm DTH	993	1.8	0.131	1	0.0040	32560	255	621
Paratherm HE	820	2.2	0.127	5.5	0.0003	46300	227	371
MultiTherm IG-4	811	2.3	0.128	5.08	<0.0001	45300	227	355
Duratherm HTO	767	2.1	0.133	4.6	<0.0001	-	218	360
Daphne Alpha Thermo 32B	824	2.2	0.127	3.63	<0.0001	-	188	-
Daphne Alpha Thermo 32 (i.e. Idemitsu Daphne Thermic 32-S oil)	816	1.93	0.127	4.4	<0.0001	-	220	-

2 Note: *indicates properties at 100 °C where available.

4 A series of experiments and tests were therefore conducted to study the behaviour of the heat
 6 transfer fluid (Idemitsu Daphne Thermic 32-S oil) when it is subjected to excessive temperatures
 6 namely:

- i. Differential scanning calorimetry (DSC)
- 8 ii. Simultaneous DSC-TGA (SDT)
- iii. Pressure-temperature analysis (closed system)

10

12 **4.3.1 Differential scanning calorimetry of heat transfer fluid**

14 Samples of fresh Idemitsu Daphne Thermic 32-S oil (i.e. heat transfer fluid - newly purchased,
 obtained from MOM) and samples of HTF obtained from the accident site (Exhibit 250221-2b), were
 16 tested using a Mettler Toledo Differential Scanning Calorimeter (DSC). The detailed DSC test results
 can be found in **Appendix C**.

18

The two liquid samples were each heated at a temperature ramp of rate 10 °C/min from -50 °C to 250 °C before being cooled back from 250 °C to -50 °C at the same rate of 10°C/min. The samples were then subjected to another heating cycle to 250 °C.

For both test samples, the three DSC thermograms generated for each of the heating and cooling cycles did not indicate any significant exothermic reactions (e.g. decompositions) occurring up to 250°C.

4.3.2 Simultaneous DSC-TGA (SDT) testing of heat transfer fluid

The two liquid samples (i.e. fresh Idemitsu Daphne Thermic 32-S oil and the sample obtained from Stars Engrg factory unit (Exhibit 250221-2b)) were tested to higher temperatures of up to 800 °C under an inert nitrogen environment using a TA Instruments Q600 SDT. The SDT tests were conducted in accordance to ASTM E1131-20. The detailed SDT test results can be seen in **Appendix D**. Some of the key results from these tests are listed in **Table 4**.

Table 4. Results from SDT tests conducted on heat transfer fluid

Sample	Ramp rate (°C/min)	Mass loss onset temperature °C	Peak mass loss temperature °C
Liquid (Exhibit 250221-2b)	2	216	280
	5	240	304
	10	257	321
Fresh Idemitsu Daphne Thermic 32-S oil	2	227	289
	5	241	318
	10	264	320

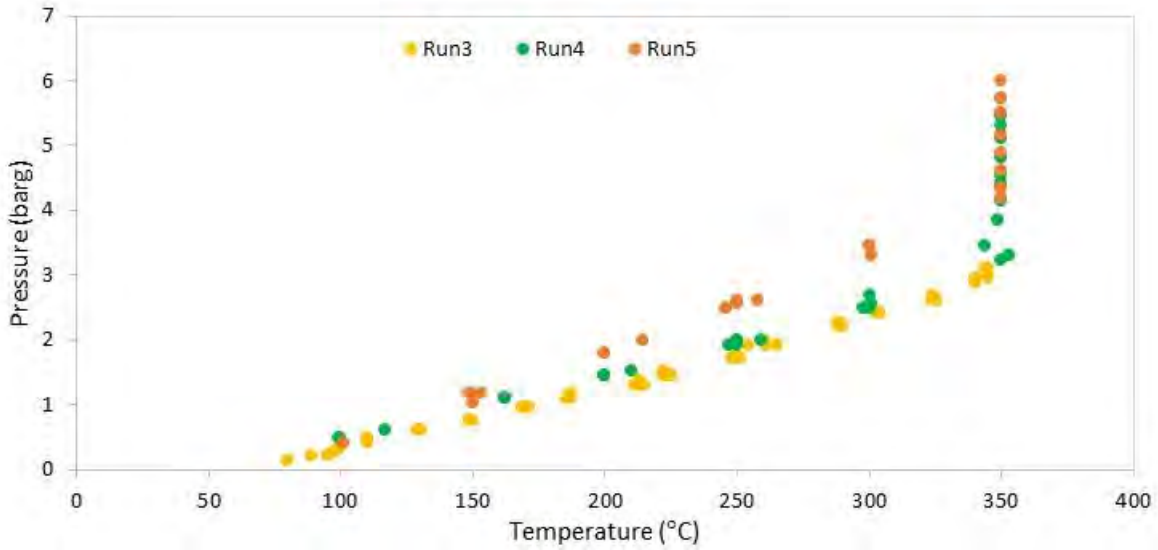
1 A qualitative review of the SDT curves obtained, indicated that both the liquid samples experienced
2 an almost total loss of mass (> 99 wt%). The peak mass loss rate occurred at a temperature range
3 from 280 °C to 321 °C as shown in **Table 4**. It was also observed that all the thermograms exhibited a
4 double exotherm profile with one relatively smaller exothermic reaction occurring before 250 °C and
5 another larger exothermic reaction occurring after 250 °C. The exothermicity of these peaks coupled
6 with the significant mass loss, suggests that the HTF samples had experienced decomposition
7 reactions.

8
9 For the liquid sample (Exhibit 250221-2b) of HTF taken from the incident site, it was also observed
10 that the onset of this decomposition occurred at a slightly lower temperature starting from 216 °C
11 compared to 227 °C for the fresh Idemitsu Daphne Thermic 32-S oil.

12 4.3.3 Pressure-temperature analysis (closed system) of heat transfer fluid

13
14 In order to study the pressure-temperature behaviour of the HTF, a series of experiments were
15 carried out with the fresh Idemitsu Daphne Thermic 32-S oil in a 300 ml hastelloy Parr Instruments
16 pressure vessel. The detailed description of the experiments and the corresponding results are shown
17 in **Appendix E**.

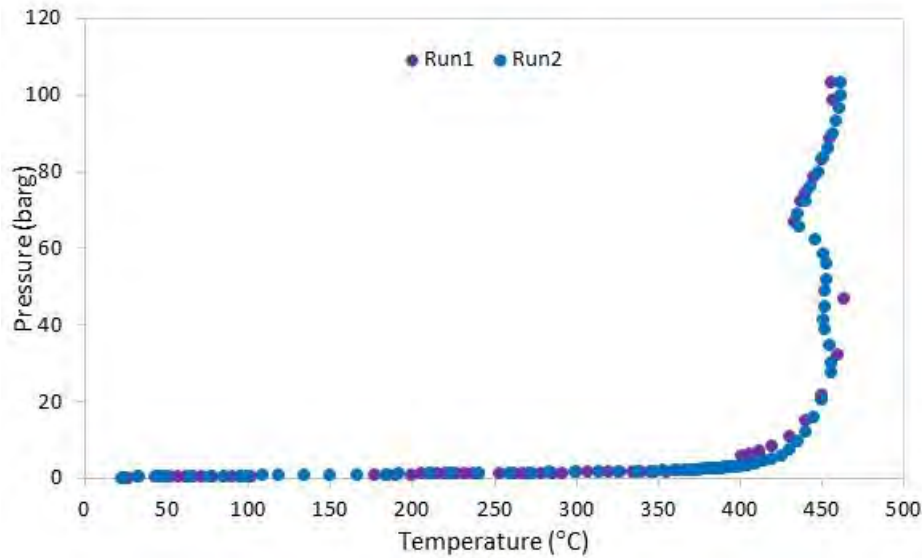
18
19 Based on the results obtained for all five experimental runs, it can be seen that at temperatures
20 below 300 °C, there does not seem to be any significant or abrupt pressure increases that would
21 indicate an exothermic or decomposition reaction happening within the HTF. However, at around
22 350 °C, it was observed that there was a significant pressure increase during experimental Run 4 and
23 Run 5 which was not present in Run 3 which ended at 340 °C. These observations can be seen in the
24 consolidated graphical plots for Runs 3, 4 and 5 as shown in **Figure 11**.



2 **Figure 11.** Consolidated graph of pressure against temperature for experimental Runs 3, 4 and 5

4 From **Figure 11**, the pressure was seen to increase to around 6 barg when the temperature was held
 at 350 °C. However, when the experimental temperature range was extended up to 450 °C for
 6 experimental Run 1 and Run 2, a larger pressure increase of up to 103 barg was observed. The
 experimental runs were terminated and the system was cooled once the system pressure was seen
 8 to exceed 100 barg due to safety reasons. The consolidated graphical plots of pressure against
 temperature for Runs 1 and 2 are shown in **Figure 12**.

10

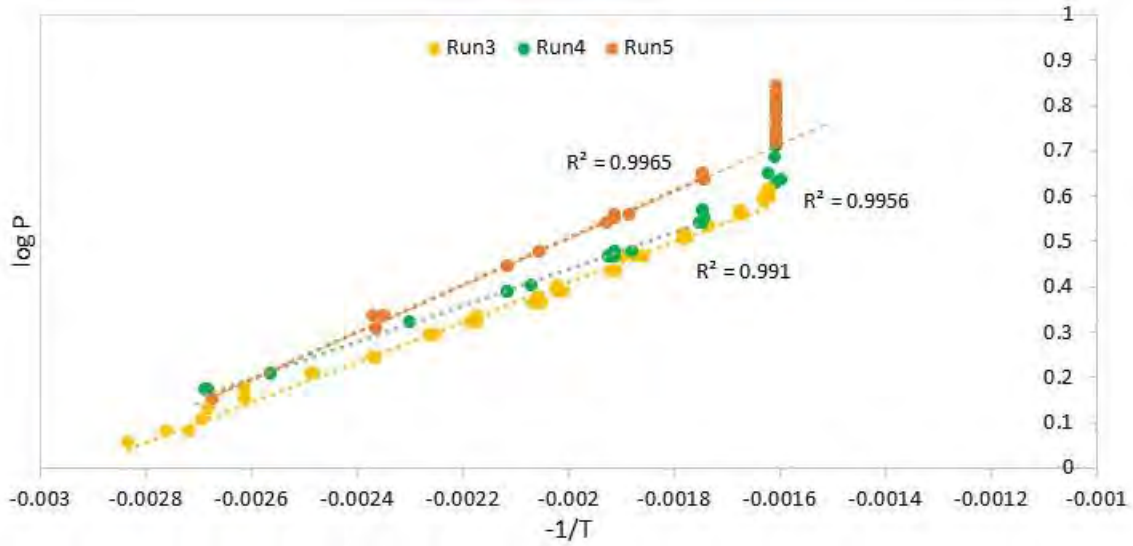


2 **Figure 12.** Consolidated graph of pressure against temperature for experimental Runs 1 and 2

4 As shown by the consolidated graphical plots in **Figure 11** and **Figure 12**, prior to the sharp pressure
 increases at 350 °C and 450 °C, the pressures were seen to be increasing gradually. It is likely that in
 6 the initial stage of the experiments at temperatures less than 340 °C, the pressure increases were
 due to vapourisation of the HTF along with the thermal expansion of the gas in the headspace above
 8 the liquid. Under a vapour pressure dominated regime, a graphical plot of the pressure logarithm
 against the reciprocal of temperature would generate a straight line as the system tends towards
 10 ideal/real gas behaviour. In addition, when the system behaviour deviates from this straight line, it
 would also indicate a transition into a gas generating, thermal decomposition regime.

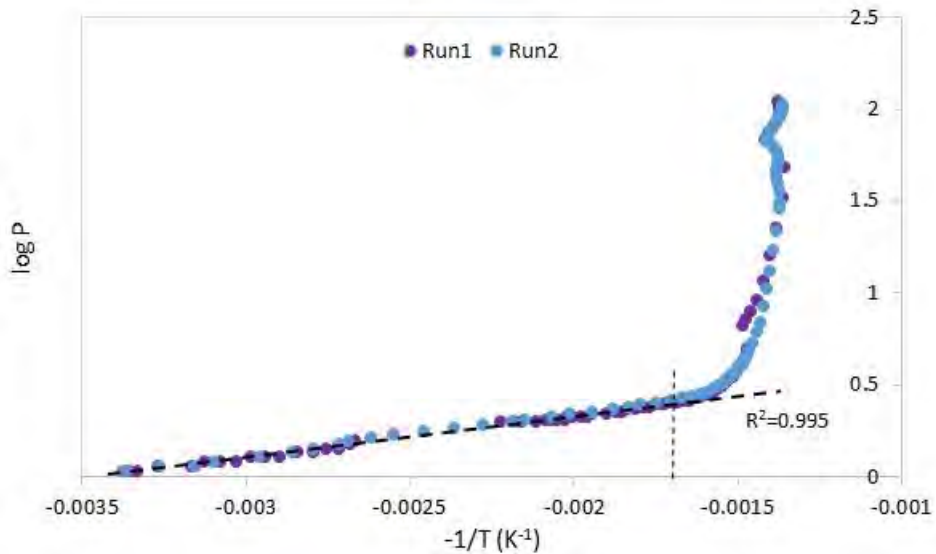
12

The consolidated graphs of the pressure logarithm plotted against the reciprocal of temperature for
 14 all five experimental runs are shown in **Figure 13** and **Figure 14**.



2 **Figure 13.** Consolidated graph of pressure logarithm against reciprocal temperature for experimental Runs 3,
4 and 5

4



6 **Figure 14.** Consolidated graph of pressure logarithm against reciprocal temperature for experimental Runs 1
and 2

8

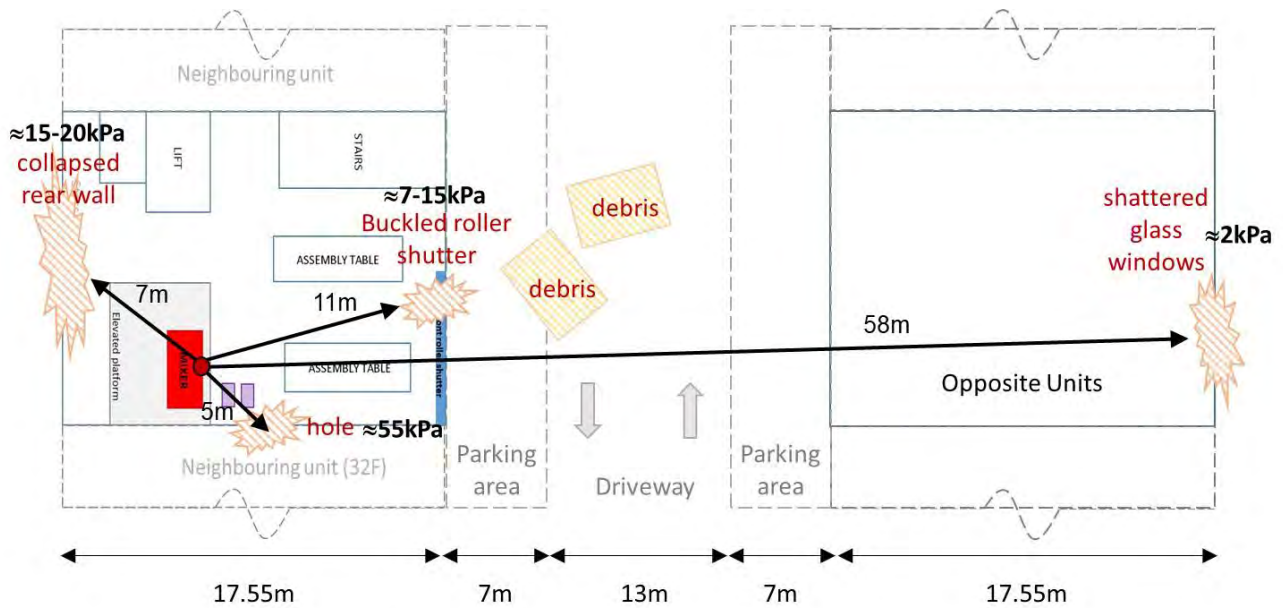
10 As seen in **Figure 13** and **Figure 14**, the system behaves linearly up to around 320 °C. After this, the pressure-temperature relationship starts to deviate, with the pressure increasing significantly. This suggests that the system is no longer within the vapour pressure dominated regime and has likely

2 transitioned into a situation where there is a significant amount of gasses being generated through a
 2 thermal decomposition of the HTF.

4 **4.4 Explosion Evaluation – Deflagration Overpressures**

6 The explosion caused a significant amount of damage to Stars Engrg’s factory unit (32E), the
 neighbouring unit (32F) and the unit across the driveway (Unit 38A). A schematic representation of
 8 some of the specific damage caused by the accident is illustrated in **Figure 15**. This illustration was
 prepared based on information and measurements provided by MOM.

10



12 **Figure 15.** Schematic representation of the damage caused by the accident

14 The specific physical damage illustrated in **Figure 15** will be used as key references in evaluating
 whether the explosion event was purely a physical explosion due to the physical/mechanical energy
 16 released from an exploding compressed gas build-up within the mixer’s heating jacket or whether it
 was a chemical explosion involving combustion/deflagration of the HTF released from the mixer’s
 18 heating jacket. In addition, the calculated explosion overpressures will also be compared against the
 corresponding damage descriptors listed in **Table 5** below.

2

Table 5. Damage produced by blast, overpressures⁸

Description of Damage	Side-on overpressure (kPa)				
Threshold for glass breakage	1	Light damage	Moderate damage	Severe damage	Total destruction
“Safe distance,” probability of 0.95 of no serious damage beyond this value; some damage to house ceilings; 10% window glass broken.	2				
Large and small windows usually shattered; occasional damage to window frames	3.5 - 7				
Corrugated steel or aluminium window frames panels fastenings fail, followed by buckling;	7 - 15	3.5-17			
Partial collapse of walls and roofs of houses	15				
Concrete or cinderblock walls, not reinforced, shattered	15 - 20	17-35			
Unreinforced brick panels, 25-35 cm thick, fail by shearing or flexure	50 - 55				
Probable total destruction of buildings; heavy machine tools moved and badly damaged	70		35-83		
Building totally destroyed i.e. damaged beyond economical repair	83	> 83			

4 Based on the actual physical damage observed at the accident site and comparison with **Table 5**, we
 can deduce that the peak overpressures generated during the primary deflagration should range
 6 from around 2 kPa to 55 kPa. Simplified overpressure calculations considering both physical and
 chemical explosion mechanisms were conducted and compared against this criterion.

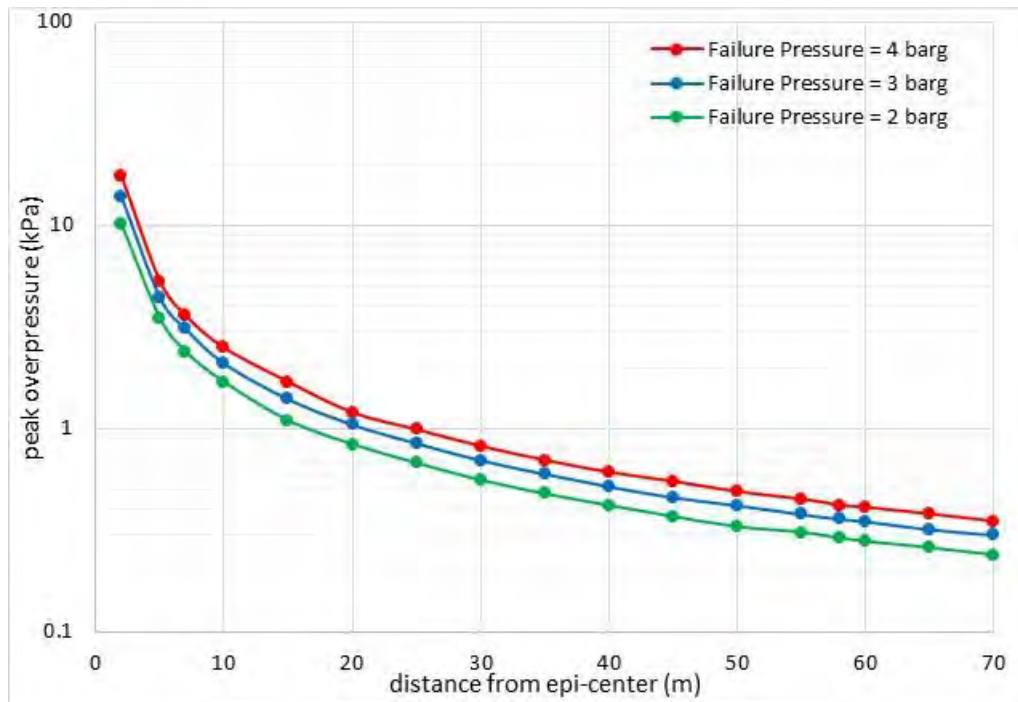
8

⁸ Adapted from Guidelines for evaluating the characteristics of vapor cloud explosions, flash fires, and BLEVES. Center for Chemical Process Safety (CCPS), 1994.

2 4.4.1 Physical explosion – estimation of overpressures

4 Increases in temperature could lead to a build-up of pressure due to thermal expansion of gasses,
 6 generation of HTF vapour and gas generation from decomposition/cracking reactions of HTF within
 8 the mixer’s heating jacket. When the heating jacket abruptly fails, the sudden energy release from
 10 the physical expansion of the compressed gasses could then result in an explosion. The peak
 overpressures arising from such a physical explosion were calculated as shown in **Appendix F**. The
 results of the physical explosion calculations are presented in **Figure 16**, indicating the peak
 overpressures generated upon failure of the heating jacket. The failure pressures used in the
 calculations were based on up to twice the rated pressure (i.e. 2 barg) of the mixer.

12



14 **Figure 16.** Graph of overpressure against distance for heating jacket failure at pressure P = 2, 3 and 4 barg

16 A comparison between the calculated overpressure and the specific damage found at the accident
 18 site is listed in **Table 6** below.

2 **Table 6.** Comparison between calculated physical overpressure and accident site damage

Accident Site Damage	Calculated peak overpressure (kPa)	Reference overpressure ⁹ (kPa)
Blast hole in wall ≈ 5 m from epicentre	5.3	50 - 55
Collapsed rear wall ≈ 7 m from epicentre	3.6	15 - 20
Damaged, buckled roller shutter ≈ 11 m from epicentre	2.5	7 - 15
Shattered glass windows ≈ 58 m from epicentre	0.42	2 – 3.5

4 Overall, it can be seen that the overpressures generated from a physical explosion arising only from
 6 compressed energy release would generate overpressures ranging from a low of about 0.3 kPa at 60
 8 m to a high of about 17 kPa at 2 m. These overpressures are much lower than the damage criterion
 10 of 2 to 55 kPa for the accident site. When compared to the specific damage found at the accident site
 12 in **Table 6**, the calculated overpressure values were lower than the reference overpressures that
 could be expected for that level of damage. Furthermore, a strictly physical explosion could not
 account for the bright flash, fires and burn injuries that corresponded with the primary explosion
 event for this incident at Stars Engrg. Therefore, it would be unlikely that the primary explosion event
 was strictly a physical explosion.

14 **4.4.2 Chemical explosion – estimation of overpressures**

16 The HTF used in the mixer’s heating jacket is classified as a combustible liquid with flash point of
 18 around 220 °C. After several cycles of use, it is known that the HTF could experience a reduction in
 its flash point. According to testing done by the Health Sciences Authority (HSA) on a sample of used
 HTF taken from the accident site, the sample had a flash point of about 135±4°C¹⁰. In spite of this

⁹ Extracted from Appendix F, Table F.2

¹⁰ Information furnished by MOM

flash point reduction, the HTF's low volatility would mean that it will be unlikely that a typical vapour
2 cloud explosion of the HTF occurred when the mixer's heating jacket ruptured.

4 An alternative mechanism for a chemical explosion that involves the HTF (Samirant 1999) would be
through the formation of aerosols. Liquids held under pressure when released suddenly can atomise
6 (Krishna et al. 2001) and form a dispersion of liquid droplets in air (i.e. aerosol or mist). Pressures of
only a few bars above atmospheric, have been shown to be enough to atomize industrially used
8 liquids (Bowen and Shirvill 1994) and ignited by energy sources as low as 100 mJ.

10 Such aerosolised liquids, could be as explosive as vapour-air mixtures even at temperatures well
below the bulk liquid's flash point. The use of flash point to evaluate a liquid's fire and explosion
12 hazard is therefore inappropriate when the liquids are aerosolised. HTFs with flash points ranging
from 149 °C to 260 °C have been shown to ignite at room temperature (Lian et al. 2010). This
14 phenomena is the basis for many industrial combustion processes such as diesel engines, gas turbines
and furnaces.

16

The flammability of an aerosol depends upon the properties of the liquid (e.g. viscosity, surface
18 tension, volatility, density, purity, flash point, autoignition temperature), air-fuel ratio (i.e.
stoichiometry) and particle size distribution which depends on the pressure and orifice size of the
20 release (Santon 2009). Furthermore, upon release, a fluid's impingement onto a secondary surface
could result in a reduction of aerosol particle sizes by 50% (Maragkos and Bowen 2002) thus
22 increasing its flammability. It is also known that aerosol explosions could be even more severe than
their corresponding vapour explosions (Krishna et al. 2003). One factor for this is that liquid droplets
24 contain more combustible matter per unit volume thus having a larger net enthalpy compared to the
vapour.

26

Incidents involving aerosolised combustible liquids such as HTFs and other heavy hydrocarbons such
28 as pump oils have been reported to occur (Yuan et al. 2021). An example of such an incident occurred

in Georgia USA (1995) where a carpet mill suffered a HTF leak from a faulty rotating coupling. The high temperature and high pressure leak resulted in aerosolisation and ignition of the HTF. Although there were no reported fatalities or injuries from this incident, the economic loss amounted to over US\$ 200 million. In a publication (Febo and Valiulis 1995), Factory Mutual Engineering and Research statistics showed that over a 10 year period, there were 54 fires and explosions involving HTFs. These incidents resulted in US\$ 150 million in losses. In another survey (Santon 2009), 37 accidents located in Europe and the United States were identified. These incidents involved the ignition of aerosols that are in most cases near or below the liquids' flash point. Out of these 37 accidents, 9 of them were large explosions that resulted in 29 fatalities. A breakdown of these 37 incidents in terms of fuel source and ignition sources are shown in **Figure 17** and **Figure 18**.

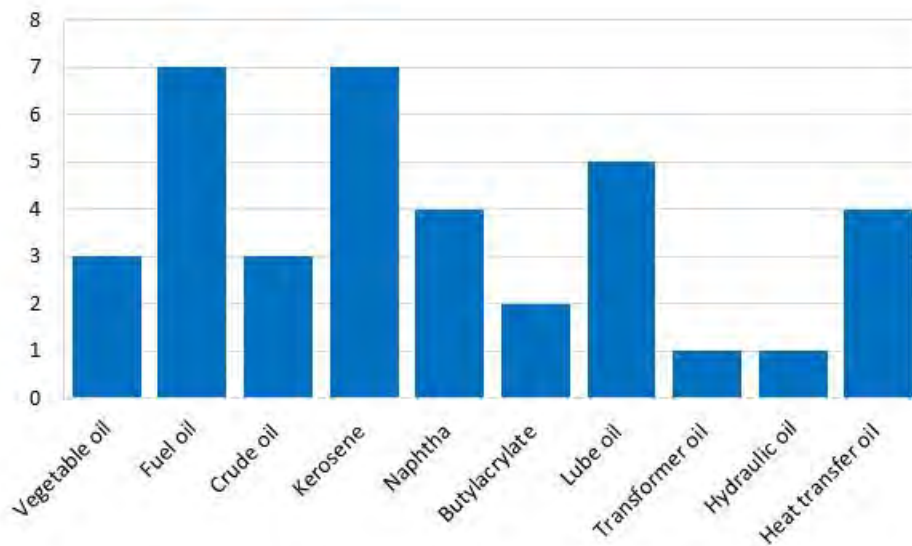
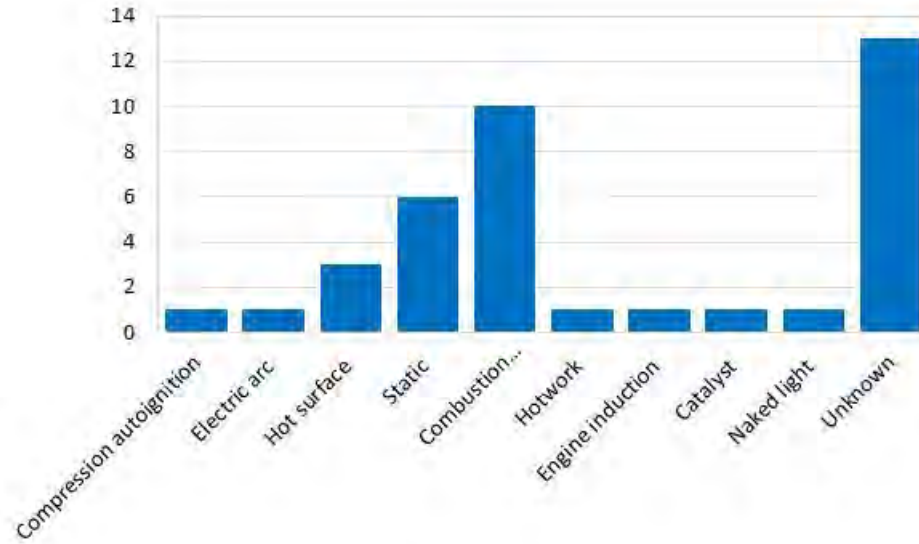


Figure 17. Breakdown of aerosol related fires and explosions according to fuel type

12



2 **Figure 18.** Breakdown of aerosol related incidents according to ignition sources

4 Based on the available literature, it is therefore possible to consider the following scenario as an explanation for the failure of the mixer:

- 6 i. Excessive heating of the HTF resulted in a pressure build-up within the heating jacket.
- ii. The high pressure led to a mechanical failure of the welded seams in the heating jacket.
- 8 iii. The sudden release of the high temperature, high pressure HTF from the heating jacket resulted in aerosol formation.
- 10 iv. The aerosol generated found an ignition source (e.g. hot surface) and ignited causing a deflagration with its associated overpressures

12

The overpressures generated from an aerosolised HTF would be dependent on the amount of fuel
 14 combusted. Hence, for the overpressure calculations here, a series of HTF volumes were considered to account for various fill levels within the mixer’s heating jacket. In addition, since the heat of combustion of Idemitsu Daphne Thermic 32-S oil is not available, an average of the available heat of
 16 combustions ($H_c \approx 40,000$ kJ/kg) of other common HTFs as listed in **Table 3** was used as a proxy for
 18 Idemitsu Daphne Thermic 32-S oil.

The peak overpressures arising from the chemical explosion of aerosolised HTF were calculated^{11,12} as described in **Appendix F** and the results are shown in **Figure 19** to **Figure 24**.

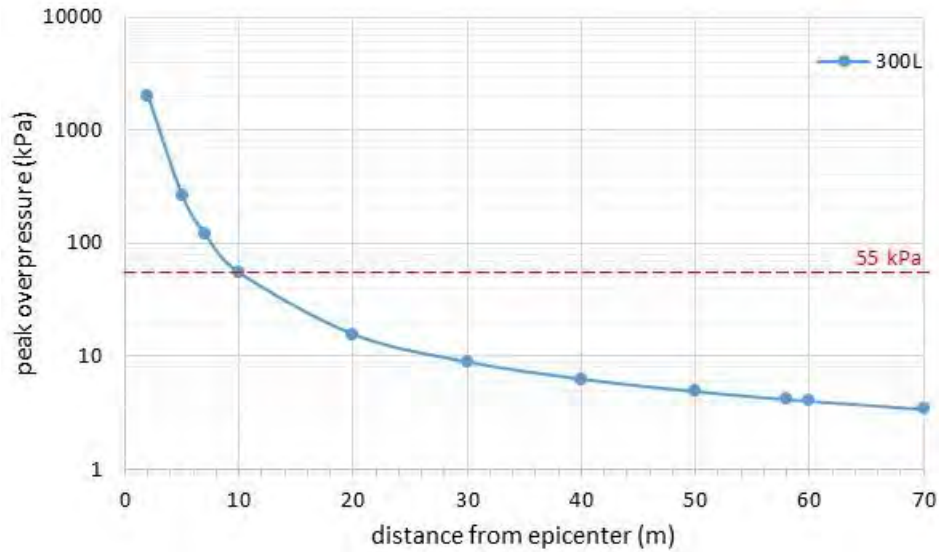


Figure 19. Graph of overpressure against distance for HTF volume = 300L

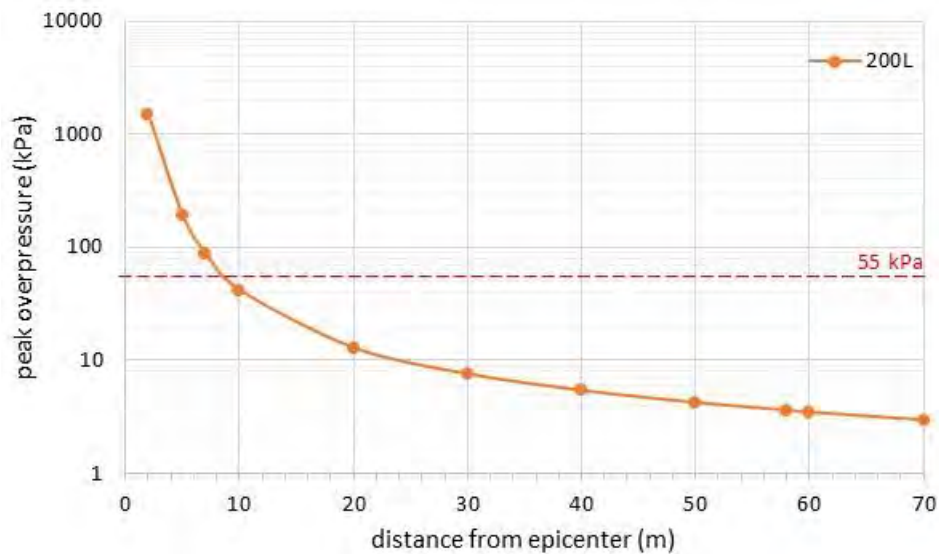


Figure 20. Graph of overpressure against distance for HTF volume = 200L

¹¹ Kumar, Ashok. (1994). Guidelines for evaluating the characteristics of vapor cloud explosions, flash fires, and BLEVEs, CCPS.

¹² Grossel, S. S. (2013). Guidelines for Evaluating Process Plant Buildings for External Explosions, Fires, and Toxic Releases, CCPS

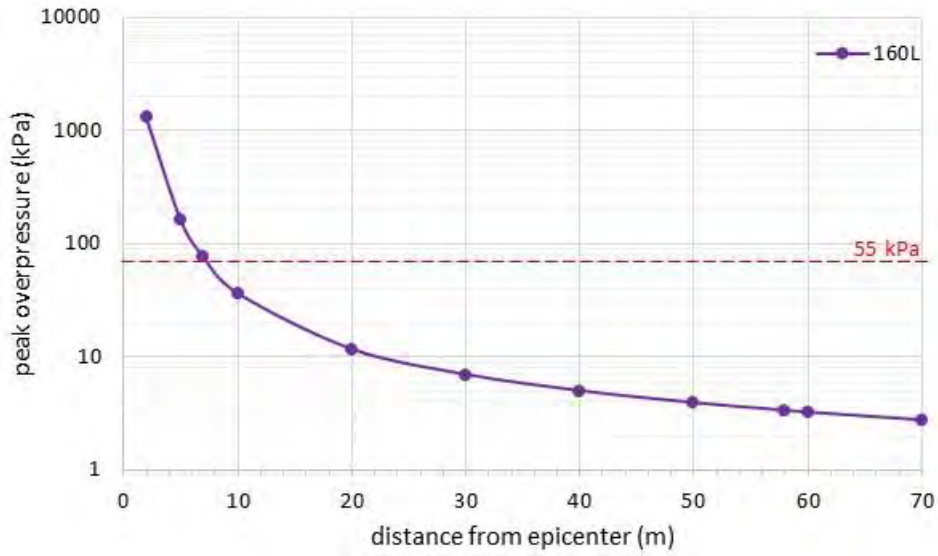


Figure 21. Graph of overpressure against distance for HTF volume = 160L

2

4

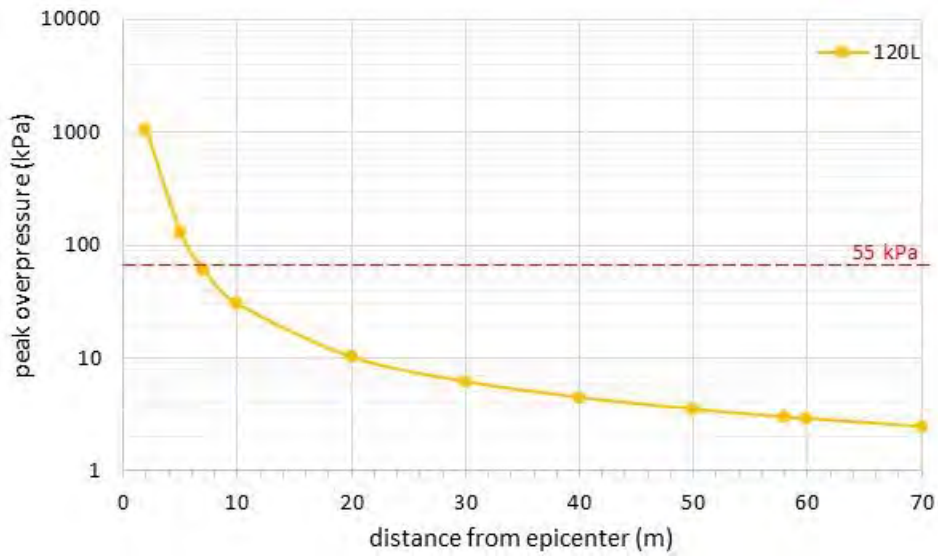
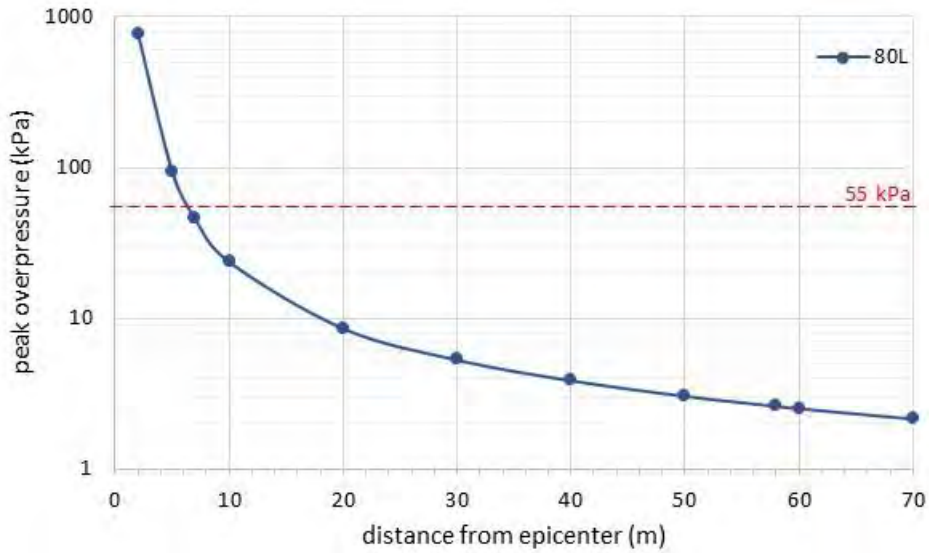


Figure 22. Graph of overpressure against distance for HTF volume = 120L

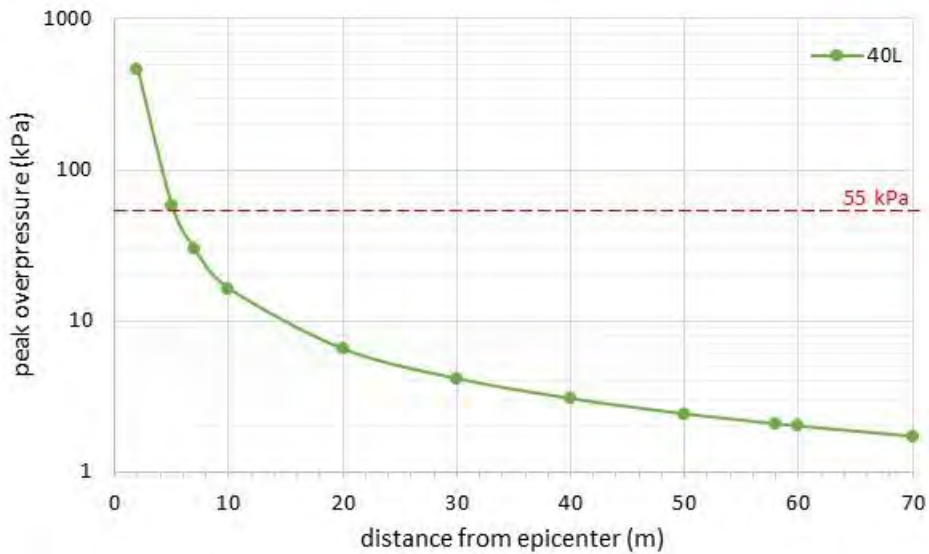
6

8



2 **Figure 23.** Graph of overpressure against distance for HTF volume = 80L

4



6 **Figure 24.** Graph of overpressure against distance for HTF volume = 40L

8 The criteria used for evaluating the chemical explosion’s overpressure are the same as that used
 10 previously for the physical explosion. It can be seen from **Figure 19** to **Figure 23**, overpressures at a
 12 distance of 5 m away from the epicentre were greater than 55 kPa when the volume of HTFs were
 between 80 litres and 300 litres. However, when the HTF volume was at 40 litres, all the
 overpressures at distances of at least 5 m away from the epicentre were about 55 kPa or lower.

Focussing on the 40 litres fluid volume, the comparison of the calculated overpressure against the specific accident deflagration damage indicates that there is some degree of alignment between the actual damage found at the site and the reference overpressures as highlighted in **Table 7**.

4

Table 7. Comparison between calculated chemical explosion overpressure and incident site damage

Incident Site Damage	Calculated peak overpressure (kPa)	Reference overpressure ¹³ (kPa)
Blast hole in wall ≈ 5 m from epicentre	58	50 - 55
Collapsed rear wall ≈ 7 m from epicentre	30	15 - 20
Damaged, buckled roller shutter ≈ 11 m from epicentre	16	7 - 15
Shattered glass windows ≈ 58 m from epicentre	2.1	2 – 3.5

6

From the analysis of overpressures arising from an ignition of aerosolised HTF, it can be deduced that such a scenario could give rise to the damage found at the accident site. In addition to the overpressure, the chemical explosion (deflagration) would also give rise to a flame front which would be consistent with the bright flash, fires and burn injuries observed during the primary explosion event.

12

¹³ Extracted from Appendix F, Table F.2

5 Secondary Flash Fire Analysis

2

In addition to the primary deflagration event that occurred at the accident site, the CCTV videos
4 indicated that up to three other flashes occurred after the initial event. These secondary events were
not accompanied by any evidence of vibrations or sound (bang). Therefore, each of these secondary
6 events were likely to be flash fires that did not generate a corresponding overpressure wave.

8 Apart from the HTF in the mixer, the following materials were used in the Stars Engrg manufacturing
process:

- 10 i. water
- ii. potato starch (powder)
- 12 iii. boric acid (powder)
- iv. bentonite clay (powder)
- 14 v. alumina trihydrate, ATH (powder)
- vi. liquid silicone rubber

16

The relevant flammability and dust combustibility related information for the process materials are
18 listed in **Table 8**.

CONFIDENTIAL

Table 8. Flammability and dust combustibility data for process materials used in mixer

Material	Physical state	NFPA704 rating ¹⁴		Combustible Dust Parameters ¹⁵						
		Fire	Reactivity	BZ	P _{max} (bar)	K _{st} (bar.m/s)	Explosion class	MIT °C	MIE (mJ)	MEC (g/m ³)
potato starch	powder	0	0	2-3	6.5-9.4	19-116	St1	380-520	100 to >1000	15-200
boric acid	powder	0	1	Not available						
bentonite clay ¹⁶	powder	0	0	2	7.7	197	St1	-	-	30-200
alumina trihydrate	powder	0	0	Not available						
liquid silicone rubber	liquid	0	1	Not applicable						

2

From **Table 8**, we can see that potato starch and bentonite clay are the only process material that have the potential to form a combustible dust cloud. The potential for bentonite to cause a combustible dust explosion or fire is not widely known and the only information publicly available on bentonite’s dust combustibility is from the Germany’s GESTIS-DUST-EX Database. The Safety Data Sheet (SDS) of the bentonite clay used by Stars Engrg¹⁷ did not provide any data that would indicate a potential combustible dust hazard. A review of various publicly available SDS for bentonite also did not turn up information that would indicate that bentonite could pose a combustible dust hazard.

10

On the other hand, commonly used starches (e.g. rice, maize, wheat, potato) are generally known to pose a combustible dust hazard. Starches are usually classified as an St1 Class combustible dust but they have large variations in the other dust combustibility parameters.

14

¹⁴ Information obtained from publicly available Safety Data Sheets

¹⁵ Information obtained from NFPA 652 (2019) and GESTIS-DUST-EX Database on Combustion and explosion characteristics of dusts, Institute for Occupational Safety and Health of the German Social Accident Insurance

¹⁶ Dust combustibility data for bentonite clay was obtained from database as “bentonite”. No data available from NFPA 652 (2019).

¹⁷ Furnished by MOM

5.1 Materials sampling and analysis

2

Based on the higher likelihood that the potato starch could contribute to a combustible dust fire or explosion, a number of samples were taken from various surfaces within the Stars Engrg factory unit. The purpose of this sampling was to identify the presence of starch within the workplace. This is because surface accumulations of combustible dust within the factory unit have been known to cause large combustible dust explosions (Giby et al. 2007, Yuan et al. 2015).

8

According to SS 667¹⁸, Clause 8.2.1, where dust accumulates in an area to a sufficient depth such that it obscures the underlying surface colour, that area should be evaluated to ascertain the dust explosion or flash fire hazard. SS 667, Clause F2.2 also specifies a layer depth criterion that in general, dust flash fire or explosion hazards exists in areas where the dust accumulation is greater than 0.8 mm in depth.

14

Sampling of accumulated dust layers has also been described in a number of combustible dust standards including NFPA 652¹⁹. MOM sampled a total of six surfaces and collected three bulk samples from Stars Engrg's factory unit. An additional five raw material samples from Stars Engrg storage area (level 2) were also collected and analysed as comparison for the samples taken from the accident site. The collected samples were then analysed by ICES, A*STAR as listed in **Table 9**. The locations where the sampling was conducted are shown in Appendix G (as provided by MOM).

22

¹⁸ SS 667: Code of practice for the handling, storage and processing of combustible dust.

¹⁹ NFPA 65: 2Standard on the Fundamentals of Combustible Dust.

2

Table 9. Types of analysis conducted on dust layer samples obtained from accident site (Stars Engrg factory unit).

No.	Analysis Type	Analytical Instrument & Method	Purpose
1	CHNS Element Analysis	Thermo Flash 2000 Elemental Analyzer using in-house method	Elemental analysis for the detection of carbon and hydrogen components to indicate the presence of starch
2	SEM/EDX Analysis	FE-SEM - JEOL Scanning Electron Microscope (SEM) JSM-7900F coupled with Oxford Instruments Energy Dispersive Analyzer Coupled with X-Ray Detector (EDS) using Acceleration Voltage of 20.0 kV under low-vacuum as LV-SED mode	Elemental analysis for the detection of inorganics to confirm the presence of ATH, clay and boric acid.
3	SDT Analysis	TA Instruments Q600 SDT using standards ASTM E1131-20 method.	Qualitative detection of organic matter (e.g. starch) via decomposition weight loss
4	FTIR analysis	PerkinElmer Frontier MIR/NIR Spectrometer using pelletised KBr-sample mixture for FTIR (Fourier Transform Infra-Red) analysis and data collected in the range of 4000 to 450 cm^{-1} .	Detection of starch via its characteristic/signature bands within the infra-red spectral range.
5	UV-Vis analysis	PerkinElmer Lambda 950 UV/Vis/NIR Spectrophotometer with sample reacted with $\text{I}_2\text{-KI}$ solution	Qualitative detection of presence of starch
6	Minimum Ignition Energy (MIE)	Chilworth Technology MIE III Cloud apparatus using ISO/IEC 80079-20-2 method	Check the minimum ignition energy of potato starch dust cloud
7	Minimum Ignition Temperature (MIT)	Chilworth Technology MIT Cloud apparatus using ISO/IEC 80079-20-2 method	Check the minimum ignition temperature of potato starch dust cloud

4

2 5.2 Materials testing and analysis results

4 The detailed results from the analytical tests of the nine samples from the Stars Engrg factory unit
and the five bulk samples from storage can be found in **Appendix H** and are summarised in **Table 10**
6 and **Table 11** respectively.

8 Notes for **Table 10** and **Table 11**:

1. CHNS analysis indicates the presence of carbon of hydrogen in the sample.
- 10 2. SEM/EDX analysis shows the elements in order of abundance, semi-quantitative wt%.
3. SEM/EDX uses carbon tape hence elemental carbon is ignored in the analysis and used only
12 to determine presence of aluminium trihydrate (Al as marker), bentonite clay (Si as marker)
and boric acid (B as marker)²⁰.
- 14 4. SDT analysis shows the temperatures for the peak weight loss rates, main followed by
secondary peaks.
- 16 5. FTIR analysis shows the degree of match of sample spectra to the reference potato starch
spectra.
- 18 6. UV/Vis analysis indicates whether the absorbance values exceed the threshold for the blue
colouration as referenced by the potato starch sample.
- 20 7. Aluminium Dihydrogen Phosphate was not used in the manufacturing process, as informed
by MOM.

22

²⁰ Note: Al represents aluminium, Si represents silicon and B represents boron

Table 10. Overview of analytical test results for powder samples taken from the Stars Engrg factory unit

S/N	Sample Description	Exhibit No.	CHNS Element Analysis	SEM/EDX Analysis	SDT Analysis	FTIR analysis	UV-Vis analysis	Conclusion
1	Bulk Point 1	170321-1b	C and H detected	O, C, Al , Si , Ca	280, 230	Inconclusive	Faint	trace starch, ATH and clay
2	Bulk Point 2	170321 -2b	C and H detected	O, C, Al , Si , Ca	280, 230	Inconclusive	Yes	trace starch, ATH and clay
3	Bulk Point 3	170321 -3b	C and H detected	O, C, Al , Si , Ca	280, 230	Inconclusive	Faint	trace starch, ATH and clay
4	Bulk (Under Pallet) 4	170321-4b	C and H detected	O, C, Al , Si , Ca	280, 230	Inconclusive	Faint	trace starch
5	Bulk (Platform) 5	170321-5b	C and H detected	O, C, Al	305	High	Yes	starch and ATH
6	Bulk (Outside Toilet) 6	170321-6b	C and H detected	O, Al , C, Si	280, 310 , 230	Inconclusive	Yes	starch, ATH and clay
7	Bulk	250221-1 b	C and H detected	C, O	305	High	Yes	starch present
8	Bulk (Bulk Bag Left)	080321-1 b	H detected	O, Al , C, Si	280, 230	Inconclusive	No	ATH and clay (starch NOT present)
9	Bulk (Bulk Bag Right)	080321-2b	C and H detected	O, C, Al , Si	310 , 230	Inconclusive	Yes	Starch, ATH and clay

Table 11. Overview of analytical test results of raw material samples taken from Stars Engng storage (level 2).

S/N	Sample Description	Exhibit No.	CHNS Element Analysis	SEM/EDX Analysis	SDT Analysis	FTIR analysis	UV-Vis analysis	Conclusion
10	Bulk (Aluminium Hydroxide)	080321-3b	H detected	O, Al, C	280, 230	Low	No	Not applicable
11	Bulk (Potato Starch)	080321-4b	C and H detected	O, C	305	Reference	Yes	Not applicable
12	Bulk (Aluminium Dihydrogen Phosphate)	170321-7b	H detected	O, P, C, Al	245 & 520	Low	No	Not applicable
13	Bulk (Boric Acid)	170321-8b	H detected	O, B, C	130	Low	No	Not applicable
14	Bulk (Clay)	170321-9b	C and H detected	O, Si, C, Al, Na, Mg, Ca, Fe, K	60, 660	Low	No	Not applicable

CONFIDENTIAL

In order to conclude the presence of starch in the samples, four out of the five different methods (i.e. CHNS, SDT, FTIR and UV/Vis) were considered as a whole. In particular, comparisons were made with the raw material samples taken from Stars Engrg's storage. In order to conclude at least the trace presence of starch, at least three out of the four analytical methods should be positive for starch. The criteria used for each of the analytical methods is as follows:

- i. CHNS Analysis – Carbon and hydrogen present
- ii. SDT Analysis – Rate of mass loss peak at about 305 °C
- iii. FTIR Analysis – Detection of at least three out of the five characteristic infra-red bands associated with the reference potato starch sample
- iv. UV/Vis Analysis – Detection of absorbance for blue colouration within the wavelength band of 400 to 800 nm.

The analytical results shown in **Table 10** shows that starch is present in at least trace quantities on all of the surfaces sampled²¹ in the immediate vicinity of the mixer. In addition, the bulk sample obtained on the raised platform (Exhibit 250221-1b) clearly indicated the presence of starch. Of the two bulk samples obtained on the ground floor close to the mixer, one of the samples (Exhibit 080321-2b) also indicated the presence of starch.

These results indicate that potato starch residues were present in various locations and surfaces throughout the Stars Engrg factory unit. These potato starch residues point to the likelihood that prior to the accident, significant quantities of potato starch may have accumulated on various surfaces throughout the factory unit. It is also highly likely that there was significant accumulation of potato starch powder on the surfaces of the raised platform.

In addition to the analytical tests conducted to ascertain the presence of starch on the surfaces within the working environment, the bulk sample of potato starch (Exhibit: 080321-4b) was also tested for

²¹ Exhibits 170321-1b, 170321 -2b, 170321 -3b, 170321-4b, 170321-5b and 170321-6b

its Minimum Ignition Energy (MIE) and Minimum Ignition Temperature (MIT) as a check against the
2 published values. The moisture content (LOD²²) of the potato starch as received was 18.95 wt%. The
MIE test results indicated that the potato starch did not ignite at spark energies up to 683 mJ.
4 Additional tests conducted on three different brands of commercially available potato starch also did
not shown any ignitions of the dust cloud up to 683 mJ. On the other hand, the MIT tests conducted
6 found that the potato starch sample ignited at a temperature of 422 °C. This ignition temperature
lies within the MIT data range for potato starch shown in **Table 8**.

8

In order to check the combustibility of bentonite clay, MIE and MIT tests were also conducted on the
10 sample obtained from Stars Engrg storage (level 2) i.e. Exhibit 170321-9b. There were no ignitions
observed for the bentonite clay dust cloud at spark energies up to 683 mJ and temperatures up to
12 900 °C.

²² Loss on Drying

6 Discussion

2

This technical investigation into the accident at Stars Engrg utilised various methods to gather evidence in order to find out the cause of the fires and explosion that occurred on 24 Feb 2021 at about 11.22 am as listed below:

6

- i. Review of CCTV video clips to ascertain chain of events.
- 8 ii. FEA to ascertain the heat transfer behavioural trends of the mixer's heating jacket's surface and the HTF within the heating jacket.
- 10 iii. Analysis of the HTF characteristics under elevated temperatures via DSC, SDT and Pressure-Temperature tests.
- 12 iv. Estimation of explosion overpressure and comparison with actual damage at the incident site to ascertain the likely mechanism (physical or chemical) of the primary deflagration event.
- 14 v. Analytical testing (CHNS, SEM/EDX, SDT, FTIR and UV/Vis) of samples in the immediate vicinity of the incident site to determine the presence of potato starch as a potential combustible dust hazard that could have caused the secondary deflagration event or flash fire.
- 16

18 The CCTV video clips revealed that there was a large primary deflagration that was accompanied with significant overpressures as evidenced by vibrations and movement of objects seen in the video clips
20 as well as the extent of damage observed on site after the accident. The vibrations were evidenced by the shaking of the CCTV cameras (i.e. Cameras 3 and 4), and flying debris were recorded by
22 Cameras 5 and 6. Although Camera 6 was damaged by the accident, from the intact portions of the video clip, it was possible to observe that the overpressures of the primary deflagration were severe
24 enough to cause the dislodging and translation of large metal sheets on to the driveway of the industrial complex as shown in **Figure 25**. In addition, Camera 1 also recorded the toppling of a
26 dustbin whilst Camera 8 showed ladders being shaken during the primary deflagration event.

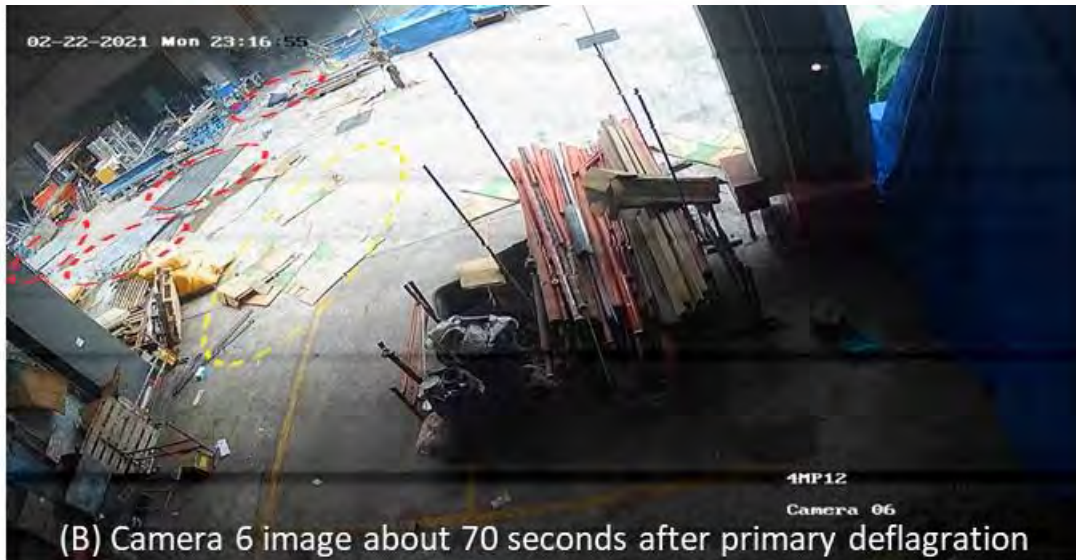
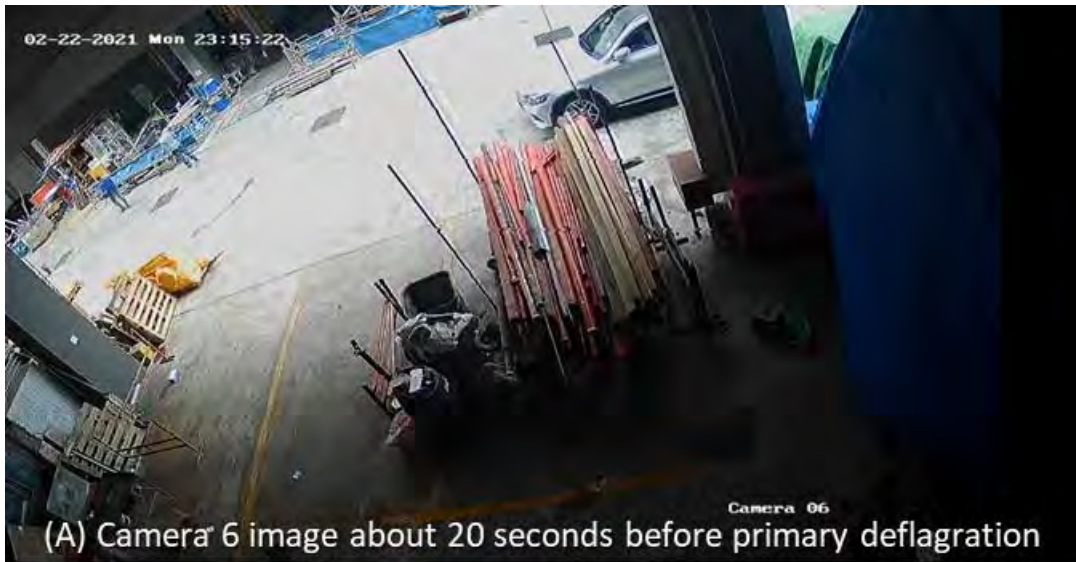


Figure 25. Images from CCTV Camera 6 showing the translation of large metal and cardboard sheets

- 2 After this primary deflagration, the CCTV video clips also indicated that there were up to three
- secondary deflagration events as recorded by Cameras 7 and 8 at about 85 seconds, 125 seconds and
- 4 155 seconds after the primary deflagration event. However, these secondary deflagration events
- were not accompanied by any observable signs of overpressure. It is likely that these secondary
- 6 deflagrations manifested as flash fires.

1 An inspection of the incident site on 9 March 2021 provided information on the physical damage
2 caused by the accident, and in particular the damage experienced by the mixer located on the raised
platform. A schematic diagram indicating the location of the damage in relation to the suspected
4 epicentre of the explosion (i.e. the mixer) is shown in **Figure 15**. Based on the extent of physical
damage observed at the accident site and the evidence from the CCTV cameras, it can be deduced
6 that the primary deflagration event was an explosion centred at the mixer which generated
overpressures high enough to cause significant physical damage at distances up to approximately
8 508 m. It can be further deduced that following this primary deflagration, there were up to three
further deflagrations that likely manifested as flash fires with negligible overpressures.

10

The next step taken was to study how the primary deflagration event could have occurred. The first
12 step taken was to understand how the mixer could have sustained the damage to its heating jacket.
A FEA modelling of the mixer with HTF inside the heating jacket was done to study the factors that
14 could potentially lead to the rupture of the heating jacket. The FEA results showed that when a total
of 45 kW of heat (corresponding to the total heat source from the mixer's nine heaters) was
16 introduced into the system, the HTF within the heating jacket could reach temperatures ranging from
427 °C to 715 °C under moderate convection conditions within the mixing chamber. The FEA
18 simulations also showed that under the various thermal conditions studied, the temperatures around
the bottom of the heater, closest to the heating elements tends to be highest. These results are
20 supported by a picture obtained from MOM (**Figure 26**) that showed a bright glow around the flanges
of one of the heating element taken on 24 February at 8.45 am (before incident) by one of the
22 workers at the Stars Enrg factory unit.



2 **Figure 26.** Image showing glowing flange connection of one of the mixer’s heating element

4 When steel is heated in air, the oxide film on the surface of the hot steel gives off a glow with a range
 6 colours which is characteristic of the surface temperature (Canale et al. 2014). **Table 12** below
 6 provides the temperatures associated with the different colours of the oxide surface of steel.

8 **Table 12.** Characteristic colour – temperature relationship of the surface oxide film on steel

Colour of surface oxide film	Characteristic temperature (°C)
Faint yellow	238
Light straw	265
Dark straw	293
Brown	321
Purple	337
Dark blue	349
Light blue	376

Based on the values given in **Table 12**, the temperatures around the glowing flange in **Figure 26**
2 should be in excess of 250 °C.

4 Another trend observed from the FEA simulations is that the temperature of the HTF increases as the
fill volume in the heating jacket decreases. There is evidence provided by MOM that the mixer's
6 heating jacket was operated with very low volumes of the HTF. I am instructed by MOM that the
maximum fill volume used at any time would have been between 40 litres and 160 litres.

8

Overall, based on the FEA simulations, we can deduce that the temperature of the HTF (i.e. Idemitsu
10 Daphne Thermic 32-S oil) within the mixer's heating jacket could have exceeded its normal operating
temperature of up to 300 °C with lower fill volumes leading to higher temperatures. In addition,
12 surfaces near the flanges of the heating elements could also exceed the design temperature of the
mixer which is rated up to 200 °C.

14

Since the FEA simulations showed that the HTF could reach temperatures above its flash point (220
16 °C) and operating temperature (300 °C), we proceeded to study how such elevated temperatures
affected the HTF. The DSC, SDT tests on the HTF samples indicated that the fluid showed significant
18 decomposition at a temperature range from 280 °C to 321 °C. It was also observed that for used HTF,
the onset of this decomposition occurred at a slightly lower temperature starting from 216 °C
20 compared to 227 °C for the fresh Idemitsu Daphne Thermic 32-S oil.

22 In terms of its pressure-temperature behaviour, the pressure exerted by the HTF in a closed system
increased linearly up to around 320 °C. At around 350 °C, it was observed that there was a significant
24 pressure increase of around 6 barg and when the temperature was increased further up to 450 °C, a
larger pressure increase of up to 103 barg was observed. Such pressures are far in excess of the
26 mixer's maximum working pressure of 2 barg.

CONFIDENTIAL

1 The likelihood of such elevated temperatures and pressures within the mixer's heating jacket could
2 therefore have led to the failure and rupture of the heating jacket. This sudden pressure release could
3 result in either a physical or chemical explosion. Estimates of overpressure for a purely physical
4 explosion arising only from compressed gas energy release would generate overpressures ranging
5 from 0.3 kPa to 17 kPa. These overpressures are much lower than the actual damage observed at the
6 accident site which should be in the range of 2 to 55 kPa.

8 Alternatively, the sudden release of high temperature HTF from the heating jacket could lead to the
9 formation and ignition of an aerosol. Estimates of overpressures generated from such a chemical
10 explosion ranged from 2.1 kPa to 58 kPa. Such overpressures are in alignment with the expected
11 overpressures of the actual damage at the accident site which should range from 2 to 55 kPa. In
12 addition, such a chemical explosion (deflagration) would also give rise to a flame front which would
13 be consistent with the bright flash, fires and burn injuries observed during the primary explosion
14 event. Such a flame front would not be generated from a purely physical explosion.

16 Following the initiation of the primary deflagration event, up to three secondary deflagrations were
17 likely to have occurred over an approximately three minute period. These secondary deflagrations
18 were probably in the form of flash fires with negligible overpressures generated. The most likely
19 combustible material present in the workplace that could have contributed to the secondary
20 deflagrations would be potato starch as it was one of the main ingredients used in the product being
21 manufactured by Stars Engrg at the factory unit. Samples taken from various surfaces within the
22 accident site were analysed for the presence of starch as accumulations of combustible powders in
23 workplaces have been known to cause large combustible dust fires and explosions. The results of the
24 analyses show that at least trace amounts of potato starch were found on all the surfaces within Stars
25 Engrg factory unit with the raised platform showing the most significant presence of potato starch.

26

27 The presence of residual potato starch points to the likelihood that prior to the accident, there had
28 been significant accumulation of potato starch within the workplace. The primary deflagration event
generated overpressures that could suspend the potato starch layers that have accumulated on

CONFIDENTIAL

- various surfaces. The suspended potato starch dust could then be ignited by the fires that were
- 2 initiated by the primary deflagration event which then resulted in a secondary deflagration/flash fire.
- This process of dust suspension could be repeated a number of times after each deflagration/flash
- 4 fire, thus resulting in the three flash fires that occurred.
- 6 The overall flow diagram showing the likely sequence of events is shown in **Figure 27**.

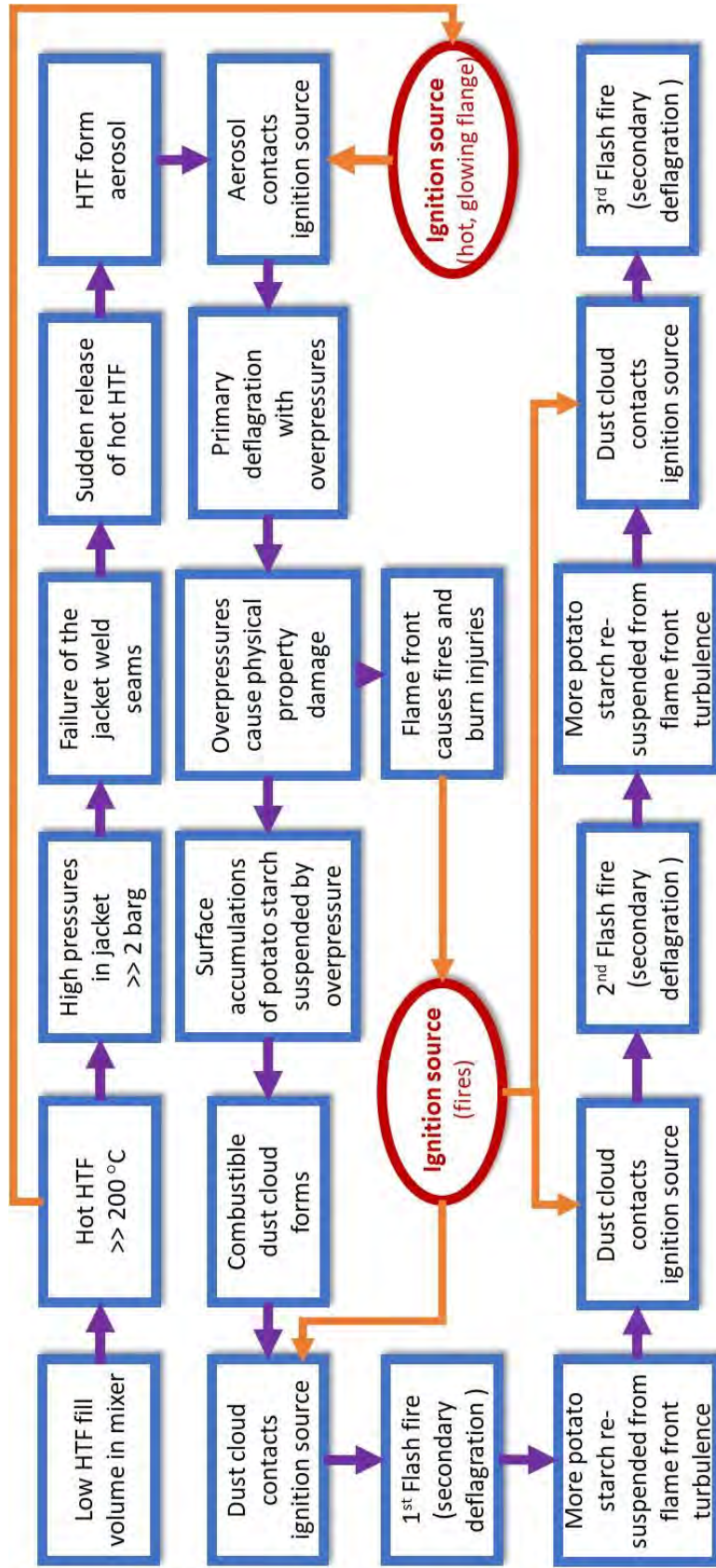


Figure 27. Overview of the likely sequence of events that resulted in the primary and secondary deflagrations at Stars Engr.

7 Conclusion

2

The root-cause of the incident on 24 February 2021 at Stars Engrg was likely due to the low amounts
4 of HTF used in the mixer. There was evidence that the mixer's heating jacket had a low fill volume (a
maximum of 160 litres at any point in time) of the required HTF. FEA simulations indicated that low
6 levels of HTF (i.e. less than 220 litres) within the heating jacket results in higher temperatures for the
HTFs and the heating jacket surfaces. The elevated temperature of the HTF will cause a build-up in
8 the pressure within the heating jacket since, as informed by MOM, the ports/pipes on the heating
jacket were sealed shut when the mixer was in operation, which would have resulted in a closed
10 system. This increase in pressures were confirmed by the pressure-temperature tests conducted on
the HTF which resulted in pressures ranging from 6 to 103 barg. The high pressures then caused the
12 mixer's heating jacket which was rated to operate at pressures less than 2 barg, to rupture abruptly
thus releasing the hot, pressurised HTF into the environment.

14

This pressurised release likely atomised the HTF to form a liquid aerosol. This aerosol or mist
16 containing very fine droplets of combustible liquid was then probably ignited by a hot surface. The
ignition source may have been any heated surface, including the hot glowing flange observed at 8.45
18 am on 24 February 2021 shown in **Figure 26**, which may have recurred if the mixer was restarted
later in the morning. The ignited aerosol cloud resulted in the primary deflagration event comprising
20 of a flame front with estimated overpressures in the range of 2.1 kPa to 58 kPa at distances of
between 58 m to 5 m respectively. These overpressures from the primary deflagration were sufficient
22 to cause physical damage which included a collapsed rear wall, a punctured side wall, large flying
debris (e.g. metal sheets) and shattered glass windows.

24

This primary deflagration event was followed by up to three secondary deflagrations in the form of
26 flash fires. These flash fires were likely the result of potato starch accumulation in the Stars Engrg
factory unit that were initially agitated and suspended by the overpressure from the primary
deflagration to form a combustible dust cloud. This combustible dust cloud was probably ignited by
28 the fires that were also initiated by the primary deflagration. As the flash fire proceeded through the

CONFIDENTIAL

combustible dust cloud, the turbulence generated could then re-suspend more potato starch that
2 then triggered the other two secondary deflagrations or flash fires.

References

- ASTM (2020). Standard Test Method for Compositional Analysis by Thermogravimetry. ASTM E1131-20, ASTM International.
- (2021). GESTIS-DUST-EX Database on Combustion and explosion characteristics of dusts, Institute for Occupational Safety and Health of the German Social Accident Insurance.
- Bowen, P. J. and L. C. Shirvill (1994). "Combustion hazards posed by the pressurized atomization of high-flashpoint liquids." *Journal of Loss Prevention in the Process Industries* 7(3): 233-241.
- Canale, L. C. F., J. Vatauvuk, et al. (2014). 12.02 - Introduction to Steel Heat Treatment. *Comprehensive Materials Processing*. Oxford, Elsevier: 3-37.
- Crowl, Daniel A. *Understanding explosions*, Vol. 16 (2010). John Wiley & Sons.
- Crowl, Daniel A., and Joseph F. Louvarm (2001). *Chemical process safety: fundamentals with applications*. Pearson Education.
- Febo, H. and J. Valiulis (1995). Heat transfer fluid mist explosion potential an important consideration for users. *Proceedings of the AIChE Loss Prevention Symposium*, Norwood, MA.
- Grossel, S. S. (2013). *Guidelines for Evaluating Process Plant Buildings for External Explosions, Fires, and Toxic Releases*, CCPS, John Wiley & Sons.
- Hadgu, T., S. W. Webb, et al. (2004). Comparison of CFD Natural Convection and Conduction-Only Models for Heat Transfer in the Yucca Mountain Drifts. *Heat Transfer Summer Conference*.
- Joseph, G. and C. H. I. Team (2007). "Combustible dusts: A serious industrial hazard." *Journal of Hazardous Materials* 142(3): 589-591.
- Krishna, K., T. Kim, et al. (2001). Understanding the formation of heat transfer fluid aerosols in air. *Proceedings of the 4th Annual Mary Kay O'Connor Process Safety Center Symposium—Beyond Regulatory Compliance: Making Safety Second Nature*, College Station, Texas.
- Krishna, K., W. J. Rogers, et al. (2003). "The use of aerosol formation, flammability, and explosion information for heat-transfer fluid selection." *Journal of Hazardous Materials* 104(1): 215-226.
- Kumar, Ashok (1994). *Guidelines for evaluating the characteristics of vapor cloud explosions, flash fires, and BLEVEs*. Center for Chemical Process Safety (CCPS).
- Lees, Frank. *Lees' Loss prevention in the process industries: Hazard identification, assessment and control*, Volume 2 (2012). Butterworth-Heinemann, 2012.

CONFIDENTIAL

Lian, P., A. F. Mejia, et al. (2010). "Flammability of heat transfer fluid aerosols produced by electrospray measured by laser diffraction analysis." *Journal of Loss Prevention in the Process Industries* 23(2): 337-345.

Maragkos, A. and P. J. Bowen (2002). "Combustion hazards due to impingement of pressurized releases of high-flashpoint liquid fuels." *Proceedings of the Combustion Institute* 29(1): 305-311.

NFPA (2019). *Standard on the Fundamentals of Combustible Dust*. NFPA 652, National Fire Prevention Association.

Robles, J., C. Bajwa, et al. (2009). *A Comparative Analysis of Natural Convection Modeling Methods in a Horizontal Annulus and Its Application to Spent Nuclear Fuel Transfer Operations-9206*. New York.

Samirant, M. (1999). *Dispersion-initiation and detonation of liquid and dust aerosols-experiences derived from military fuel-air explosives*. *Prevention of Hazardous Fires and Explosions*, Springer: 123-134.

Santon, R. (2009). *Mist fires and explosions-an incident survey*. *Proc. IChemE Hazards XXI Symposium & Workshop*.

SSC (2020). *Code of practice for the handling, storage and processing of combustible dust*. SS 667, Singapore Standards Council.

Yuan, S., C. Ji, et al. (2021). "A review of aerosol flammability and explosion related incidents, standards, studies, and risk analysis." *Process Safety and Environmental Protection* 146: 499-514.

Yuan, Z., N. Khakzad, et al. (2015). "Dust explosions: A threat to the process industries." *Process Safety and Environmental Protection* 98: 57-71.

Appendices

Appendix A: Observations log of significant events from CCTV video clips

Appendix B: Finite Element Analysis (FEA) modelling conducted on mixer

Appendix C: Differential Scanning Calorimetry (DSC) - testing of heat transfer fluid

Appendix D: Simultaneous DSC-TGA (SDT) - testing of heat transfer fluid

Appendix E: Pressure – temperature analysis of heat transfer fluid

Appendix F: Explosion calculations – estimation of overpressures

Appendix G: Dust layer and HTF sampling locations

Appendix H: Details of CHNS, SEM/EDX, SDT, FTIR and UV-Vis analysis - testing of solid powder samples

Contact us:

Shaik Salim

Institute of Chemical & Engineering Sciences

Principal Specialist

Tel: 67963950 / 98285341

shaik_salim@ices.a-star.edu.sg

Norhazry Johari

Institute of Chemical & Engineering Sciences

Director Business Development

Tel: 67963871

Norhazry_Johari@ices.a-star.edu.sg



CREATING GROWTH, ENHANCING LIVES

Mission | We advance science and develop innovative technology to further economic growth and improve lives.

Vision | A global leader in science, technology and open innovation.

Appendix A: Observations log of significant events from CCTV video clips

Timestamp	Original	22 Feb 2021	23:15:40	23:15:41	23:15:42	23:15:49	23:15:52	23:16:41	23:16:48	23:16:54	23:16:55	23:17:05	23:17:29	23:17:34	23:17:45	23:18:15	23:18:17	23:19:45
	Adjusted	24 Feb 2021	11:22:28	11:22:29	11:22:30	11:22:37	11:22:40	11:23:29	11:23:36	11:23:42	11:23:43	11:23:53	11:24:17	11:24:22	11:24:33	11:25:03	11:25:05	11:26:33
No.	Location																	
CAMERA 1	level 3 FCD - lift lobby				pressure wave - dustbin topples		metal sheet behind dustbin falls over and fire alarm is activated											
CAMERA 2	level 3 FCD – rear corridor				pressure wave, black smoke													
CAMERA 3	level 2 office - front/driveway facing			bright flash and vibration, short duration (≈1s)					smoke outside window, office lady runs away from window									
CAMERA 4	level 2 office – rear facing			vibration, pressure wave						lady running to exit								
CAMERA 5	level 1 -external, driveway facing		glow observed on the left of the camera	bright flash, short duration (≈1s), flying debris		black smoke				black smoke			lady opens exit door	burn victim seen			worker opens exit door	grey smoke seen, small dropping debris
CAMERA 6	level 1 external driveway facing (damaged)		bright flash, followed by video loss, driveway clear															
CAMERA 7	level 1- main entrance			bright flash, short duration (≈1s), small flying debris				lighter coloured dust/ smoke seen										bright flash
CAMERA 8	level 1 - rear entrance			bright flash, short duration (≈1s), pressure wave - ladders move, followed by black smoke		black smoke						thick black smoke/cloud followed by flash			thick black smoke/cloud followed by flash			

Appendix B: Finite Element Analysis (FEA) modelling conducted on mixer

2

B.1. Modelling Method

4 The meshed mixer structure as shown in **Figure B.1** was composed of approximately 90,000 hex-
dominated elements across three layers with an average length of 12mm. Meanwhile, the heat
6 transfer fluid within the heating jacket was modelled as a mesh comprising of about 1.26 million
tetrahedral elements. The meshed elements for the heat transfer fluid is shown in **Figure B.2**.

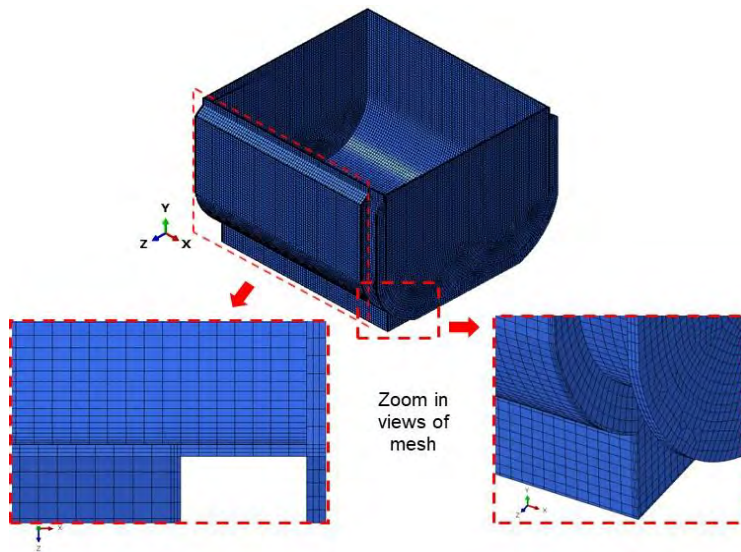


Figure B.1. FEA mesh for mixer structure

10

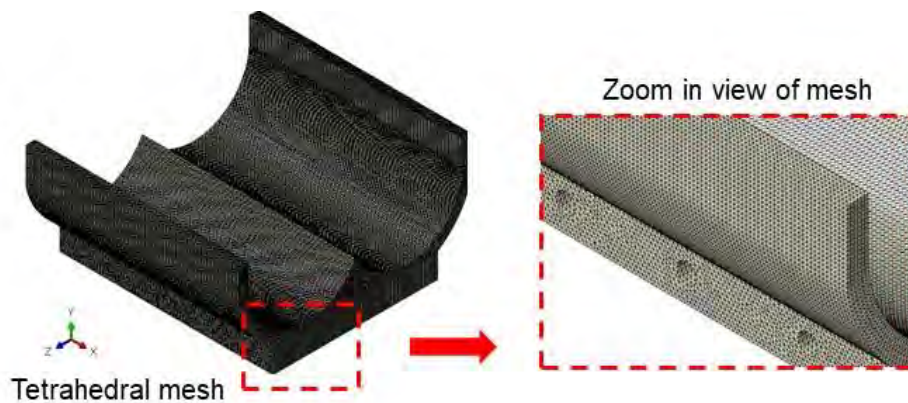


Figure B.2. FEA mesh for heat transfer fluid within the jacket

The Equivalent Thermal Conductivity (k_{eq}) Method (Febo and Valiulis 1995, Hadgu et al. 2004) was used to model heat flow in the heat transfer fluid (HTF). This method consists of determining a value of thermal conductivity that would allow the same amount of heat transfer as natural convection would. The equivalent thermal conductivity is defined as:

$$k_{eq} = \frac{Q_{cond+conv(HTF)}}{Q_{cond(HTF)}}$$

The effective thermal conductivity, k_{eff} , models natural convection by specifying an enhanced thermal conductivity for use in a conduction-only model:

$$k_{eff} = k_{eq} \times k_{HTF}$$

Since Q_{conv} tends to be much larger than Q_{cond} , and both thermal conductivity (k) and heat transfer coefficient (h) are positively related to Q , therefore:

$$\frac{Q_{conv}}{Q_{cond}} \propto \frac{h}{k} = k_{eq}$$

Based on typical literature values¹ the heat transfer coefficient of the fluid, h_{HTF} (natural convection) ranges from 50 to 600 W/m²K. Therefore for the purposes of this FEA analysis, we assume three values of $k_{eff} = 50$ W/mK, 200 W/mK and 600 W/mK to simulate the typical lower and upper bounds for the heat transfer fluid. This heat load condition is more realistic as there will be a temperature distribution along the mixer surface instead of assuming it to have a uniform heat flux.

Further, surface heat flux is applied at the heating element tube surfaces to conduct heat to the heat transfer fluid before reaching the mixer surfaces. Using this equivalent conductivity method, the convection phenomena is thus simplified into an equivalent conduction term to calculate the total heat transfer. This method is advantageous as it provides a quick and simplified way of

¹ https://www.engineersedge.com/thermodynamics/overall_heat_transfer-table.htm and <https://www.thermopedia.com/content/841/>

calculating heat transfer. However, it should be noted that localized and fluid flow effects may not be fully represented by this modelling approach.

B.2. Material Properties

Table B.1. Material properties used for FEA simulations

Component	Density (kg/m ³)	Thermal Conductivity (W/mK)	Specific Heat (J/kgK)	Comment
Mixer	8000	19.2	500	Stainless steel: SS304 and SS316 have similar properties
	7840	54		Carbon steel: properties of LCS and MCS are not significantly different*
Heat Transfer Fluid	800	k _{eff} = 50, 200, 600	9734.3	Daphne Alpha Thermo 32, High Performance Heat Transfer Oil information obtained from product information sheet

Note: *Thermal-jacket is made of carbon steel i.e. low carbon steel (LCS) or medium carbon steel (MCS). Based on typical values^{2,3} of LCS and MCS:

- Density of LCS \approx 7833 kg/m³ and MCS \approx 7801 kg/m³ (i.e. 0.4% difference)
- Thermal conductivity: k_{LCS} \approx 58.5 W/mK and k_{MCS} \approx 52 W/mK (i.e. 11.8% difference)

B.3 Boundary and Load Conditions

Based on relative CAD dimensions, the heating tube diameters are assumed to be 50 mm. The “NH Sigma Kneader User Guide” obtained from MOM indicated that the heat source had “A heating power of 800 W, a total of three.” This was taken to mean that each heating element provided 800 W of heat into the system. Hence, it was initially assumed that the heat source for the mixer was:

- 800W x 9 tubes = 7.2 kW (Total)

² https://www.engineersedge.com/properties_of_metals.htm

³ <http://www.matweb.com/>

2 Subsequently, investigations revealed that each heating element unit had a power rating of 5 kW
as shown in **Figure B.3** below. Hence, FEA simulations were also conducted to study the effects
4 of a higher heat load on the mixer system.



6 **Figure B.3.** Photograph of heating element of the NH Sigma Kneader taken by Matcor

8
With regards to the internal contents of the mixer, MOM had instructed that just prior to the
10 incident, the workers had started working on a new batch by introducing water into the mixing
chamber. Hence, for the liquid contents within the mixing chamber, the following heat transfer
12 coefficients^{4,5} were applied to the mixer's inner surface to take into account three different
scenarios:

- 14 i. Low heat transfer: $h = 5 \text{ W/m}^2\text{K}$ (air natural convection, i.e. empty and no rotation/agitation)
- 16 ii. Moderate heat transfer: $h = 50 \text{ W/m}^2\text{K}$ (water natural convection i.e. liquid with no rotation/agitation)
- 18 iii. High heat transfer: $h = 500 \text{ W/m}^2\text{K}$ (water forced convection, i.e. liquid with rotation/agitation)

20

⁴ <https://www.thermopedia.com/content/841/>

⁵ https://www.engineersedge.com/heat_transfer/convective_heat_transfer_coefficients__13378.htm

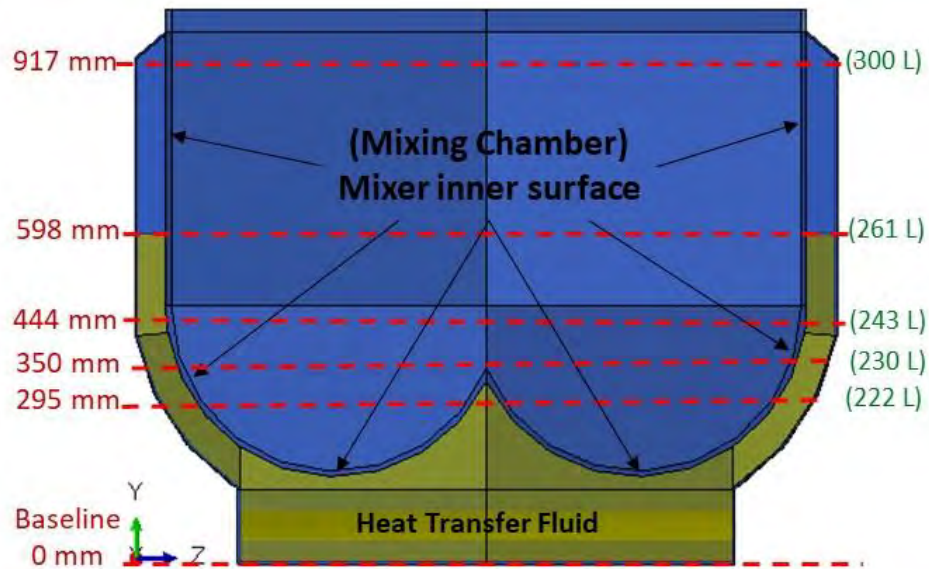
B.4. Modelling assumptions

2 In addition to the material properties and boundary conditions stated, the following assumptions
were used in the FEA modelling:

- 4 i. Assume steady state heat transfer during operational conditions.
- 6 ii. Effective k (k_{eff}) approach used to model convective flow of HTF within heating jacket
enclosure.
- 8 iii. Assume that heat from heating tube is uniformly dissipated/transferred to the HTF that
in turn is fully transferred to the mixer internal surface, under steady state.
- 10 iv. Assume perfect heat conduction of the interfaces (e.g. between HTF and mixer).
- 12 v. Assume constant heat transfer coefficient for mixer exterior surfaces (i.e. no insulation).
- vi. Assume different volumes of heat transfer fluid within the heating jacket (see details
below).

14 *B.4.1. Quantity of heat transfer fluid*

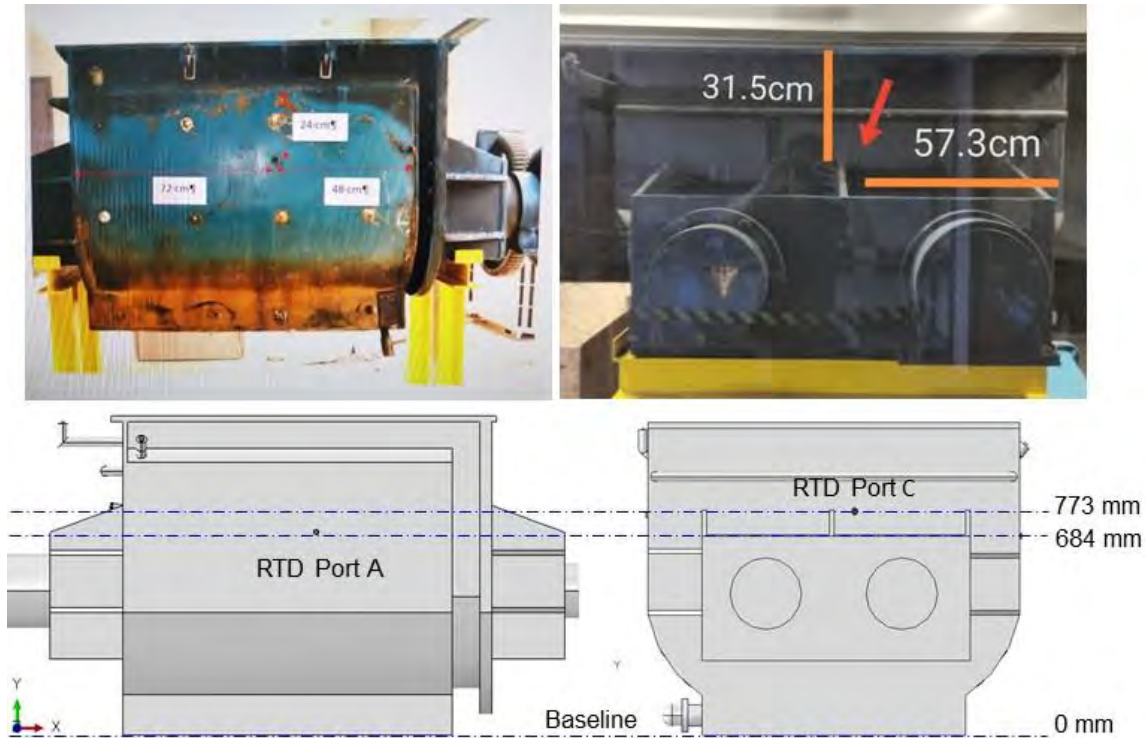
Since the amount of heat transfer fluid within the mixer's heating jacket is not definitively known,
16 the FEA modelling used several reference points to simulate the effects of varying amounts of
fluid. Several arbitrary liquid levels were defined for the model that corresponds with varying
18 heat transfer fluid fill volumes as shown in **Figure B.4** below. The liquid levels (in mm) accounts
for both the heat transfer fluid volume as indicated in **Figure B.4** and the volume displaced by the
20 heating elements' tubes which was assumed to be about 5.3 litres.



2 **Figure B.4.** Variation of heat transfer fluid volumes and their corresponding levels within the heating
 jacket.

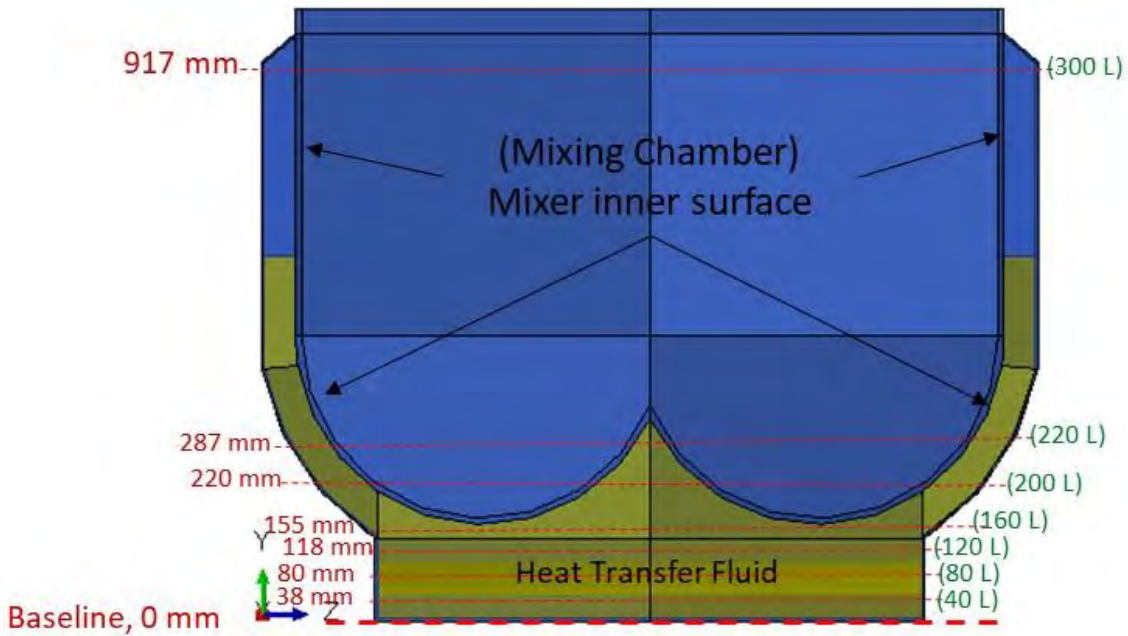
4

In addition to the fluid levels shown in **Figure B.4**, heat transfer fluid levels that were aligned with
 6 the positions of RTD sensor ports available in the mixer's heating jacket were also considered.
 The positioning of the RTD sensor ports were provided in Matcor's CAD drawing of the mixer
 8 provided by MOM and illustrated in **Figure B.5** below.



2 **Figure B.5.** Positions of RTD sensor ports A and C for the mixer's heating jacket

4 Apart from these levels, based on information provided by MOM, the amount of heat transfer
 6 fluid added into the jacket by the workers from Stars Engrg could range from 40 litres to 160
 8 litres. A fill volume of 160 litres would result in a fluid level of 155 mm as illustrated **Figure B.6**
 below. Meanwhile, a fill volume of just 40 litres (32 kg of heat transfer fluid) would result in a
 fluid level that is only 38 mm above the base of the mixer's heating jacket as illustrated in **Figure**
B.6 below.



2 **Figure B.6.** Low heat transfer fluid volumes within the mixer’s jacket

4 At fill volumes of about 220 to 40 litres, the heat transfer fluid will not be fully in contact with the
 6 mixer’s inner surface. This would result in low heat transfer to the mixing chamber. In such a
 8 situation, the temperature of the heat transfer fluid will be expected to be very high and would
 likely result in phase changes with vapours accumulating in the void space above the HTF level.
 Since phase change and latent heat models have not been included in the current FEA modelling,
 HTF volumes less than 222 litres were therefore not simulated.

10

B.5. FEA analysis results

12

Table B.2. High convection at mixer’s inner surface ($h=500 \text{ W/m}^2\text{K}$) and total heat source = 7.2 kW

Effective thermal conductivity (k_{eff})	50 W/mK	200 W/mK	600 W/mK	Notes
HTF Level (mm)				
295	66	50	45	222 L HTF fill volume
444	66	49	43	243 L HTF fill volume
598	66	49	43	261 L HTF fill volume
917	66	49	43	300 L HTF fill volume

14

2 **Table B.3.** Moderate convection at mixer's inner surface ($h=50 \text{ W/m}^2\text{K}$) and total heat source = 7.2 kW

Effective thermal conductivity (k_{eff})	50 W/mK	200 W/mK	600 W/mK	Notes
HTF Level (mm)				
295	140	112	104	222 L HTF fill volume
350	139	104	94	230 L HTF fill volume
444	136	104	93	243 L HTF fill volume
598	135	100	87	261 L HTF fill volume
917	135	98	81	300 L HTF fill volume
684	138	101	88	RTD sensor port position (A)
773	138	101	88	RTD sensor port position (C)

4

Table B.4. Low convection at mixer's inner surface ($h=5 \text{ W/m}^2\text{K}$) and total heat source = 7.2 kW

Effective thermal conductivity ($k_{\text{HTF,eff}}$)	50 W/mK	200 W/mK	600 W/mK	Notes
HTF Level (mm)				
295	353	309	298	222 L HTF fill volume
350	313	259	243	230 L HTF fill volume
444	332	280	262	243 L HTF fill volume
598	320	258	236	261 L HTF fill volume
917	314	237	208	300 L HTF fill volume
684	298	228	204	RTD sensor port position (A)
773	296	224	198	RTD sensor port position (C)

6

8 **Table B.5.** Comparison of FEA simulations using heat sources = 7.2 kW and 45 kW, Fill volume =230 L

Effective thermal conductivity, k_{eff} (W/mK)	Mixer inner surface convection		h=50 W/m ² K	
	h=5 W/m ² K	45kW	7.2kW	45kW
50	313	1801	139	714
200	259	1464	104	494
600	243	1365	94	427

10

**Appendix C: Differential Scanning Calorimetry (DSC) -
Testing of Heat Transfer Fluid**

REPORT

REPORT REFERENCE: ICES/AC/21013_Part5 **DATE:** 20th Apr 2021

SUBJECT: DSC Analysis for oil samples

COMPANY: ICES, A*STAR
1, Pesek Road, Jurong Island,
Singapore 627833

ATTENTION: Dr. Shaik Salim

DATE SAMPLE RECEIVED: 8th Apr 2021

DATE ANALYSED: 16th Apr 2021

DATE TEST COMPLETED: 20th Apr 2021

DESCRIPTION OF SAMPLE(S):

2 liquid oil samples (~ 500ml) were received.

S/N	Sample Description	Exhibit No.
1	Liquid	250221-2b
2	Daphne Thermic Oil 32 (20L)	-

METHOD OF TEST:

The two samples were analysed as received with Mettler Toledo Differential Scanning Calorimeter (DSC) 3 using inert N₂ gas purge and high-pressure stainless steel crucibles (30µl).

Test condition: Heat from -50°C to 250°C, ramp rate 10°C/min

Cool down from 250°C to -50°C, ramp rate 10°C/min

Heat from -50°C to 250°C, ramp rate 10°C/min

RESULTS:

S/N	Sample Description	Exhibit No.	Temperature, °C	Status	Reference
1	Liquid	250221-2b	-21.49	Crystallisation Point	Fig 1
2	Daphne Thermic Oil 32 (20L)	-	-17.28	Crystallisation Point	Fig 2

TESTED BY:

Mr. Yeo Wen Cong
Senior Research Engineer

APPROVED BY:

Mr. Andrew Lim
Team Leader
Analytics & Characterisation
Scientific Infrastructure & Analytics

Note: This report shall not be reproduced except in full, without written approval from ICES. This report does not constitute an endorsement of any item or material tested and must not be used for any publicity materials, and/or for advertising purposes without approval from ICES. Test results relate only to sample(s) submitted by the client for technical studies and shall not be used for any purpose of technical litigation.

Figure 1

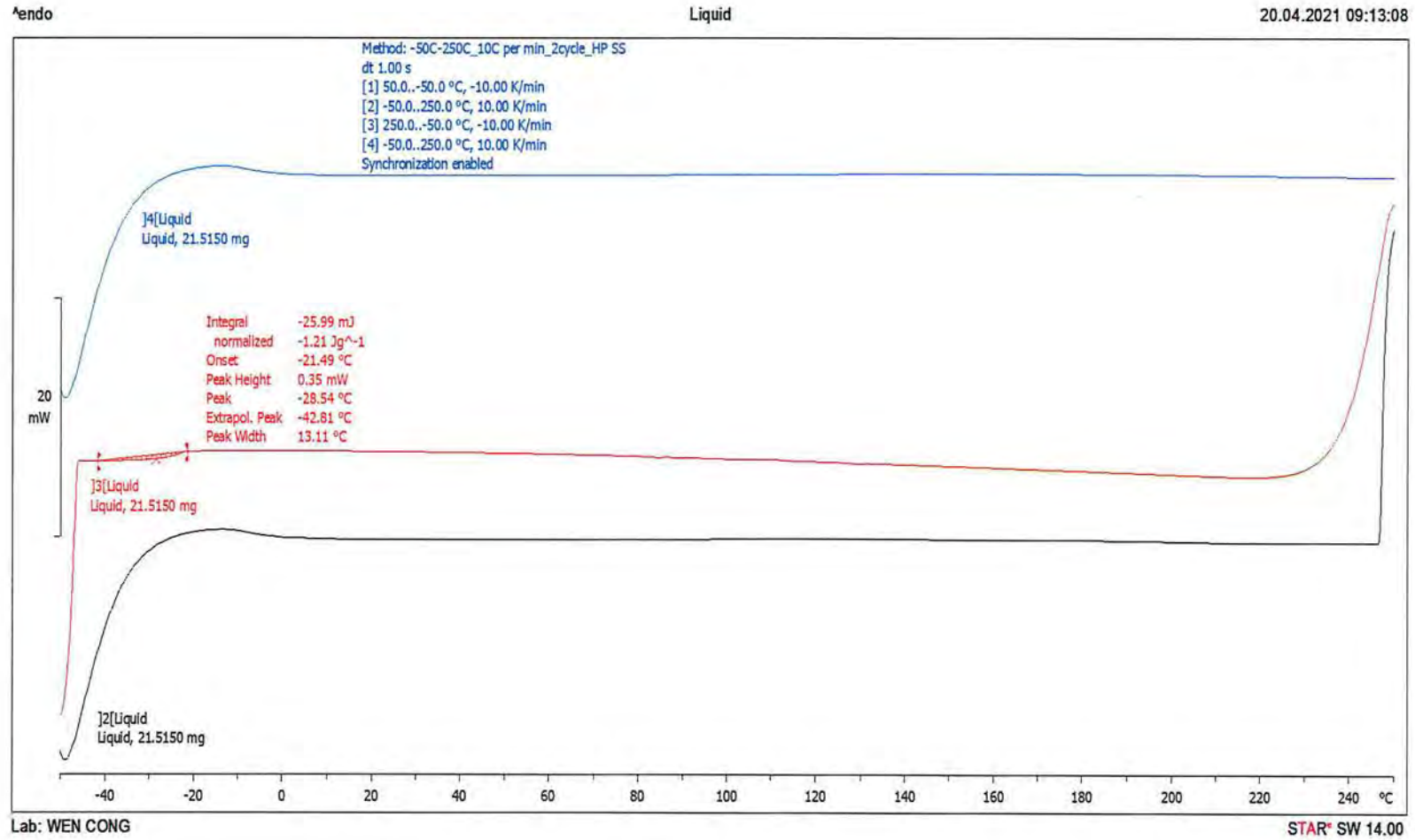
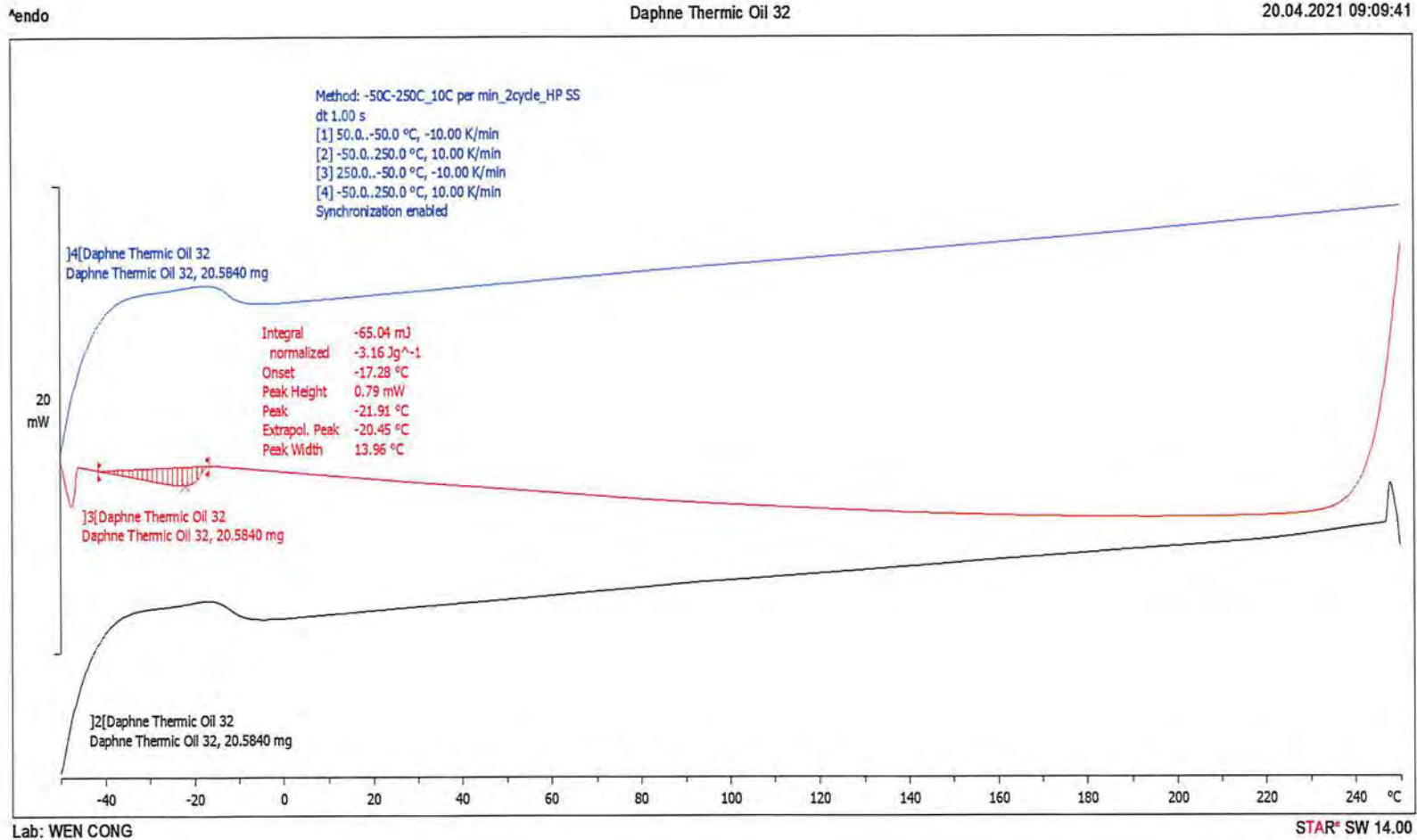


Figure 2



**Appendix D: Simultaneous DSC-TGA (SDT) - Testing of
Heat Transfer Fluid**

REPORT

REPORT REFERENCE: ICES/AC/21013_Part2b **DATE:** 3rd May 2021

SUBJECT: SDT Analysis on oil samples

COMPANY: ICES, A*STAR
1, Pesek Road, Jurong Island,
Singapore 627833

ATTENTION: Dr. Shaik Salim

DATE SAMPLE RECEIVED: 1st Apr 2021

DATE ANALYSED: 13th Apr 2021

DATE TEST COMPLETED: 3rd May 2021

DESCRIPTION OF SAMPLE(S):

2 liquid oil samples (~500mL each) were received.

S/N	Sample Description	Exhibit No.
1	Liquid	250221-2b
2	Daphne Thermic Oil 32 (20L)	-

METHOD OF TEST:

Standard test method for compositional analysis by thermogravimetry – SDT method as per ASTM E1131-20. Perform SDT analysis as received using TA SDT Q600 and test according to test condition. Analysis is done at different ramp rate of 2°C/min, 5°C/min and 10°C/min.

Test condition: Heat from 30°C to 800°C in N₂

RESULTS:

S/N	Sample Description	Exhibit No.	Ramp Rate °C/min	Weight Loss % 30°C to 800°C	Residue %	Ref
1	Liquid	250221-2b	2	99.46	0.54	Fig 1
			5	100.40	0.01	Fig 2
			10	99.42	0.50	Fig 3
2	Daphne Thermic Oil 32 (20L)	-	2	99.91	0.09	Fig 4
			5	99.81	0.20	Fig 5
			10	99.67	0.32	Fig 6

TESTED BY: Mr. Yeo Wen Cong
Senior Research Engineer



APPROVED BY: Mr. Andrew Lim
Team Leader
Analytics & Characterisation
Scientific Infrastructure & Analytics



Note: This report shall not be reproduced except in full, without written approval from ICES. This report does not constitute an endorsement of any item or material tested and must not be used for any publicity materials, and/or for advertising purposes without approval from ICES. Test results relate only to sample(s) submitted by the client for technical studies and shall not be used for any purpose of technical litigation.

Figure 1

Sample: Liquid Run 2
Size: 32.6180 mg
Comment: Ramp 2C/min

File: C:\...VAR21SDT10075\Liquid Run 2.001
Run Date: 30-Apr-2021 16:03
Instrument: SDT Q600 V20.9 Build 20

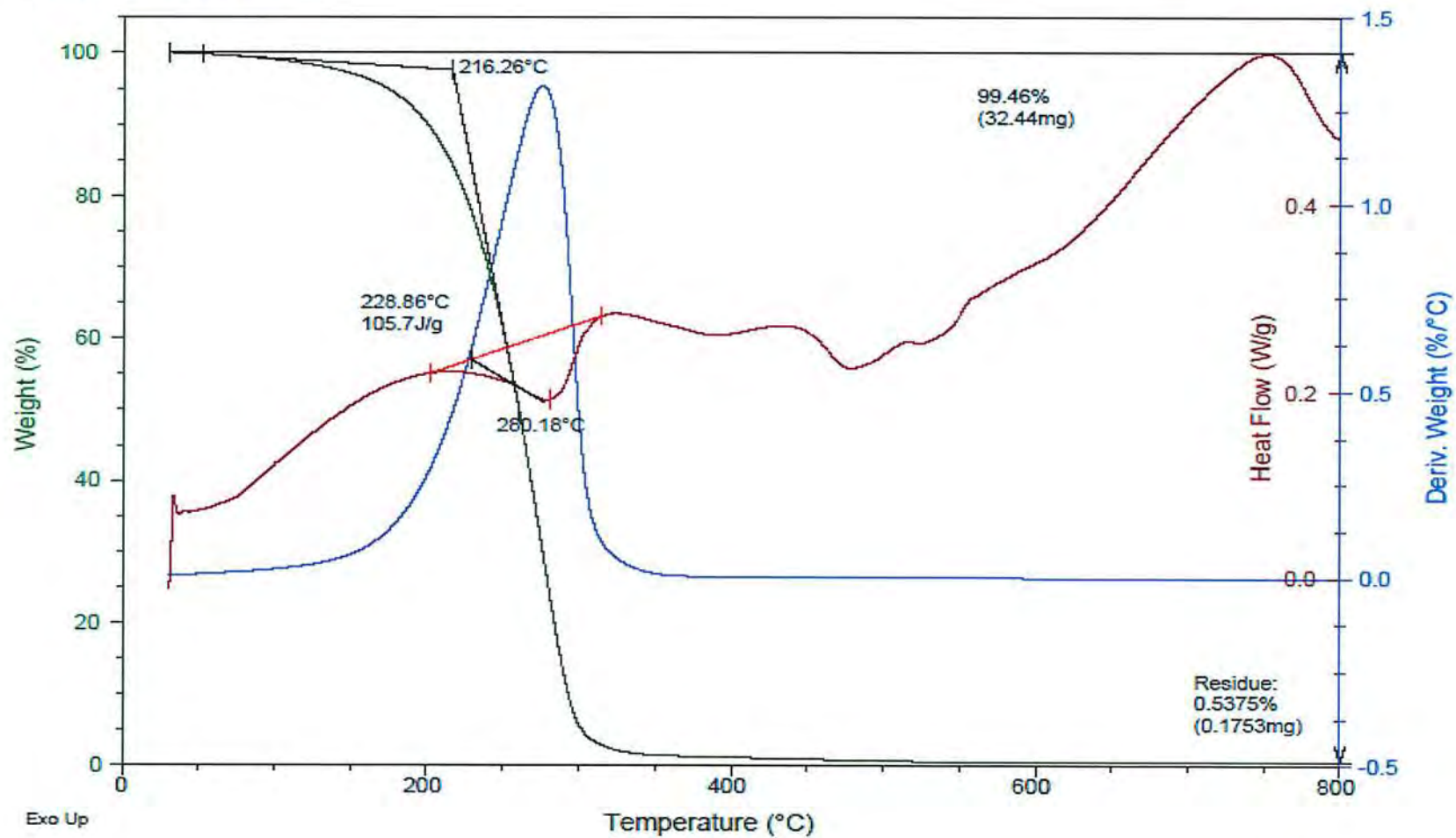


Figure 2

Sample: Liquid Run 3
Size: 27.3430 mg
Comment: Ramp 5C/min

File: C:\...LAR21SDT10075\Liquid Run 3.001
Run Date: 29-Apr-2021 18:58
Instrument: SDT Q600 V20.9 Build 20

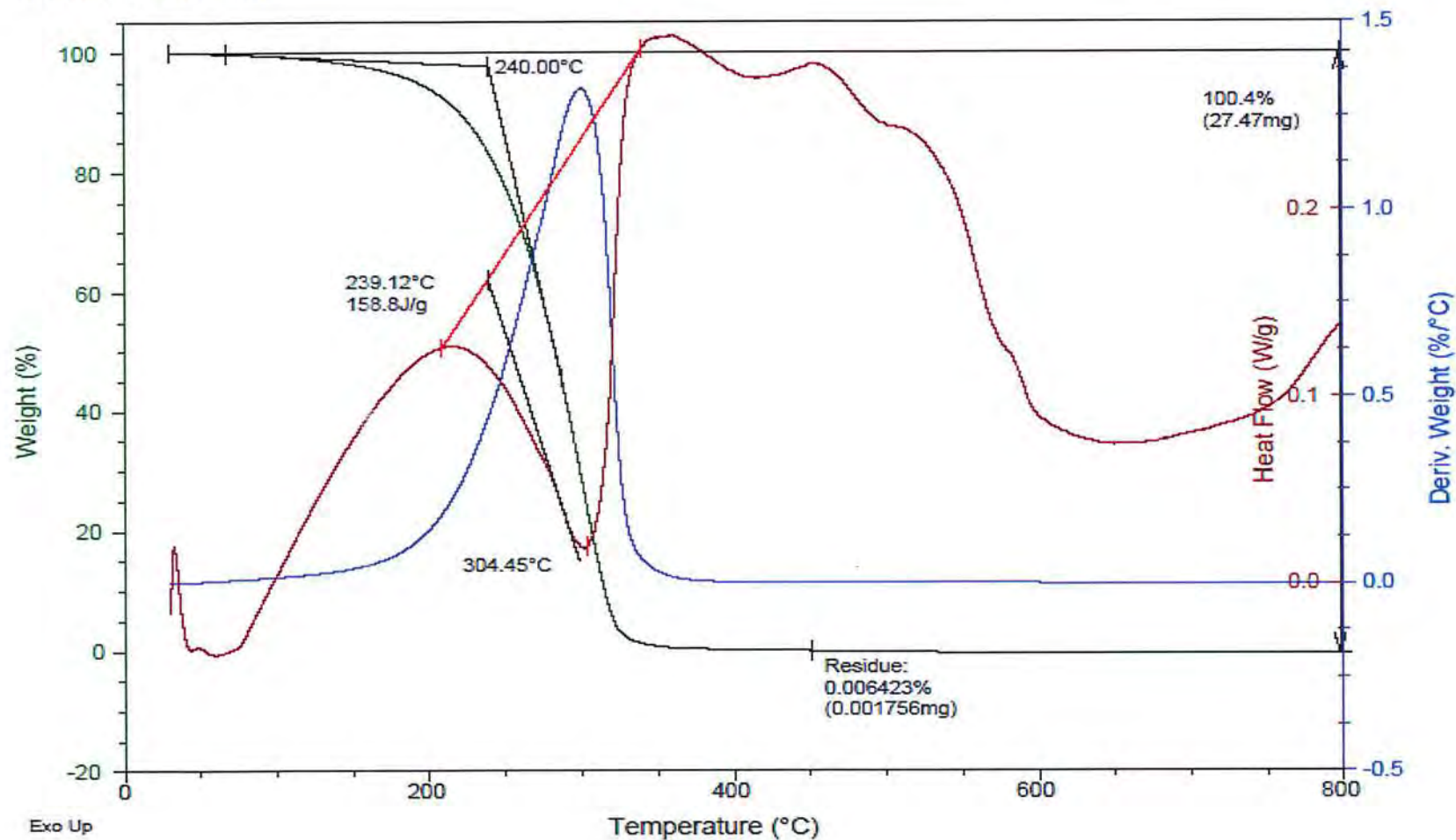


Figure 3

Sample: Liquid
Size: 32.7100 mg

File: C:\...Wen Cong\AR21SDT10066\Liquid.001
Run Date: 16-Apr-2021 08:36
Instrument: SDT Q600 V20.9 Build 20

Comment: 2104T02_O1

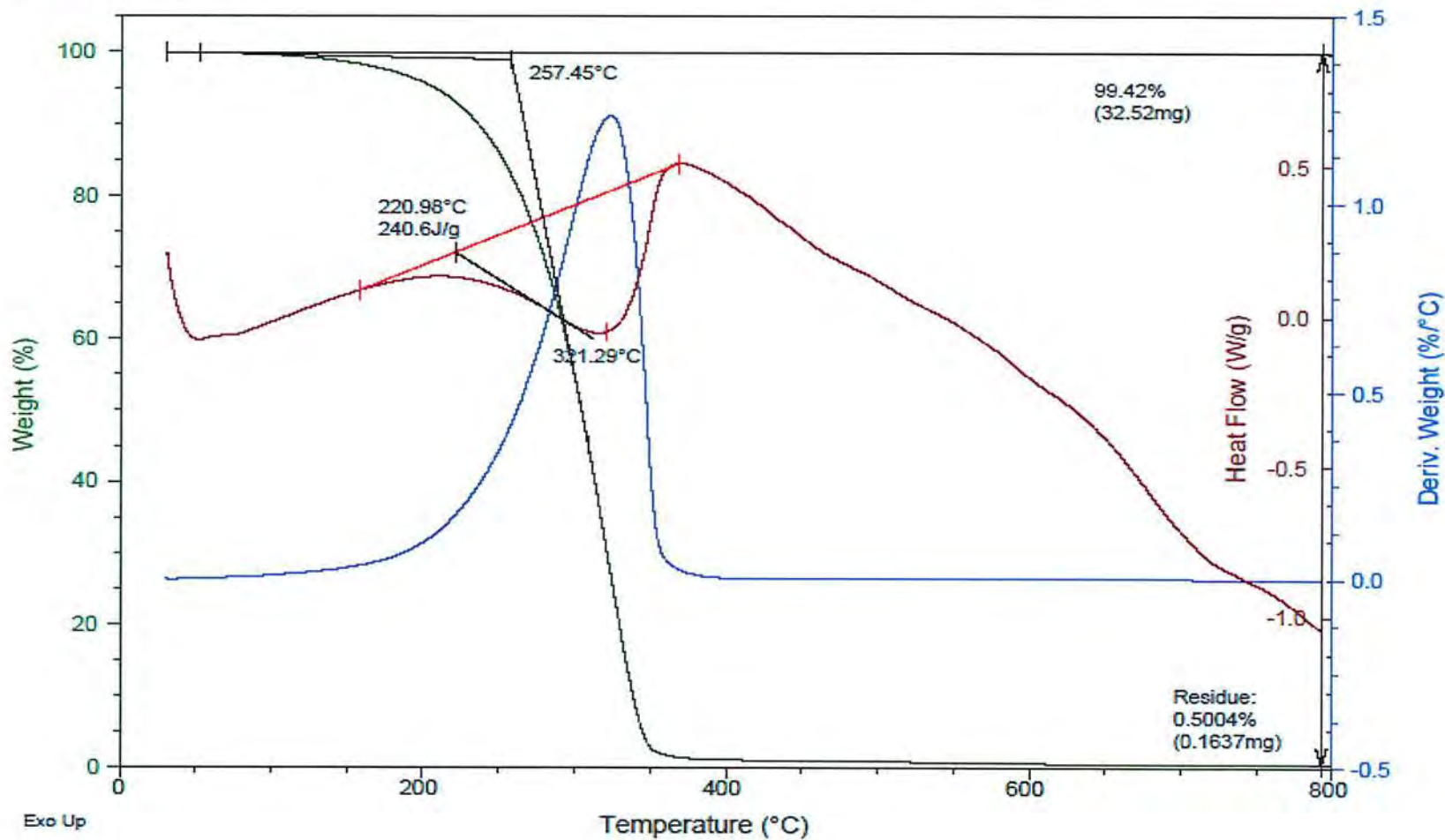


Figure 4

Sample: Daphne Thermic Oil 32 Run 2
Size: 25.1790 mg

File: C:\...Daphne Thermic Oil 32 Run 2.001
Run Date: 28-Apr-2021 14:04
Instrument: SDT Q600 V20.9 Build 20

Comment: Ramp 2C/min

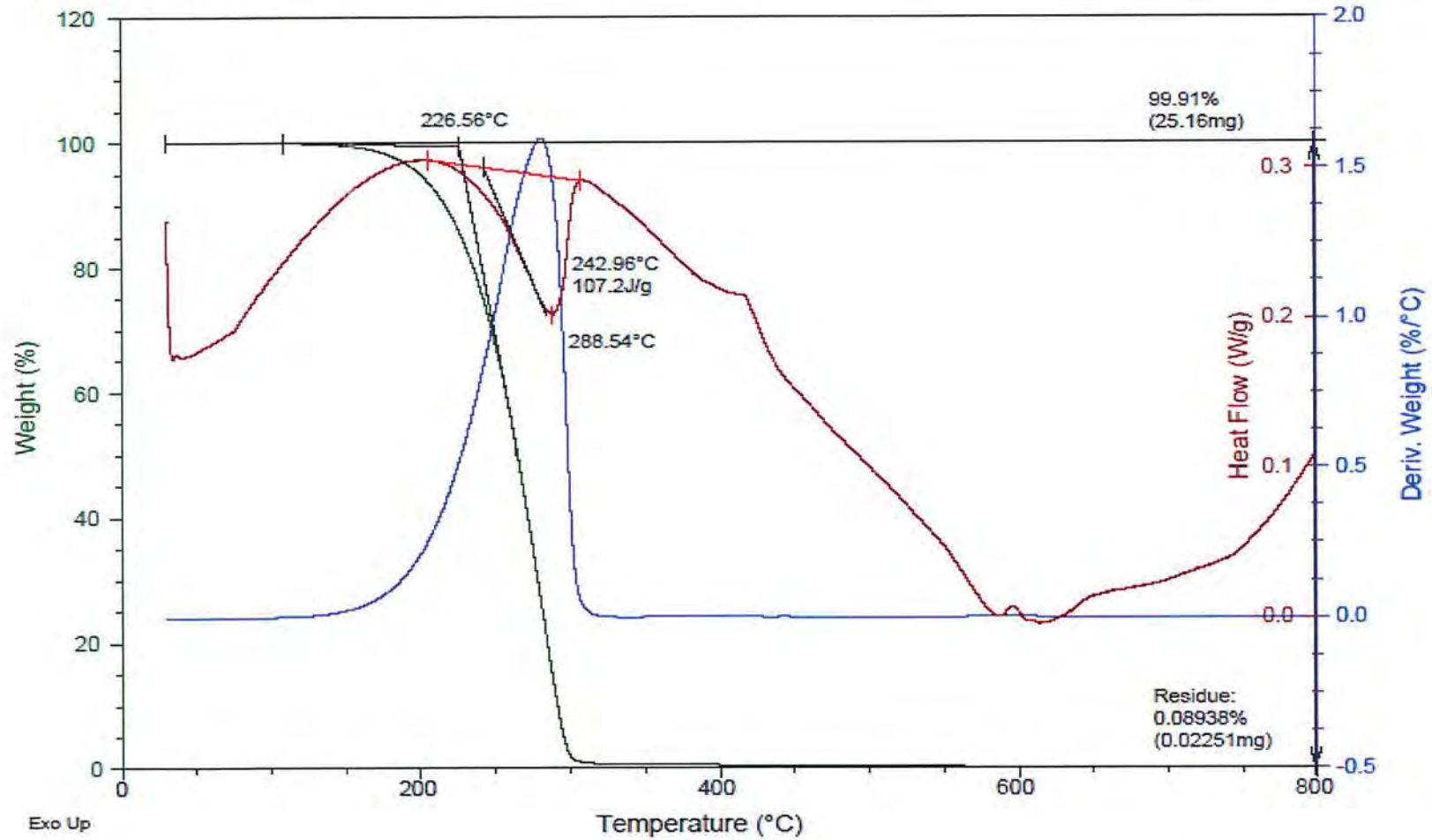


Figure 5

Sample: Daphne Thermic Oil 32 Run 3
Size: 31.2570 mg
Comment: Ramp 5C/min

File: C:\...\Daphne Thermic Oil 32 Run 3.001
Run Date: 29-Apr-2021 15:55
Instrument: SDT Q600 V20.9 Build 20

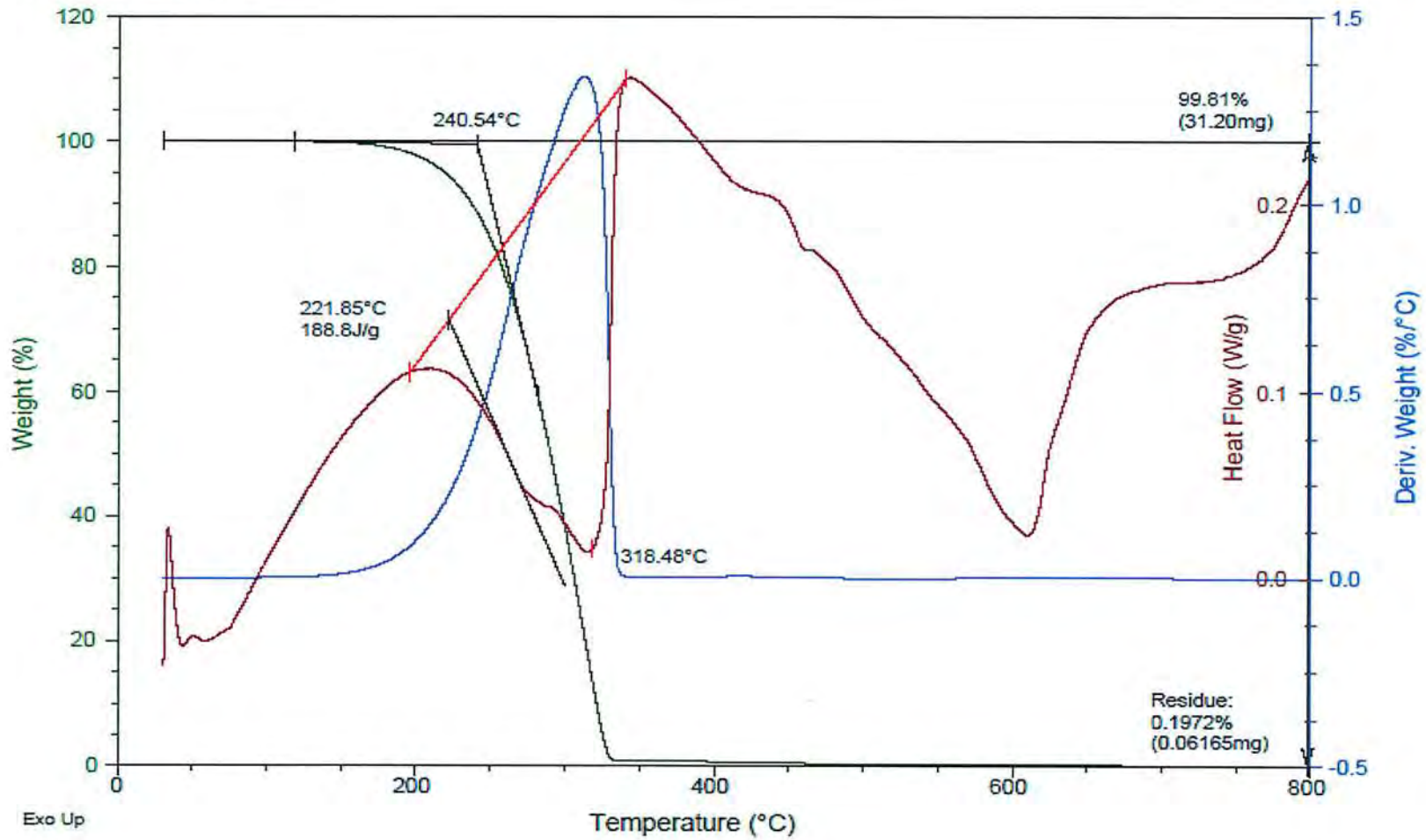
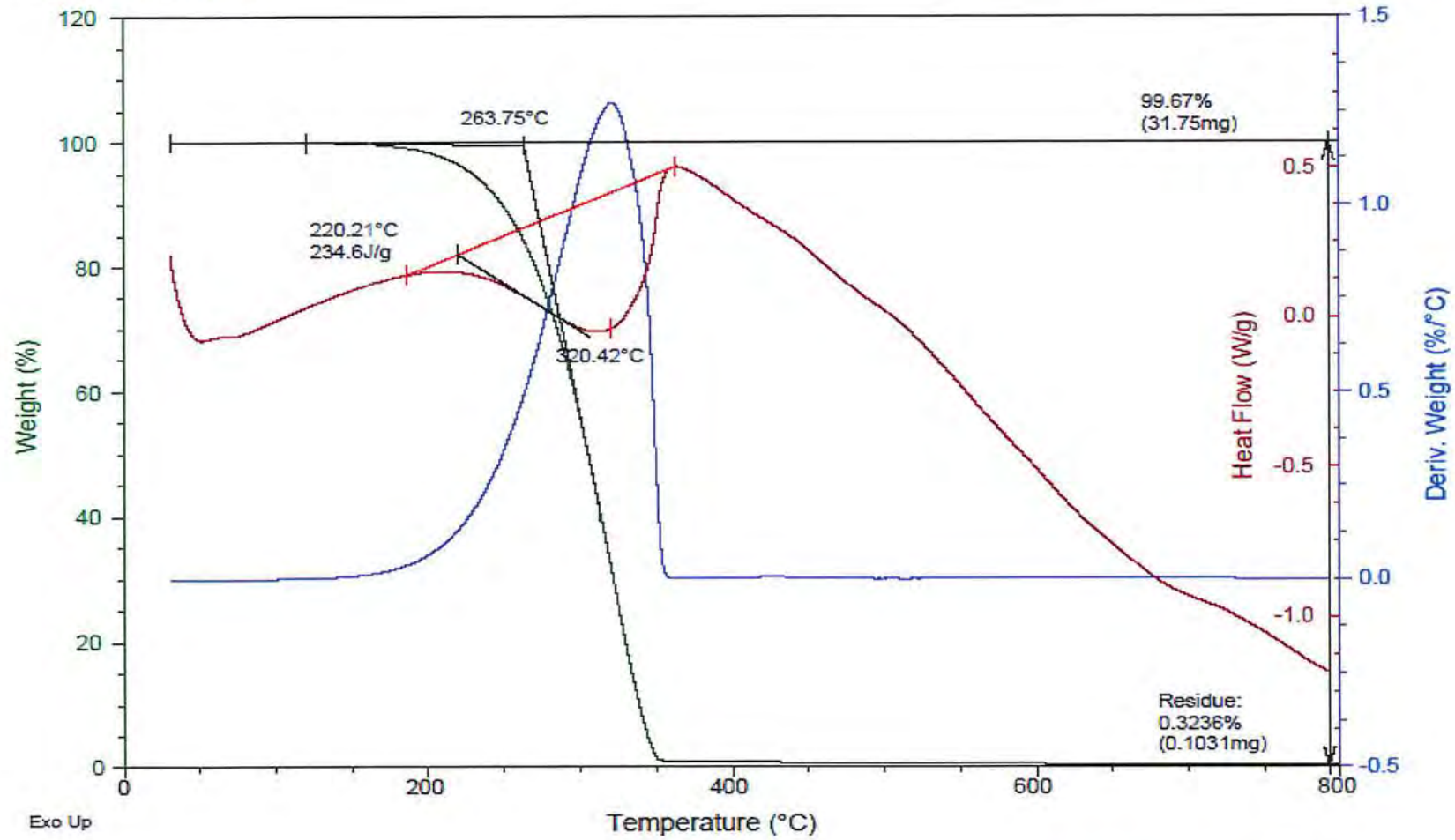


Figure 6

Sample: Daphne Thermic Oil 32
Size: 31.8560 mg
Comment: 2104T02_P1

File: C:\...\Daphne Thermic Oil 32.001
Run Date: 15-Apr-2021 17:49
Instrument: SDT Q600 V20.9 Build 20



Appendix E: Pressure – Temperature Analysis of Heat Transfer Fluid

2

The pressure-temperature behaviour of the heat transfer fluid, was studied using a 300 ml
4 hastelloy Parr Instruments pressure vessel. The pressure vessel is equipped with an impeller and
is rated to operate up to 500 °C and 340 barg. However, a bursting disc rated at 135 bars was
6 attached to the system to ensure a large safety margin in case of overpressure. The set-up is
controlled using a Parr 4848 controller that also continuously measures the Parr reactor's internal
8 temperature and pressure.

10 A manual heat-wait-search protocol was implemented for this pressure-temperature analysis.
Each experimental run was conducted with a 10 °C/min temperature ramp rate. The temperature
12 was raised in 10 °C intervals to allow for the pressure to stabilise and to check for any large
increase in pressures that would indicate an exothermic decomposition. This was carried out until
14 350 °C. After that, the temperature was allowed to increase to 450 °C and held to monitor the
final pressure level reached.

16

A total of five experimental runs were conducted. Each experimental run was conducted over
18 approximately 5 to 7 hours. The results for each of the five experimental runs are shown in **Figure
E.1 to Figure E.5** below.

20

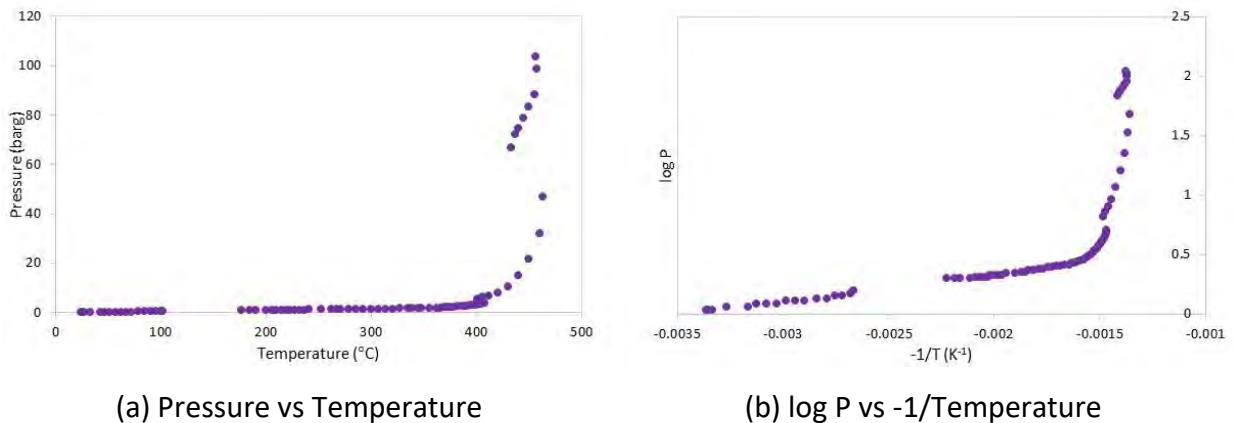
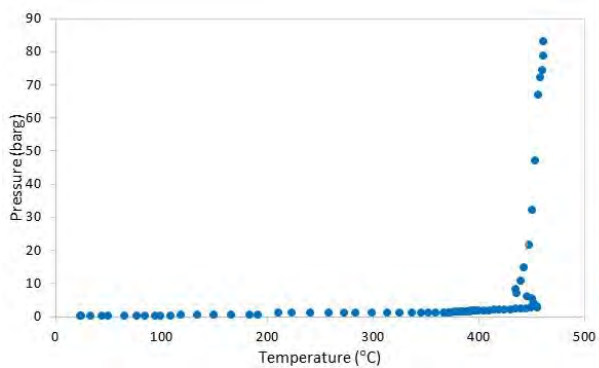
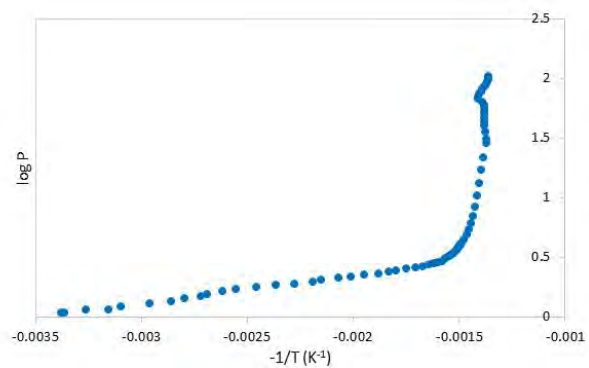


Figure E.1. Parr reactor experimental Run 1 up to 450 °C

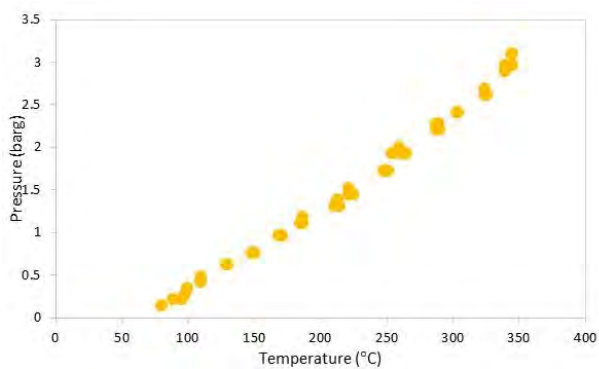


(a) Pressure vs Temperature

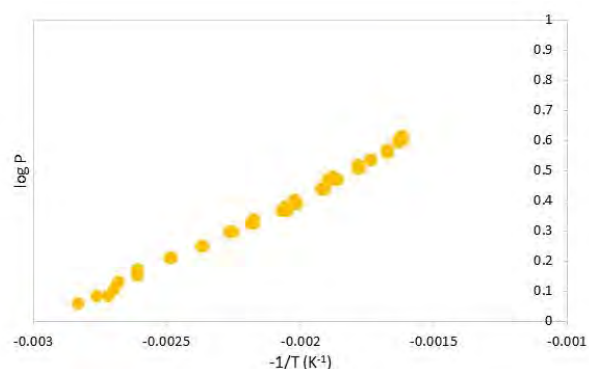


(b) log P vs $-1/\text{Temperature}$

Figure E.2. Parr Reactor experimental Run 2 up to 450 °C

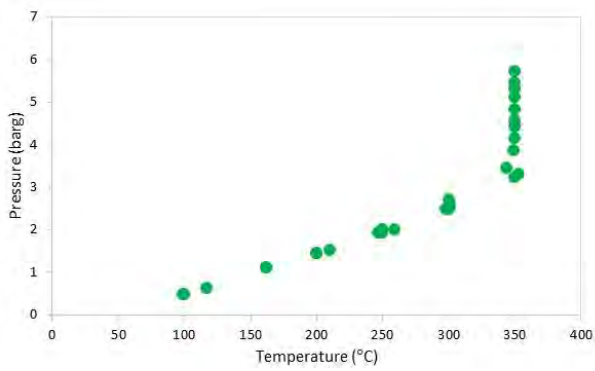


(a) Pressure vs Temperature

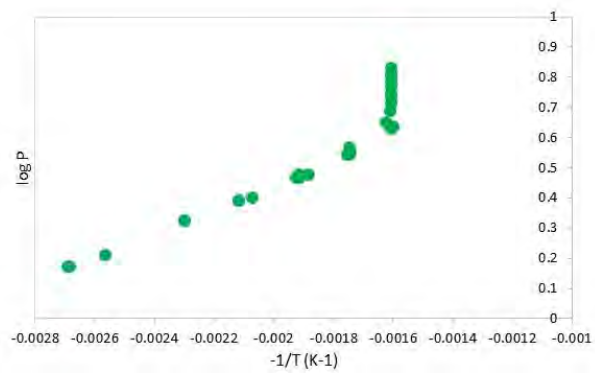


(b) log P vs $-1/\text{Temperature}$

Figure E.3. Parr Reactor experimental Run 3 up to 340 °C

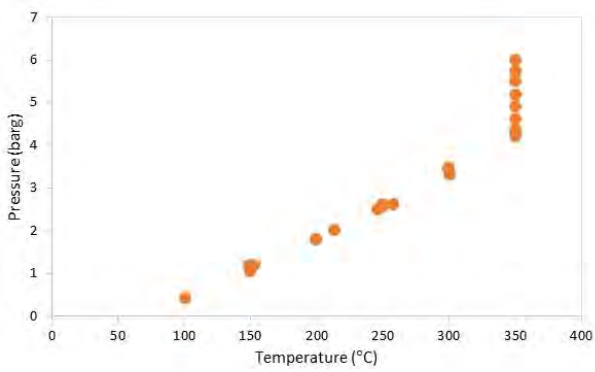


(a) Pressure vs Temperature

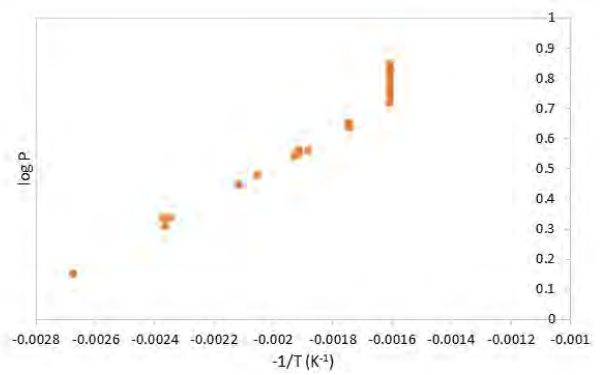


(b) log P vs -1/Temperature

Figure E.4. Parr Reactor experimental Run 4 up to 350 °C



(a) Pressure vs Temperature



(b) log P vs -1/Temperature

Figure E.5. Parr Reactor experimental Run 5 up to 350 °C

Appendix F: Explosion Calculations – Estimation of Overpressures

2 1. Physical Explosion

For the scenario where the explosion is strictly due to the physical energy released from an exploding compressed gas build-up within the mixer’s heating jacket, the following calculation method can be applied.

6 Assumptions

P_2 = initial absolute pressure (bars); this is taken as the pressure within the mixer’s heating jacket. Based on the information provided in the NH Sigma Kneader’s User Guide, the heating jacket is rated to a pressure of up to 2 barg. Usually, the rated operational pressure is less than the test pressure which is in turn lower than the design pressure in order to provide a significant safety margin. It can thus be assumed for the purposes of these calculation the value of $P_2 = 3, 4$ and 5 bars (absolute).

P_1 = final absolute pressure (bars); this is taken as atmospheric pressure, 1.013 bars

14 V = volume of heating jacket (300 litres)

16 STEP 1: Calculation of the energy of (mechanical) explosion

$$E(cal) = P_2V \left[\ln \left(\frac{P_2}{P_1} \right) - \left(1 - \frac{P_1}{P_2} \right) \right] \times 23900.6 \text{ --- Equation (1)}$$

18 The energy (in calories) of mechanical explosion¹ of the compressed gas cylinder obtained from Equation (1) is used to obtain the **TNT-equivalent**²; where

$$20 \text{ TNT – equivalent (kg TNT)} = m_{TNT} = \frac{E(cal)}{1120(cal/g \text{ of TNT}) \times 1000} \text{ --- Equation (2)}$$

¹ Crowl, Daniel A. Understanding explosions. Vol. 16. John Wiley & Sons, 2010.

² Crowl, Daniel A., and Joseph F. Louvar. Chemical process safety: fundamentals with applications. Pearson Education, 2001

STEP 2: Calculation of peak over pressure arising from the explosion

2 The scaled distance **Z** is then calculated from the equation below³.

$$Z = \frac{r}{m_{TNT}^{1/3}} \text{ --- Equation (3)}$$

4 Where *r* (m) is the distance of a receptor from the explosion epicentre. For this incident,
various distances that correspond with specific types of damage as well as the physical
6 dimensions of the factory unit and its surroundings will be used to estimate the overpressure.

8 The scaled peak overpressure, ***p_s***, is then calculated using the equation below⁴:

$$p_s = \frac{808(1+(z/4.5)^2)}{[1+(z/0.048)^2]^{1/2}[1+(z/0.32)^2]^{1/2}[1+(z/1.35)^2]^{1/2}} \text{ --- Equation (4)}$$

10

Hence, the peak overpressure, ***p_o*** is⁵:

12

$$p_o \text{ (kPa)} = p_s \times 101 \text{ --- Equation 5}$$

14 The calculated peak overpressures can then be compared to the types of overpressure
damage⁶ listed in **Table F.1** and **Table F.2** for verification and reference.

16

18

³ Crowl, Daniel A., and Joseph F. Louvar. Chemical process safety: fundamentals with applications. Pearson Education, 2001

⁴ Lees, Frank. Lees' Loss prevention in the process industries: Hazard identification, assessment and control, Volume 2. Butterworth-Heinemann, 2012

⁵ Lees, Frank. Lees' Loss prevention in the process industries: Hazard identification, assessment and control, Volume 2. Butterworth-Heinemann, 2012

⁶ Kumar, Ashok. Guidelines for evaluating the characteristics of vapor cloud explosions, flash fires, and BLEVEs. Center for Chemical Process Safety (CCPS) of the AIChE, 1994

Table F.1. Overpressure categorisation in terms of damage levels

Zone	Damage Level	Side-on overpressure (kPa)
A	Total destruction - building totally destroyed i.e. damaged beyond economical repair	> 83
B	Severe damage - partial collapse and/or failure of some bearing member	> 35
C	Moderate damage - building still usable, but structural repairs are required	> 17
D	Light damage - shattered window panes, light cracks in walls, and damage to wall panels and roofs	> 3.5

Table F.2. Damage produced by blast, overpressures

S/N	Description of Damage	Side-on overpressure (kPa)
1	Annoying noise	0.15
2	Occasional breaking of large window panes already under strain	0.2
3	Loud noise; sonic boom glass failure	0.3
4	Breakage of small windows under strain	0.7
5	Threshold for glass breakage	1
6	“Safe distance,” probability of 0.95 of no serious damage beyond this value; some damage to house ceilings; 10% window glass broken.	2
7	Limited minor structural damage	3
8	Large and small windows usually shattered; occasional damage to window frames	3.5 - 7
9	Minor damage to house structures	5
10	Partial demolition of houses, made uninhabitable	8
11	Corrugated asbestos shattered. Corrugated steel or aluminium window frames panels fastenings fail, followed by buckling; wood panel (standard housing) fastenings fail; panels blown in	7 - 15
12	Steel frame of clad building slightly distorted	10
13	Partial collapse of walls and roofs of houses	15
14	Concrete or cinderblock walls, not reinforced, shattered	15 - 20
15	Lower limit of serious structural damage 50% destruction of brickwork of houses	18
16	Heavy machines in industrial buildings suffered little damage; steel frame building distorted and pulled away from foundations	20
17	Frameless, self-framing steel panel building demolished; rupture of oil storage tanks	20 - 28
18	Cladding of light industrial buildings ruptured	30
19	Wooden utility poles snapped; tall hydraulic press in building slightly damaged	35
20	Nearly complete destruction of houses	35 - 50
21	Loaded tank cars overturned	50
22	Unreinforced brick panels, 25-35 cm thick, fail by shearing or flexure	50 - 55
23	Loaded train boxcars completely demolished	60
24	Probable total destruction of buildings; heavy machine tools moved and badly damaged	70

2. Chemical Explosion

2 For the scenario where the explosion is due to the release of energy via the combustion of a
4 fuel which in this case is the heat transfer fluid, a similar approach to the physical explosion
described previously can also be applied⁷.

The only adjustment that is required will be in Step 1 where the chemical energy released
6 due to the combustion of the fuel needs to be calculated using⁸:

$$m_{TNT} = \frac{\eta m \Delta H_c}{E_{TNT}} \quad \text{--- Equation 6}$$

8

Where:

10 m_{TNT} is the equivalent mass of TNT (kg)

η is the empirical explosion efficiency (0.01 to 0.1)

12 m is the mass of hydrocarbon (kg)

ΔH_c is heat of combustion (kJ/kg)

14 E_{TNT} is the energy of explosion of TNT = 1120 cal/g = 4686 kJ/kg

16 Assumptions

i. Explosion efficiency η , was taken as 1% or 0.01

18 ii. Heat of combustion ΔH_c , was taken as 40,000 kJ/kg

20

Following the calculation for m_{TNT} , the estimation of overpressures can proceed as described
22 previously in Step 2.

24

⁷ Kumar, Ashok. Guidelines for evaluating the characteristics of vapor cloud explosions, flash fires, and BLEVEs. Center for Chemical Process Safety (CCPS) of the AIChE, 1994

⁸ Crowl, Daniel A., and Joseph F. Louvar. Chemical process safety: fundamentals with applications. Pearson Education, 2001

Appendix G: Dust layer and HTF sampling location

Exhibit number: 080321-2b
Sample description: BULK (BULK BAG RIGHT)
Photo:



Exhibit number: 080321-1b
Sample description: BULK (BULK BAG LEFT)
Photo:



Exhibit number: 170321-4b
Sample description: BULK (UNDER PALLET) 4
Photo:

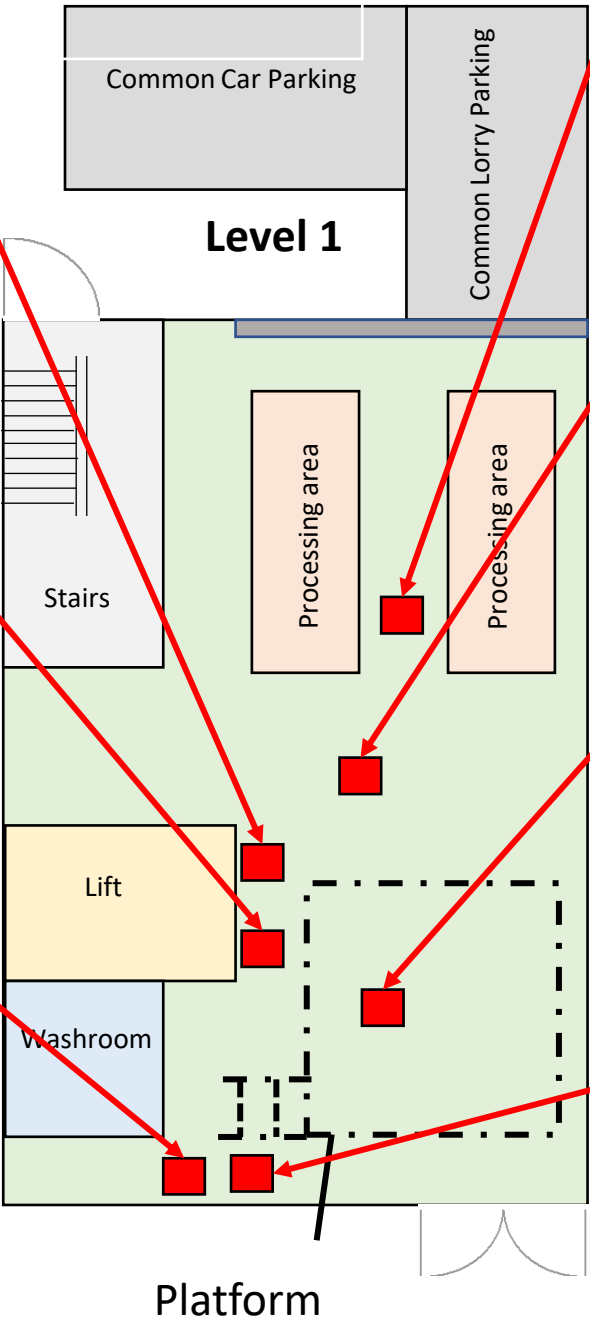


Exhibit number: 170321-1b
Sample description: BULK POINT 1 (20x20cm)
Photo:



Exhibit number: 170321-2b
Sample description: BULK POINT 2 (20x20cm)
Photo:



Exhibit number: 170321-3b
Sample description: BULK POINT 3 (20x20cm)
Photo:



Exhibit number: 170321-6b
Sample description: BULK (OUTSIDE TOILET) 6
Photo:



Schematic layout plan of platform

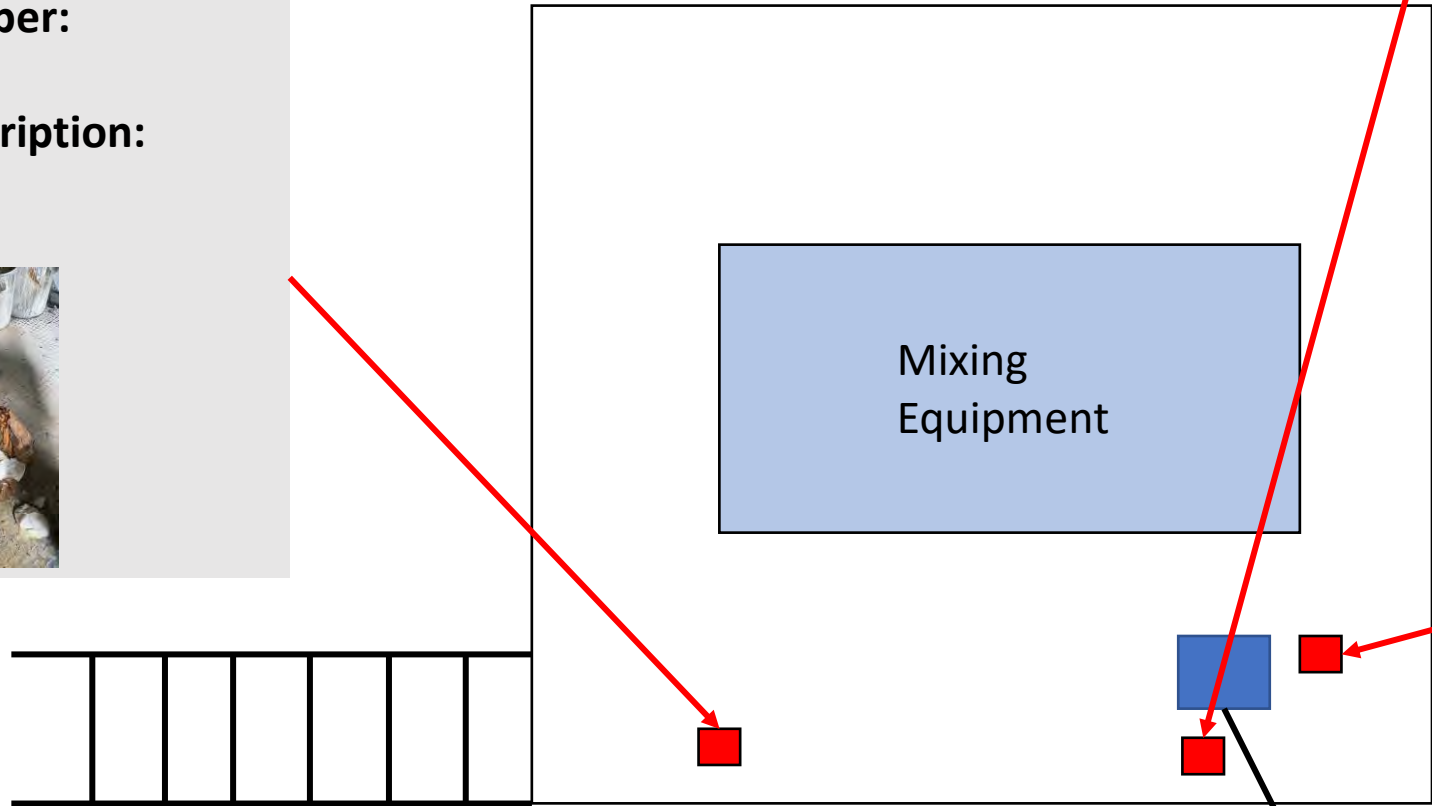
Exhibit number:
250221-1b
Sample description:
BULK
Photo:



Exhibit number:
170321-5b
Sample description:
BULK (PLATFORM) 5
Photo:



Exhibit number:
250221-2b
Sample description:
LIQUID
Photo:



Chute

Appendix H: Details of CHNS, SEM/EDX, SDT, FTIR and
UV-Vis analysis - Testing of solid powder samples

REPORT

REPORT REFERENCE: ICES/AC/21013_Part3 **DATE:** 20th April 2021

SUBJECT: CHNS Element Analysis of Powder Samples

COMPANY: ICES, A*STAR
1, Pesek Road, Jurong Island
Singapore 627833

ATTENTION: Dr. Shaik Salim

DATE SAMPLE RECEIVED: 1st April 2021

DATE ANALYSED: 20th April 2021

DATE TEST COMPLETED: 20th April 2021

DESCRIPTION OF SAMPLE(S):

Fourteen powder samples (~ 5-10g each) were received.

S/N	Sample Description	Exhibit No.
1	Bulk	250221-1b
2	Bulk (Bulk Bag Left)	080321-1b
3	Bulk (Bulk Bag Right)	080321-2b
4	Bulk (Aluminium Hydroxide)	080321-3b
5	Bulk (Potato Starch)	080321-4b
6	Bulk Point 1	170321-1b
7	Bulk Point 2	170321-2b
8	Bulk Point 3	170321-3b
9	Bulk (Under Pallet) 4	170321-4b
10	Bulk (Platform) 5	170321-5b
11	Bulk (Outside Toilet) 6	170321-6b
12	Bulk (Aluminium Dihydrogen Phosphate)	170321-7b
13	Bulk (Boric Acid)	170321-8b
14	Bulk (Clay)	170321-9b

METHOD OF TEST:

Samples were analysed as received. Perform CHNS Elemental Analysis using Thermo Flash 2000 Elemental Analyzer according to in-house developed method

RESULTS:

No	Sample Name	Nitrogen (% w/w)	Carbon (% w/w)	Hydrogen (% w/w)	Sulphur (% w/w)
1	Bulk	ND	29.25	7.81	ND
2	Bulk (Bulk Bag Left)	ND	ND	3.30	ND
3	Bulk (Bulk Bag Right)	ND	5.04	5.06	ND
4	Bulk (Aluminium Hydroxide)	ND	ND	3.80	ND
5	Bulk (Potato Starch)	ND	36.07	7.06	ND
6	Bulk Point 1	ND	4.00	3.51	ND
7	Bulk Point 2	ND	4.39	3.74	ND
8	Bulk Point 3	ND	3.77	3.77	ND
9	Bulk (Under Pallet) 4	ND	3.20	3.46	ND
10	Bulk (Platform) 5	ND	35.50	7.02	ND
11	Bulk (Outside Toilet) 6	ND	8.37	4.27	ND
12	Bulk (Aluminium Dihydrogen Phosphate)	ND	ND	2.35	ND
13	Bulk (Boric Acid)	ND	ND	4.79	ND
14	Bulk (Clay)	ND	0.81	1.69	ND

*ND refers as "Not Detected".

TESTED BY:

Ms. Angeline Seo
Senior Research Engineer

APPROVED BY:

Mr. Andrew Lim
Team Leader
Analytics & Characterisation
Scientific Infrastructure & Analytics

REPORT

REPORT REFERENCE: ICES/AC/21013_Part4 **DATE:** 19th Apr 2021

SUBJECT: SEM/EDX Analysis of powder specimens

COMPANY: ICES, A*STAR
1, Pesek Road, Jurong Island,
Singapore 627833

ATTENTION: Dr. Shaik Salim

DATE SAMPLE RECEIVED: 1st Apr 2021

DATE ANALYSED: 16th Apr 2021

DATE TEST COMPLETED: 19th Apr 2021

DESCRIPTION OF SAMPLE(S):

Fourteen samples consisting of powder specimens (~5-10g each) were received.

S/N	Sample Description	Exhibit No.
1	Bulk	250221-1b
2	Bulk (Bulk Bag Left)	080321-1b
3	Bulk (Bulk Bag Right)	080321-2b
4	Bulk (Aluminium Hydroxide)	080321-3b
5	Bulk (Potato Starch)	080321-4b
6	Bulk Point 1	170321-1b
7	Bulk Point 2	170321-2b
8	Bulk Point 3	170321-3b
9	Bulk (Under Pallet) 4	170321-4b
10	Bulk (Platform) 5	170321-5b
11	Bulk (Outside Toilet) 6	170321-6b
12	Bulk (Aluminium Dihydrogen Phosphate)	170321-7b
13	Bulk (Boric Acid)	170321-8b
14	Bulk (Clay)	170321-9b

METHOD OF TEST:

The samples were transferred onto carbon tape and analyzed as received. SEM images along with its elemental compositions were acquired by FE-SEM - JEOL Scanning Electron Microscope (SEM) JSM-7900F coupled with Oxford Instruments Energy Dispersive Analyzer Coupled with X-Ray Detector (EDS) using Acceleration Voltage of 20.0 kV under low-vacuum as LV-SED mode.

RESULTS:

1. The SEM images and EDX spectrums of "Bulk (250221-1b)" are displayed from Figure 1a to 1c.

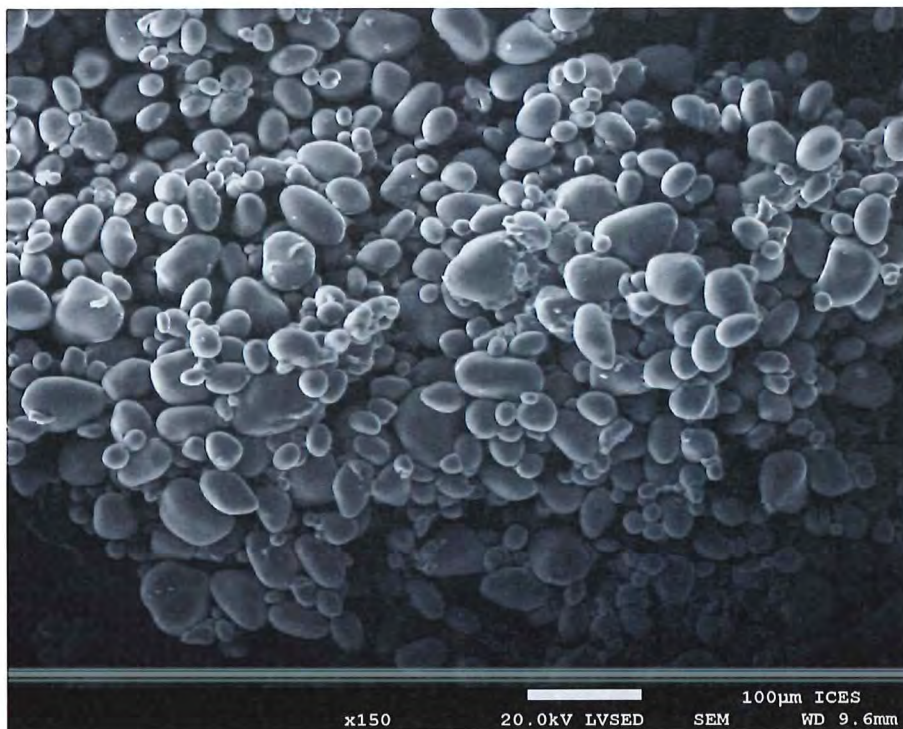


Figure 1a: SEM image of "Bulk, (250221-1b)"



Figure 1b: SEM/EDX image of "Bulk, (250221-1b)"

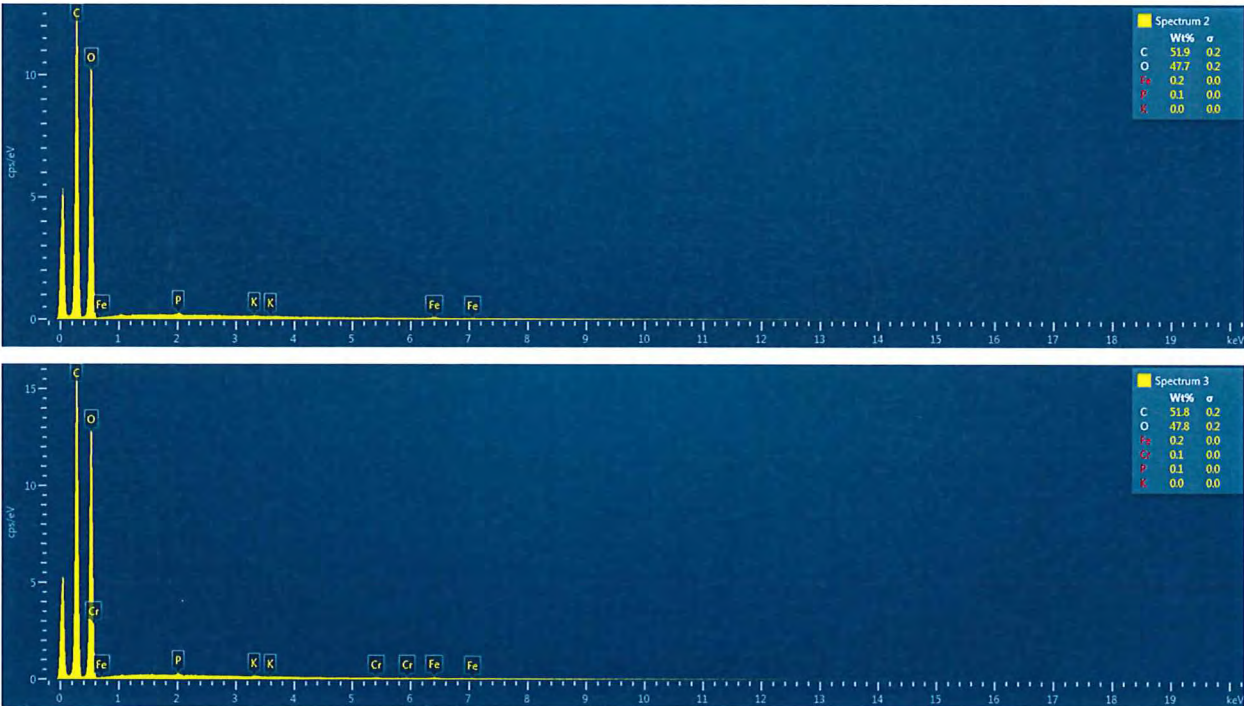


Figure 1c: EDX Spectrums 2 and 3 - Elemental Compositions of "Bulk, (250221-1b)"

2. The SEM images and EDX spectrums of “Bulk (Bulk Bag Left), (080321-1b)” are displayed from Figure 2a to 2c.

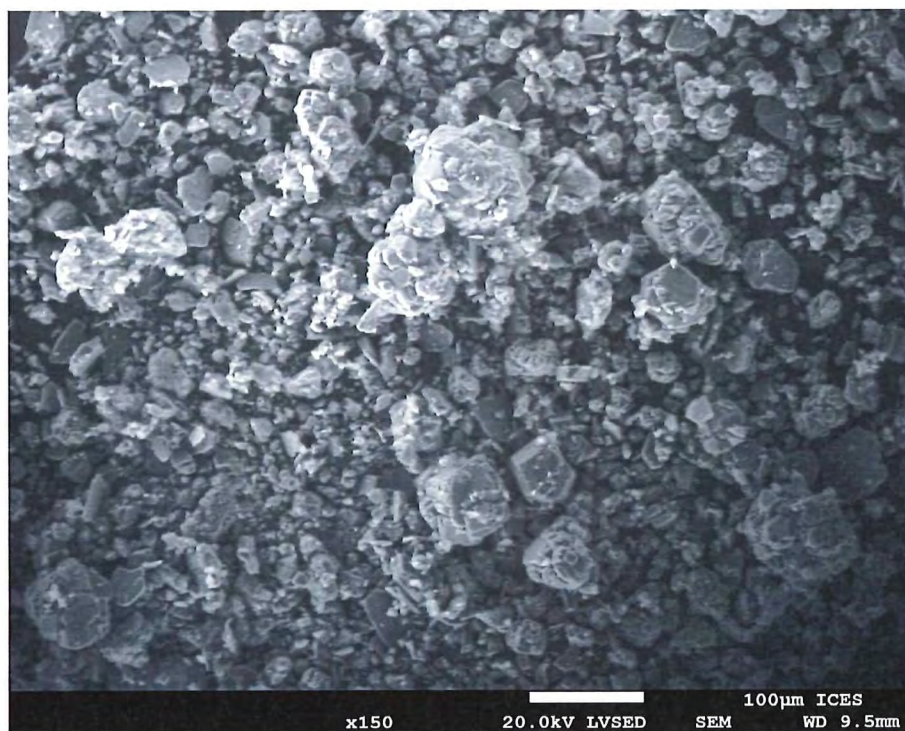


Figure 2a: SEM image of “Bulk (Bulk Bag Left), (080321-1b)”

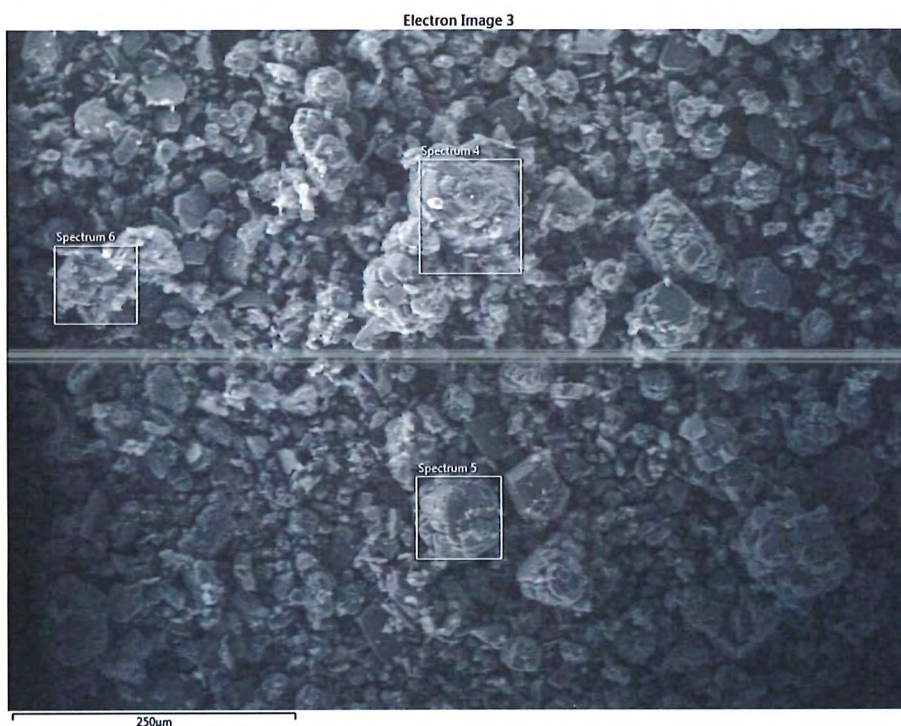


Figure 2b: SEM/EDX image of “Bulk (Bulk Bag Left), (080321-1b)”

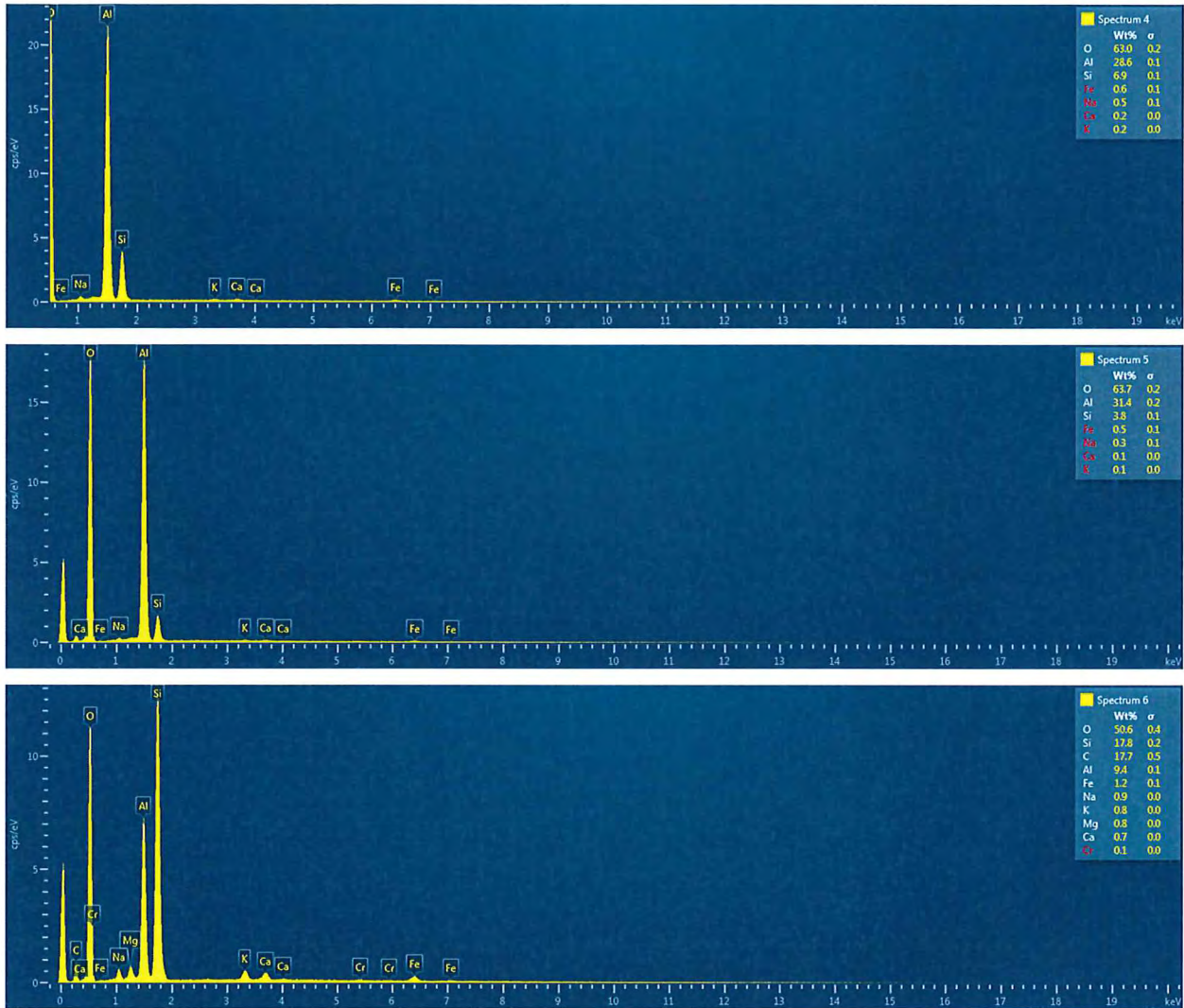


Figure 2c: EDX Spectrums 4 and 6 - Elemental Compositions of “Bulk (Bulk Bag Left), (080321-1b)”

3. The SEM images and EDX spectrums of “Bulk (Bulk Bag Right), (080321-2b)” are displayed from Figure 3a to 3c.

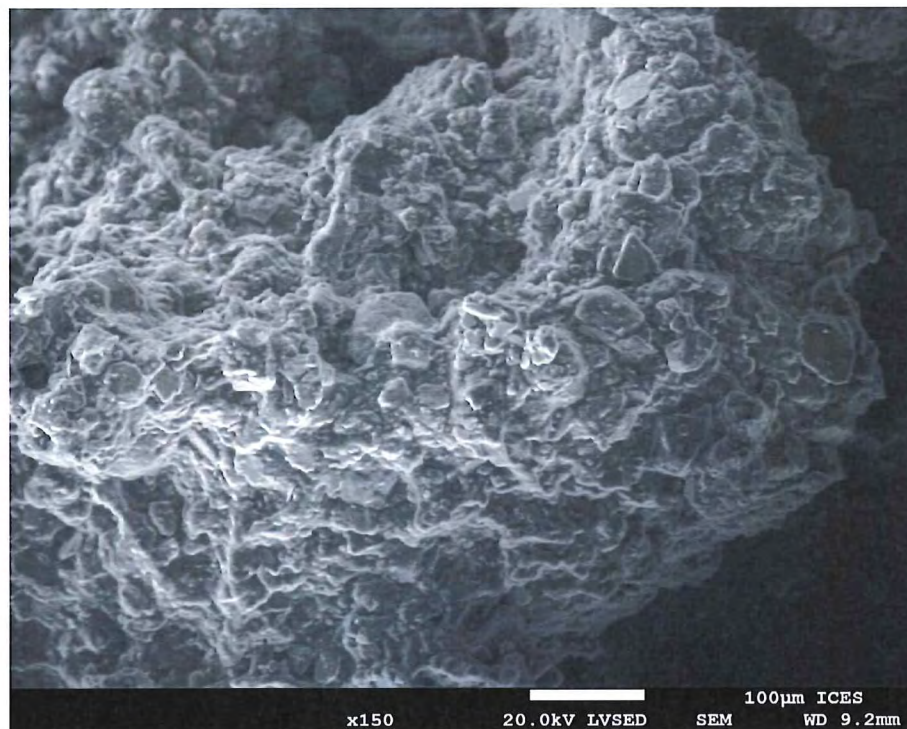


Figure 3a: SEM image of “Bulk (Bulk Bag Right), (080321-2b)”

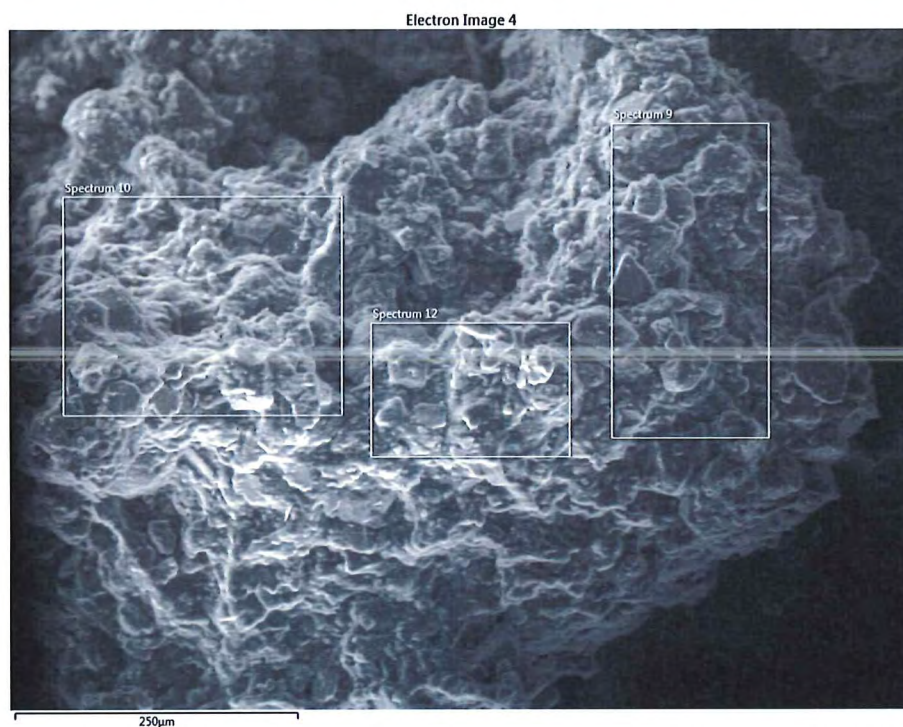


Figure 3b: SEM/EDX image of “Bulk (Bulk Bag Right), (080321-2b)”

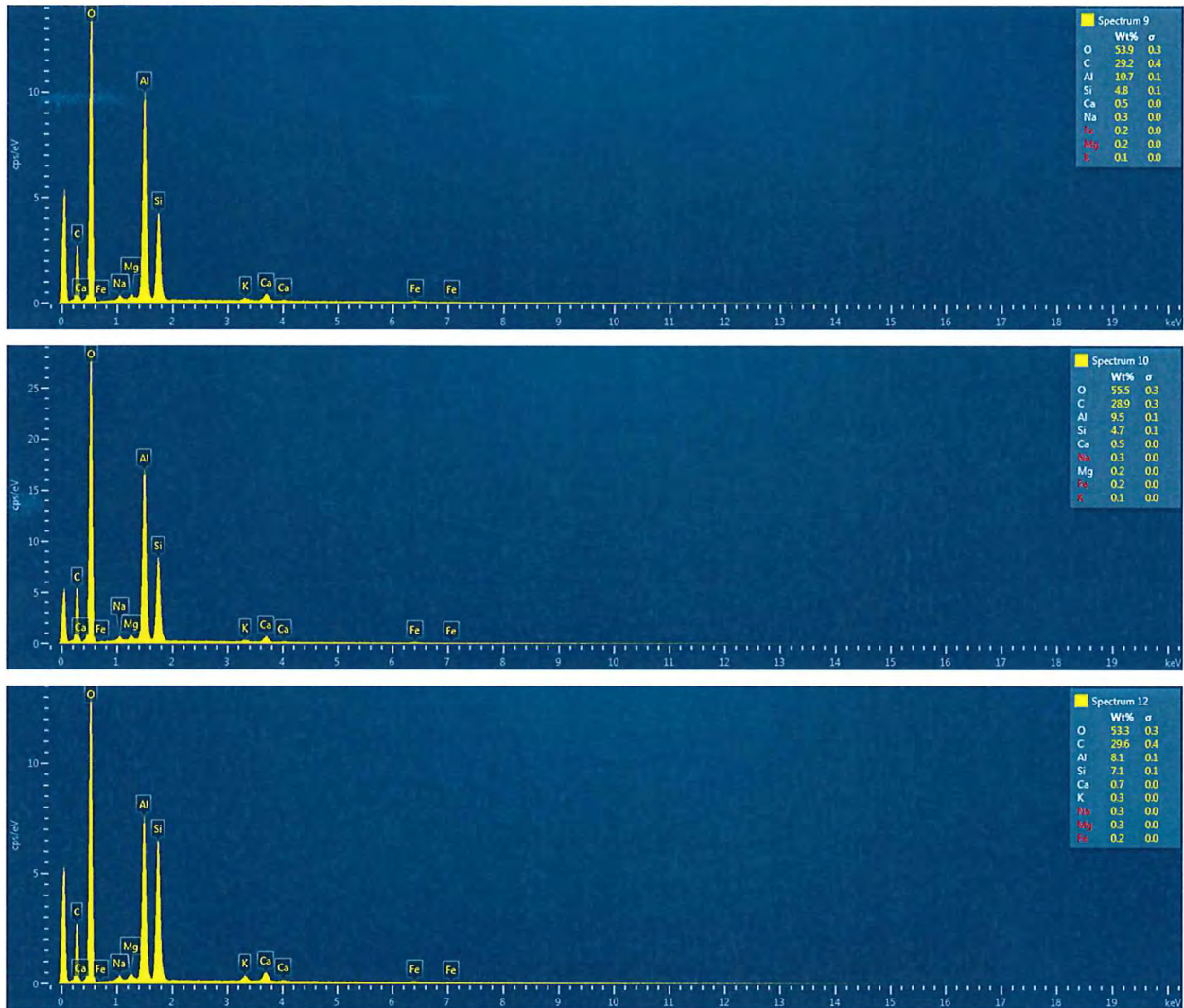


Figure 3c: EDX Spectrums 9, 10 and 12 - Elemental Compositions of “Bulk (Bulk Bag Right), (080321-2b)”

4. The SEM images and EDX spectrums of “Bulk (Aluminium Hydroxide), (080321-3b)” are displayed from Figure 4a to 4c.

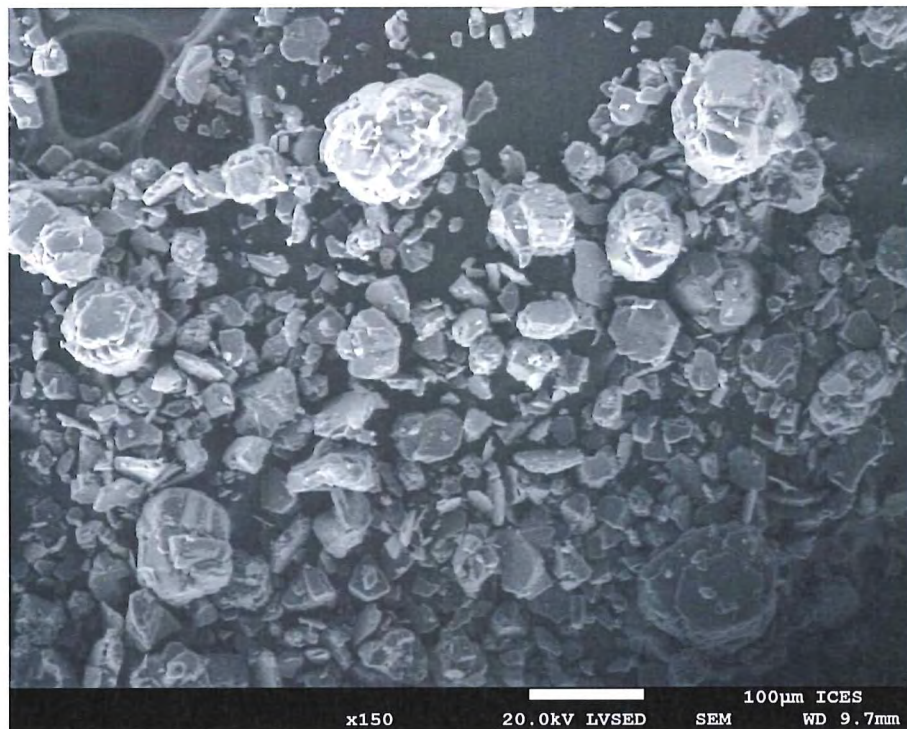


Figure 4a: SEM image of “Bulk (Aluminium Hydroxide), (080321-3b)”

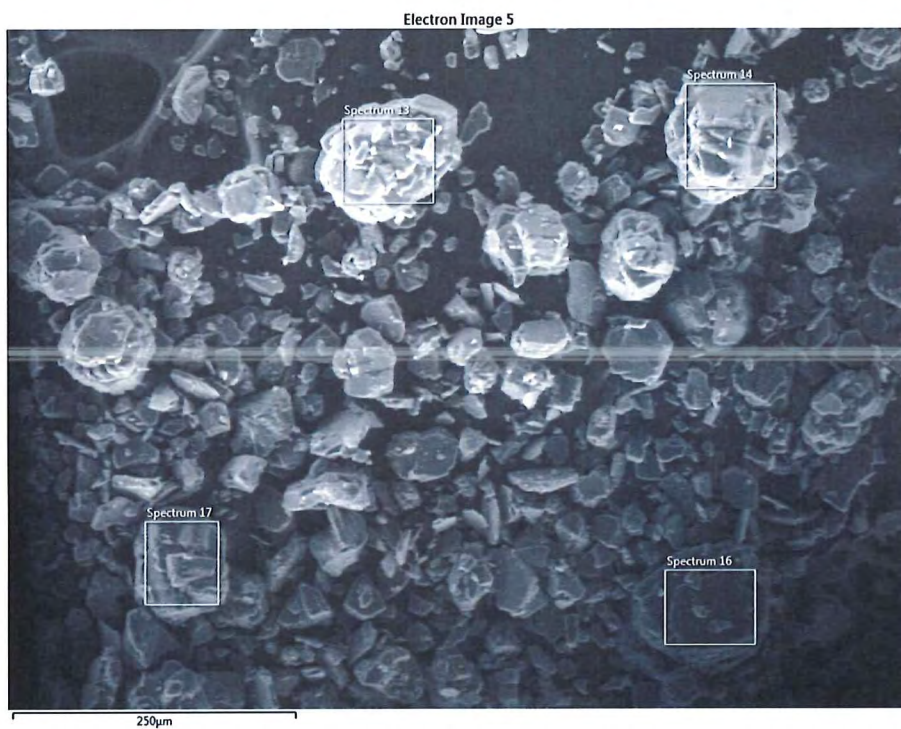


Figure 4b: SEM/EDX image of “Bulk (Aluminium Hydroxide), (080321-3b)”

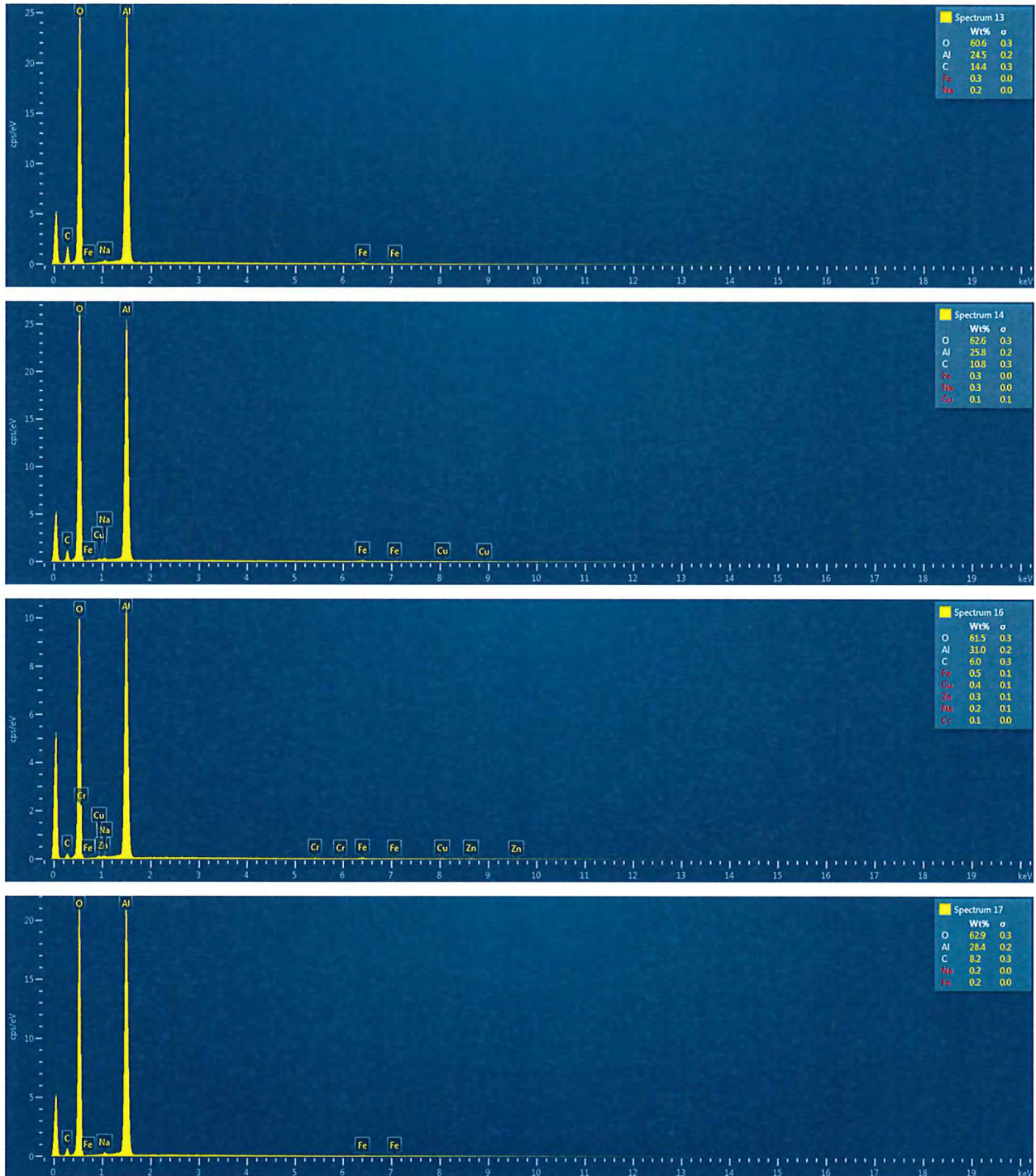


Figure 4c: EDX Spectrums 13, 14, 16 and 17 - Elemental Compositions of "Bulk (Aluminium Hydroxide), (080321-3b)"

5. The SEM images and EDX spectrums of “Bulk (Potato Starch), (080321-4b)” are displayed from Figure 5a to 5c.

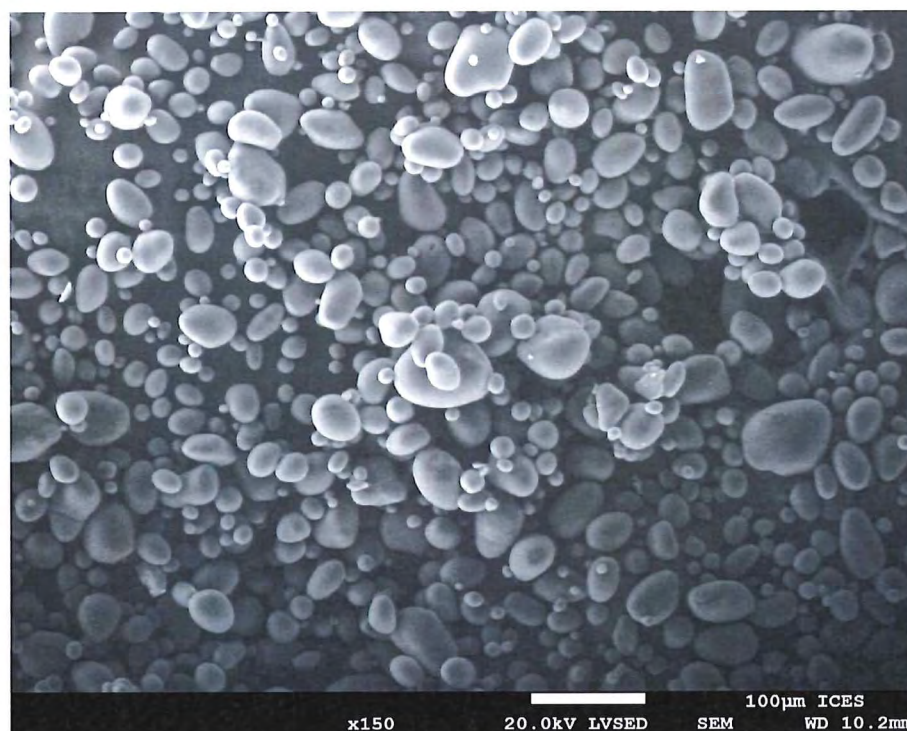


Figure 5a: SEM image of “Bulk (Potato Starch), (080321-4b)”

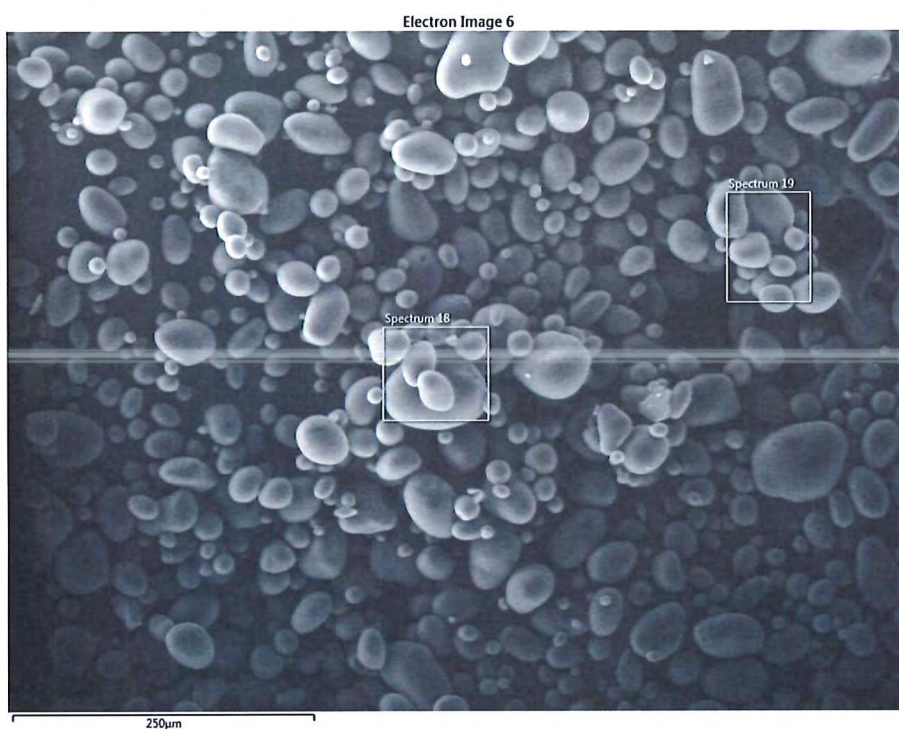


Figure 5b: SEM/EDX image of “Bulk (Potato Starch), (080321-4b)”

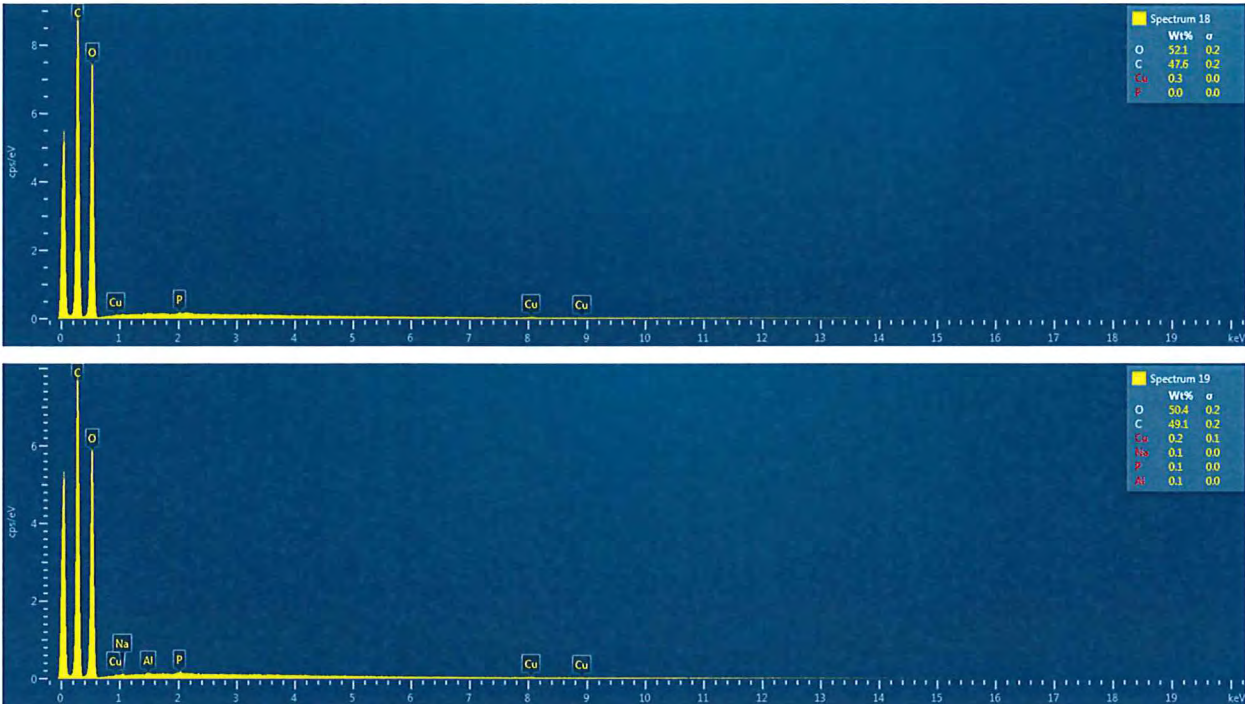


Figure 5c: EDX Spectrums 18 and 19 - Elemental Compositions of "Bulk (Potato Starch), (080321-4b)"

6. The SEM images and EDX spectrums of “Bulk Point 1, (170321-1b)” are displayed from Figure 6a to 6c.

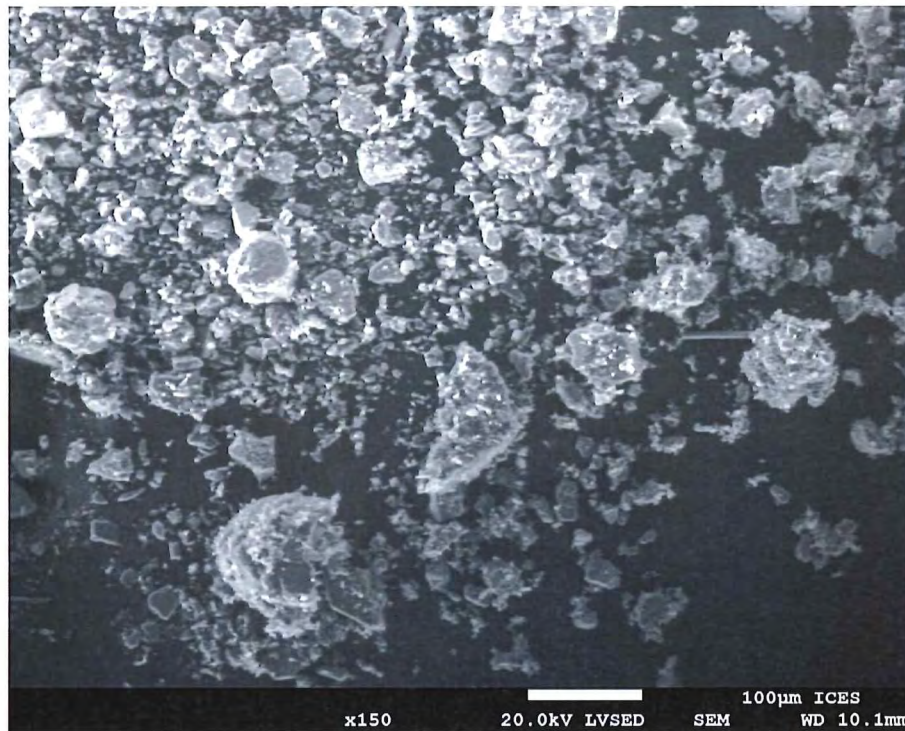


Figure 6a: SEM image of “Bulk Point 1, (170321-1b)”

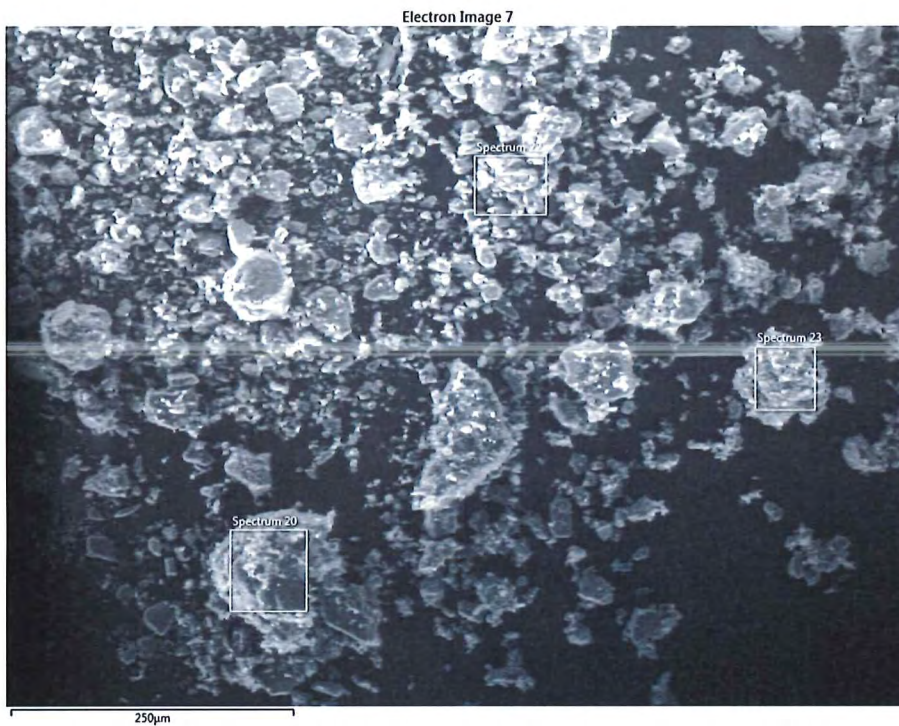


Figure 6b: SEM/EDX image of “Bulk Point 1, (170321-1b)”

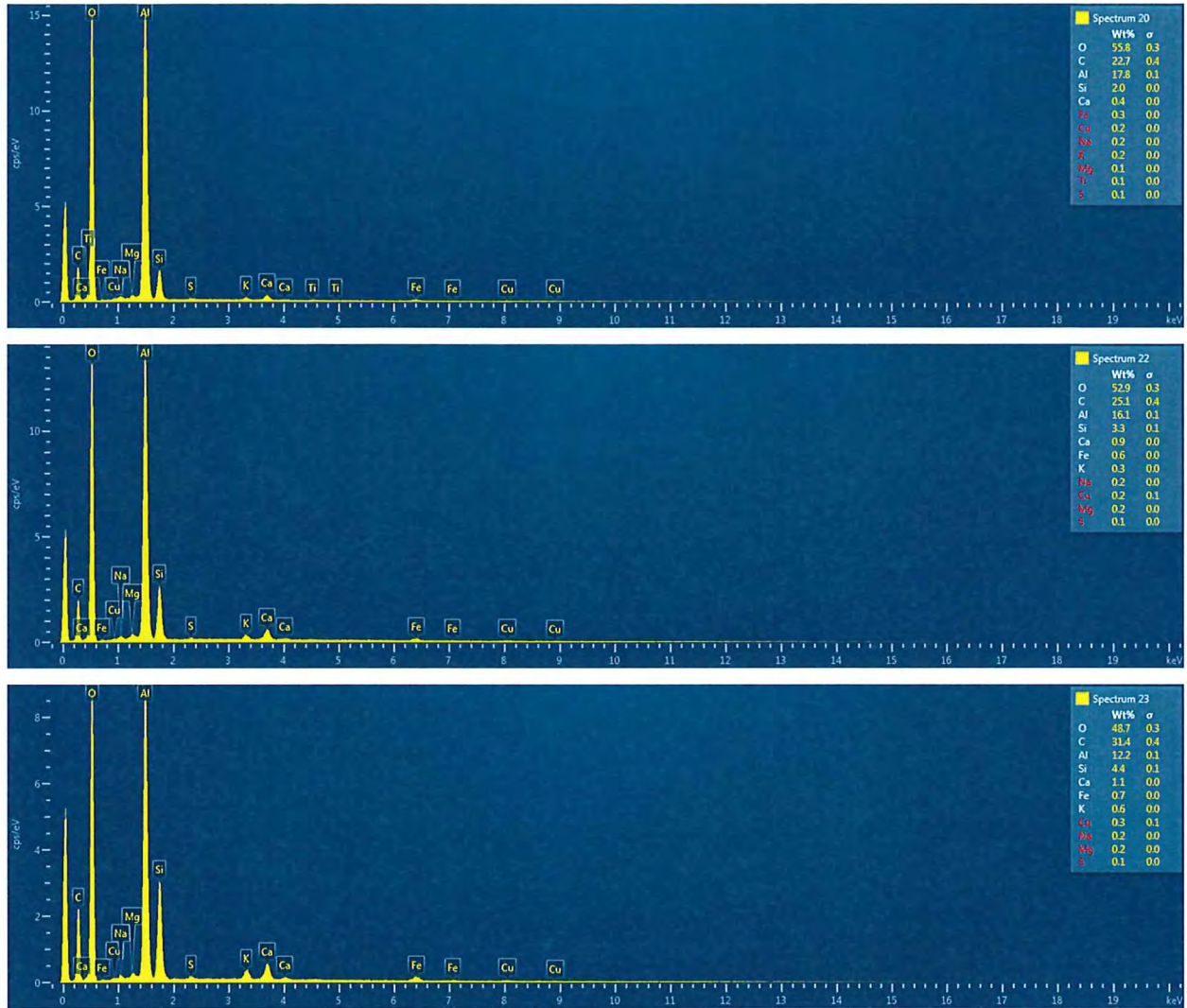


Figure 6c: EDX Spectrums 20, 22 and 23 - Elemental Compositions of “Bulk Point 1, (170321-1b)”

7. The SEM images and EDX spectrums of “Bulk Point 2, (170321-2b)” are displayed from Figure 7a to 7c.

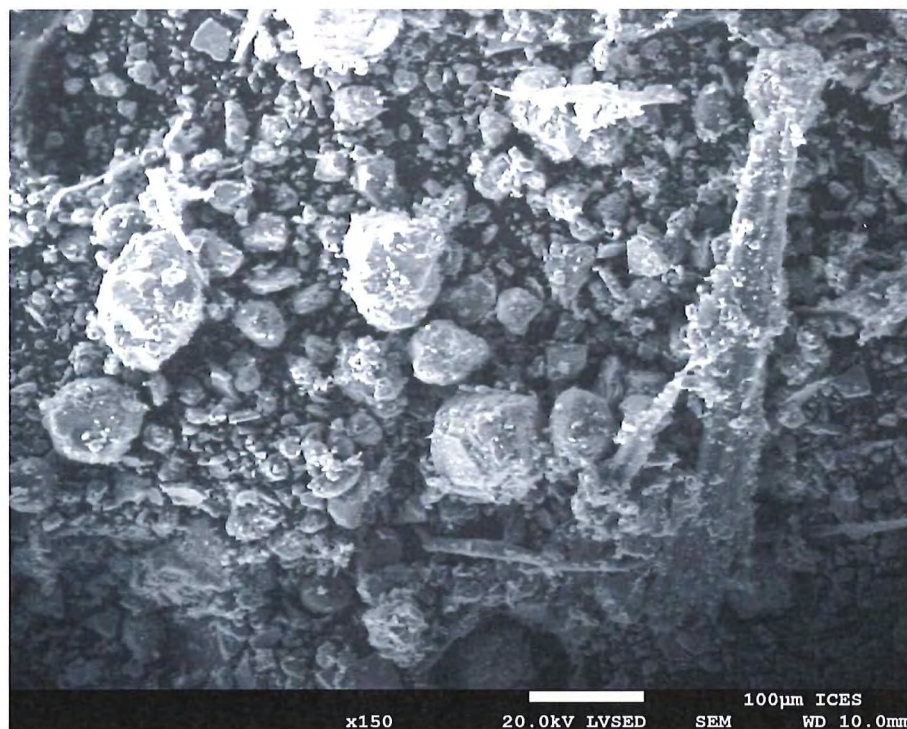


Figure 7a: SEM image of “Bulk Point 2, (170321-2b)”

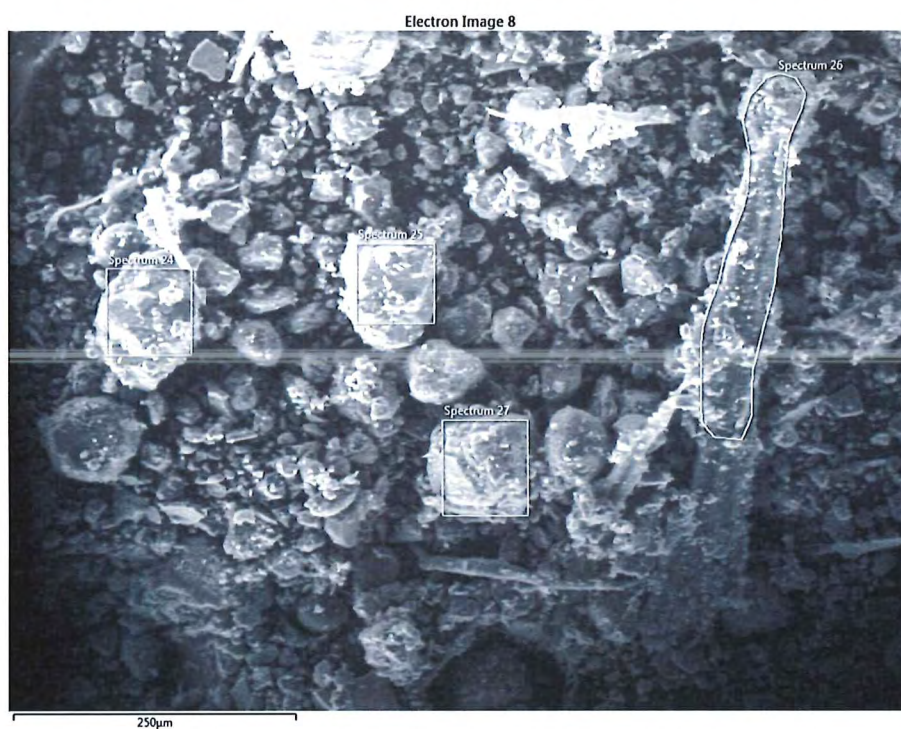


Figure 7b: SEM/EDX image of “Bulk Point 2, (170321-2b)”

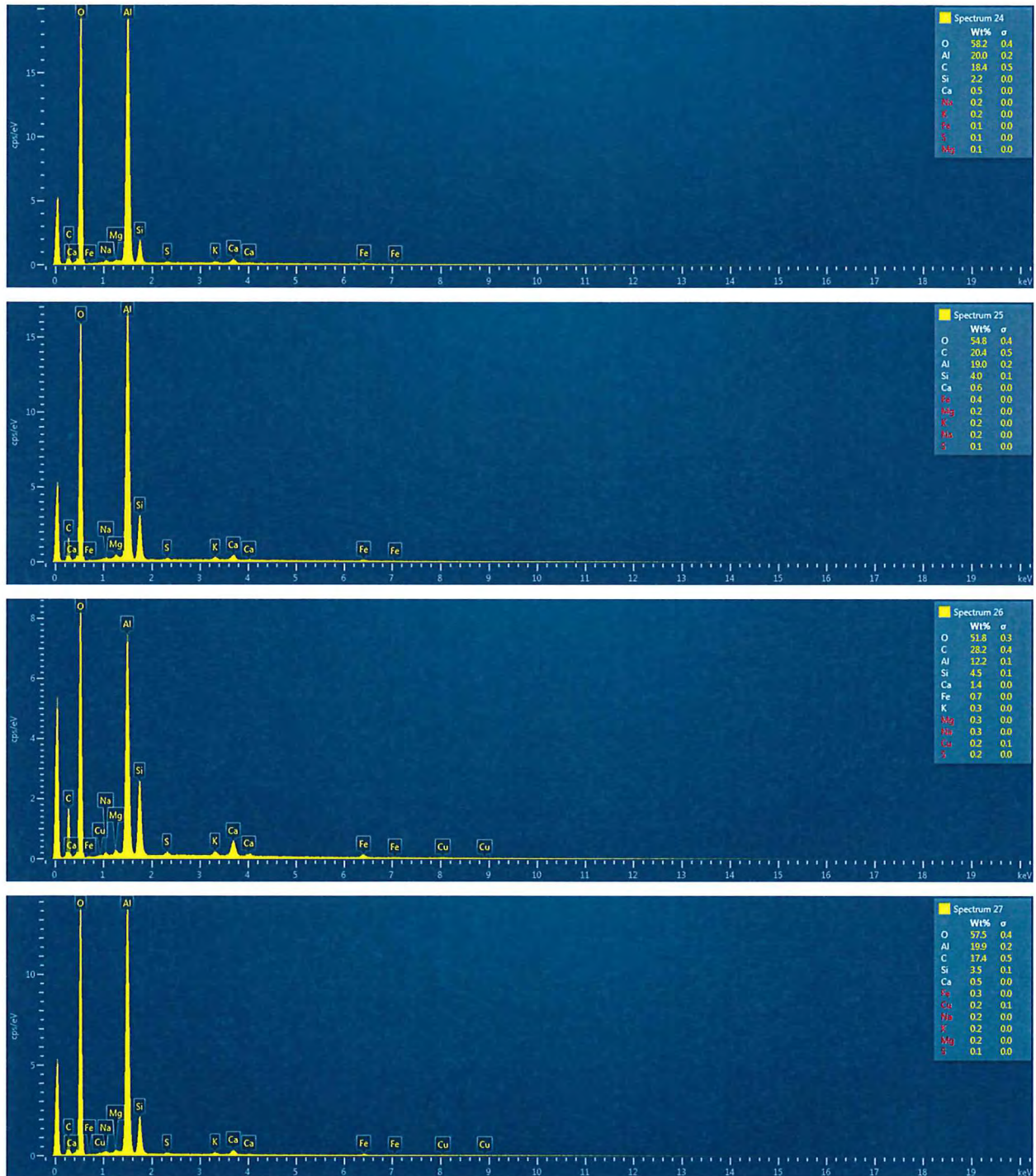


Figure 7c: EDX Spectra 24 to 27 - Elemental Compositions of "Bulk Point 2, (170321-2b)"

8. The SEM images and EDX spectrums of “Bulk Point 3, (170321-3b)” are displayed from Figure 8a to 8c.

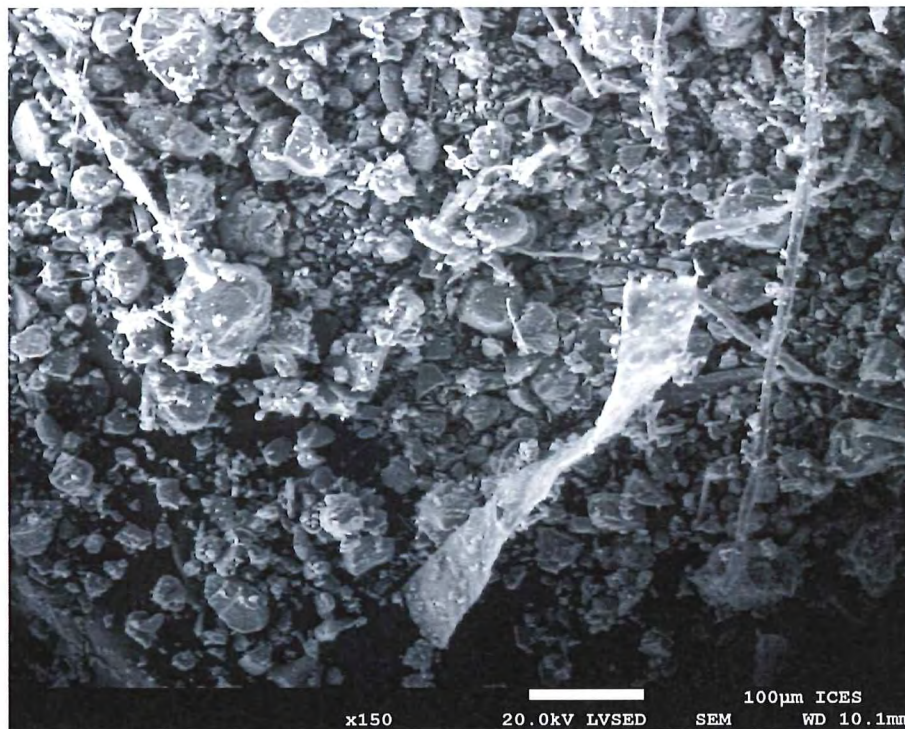


Figure 8a: SEM image of “Bulk Point 3, (170321-3b)”

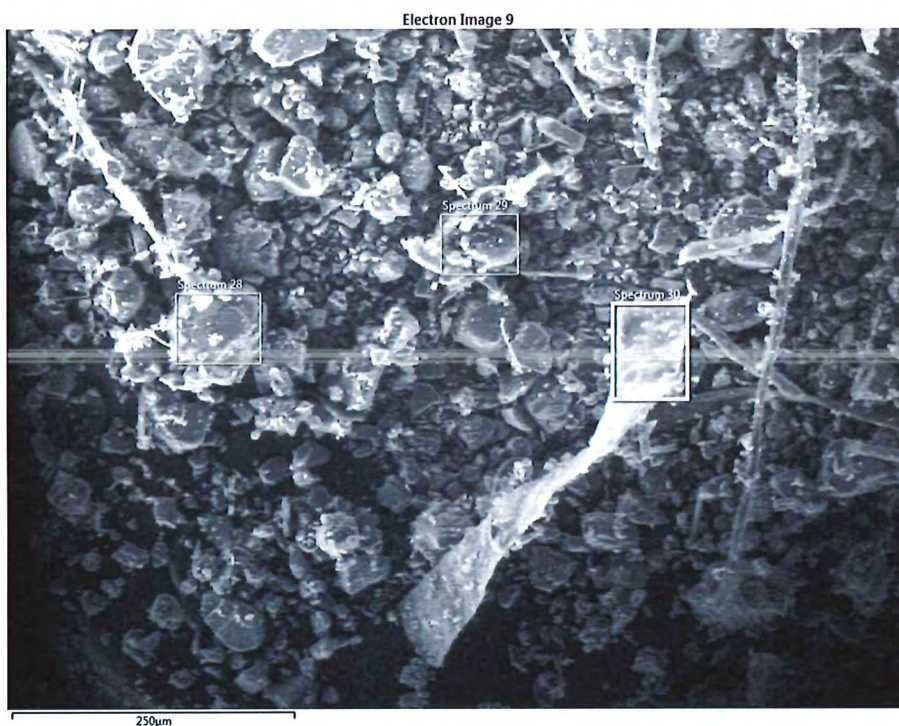


Figure 8b: SEM/EDX image of “Bulk Point 3, (170321-3b)”

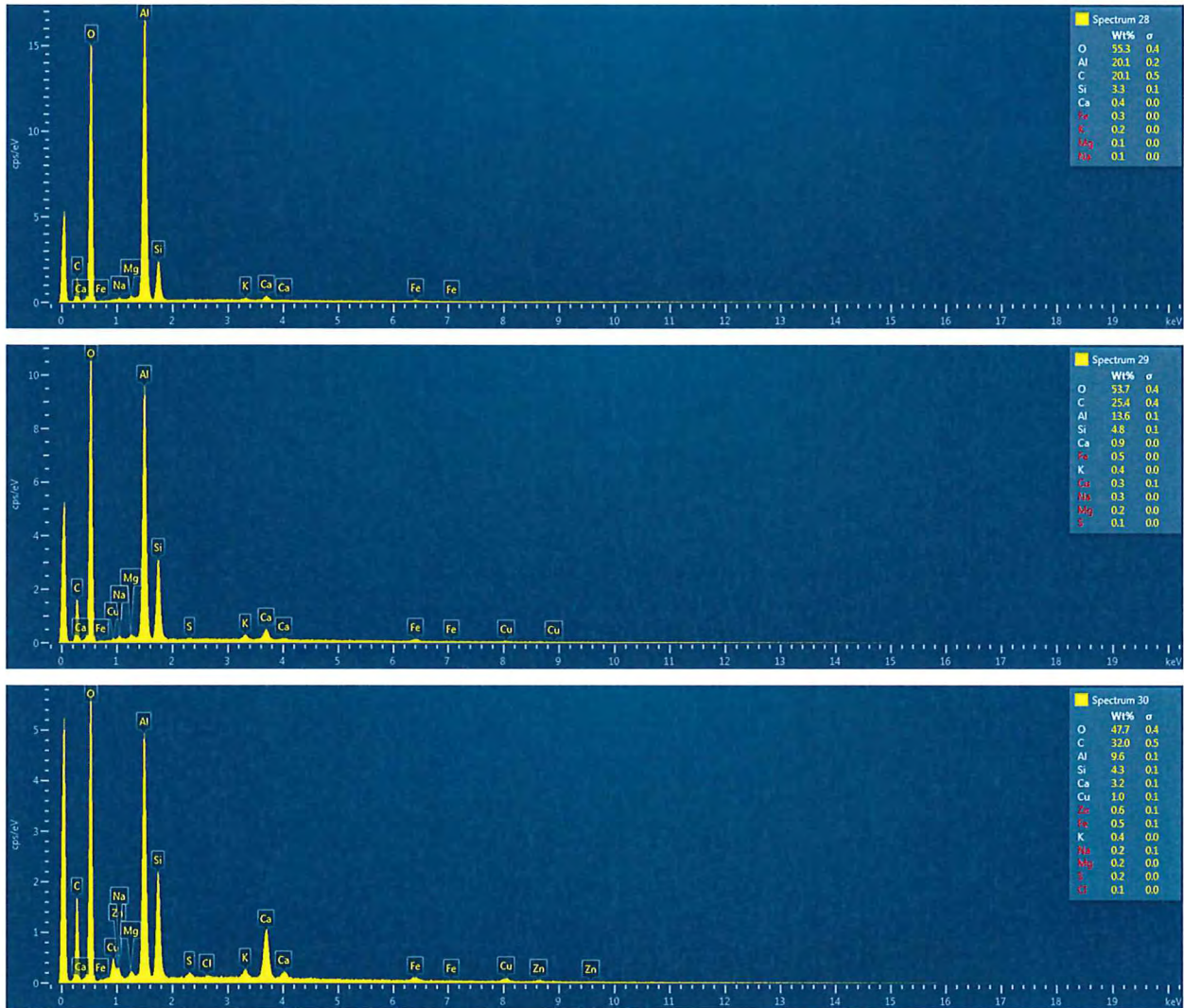


Figure 8c: EDX Spectrums 28 to 30 - Elemental Compositions of "Bulk Point 3, (170321-3b)"

9. The SEM images and EDX spectrums of “Bulk (Under Pallet) 4, (170321-4b)” are displayed from Figure 9a to 9c.

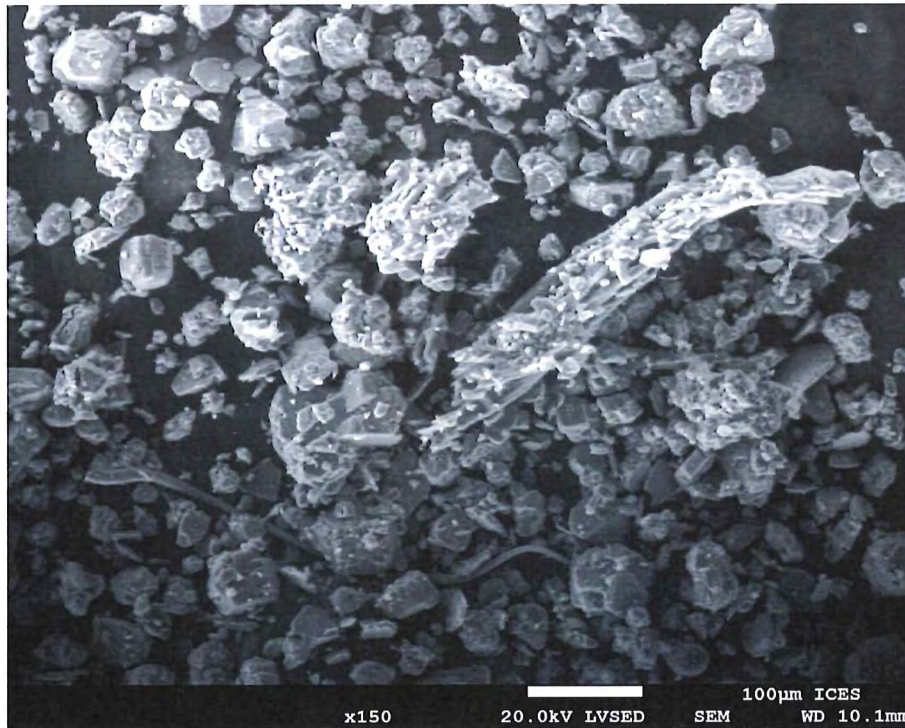


Figure 9a: SEM image of “Bulk (Under Pallet) 4, (170321-4b)”

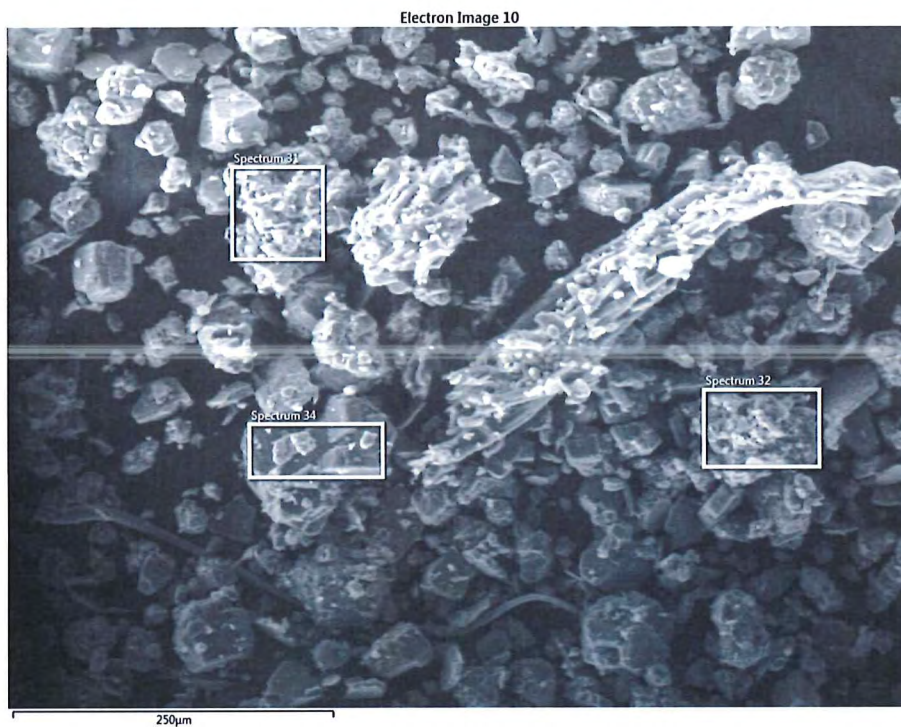


Figure 9b: SEM/EDX image of “Bulk (Under Pallet) 4, (170321-4b)”

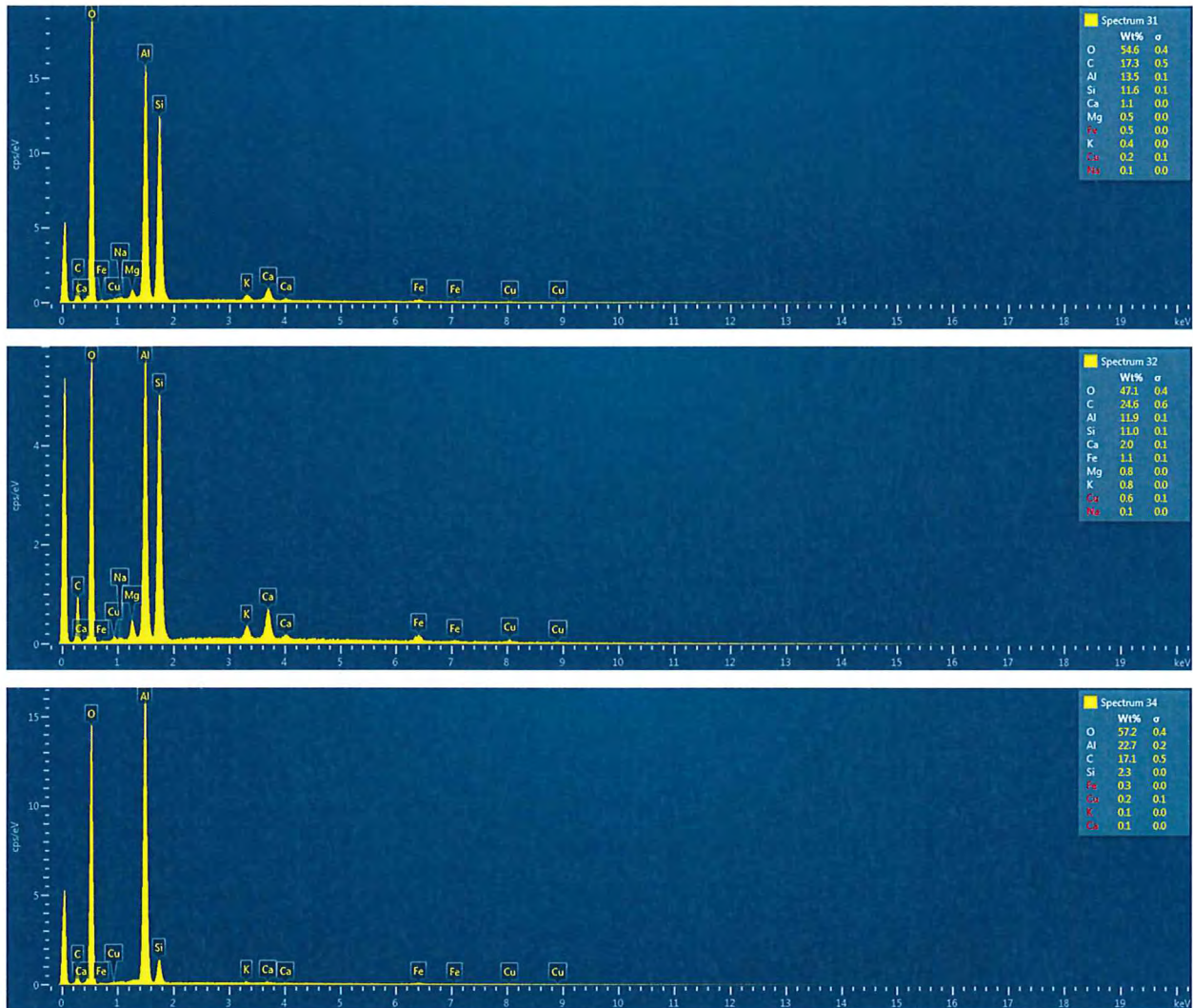


Figure 9c: EDX Spectra 31, 32 and 34 - Elemental Compositions of “Bulk (Under Pallet) 4, (170321-4b)”

10. The SEM images and EDX spectrums of “Bulk (Platform) 5, (170321-5b)” are displayed from Figure 10a to 10c.

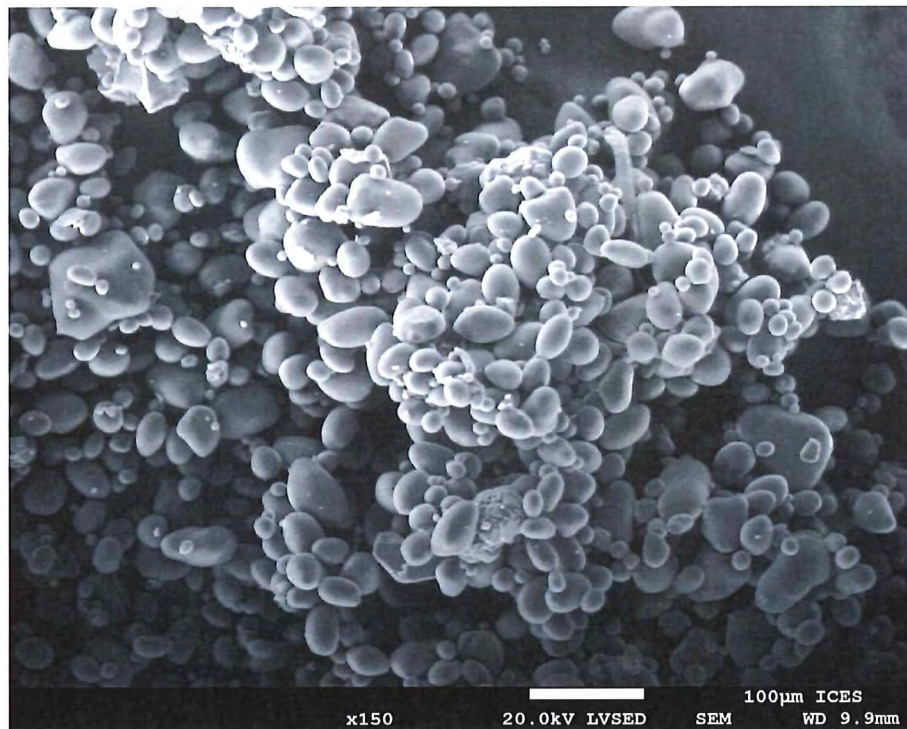


Figure 10a: SEM image of “Bulk (Platform) 5, (170321-5b)”

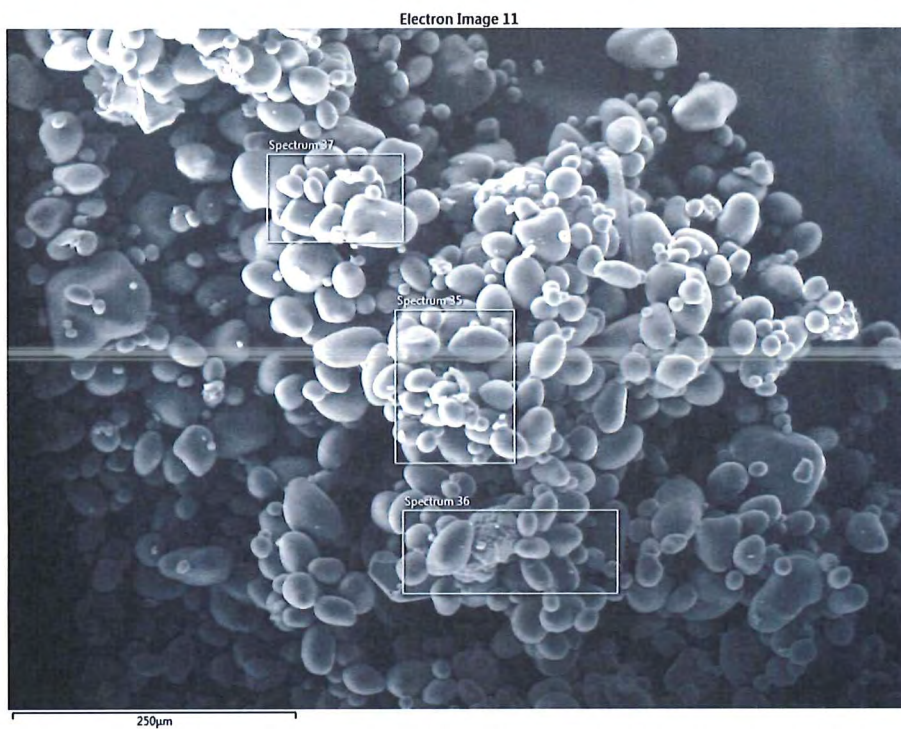


Figure 10b: SEM/EDX image of “Bulk (Platform) 5, (170321-5b)”

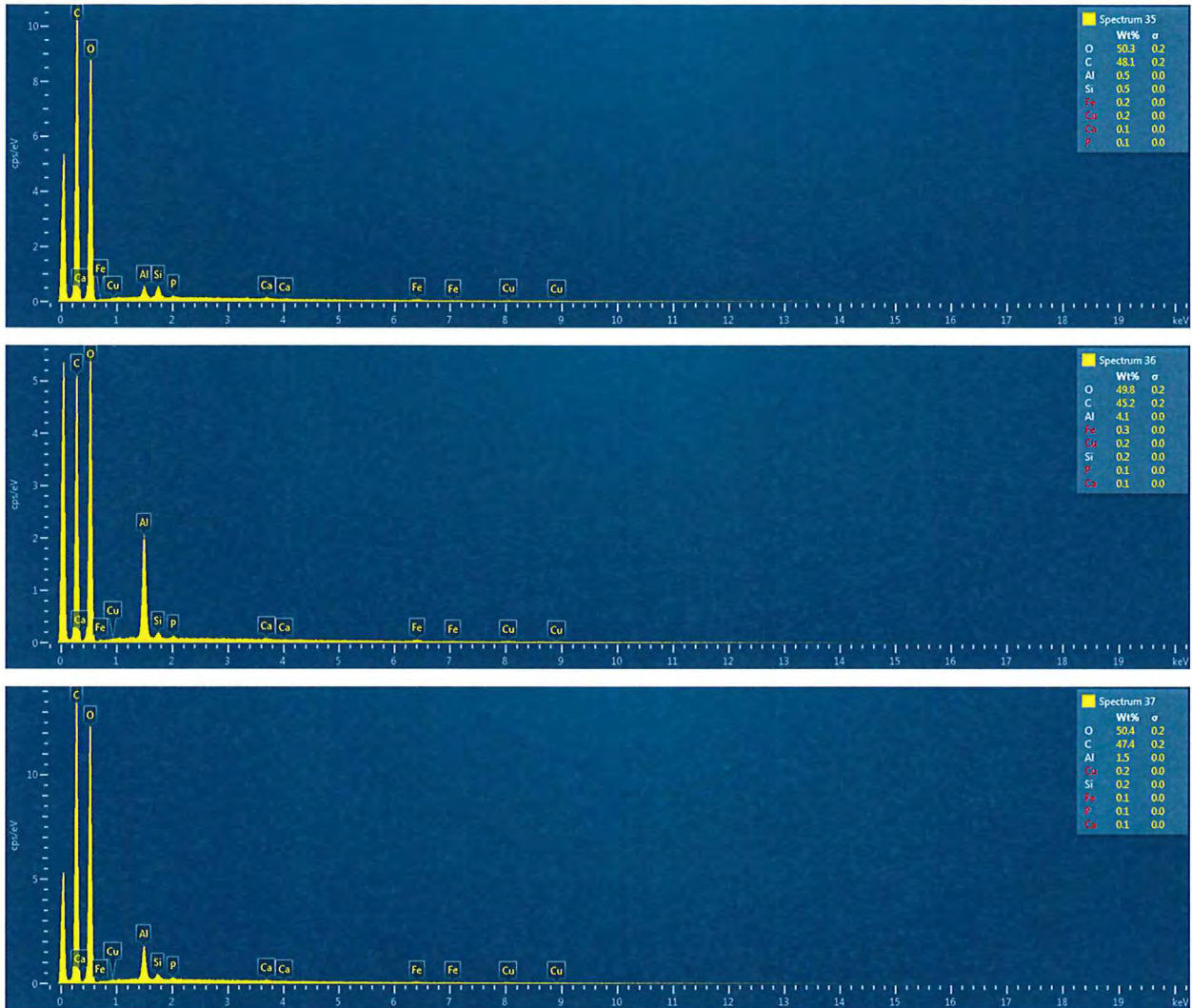


Figure 10c: EDX Spectrums 35, 36 and 37 - Elemental Compositions of “Bulk (Platform) 5, (170321-5b)”

11. The SEM images and EDX spectrums of “Bulk (Outside Toilet) 6, (170321-6b)” are displayed from Figure 11a to 11c.

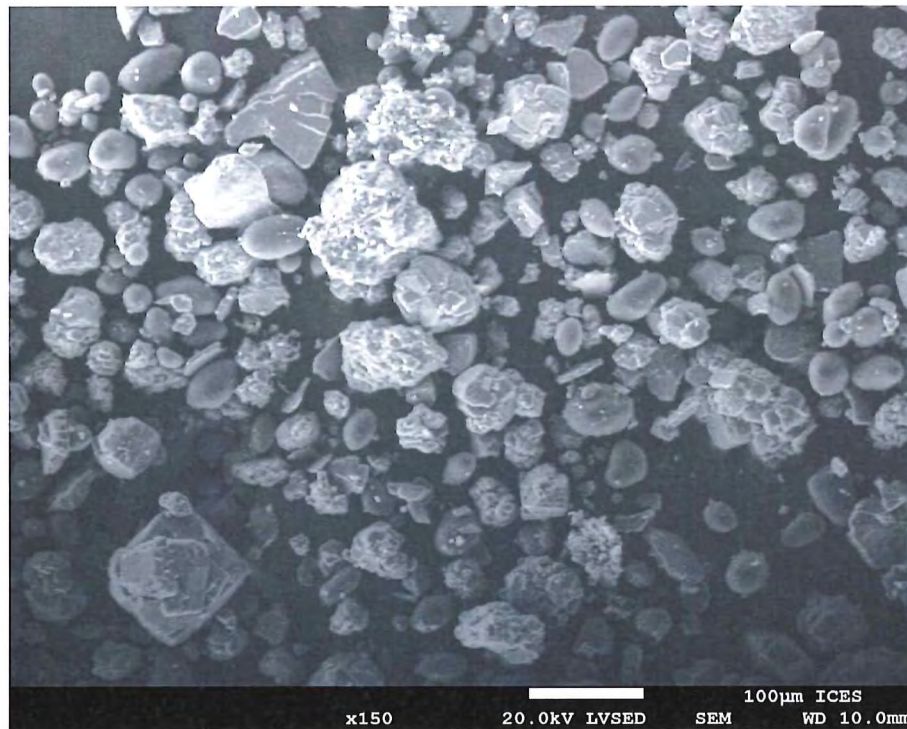


Figure 11a: SEM image of “Bulk (Outside Toilet) 6, (170321-6b)”

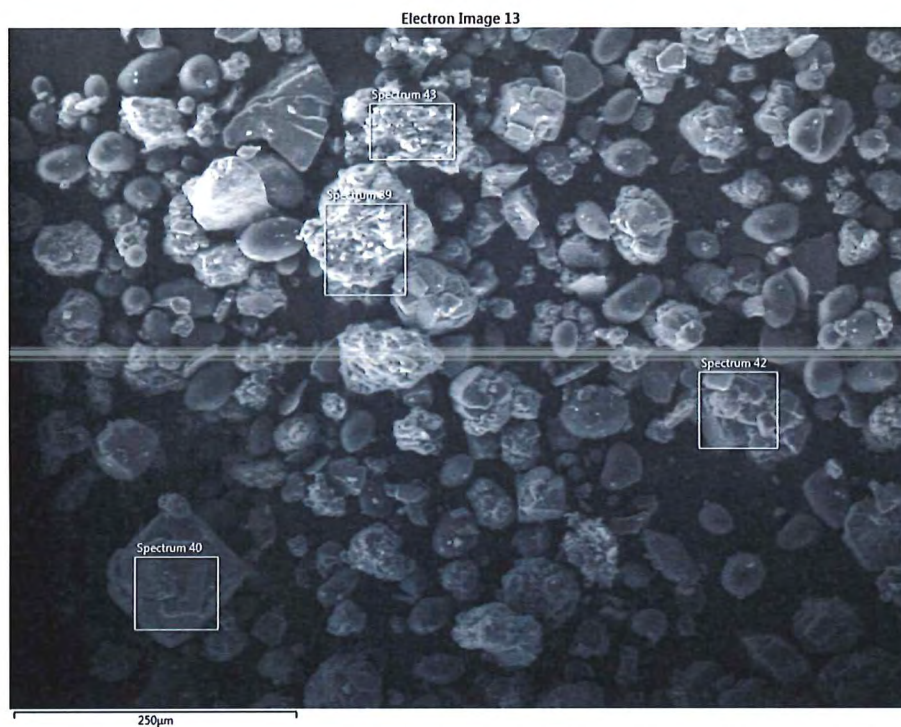


Figure 11b: SEM/EDX image of “Bulk (Outside Toilet) 6, (170321-6b)”

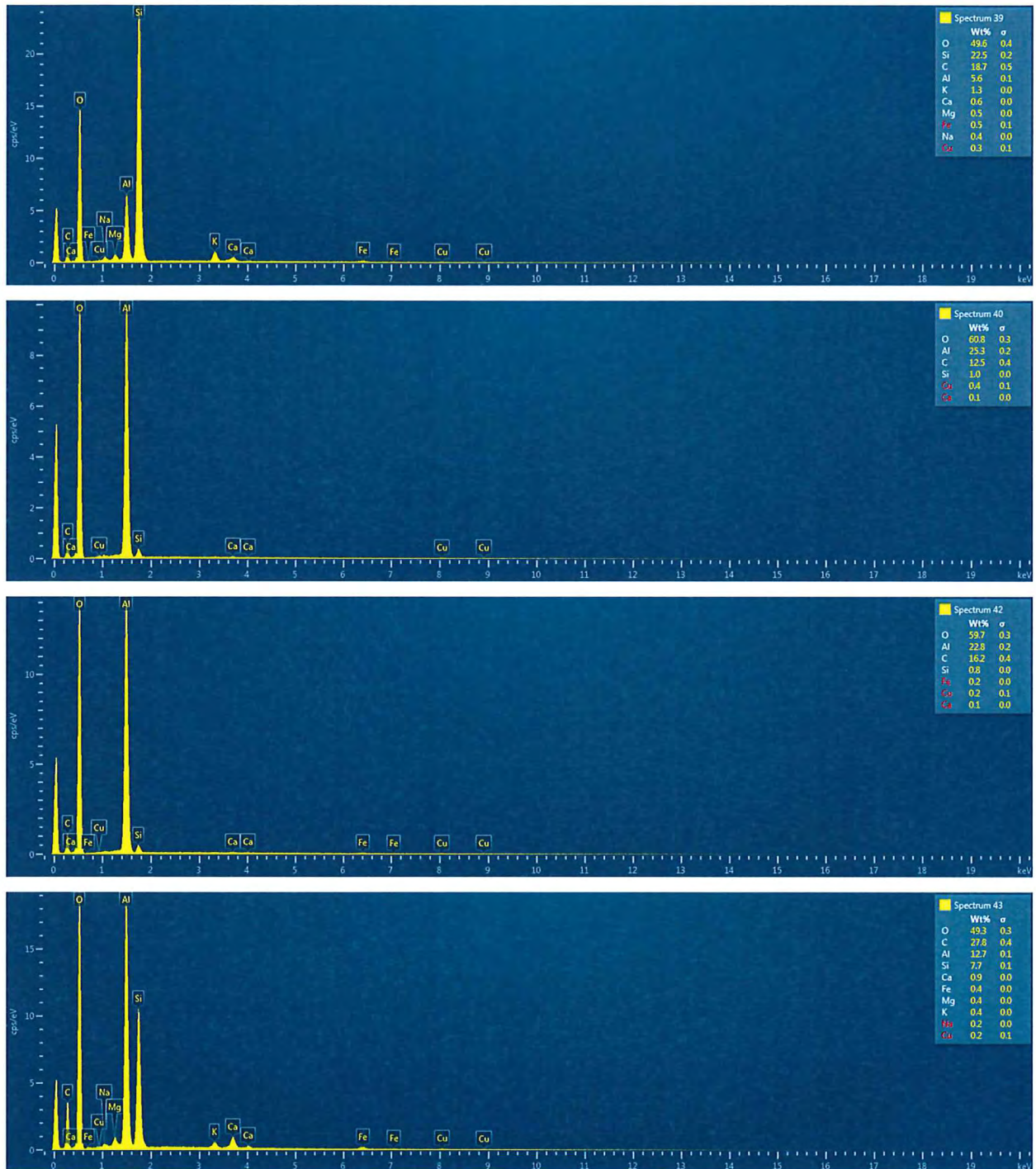


Figure 11c: EDX Spectrums 39, 40, 42 and 43 - Elemental Compositions of “Bulk (Outside Toilet 6, (170321-6b)”

12. The SEM images and EDX spectrums of “Bulk (Aluminium Dihydrogen Phosphate), (170321-7b)” are displayed from Figure 12a to 12c.

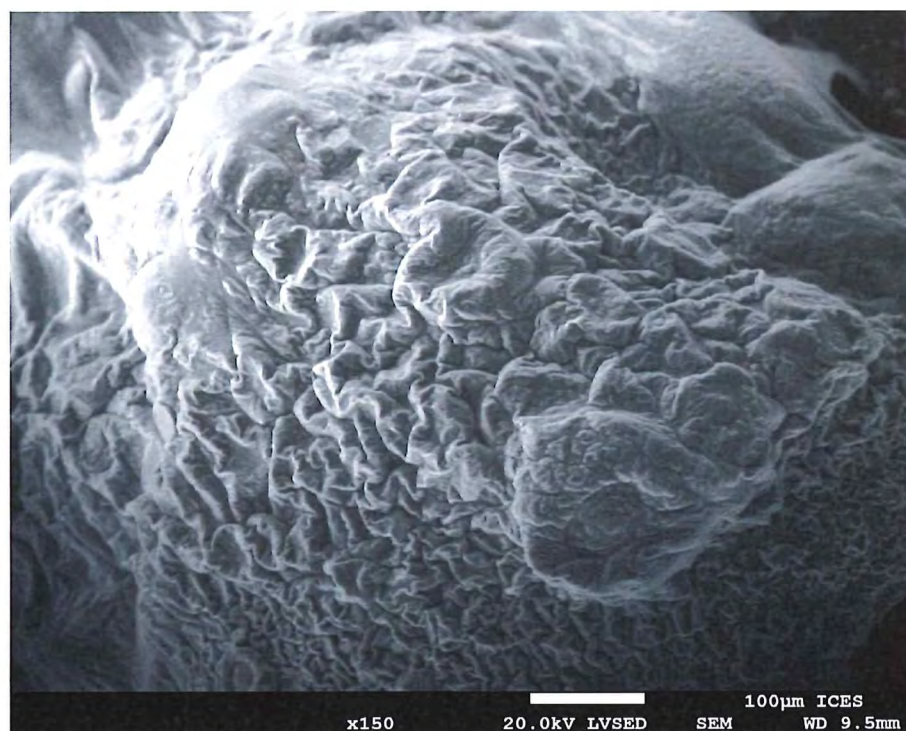


Figure 12a: SEM image of “Bulk (Aluminium Dihydrogen Phosphate), (170321-7b)”

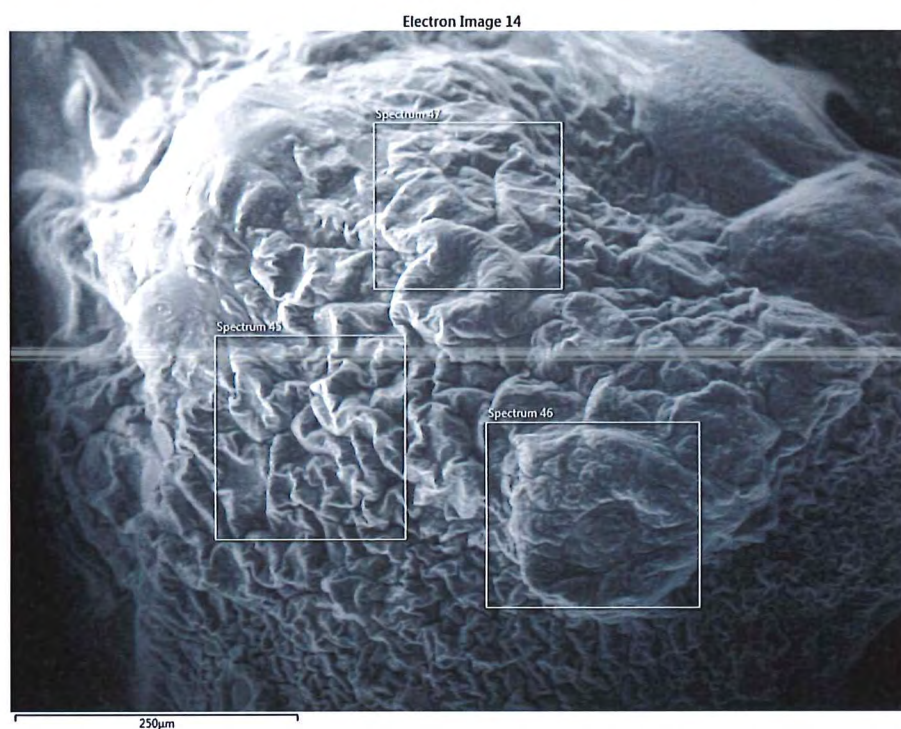


Figure 12b: SEM/EDX image of “Bulk (Aluminium Dihydrogen Phosphate), (170321-7b)”

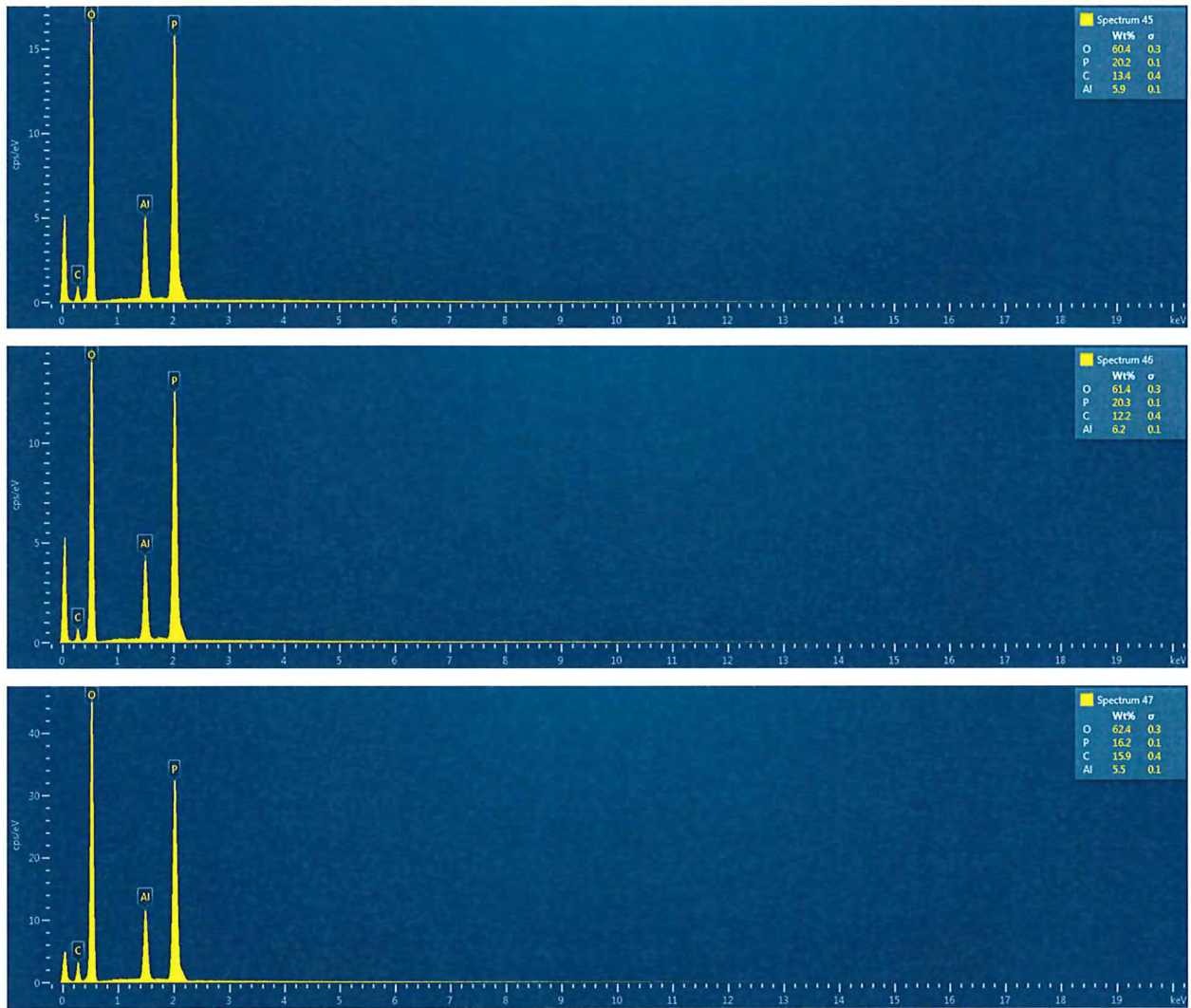


Figure 12c: EDX Spectrums 45 to 47 - Elemental Compositions of “Bulk (Aluminium Dihydrogen Phosphate), (170321-7b)”

13. The SEM images and EDX spectrums of “Bulk (Boric Acid), (170321-8b)” are displayed from Figure 13a to 13c.

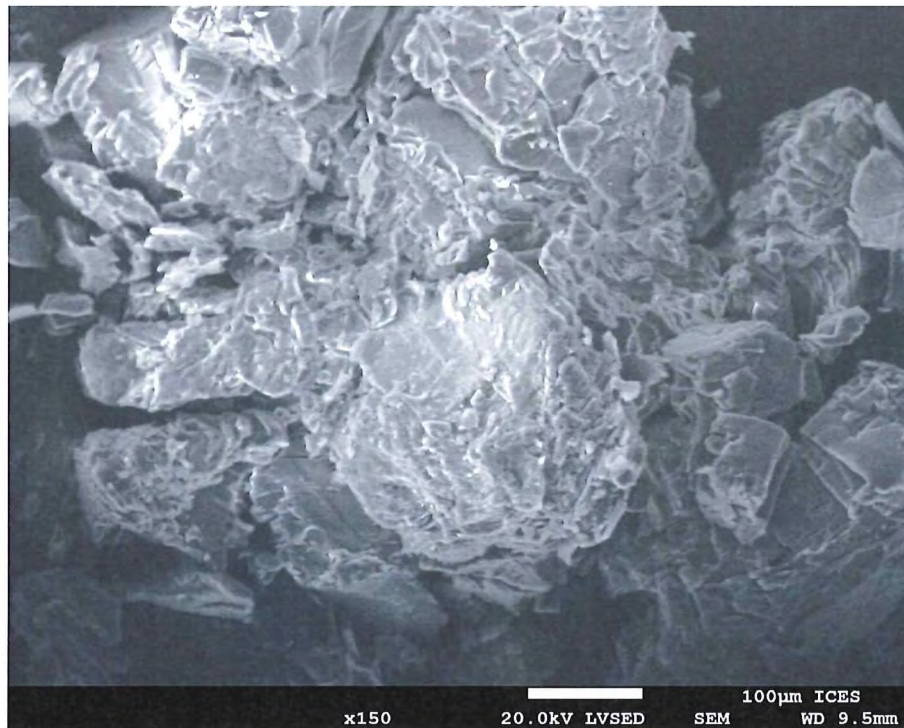


Figure 13a: SEM image of “Bulk (Boric Acid), (170321-8b)”



Figure 13b: SEM/EDX image of “Bulk (Boric Acid), (170321-8b)”

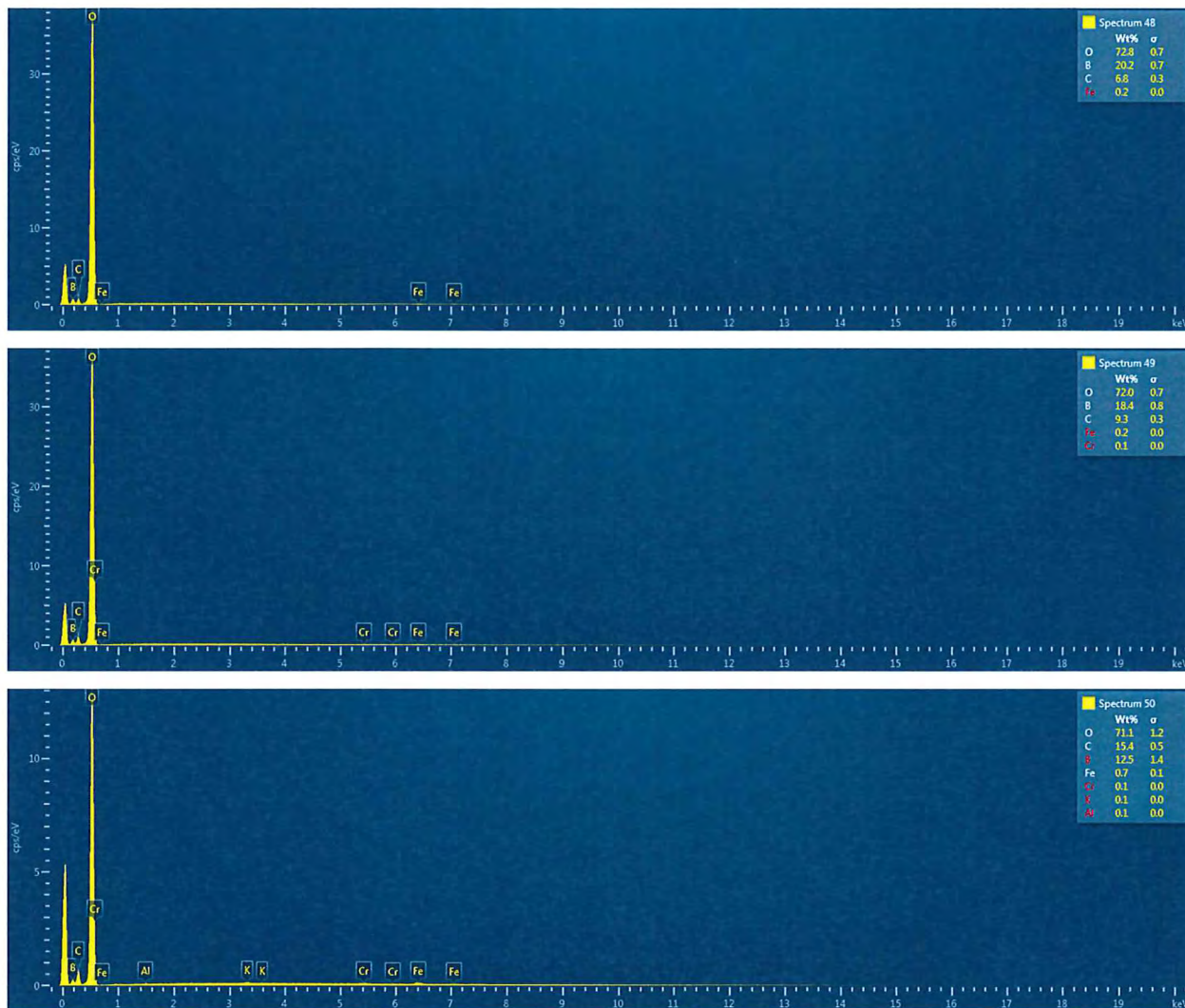


Figure 13c: EDX Spectrums 48 to 50 - Elemental Compositions of “Bulk (Boric Acid), (170321-8b)”

14. The SEM images and EDX spectrums of “Bulk (Clay), (170321-9b)” are displayed from Figure 14a to 14c.

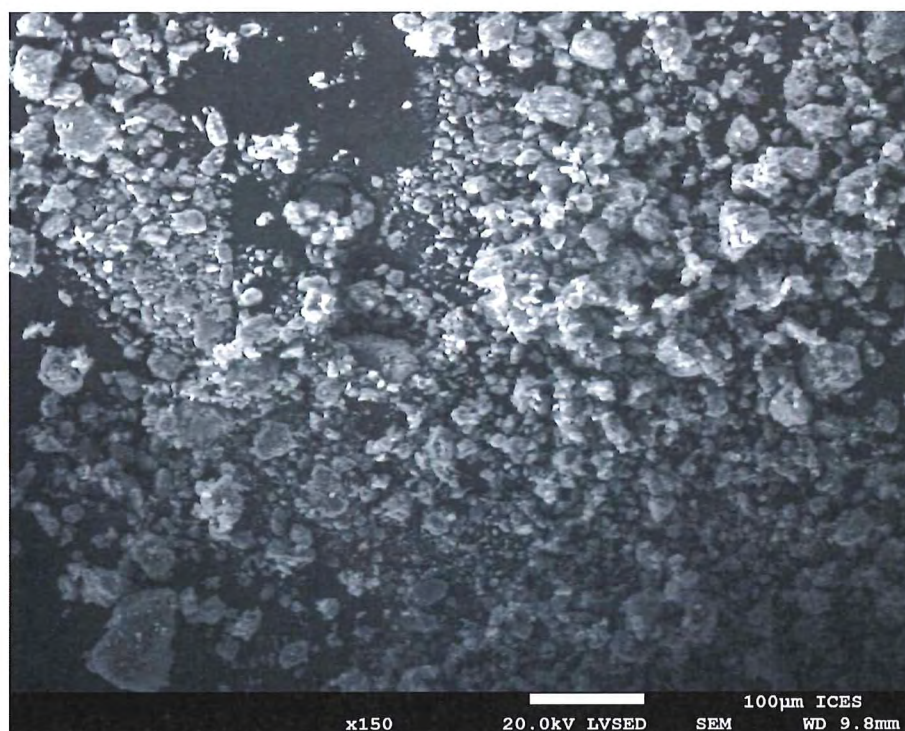


Figure 14a: SEM image of “Bulk (Clay), (170321-9b)”



Figure 14b: SEM/EDX image of “Bulk (Clay), (170321-9b)”

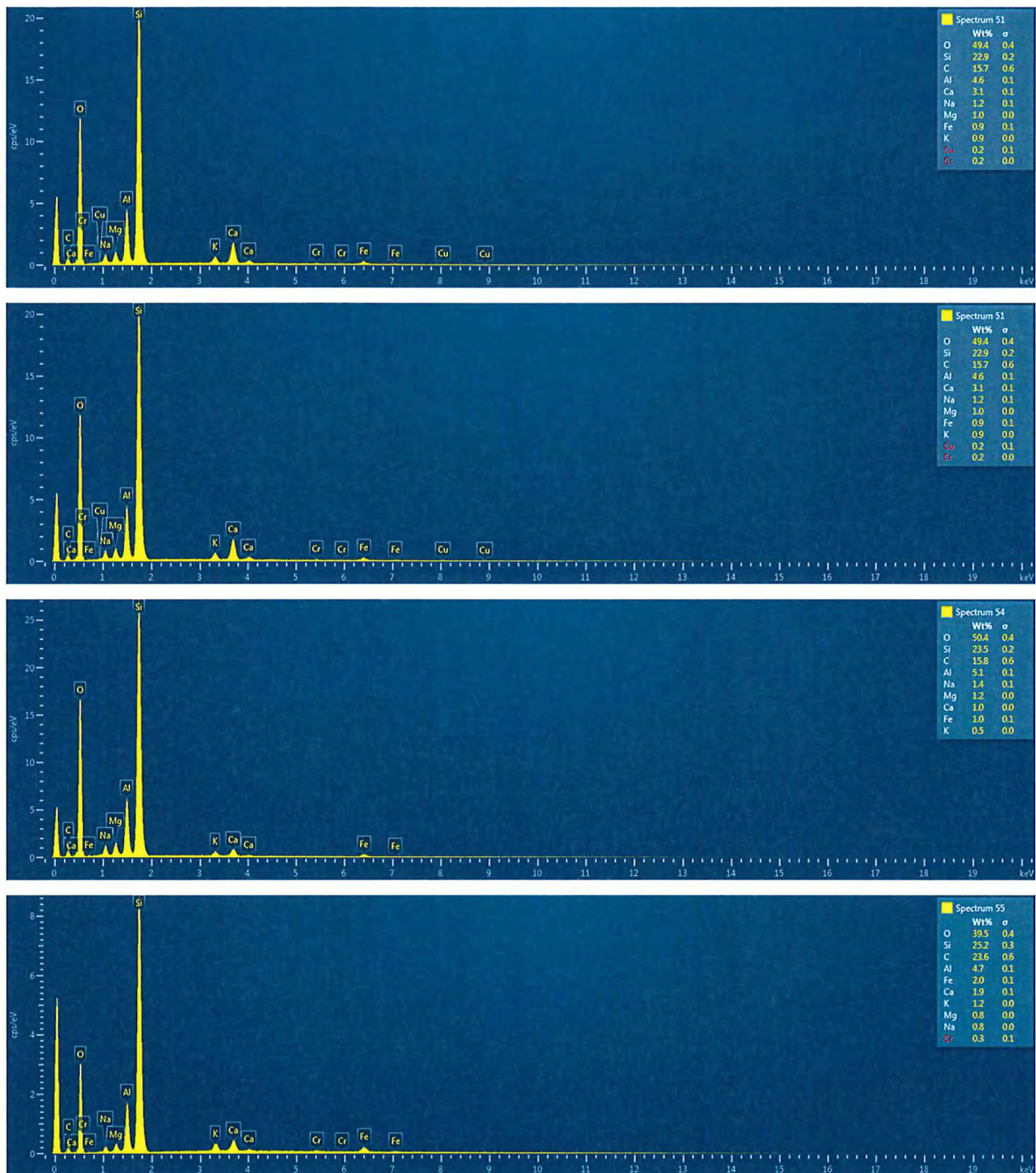


Figure 14c: EDX Spectrums 51, 52, 54 and 55 - Elemental Compositions of "Bulk (Clay, (170321-9b)"

Sample Name	Exhibit No.	SEM Image	EDX Spectrum	Elemental, (Semi-quantitative), Weight %													
				C	O	Na	P	Mg	Al	Si	K	Ca	Cr	Fe	Cu	Zn	Total
Bulk	250221-1b	Figure 1a	Spectrum 2	51.9	47.7	-	0.1	-	-	-	0.0	-	-	0.2	-	-	100.0
			Spectrum 3	51.8	47.9	-	0.1	-	-	-	0.1	-	0.1	0.2	-	-	100.0
Bulk (Bulk Bag Left)	080321-1b	Figure 2a	Spectrum 4	10.6	60.4	0.4	-	-	22.7	5.1	0.2	0.2	-	0.5	-	-	100.0
			Spectrum 5	7.7	61.9	0.3	-	-	26.5	3.0	0.1	0.1	-	0.4	-	-	100.0
			Spectrum 6	17.7	50.7	0.9	-	0.8	9.4	17.8	0.8	0.7	0.1	1.2	-	-	100.0
Bulk (Bulk Bag Right)	080321-2b	Figure 3a	Spectrum 9	29.2	53.9	0.3	-	0.2	10.7	4.8	0.1	0.6	-	0.2	-	-	100.0
			Spectrum 10	28.9	55.5	0.3	-	0.2	9.5	4.8	0.1	0.5	-	0.2	-	-	100.0
			Spectrum 12	29.6	53.3	0.3	-	0.3	8.1	7.1	0.4	0.7	-	0.2	-	-	100.0
Bulk (Aluminium Hydroxide)	080321-3b	Figure 4a	Spectrum 13	14.4	60.6	0.2	-	-	24.5	-	-	-	-	0.3	-	-	100.0
			Spectrum 14	10.8	62.7	0.3	-	-	25.8	-	-	-	-	0.3	0.1	-	100.0
			Spectrum 16	6.0	61.5	0.2	-	-	31.0	-	-	-	0.1	0.5	0.4	0.3	100.0
			Spectrum 17	8.3	63.0	0.2	-	-	28.4	-	-	-	-	0.2	-	-	100.0

Sample Name	Exhibit No.	SEM Image	EDX Spectrum	Elemental, (Semi-quantitative), Weight %																
				C	O	Na	P	Mg	Al	Si	S	Cl	K	Ca	Ti	Fe	Cu	Zn	Total	
Bulk (Potato Starch)	080321-4b	Figure 5a	Spectrum 18	47.6	52.1	-	0.0	-	-	-	-	-	-	-	-	-	-	0.3	-	100.0
			Spectrum 19	49.1	50.4	0.1	0.1	-	0.1	-	-	-	-	-	-	-	-	-	0.2	-
Bulk Point 1	170321-1b	Figure 6a	Spectrum 20	22.7	55.8	0.2	-	0.1	17.8	2.0	0.1	-	0.2	0.4	0.1	0.4	0.2	-	-	100.0
			Spectrum 22	25.2	52.9	0.3	-	0.2	16.1	3.3	0.1	-	0.3	0.9	-	0.6	0.2	-	-	100.0
			Spectrum 23	31.5	48.7	0.2	-	0.2	12.2	4.4	0.1	-	0.6	1.1	-	0.7	0.3	-	-	100.0
Bulk Point 2	170321-2b	Figure 7a	Spectrum 24	18.4	58.2	0.2	-	0.1	20.0	2.2	0.1	-	0.2	0.5	-	0.2	-	-	-	100.0
			Spectrum 25	20.4	54.8	0.2	-	0.2	19.0	4.0	0.1	-	0.2	0.6	-	0.4	-	-	-	100.0
			Spectrum 26	28.2	51.8	0.3	-	0.3	12.2	4.5	0.2	-	0.3	1.4	-	0.7	0.2	-	-	100.0
			Spectrum 27	17.4	57.5	0.2	-	0.2	19.9	3.5	0.1	-	0.2	0.5	-	0.4	0.3	-	-	100.0
Bulk Point 3	170321-3b	Figure 8a	Spectrum 28	20.1	55.3	0.1	-	0.2	20.1	3.3	-	-	0.2	0.4	-	0.3	-	-	-	100.0
			Spectrum 29	25.4	53.7	0.3	-	0.2	13.6	4.8	0.1	-	0.4	0.9	-	0.5	0.3	-	-	100.0
			Spectrum 30	32.0	47.7	0.2	-	0.2	9.6	4.3	0.2	0.1	0.4	3.2	-	0.5	1.0	0.6	-	100.0

Sample Name	Exhibit No.	SEM Image	EDX Spectrum	Elemental, (Semi-quantitative), Weight %											
				C	O	Na	P	Mg	Al	Si	K	Ca	Fe	Cu	Total
Bulk (Under Pallet) 4	170321-4b	Figure 9a	Spectrum 31	17.3	54.6	0.2	-	0.5	13.5	11.6	0.5	1.2	0.5	0.2	100.0
			Spectrum 32	24.6	47.1	0.1	-	0.8	11.9	11.0	0.8	2.0	1.1	0.6	100.0
			Spectrum 34	17.1	57.2	-	-	-	22.7	2.3	0.1	0.1	0.3	0.2	100.0
Bulk (Platform) 5	170321-5b	Figure 10a	Spectrum 35	48.1	50.3	-	0.1	-	0.5	0.5	-	0.1	0.3	0.2	100.0
			Spectrum 36	45.2	49.8	-	0.1	-	4.2	0.2	-	0.1	0.3	0.2	100.0
			Spectrum 37	47.4	50.4	-	0.1	-	1.5	0.2	-	0.1	0.2	0.2	100.0
Bulk (Outside Toilet) 6	170321-6b	Figure 11a	Spectrum 39	18.7	49.6	0.5	-	0.5	5.6	22.5	1.3	0.6	0.5	0.3	100.0
			Spectrum 40	12.5	60.8	-	-	-	25.3	1.0	-	0.1	-	0.4	100.0
			Spectrum 42	16.2	59.7	-	-	-	22.8	0.8	-	0.1	0.2	0.2	100.0
			Spectrum 43	27.8	49.3	0.2	-	0.4	12.7	7.7	0.4	0.9	0.4	0.2	100.0

Sample Name	Exhibit No.	SEM Image	EDX Spectrum	Elemental, (Semi-quantitative), Weight %														
				C	O	B	Na	P	Mg	Al	Si	K	Ca	Cr	Fe	Cu	Total	
Bulk (Aluminium Dihydrogen Phosphate)	170321-7b	Figure 12a	Spectrum 45	13.4	60.4	-	-	20.2	-	5.9	-	-	-	-	-	-	100.0	
			Spectrum 46	12.2	61.4	-	-	20.3	-	6.2	-	-	-	-	-	-	-	100.0
			Spectrum 47	15.9	62.4	-	-	16.2	-	5.5	-	-	-	-	-	-	-	100.0
Bulk (Boric Acid)	170321-8b	Figure 13a	Spectrum 48	6.8	72.9	20.2	-	-	-	-	-	-	-	-	0.2	-	100.0	
			Spectrum 49	9.3	72.0	18.4	-	-	-	-	-	-	-	0.1	0.2	-	100.0	
			Spectrum 50	15.4	71.1	12.5	-	-	-	0.1	-	0.1	-	0.1	0.7	-	100.0	
Bulk (Clay)	170321-9b	Figure 14a	Spectrum 51	15.7	49.4	-	1.2	-	1.0	4.6	22.9	0.9	3.1	0.2	0.9	0.2	100.0	
			Spectrum 52	20.4	46.1	-	1.1	-	0.8	4.4	23.9	1.3	0.9	0.2	1.0	-	100.0	
			Spectrum 54	15.8	50.4	-	1.4	-	1.2	5.1	23.5	0.5	1.0	-	1.0	-	100.0	
			Spectrum 55	23.6	39.5	-	0.8	-	0.9	4.7	25.2	1.2	1.9	0.3	2.0	-	100.0	

Table 1: Semi-Quantitative Elemental Composition of Powder Specimens

TESTED BY:

Mr. Andrew Lim
Senior Research Engineer
Analytics & Characterisation



APPROVED BY:

Dr. Brendan Burkett
Head
Scientific Infrastructure & Analytics



Note: This report shall not be reproduced except in full, without written approval from ICES. This report does not constitute an endorsement of any item or material tested and must not be used for any publicity materials, and/or for advertising purposes without approval from ICES. Test results relate only to sample(s) submitted by the client for technical studies and shall not be used for any purpose of technical litigation.

REPORT

REPORT REFERENCE: ICES/AC/21013_Part2a **DATE:** 19th Apr 2021

SUBJECT: SDT Analysis on powder samples

COMPANY: ICES, A*STAR
1, Pesek Road, Jurong Island,
Singapore 627833

ATTENTION: Dr. Shaik Salim

DATE SAMPLE RECEIVED: 1st Apr 2021

DATE ANALYSED: 13th Apr 2021

DATE TEST COMPLETED: 16th Apr 2021

DESCRIPTION OF SAMPLE(S):

14 powder samples (~5-10g each) were received.

S/N	Sample Description	Exhibit No.
1	Bulk	250221-1b
2	Bulk (Bulk Bag Left)	080321-1b
3	Bulk (Bulk Bag Right)	080321-2b
4	Bulk (Aluminium Hydroxide)	080321-3b
5	Bulk (Potato Starch)	080321-4b
6	Bulk Point 1	170321-1b
7	Bulk Point 2	170321-2b

S/N	Sample Description	Exhibit No.
8	Bulk Point 3	170321-3b
9	Bulk (Under Pallet) 4	170321-4b
10	Bulk (Platform) 5	170321-5b
11	Bulk (Outside Toilet) 6	170321-6b
12	Bulk (Aluminium Dihydrogen Phosphate)	170321-7b
13	Bulk (Boric Acid)	170321-8b
14	Bulk (Clay)	170321-9b

METHOD OF TEST:

Standard test method for compositional analysis by thermogravimetry – SDT method as per ASTM E1131-20. Perform SDT analysis as received using TA SDT Q600 and test according to test condition.

Test condition: Heat from 30°C to 800°C, ramp rate 10°C/min in N₂

RESULTS:

S/N	Sample Description	Exhibit No.	Weight Loss % 30°C to 200°C	Weight Loss % 200°C to 800°C	Residue %	Ref
1	Bulk	250221-1b	17.26	52.89	10.53	Fig 1
5	Bulk (Potato Starch)	080321-4b	8.98	67.64	13.83	Fig 5
10	Bulk (Platform) 5	170321-5b	10.36	67.79	12.60	Fig 10

S/N	Sample Description	Exhibit No.	Weight Loss % 30°C to 250°C	Weight Loss % 250°C to 350°C	Weight Loss % 350°C to 800°C	Residue %	Ref
2	Bulk (Bulk Bag Left)	080321-1b	3.02	19.37	5.60	69.38	Fig 2
4	Bulk (Aluminium Hydroxide)	080321-3b	3.90	24.11	6.69	65.29	Fig 4

S/N	Sample Description	Exhibit No.	Weight Loss % 30°C to 200°C	Weight Loss % 200°C to 250°C	Weight Loss % 250°C to 350°C	Weight Loss % 250°C to 350°C	Weight Loss % 250°C to 350°C	Residue %	Ref
3	Bulk (Bulk Bag Right)	080321 -2b	16.04	2.89	15.56	3.34	4.63	49.45	Fig 3

S/N	Sample Description	Exhibit No.	Weight Loss % 30°C to 250°C	Weight Loss % 250°C to 320°C	Weight Loss % 320°C to 450°C	Weight Loss % 450°C to 600°C	Weight Loss % 600°C to 800°C	Residue %	Ref
6	Bulk Point 1	170321 -1b	3.54	20.66	4.02	3.31	2.44	65.13	Fig 6
7	Bulk Point 2	170321 -2b	4.53	21.62	3.89	3.73	2.30	62.75	Fig 7
8	Bulk Point 3	170321 -3b	4.83	21.70	3.50	3.76	1.93	63.70	Fig 8

S/N	Sample Description	Exhibit No.	Weight Loss % 30°C to 248°C	Weight Loss % 248°C to 308°C	Weight Loss % 308°C to 450°C	Weight Loss % 450°C to 600°C	Weight Loss % 600°C to 800°C	Residue %	Ref
9	Bulk (Under Pallet) 4	170321 -4b	4.27	17.41	3.68	3.46	1.84	67.19	Fig 9

S/N	Sample Description	Exhibit No.	Weight Loss % 30°C to 250°C	Weight Loss % 250°C to 300°C	Weight Loss % 300°C to 450°C	Weight Loss % 450°C to 600°C	Weight Loss % 600°C to 800°C	Residue %	Ref
11	Bulk (Outside Toilet) 6	170321 -6b	4.41	17.44	13.17	3.56	2.04	55.35	Fig 11

S/N	Sample Description	Exhibit No.	Weight Loss % 30°C to 125°C	Weight Loss % 125°C to 175°C	Weight Loss % 175°C to 200°C	Weight Loss % 200°C to 400°C	Weight Loss % 400°C to 800°C	Residue %	Ref
12	Aluminium Dihydrogen Phosphate	170321 -7b	2.11	1.50	0.72	10.53	4.44	77.08	Fig 12

S/N	Sample Description	Exhibit No.	Weight Loss % 30°C to 150°C	Weight Loss % 150°C to 800°C	Residue %	Ref
13	Bulk (Boric Acid)	170321-8b	28.88	15.22	55.90	Fig 13

S/N	Sample Description	Exhibit No.	Weight Loss % 30°C to 100°C	Weight Loss % 100°C to 800°C	Residue %	Ref
14	Bulk (Clay)	170321-9b	2.49	5.75	82.63	Fig 14

TESTED BY:

Mr. Yeo Wen Cong
Senior Research Engineer



APPROVED BY:

Mr. Andrew Lim
Team Leader
Analytics & Characterisation
Scientific Infrastructure & Analytics



Note: This report shall not be reproduced except in full, without written approval from ICES. This report does not constitute an endorsement of any item or material tested and must not be used for any publicity materials, and/or for advertising purposes without approval from ICES. Test results relate only to sample(s) submitted by the client for technical studies and shall not be used for any purpose of technical litigation.

Figure 1

Sample: Bulk
Size: 12.1840 mg
Comment: 2104T02_A1

File: C:\...Wen Cong\AR21\SDT10065\Bulk.001
Run Date: 13-Apr-2021 08:33
Instrument: SDT Q600 V20.9 Build 20

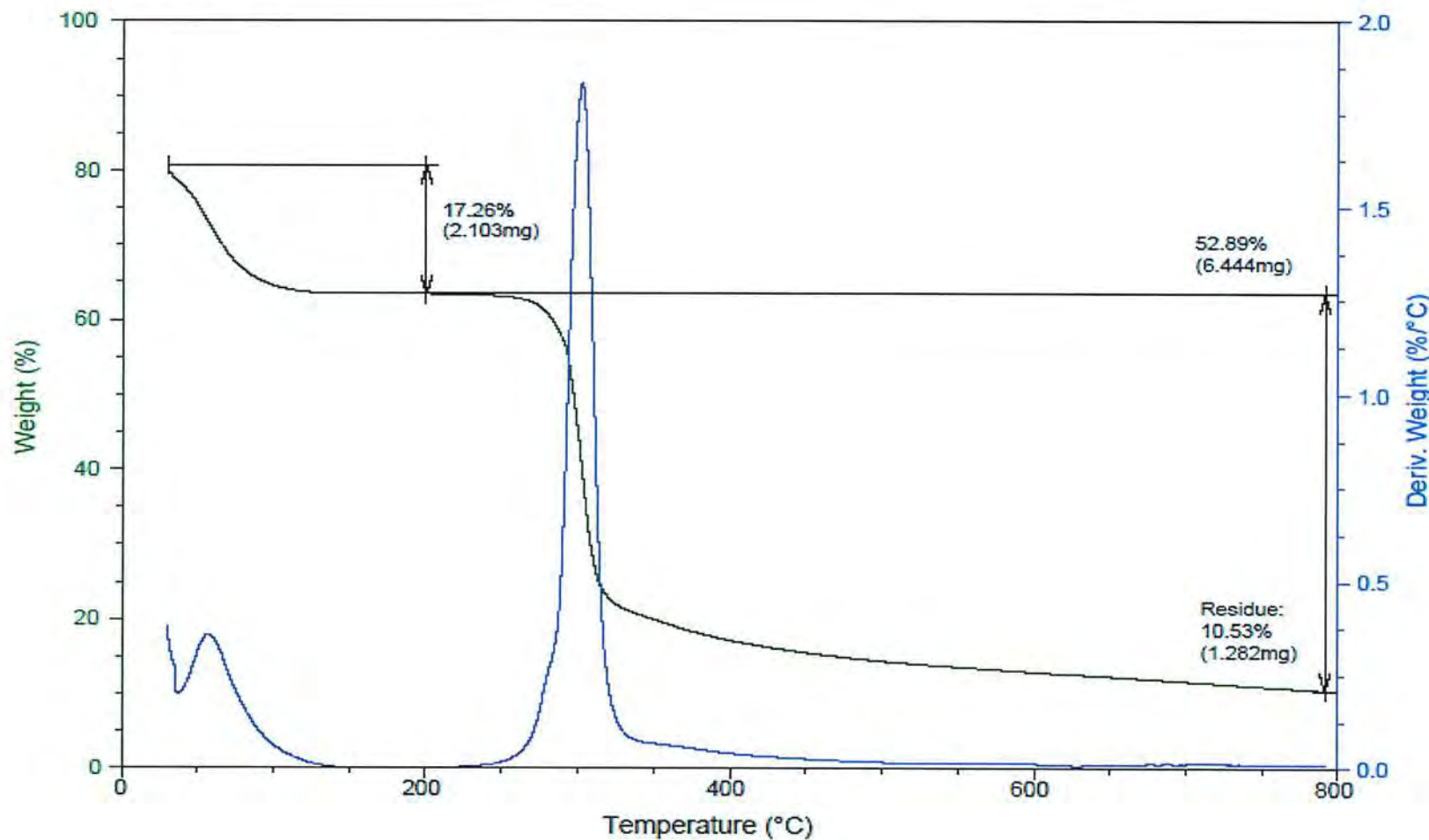


Figure 2

Sample: Bulk bag left
Size: 12.3810 mg
Comment: 2104T02_B1

File: C:\...VAR21SDT10065\Bulk bag left.001
Run Date: 13-Apr-2021 11:17
Instrument: SDT Q600 V20.9 Build 20

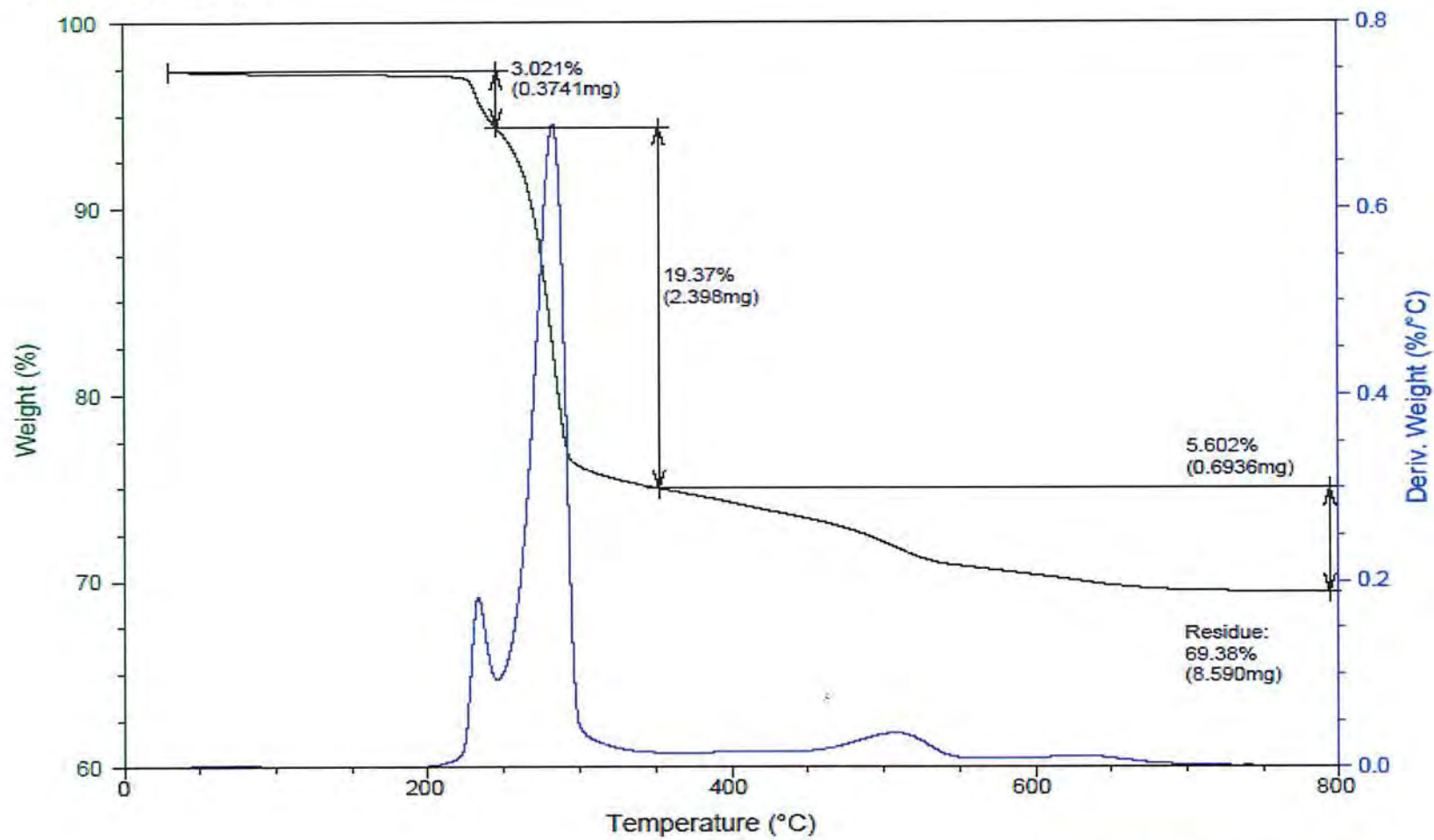


Figure 3

Sample: Bulk Bag Right
Size: 37.0230 mg

File: C:\... \AR21SDT10065\Bulk Bag Right.001
Run Date: 15-Apr-2021 15:31
Instrument: SDT Q600 V20.9 Build 20

Comment: 2104T02_C1

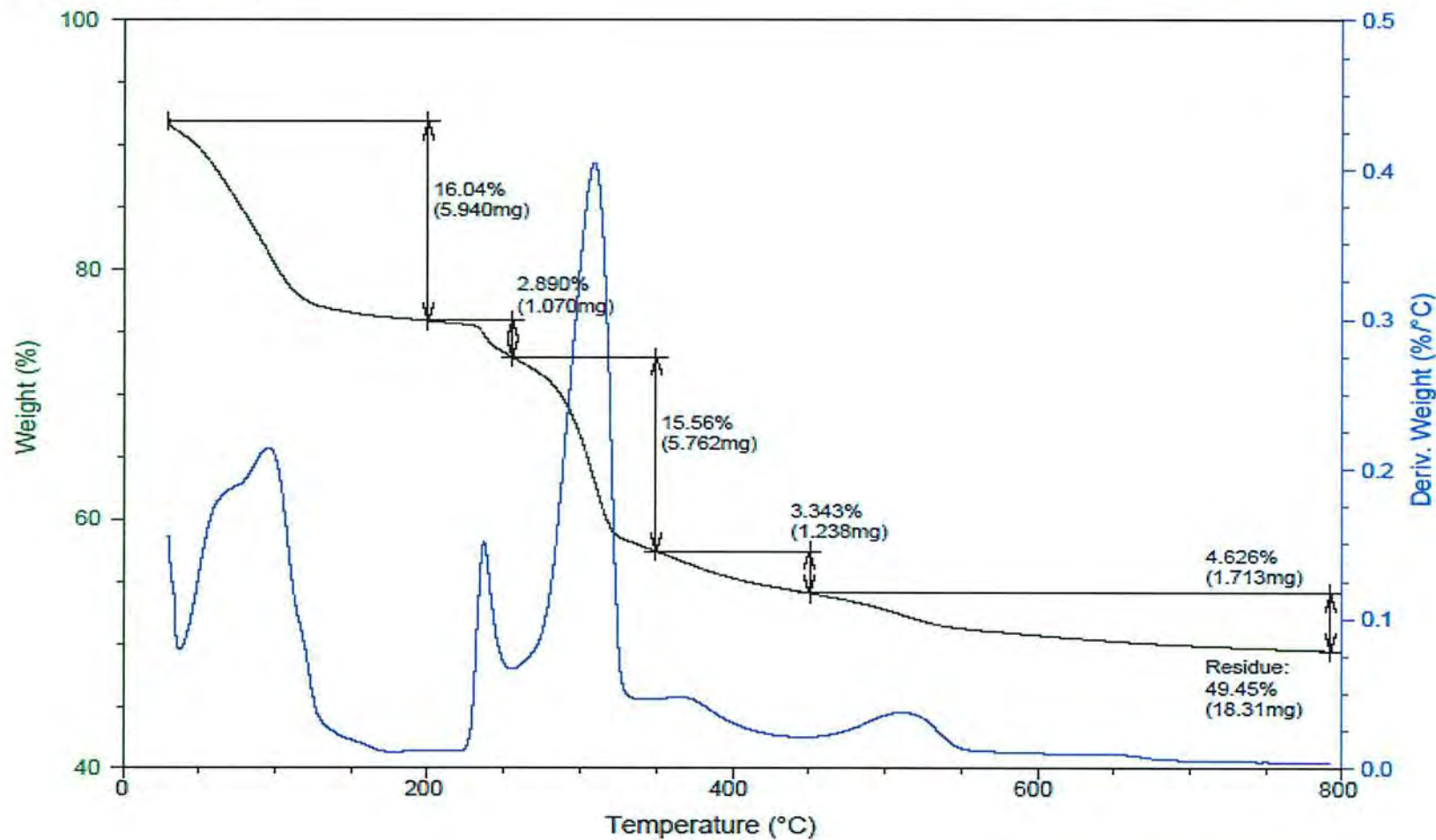


Figure 4

Sample: Bulk aluminium hydroxide
Size: 19.5450 mg

File: C:\...\Bulk aluminium hydroxide.001
Run Date: 13-Apr-2021 13:38
Instrument: SDT Q600 V20.9 Build 20

Comment: 2104T02_D1

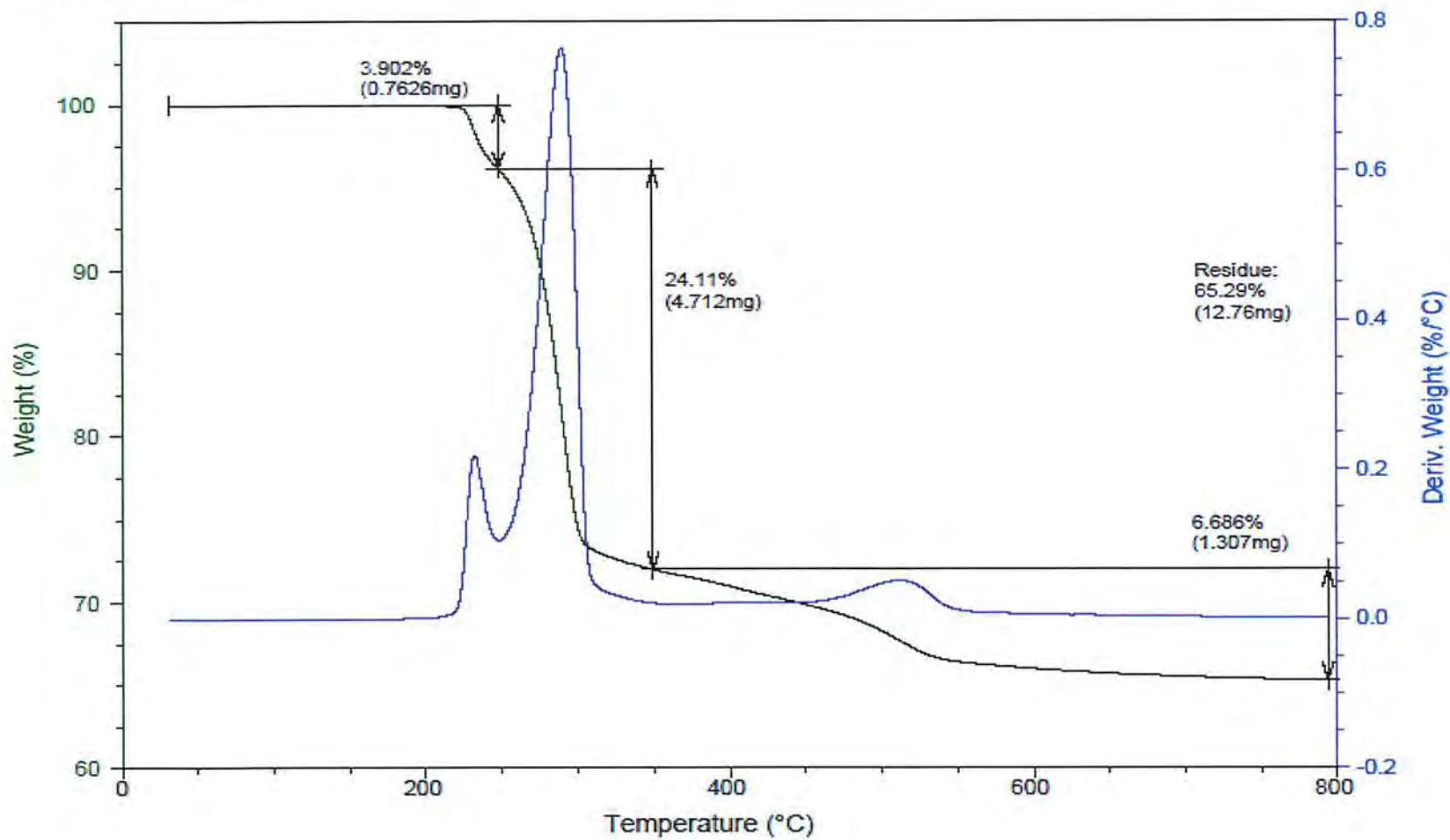


Figure 5

Sample: Bulk potato starch
Size: 9.8890 mg
Comment: 2104T02_E1

File: C:\...\Bulk potato starch.001
Run Date: 13-Apr-2021 15:53
Instrument: SDT Q600 V20.9 Build 20

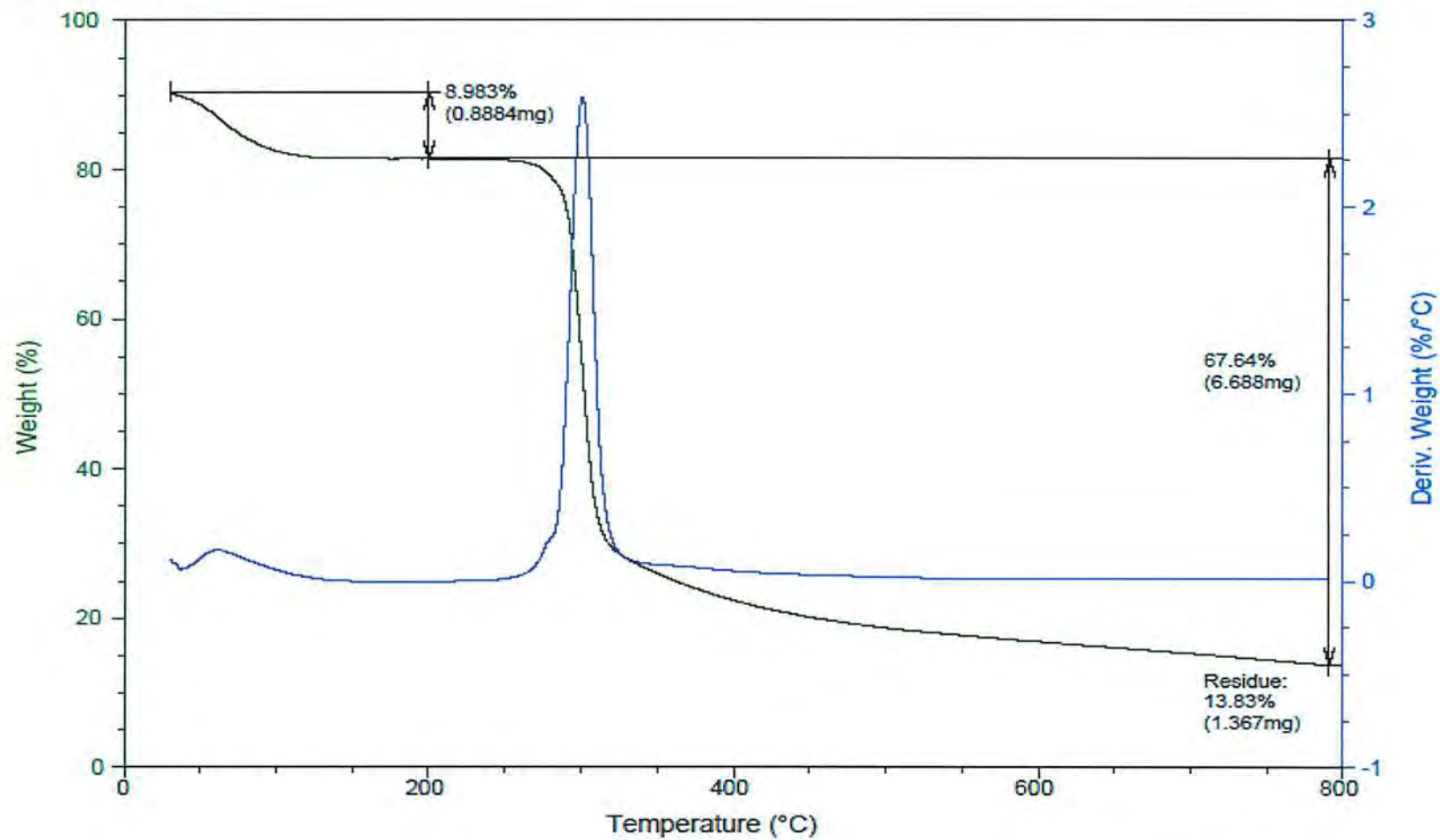


Figure 6

Sample: Bulk Point 1
Size: 12.5490 mg
Comment: 2104T02_F1

File: C:\...AR21SDT10065\Bulk Point 1.001
Run Date: 14-Apr-2021 15:27
Instrument: SDT Q600 V20.9 Build 20

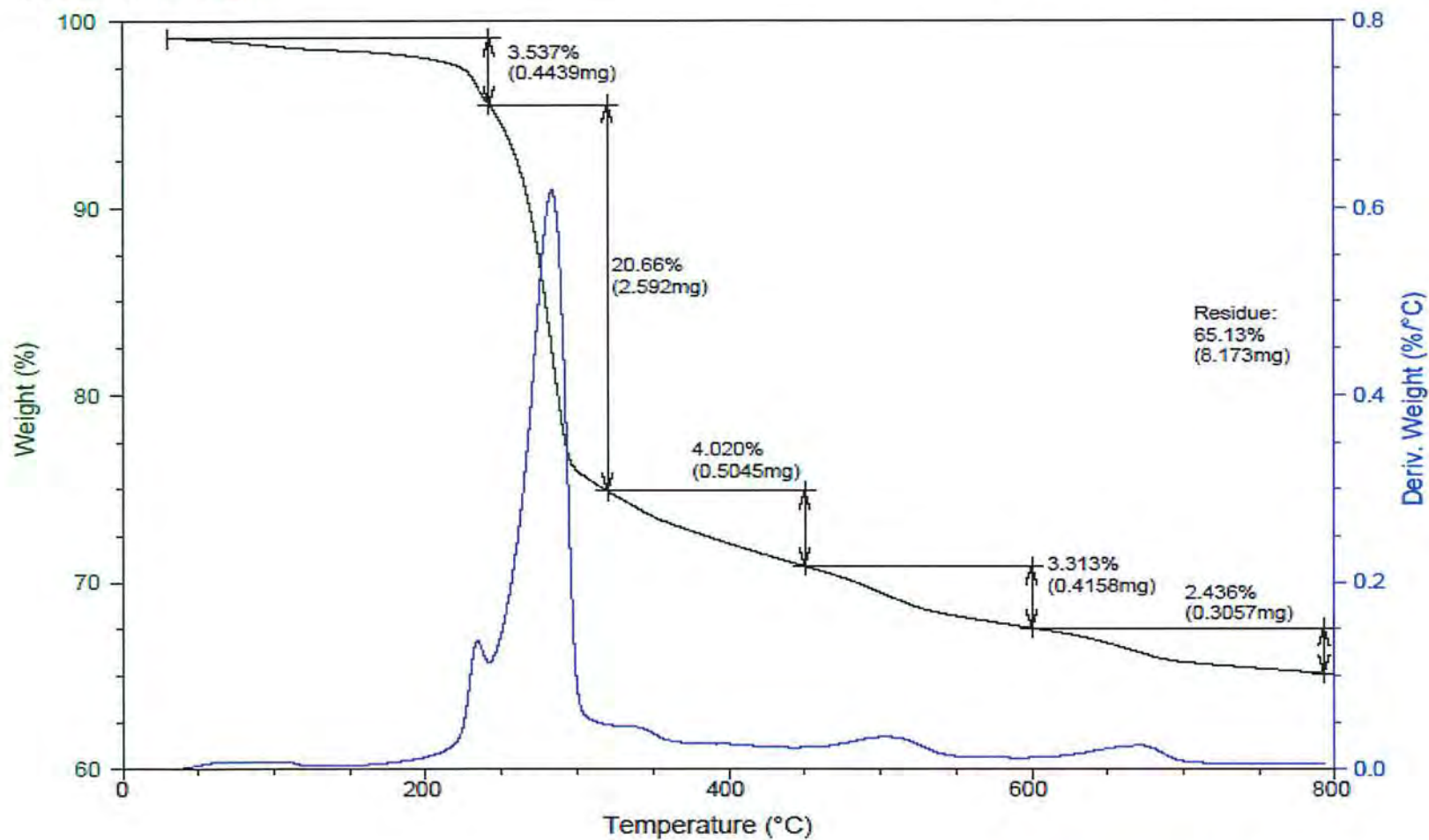


Figure 7

Sample: Bulk Point 2
Size: 8.9990 mg
Comment: 2104T02_G1

File: C:\...AR21SDT10065\Bulk Point 2.001
Run Date: 14-Apr-2021 17:45
Instrument: SDT Q600 V20.9 Build 20

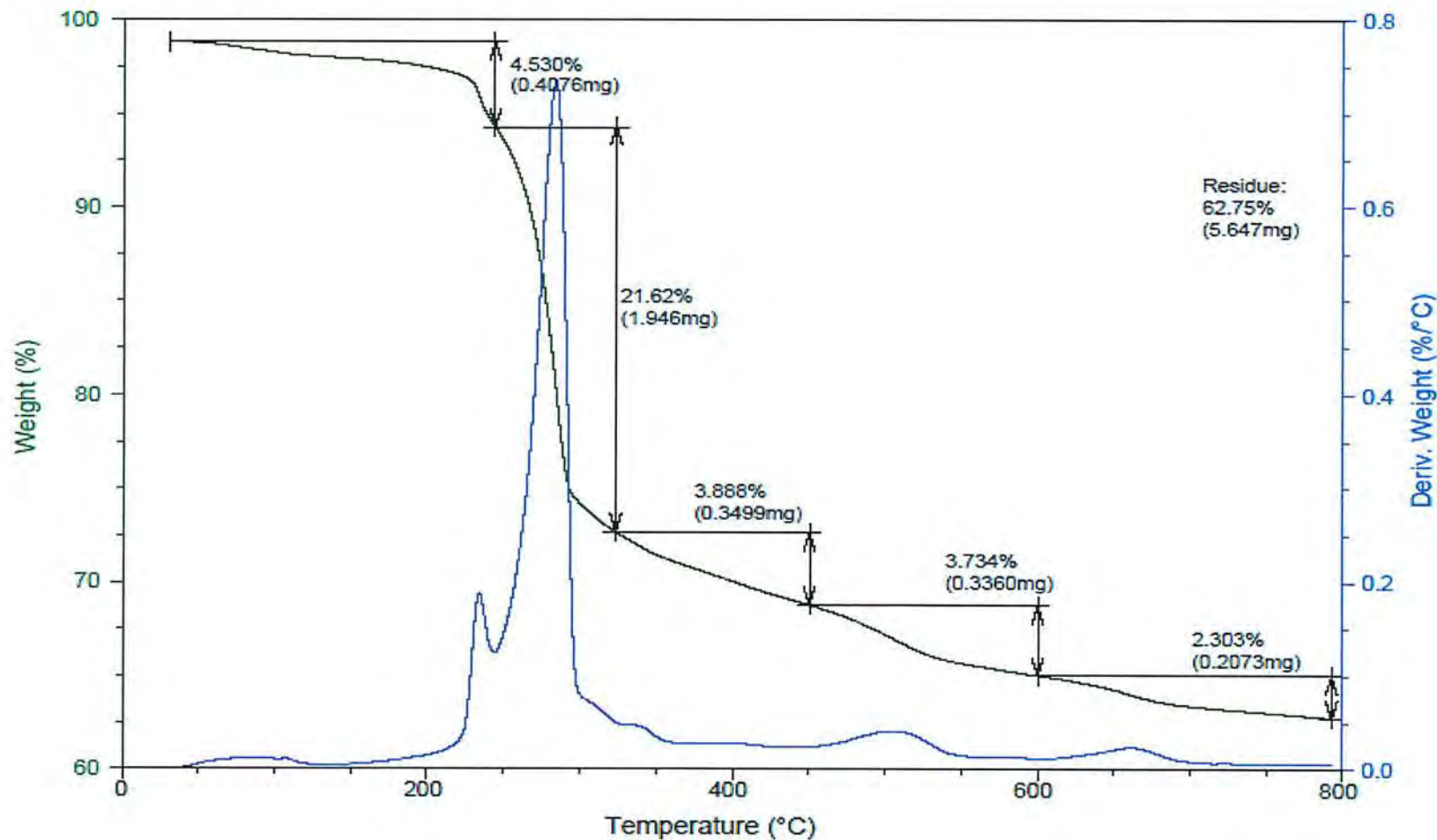


Figure 8

Sample: Bulk Point 3
Size: 15.9830 mg

File: C:\...AR21SDT10065\Bulk Point 3.001
Run Date: 14-Apr-2021 19:41
Instrument: SDT Q600 V20.9 Build 20

Comment: 2104T02_H1

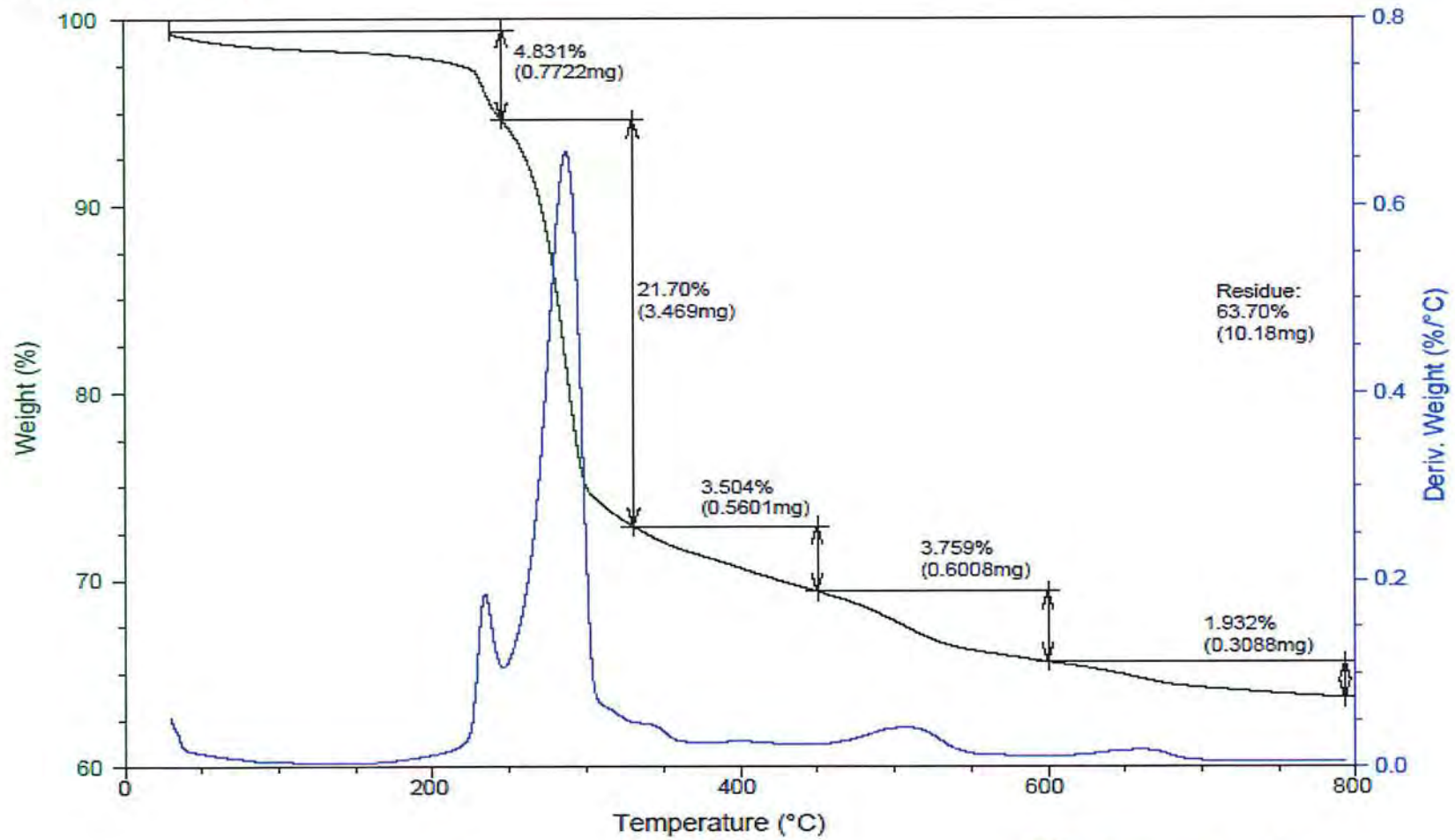
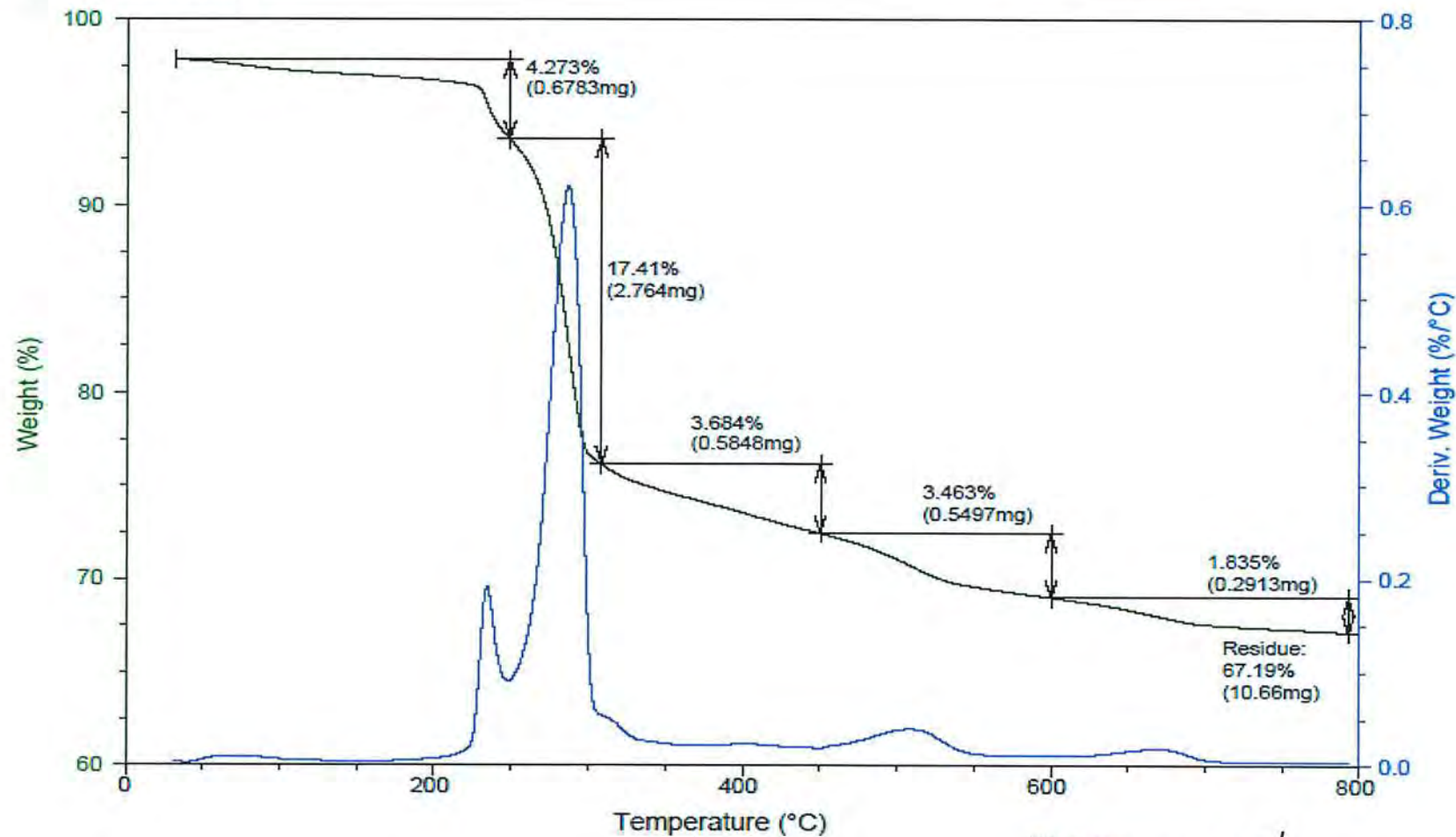


Figure 9

Sample: Bulk Under Pallet 4
Size: 15.8730 mg

File: C:\...Bulk Under Pallet 4.001
Run Date: 15-Apr-2021 08:32
Instrument: SDT Q600 V20.9 Build 20

Comment: 2104T02_I1



INSTITUTE OF CHEMICAL AND PHYSICAL SCIENCES
1 Pesek Road, Jurong Island, Singapore 627833

Figure 10

Sample: Bulk Platform 5
Size: 12.5540 mg
Comment: 2104T02_J1

File: C:\...AR21SDT10065\Bulk Platform 5.001
Run Date: 15-Apr-2021 10:45
Instrument: SDT Q600 V20.9 Build 20

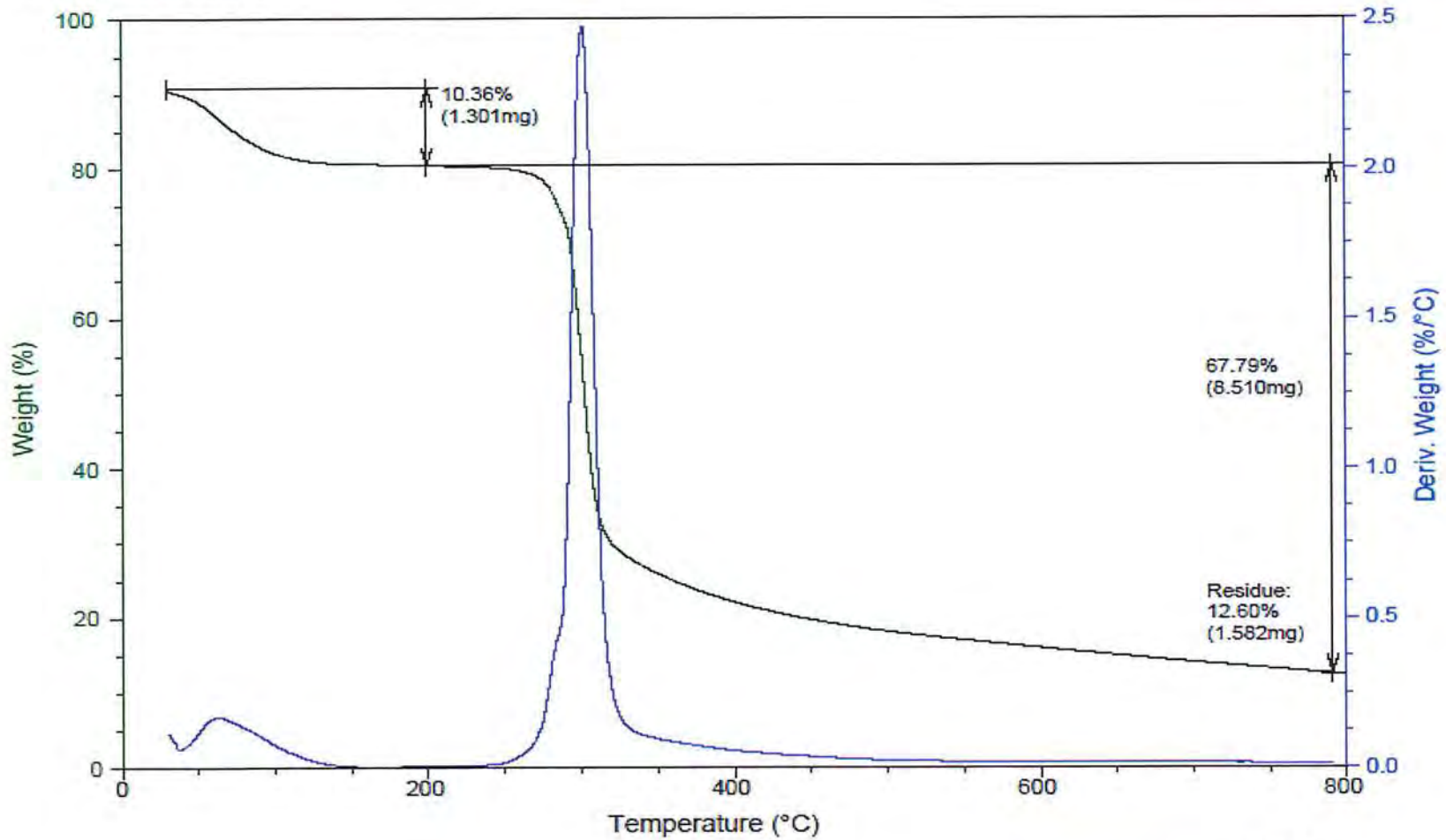


Figure 11

Sample: Bulk Outside Toilet 6
Size: 12.3640 mg

File: C:\...\Bulk Outside Toilet 6.001
Run Date: 15-Apr-2021 13:17
Instrument: SDT Q600 V20.9 Build 20

Comment: 2104T02_K1

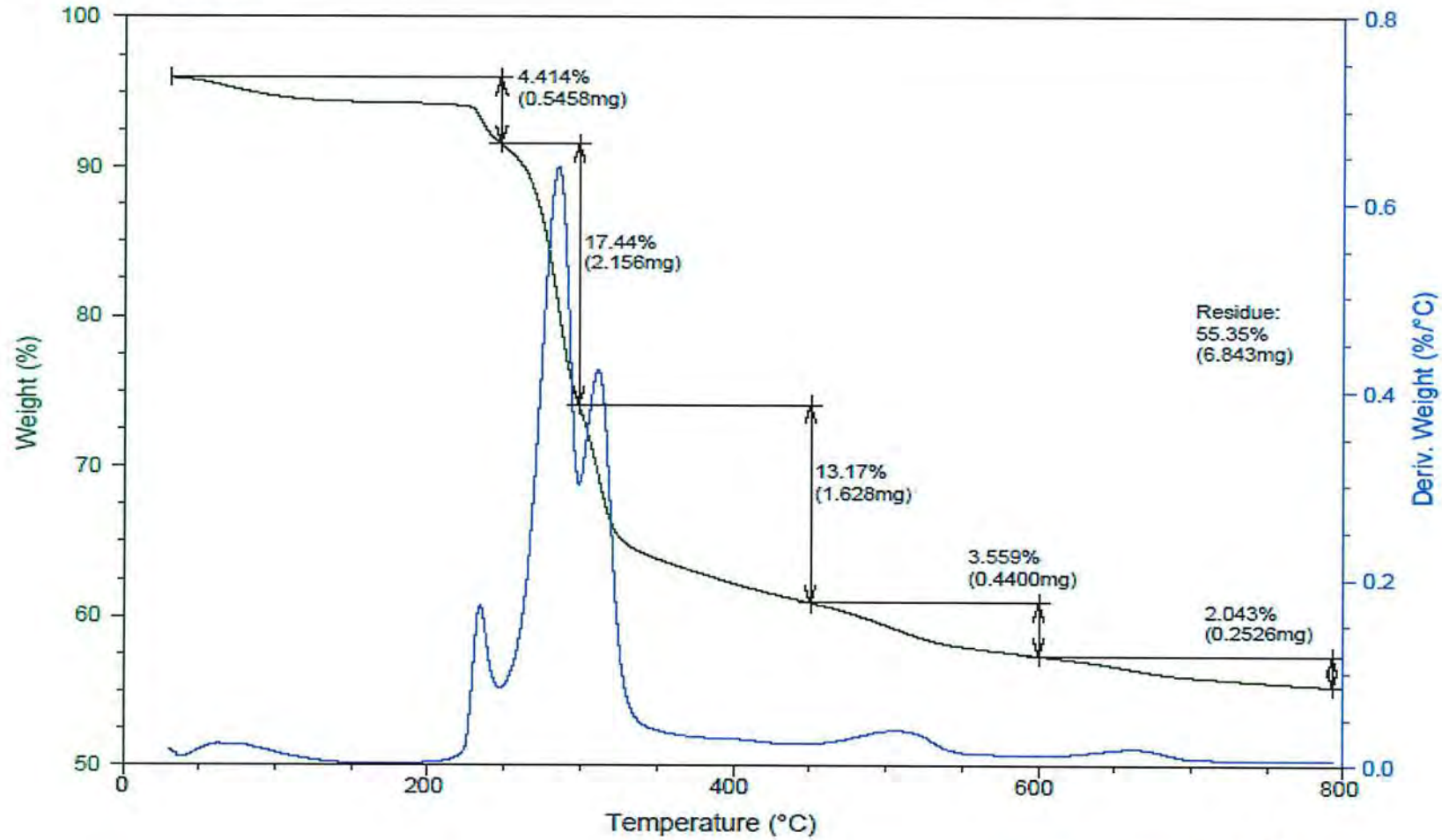


Figure 12

Sample: Aluminium Dihydrogen Phosphate
Size: 11.0860 mg

File: C:\...Aluminium Dihydrogen Phosphate.001
Run Date: 14-Apr-2021 08:34
Instrument: SDT Q600 V20.9 Build 20

Comment: 2104T02_L1

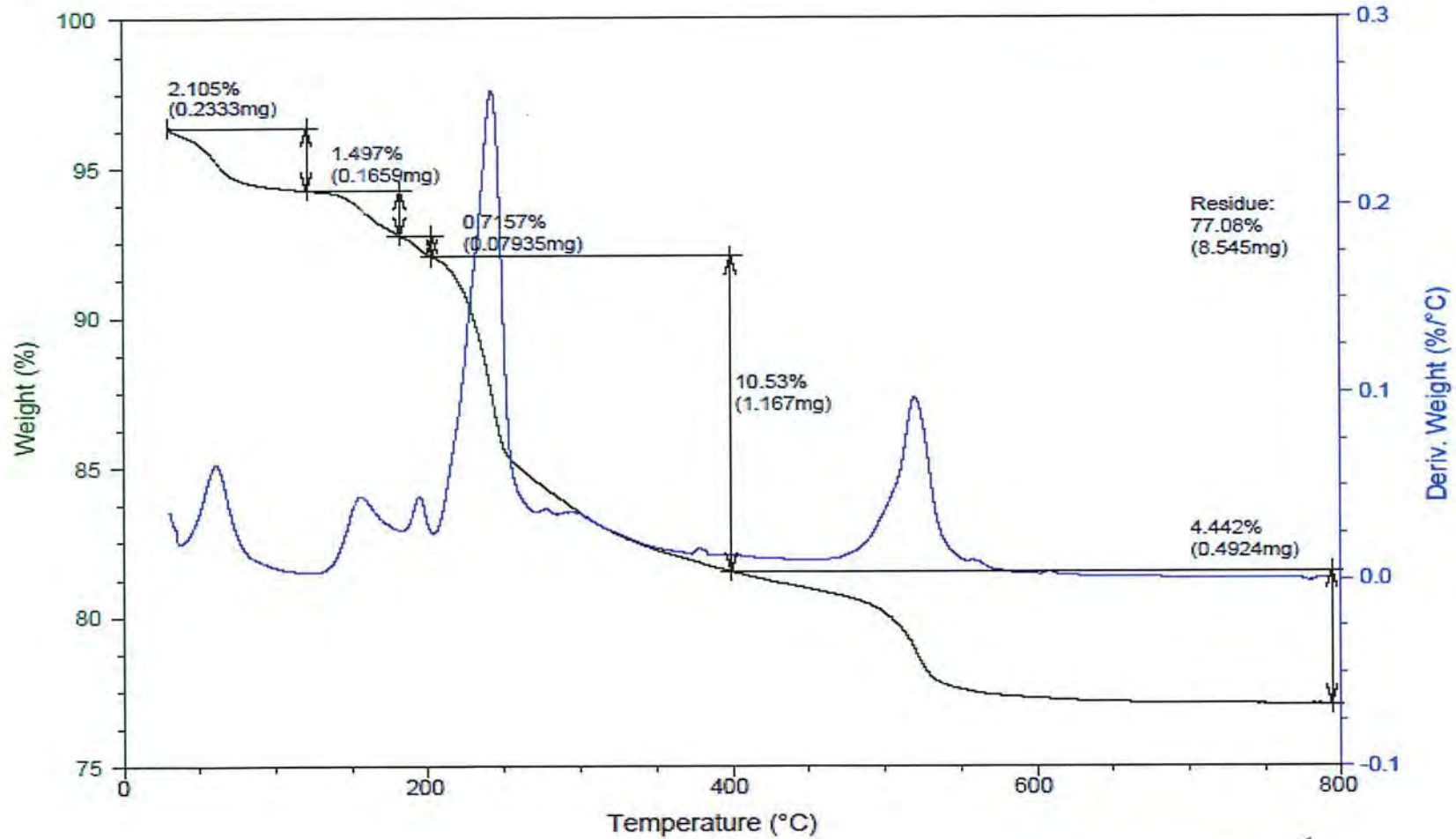


Figure 13

Sample: Bulk Boric Acid
Size: 18.3560 mg

File: C:\...AR21SDT10065\Bulk Boric Acid.001
Run Date: 14-Apr-2021 10:49
Instrument: SDT Q600 V20.9 Build 20

Comment: 2104T02_M1

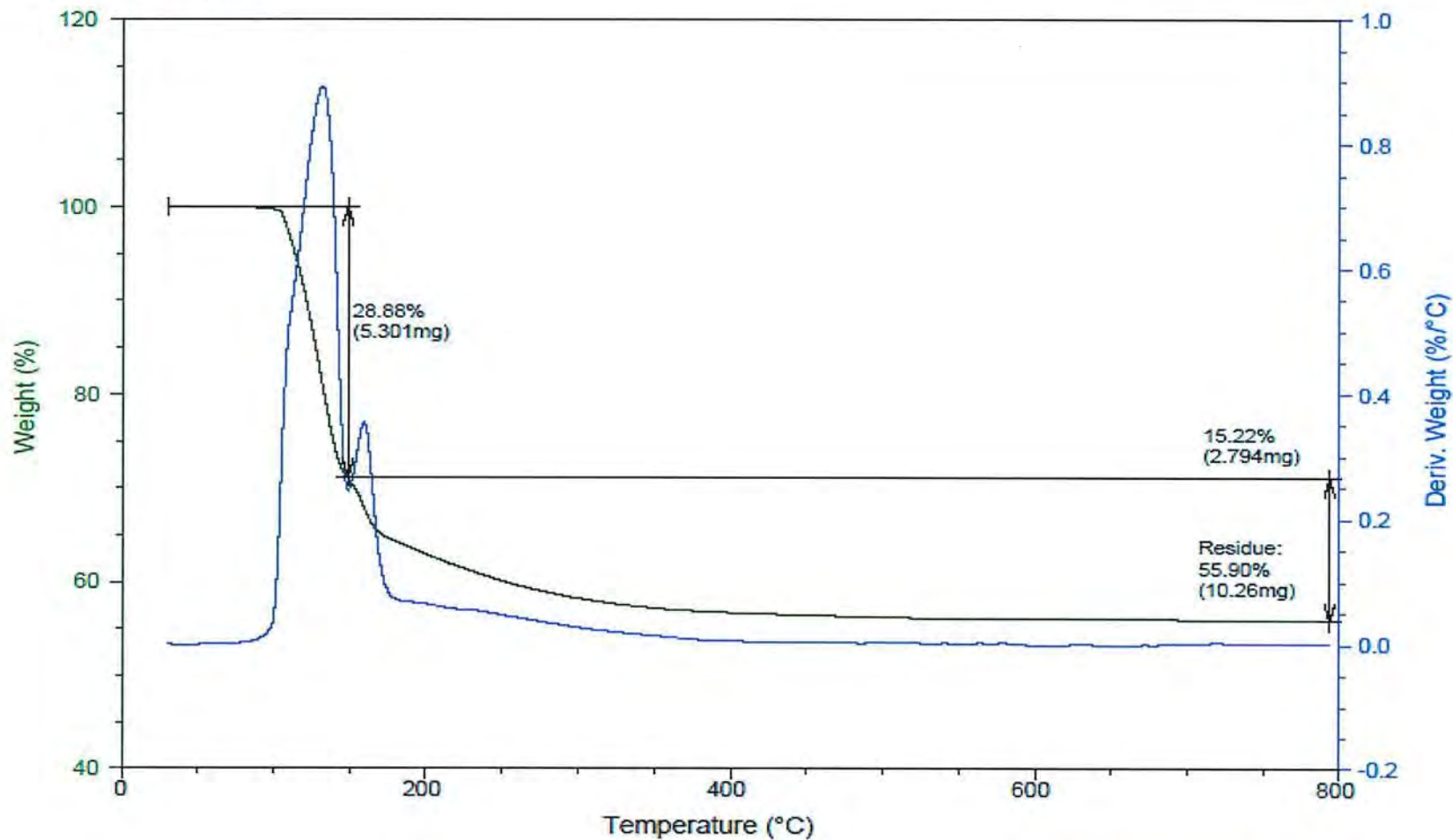
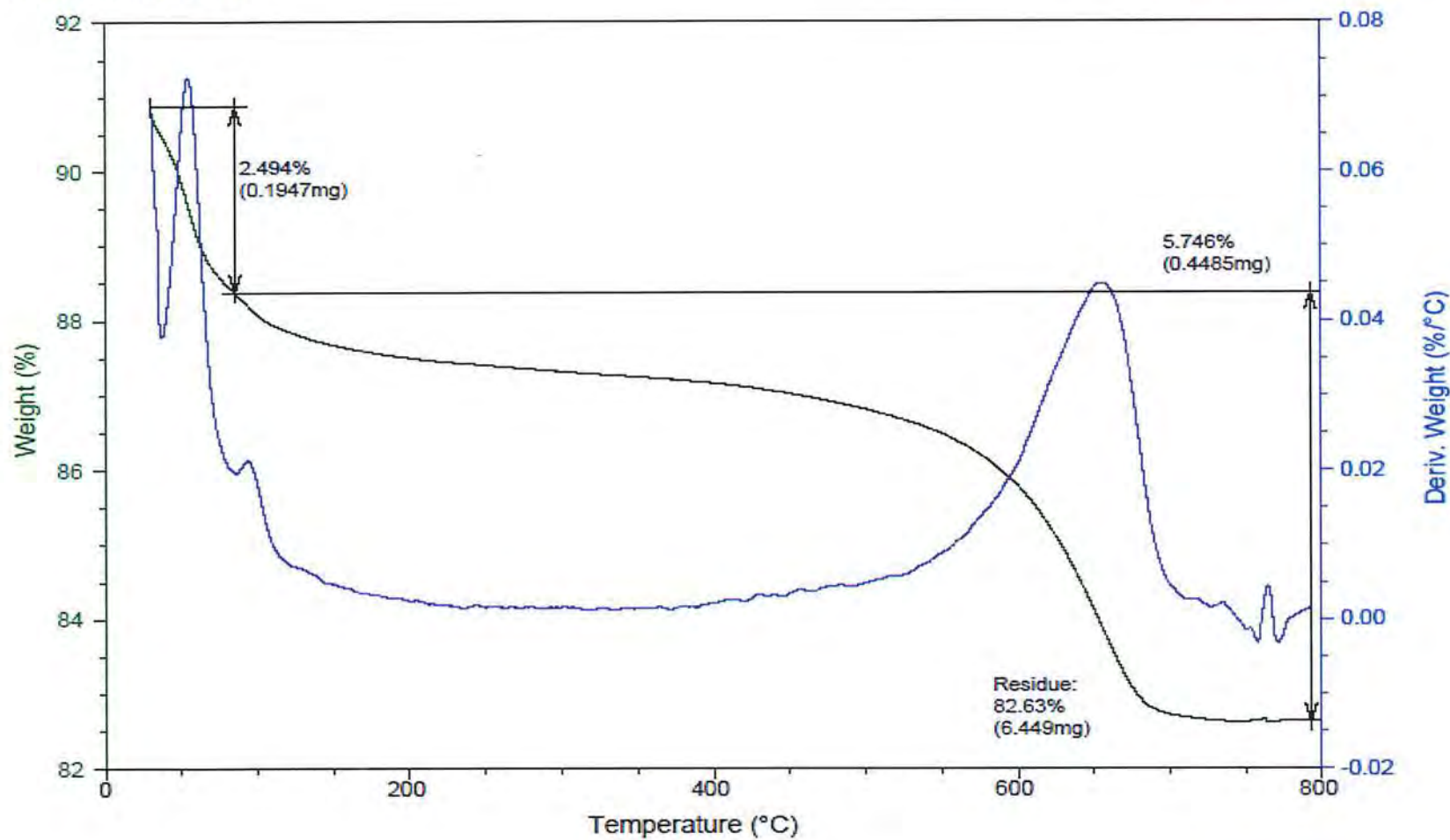


Figure 14

Sample: Bulk Clay
Size: 7.8050 mg

File: C:\...VAR21SDT10065\Bulk Clay.001
Run Date: 14-Apr-2021 13:08
Instrument: SDT Q600 V20.9 Build 20

Comment: 2104T02_N1



REPORT

REPORT REFERENCE: ICES/AC/21013_Part1a **DATE:** 6th May 2021

SUBJECT: FTIR analysis of powder specimens

COMPANY: ICES, A*STAR
1, Pesek Road, Jurong Island,
Singapore 627833

ATTENTION: Dr. Shaik Salim

DATE SAMPLE RECEIVED: 1st Apr 2021

DATE ANALYSED: 13th Apr 2021

DATE TEST COMPLETED: 3rd May 2021

DESCRIPTION OF SAMPLE(S):

Fourteen samples consisting of powder specimens (~5-10g each) were received.

S/N	Sample Description	Exhibit No.
1	Bulk	250221-1b
2	Bulk (Bulk Bag Left)	080321-1b
3	Bulk (Bulk Bag Right)	080321-2b
4	Bulk (Aluminium Hydroxide)	080321-3b
5	Bulk (Potato Starch)	080321-4b
6	Bulk Point 1	170321-1b
7	Bulk Point 2	170321-2b
8	Bulk Point 3	170321-3b
9	Bulk (Under Pallet) 4	170321-4b
10	Bulk (Platform) 5	170321-5b
11	Bulk (Outside Toilet) 6	170321-6b
12	Bulk (Aluminium Dihydrogen Phosphate)	170321-7b
13	Bulk (Boric Acid)	170321-8b
14	Bulk (Clay)	170321-9b

METHOD OF TEST:

The qualitative FTIR (Fourier Transform Infra-Red) analysis of powder specimens as received was conducted by PerkinElmer Frontier MIR/NIR Spectrometer.

Samples were prepared by means of grinding solid powder specimens and mixing it with KBr powder matrix, before pressing the resulting KBr-sample mixture into a pellet for FTIR (Fourier Transform Infra-Red) analysis and data collected in the range of 4000 to 450 cm^{-1} .

RESULTS:

1. The spectrums obtained from FTIR analysis of respective powder specimens are presented in Figures 1 to 14.

2. A summary of common FTIR band assignments (C-H stretching, C-O bending associated with OH group, CH_2 symmetric deformation, C-O-C asymmetric stretching and C-O stretching) arising from starch materials' major IR spectrum bands are presented on Table 1.

(Reference: A J D Abdullah et al 2018 IOP Conf. Ser.: Earth Environ. Sci. 160 012003, Warren, F. J., et al 2016, Carbohydrate Polymers, Volume 139, 2016)

3. Refer to Table 1, the observed peak data of Specimens 1 to 14 associated with common FTIR band assignments found in starch materials are presented.

4. Refer to Figure 15 for FTIR spectrums comparison of Specimen 1 - Bulk, Exhibit No. 250221-1b, Specimen 10 - Bulk (Platform) 5, Exhibit No. 170321-5b, and reference Specimen 5 - Bulk (Potato Starch), Exhibit No. 080321-4b. All three spectrums indicated similarities across major pronounced bands when compared with common FTIR band assignments found in starch materials as highlighted.

5. Refer to Figure 16a for FTIR spectrum comparison of Specimens 6, 7, 8, 9 and 11, and Figure 16b for FTIR spectrum comparison of Specimens 2, 3 and 4, as presented along with the common FTIR band assignments found in starch materials as highlighted.

Sample Description	Exhibit No.	Common FTIR band assignments in Starch Material					Likelihood of similarity compared with Specimen 5 - Bulk (Potato Starch), Exhibit No. 080321-4b
		C-H stretching	C-O bending associated with OH group	CH ₂ symmetric deformation	C-O-C asymmetric stretching	C-O stretching	
		~2931 cm ⁻¹	~1637 cm ⁻¹	~1458 cm ⁻¹	~1149 cm ⁻¹	~1200-800 cm ⁻¹	
Bulk	250221-1b	2930.78	1647.32	1460.07	1158.86	1080.73, 1019.89	High
Bulk (Bulk Bag Left)	080321-1b	-	1638.42	1477.92	-	1088.03, 1031.92	Inconclusive
Bulk (Bulk Bag Right)	080321-2b	2963.66	1641.00	-	-	1086.99, 1022.54	Inconclusive
Bulk (Aluminium Hydroxide)	080321-3b	-	-	-	-	1018.89, 966.59	Low
Bulk (Potato Starch)	080321-4b	2930.75	1651.10	1463.56	1165.28	1080.11, 983.65	Reference
Bulk Point 1	170321-1b	2925.16	1634.25	-	-	1020.12, 968.30	Inconclusive
Bulk Point 2	170321-2b	2925.16	-	-	-	1019.34, 967.79	Inconclusive
Bulk Point 3	170321-3b	2925.17	1632.14	-	-	1020.08, 968.13	Inconclusive
Bulk (Under Pallet) 4	170321-4b	2925.89	1637.99	-	-	1087.39, 1022.88	Inconclusive
Bulk (Platform) 5	170321-5b	2928.02	1654.92	1466.70	1167.67	1080.01, 981.68	High
Bulk (Outside Toilet) 6	170321-6b	2963.12	1644.93	-	-	1019.66, 969.17	Inconclusive
Bulk (Aluminium Dihydrogen Phosphate)	170321-7b	-	1667.62	-	1194.79	1134.83, 987.31	Low
Bulk (Boric Acid)	170321-8b	-	-	1467.72	-	1194.31	Low
Bulk (Clay)	170321-9b	-	1638.24	-	-	1088.14, 1039.40	Low

Table 1 – Summary table of observed peak data collected from FTIR spectrums of Specimens 1 to 14 and associated common FTIR band assignments in Starch Material

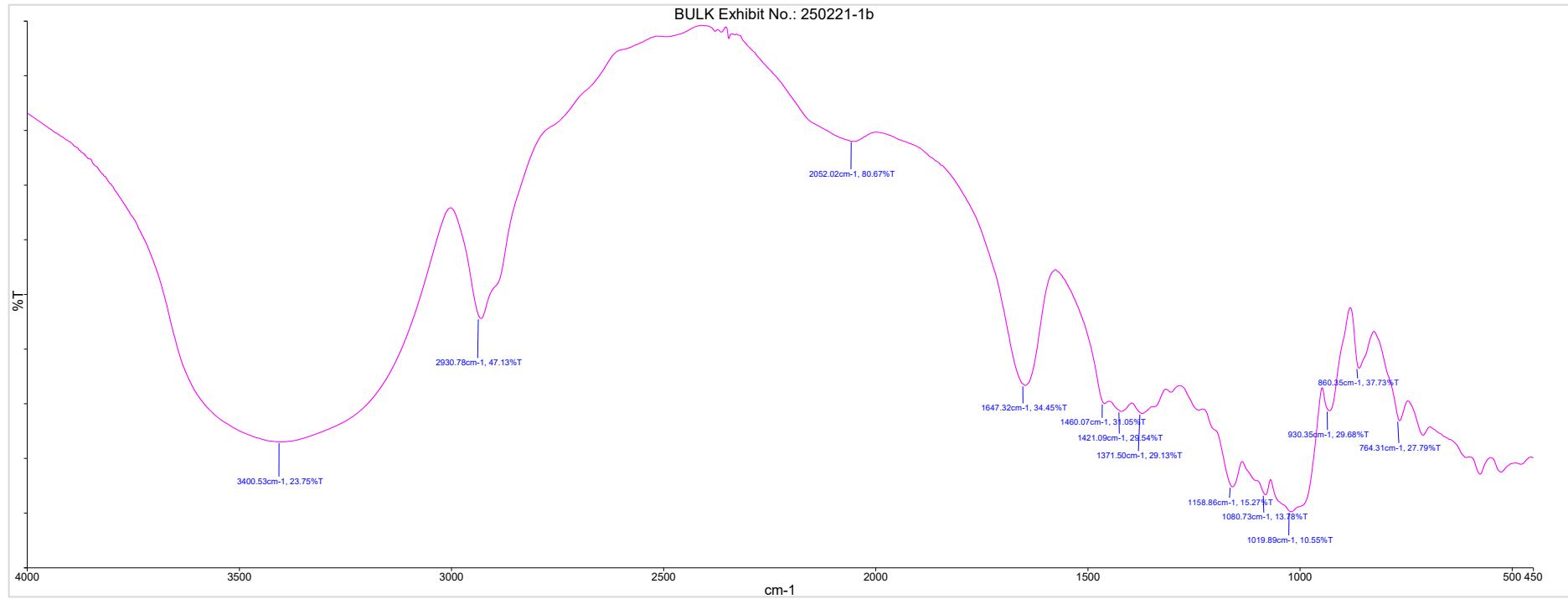


Figure 1 – FTIR spectrum of Specimen 1 - Bulk, Exhibit No. 250221-1b

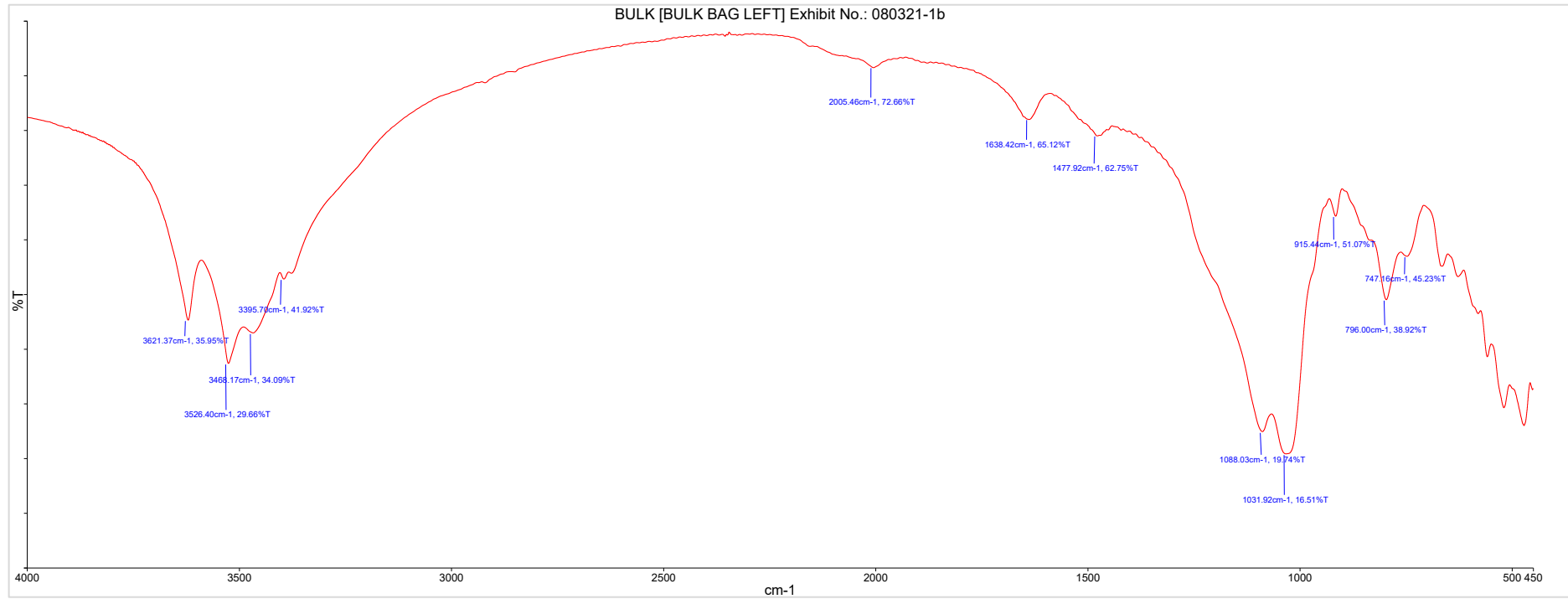


Figure 2 – FTIR spectrum of Specimen 2 - Bulk (Bulk Bag Left), Exhibit No. 080321-1b

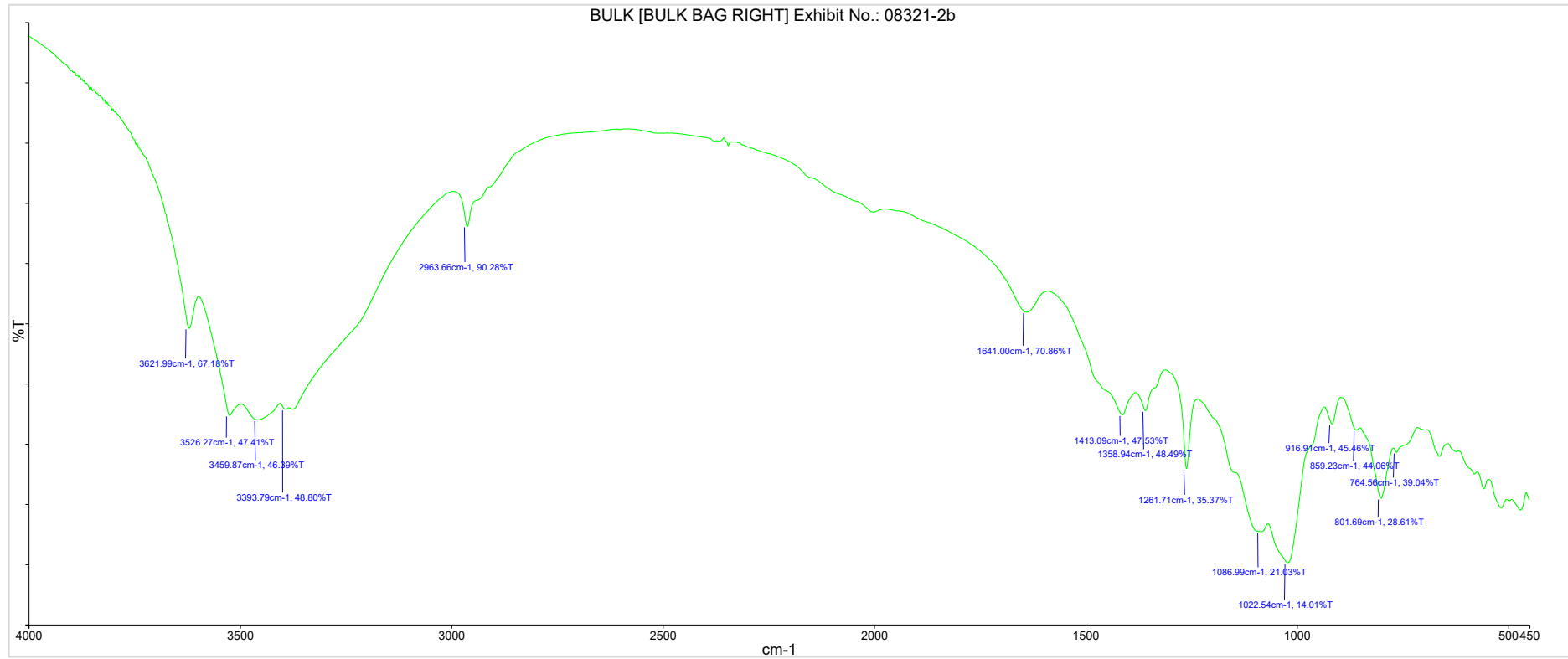


Figure 3 – FTIR spectrum of Specimen 3 - Bulk (Bulk Bag Right), Exhibit No. 080321-2b

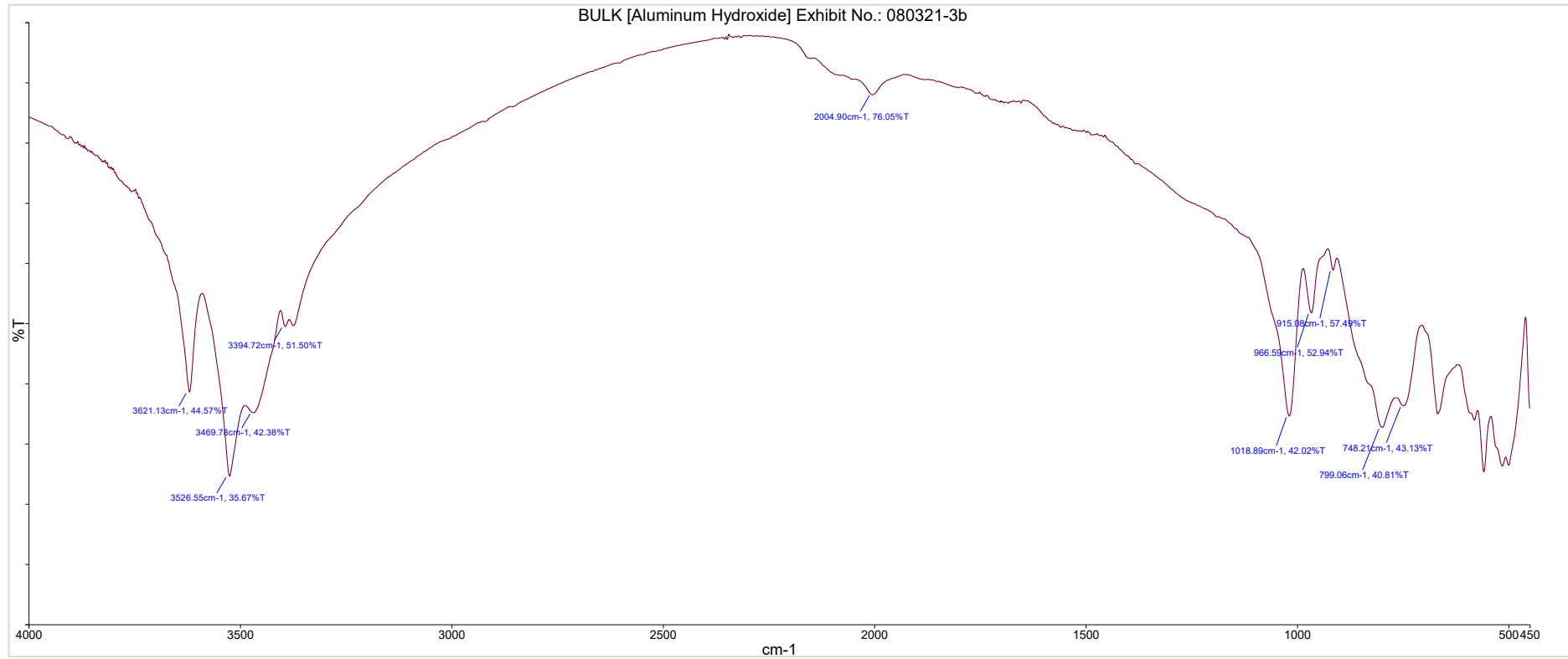


Figure 4 – FTIR spectrum of Specimen 4 - Bulk (Aluminium Hydroxide), Exhibit No. 080321-3b

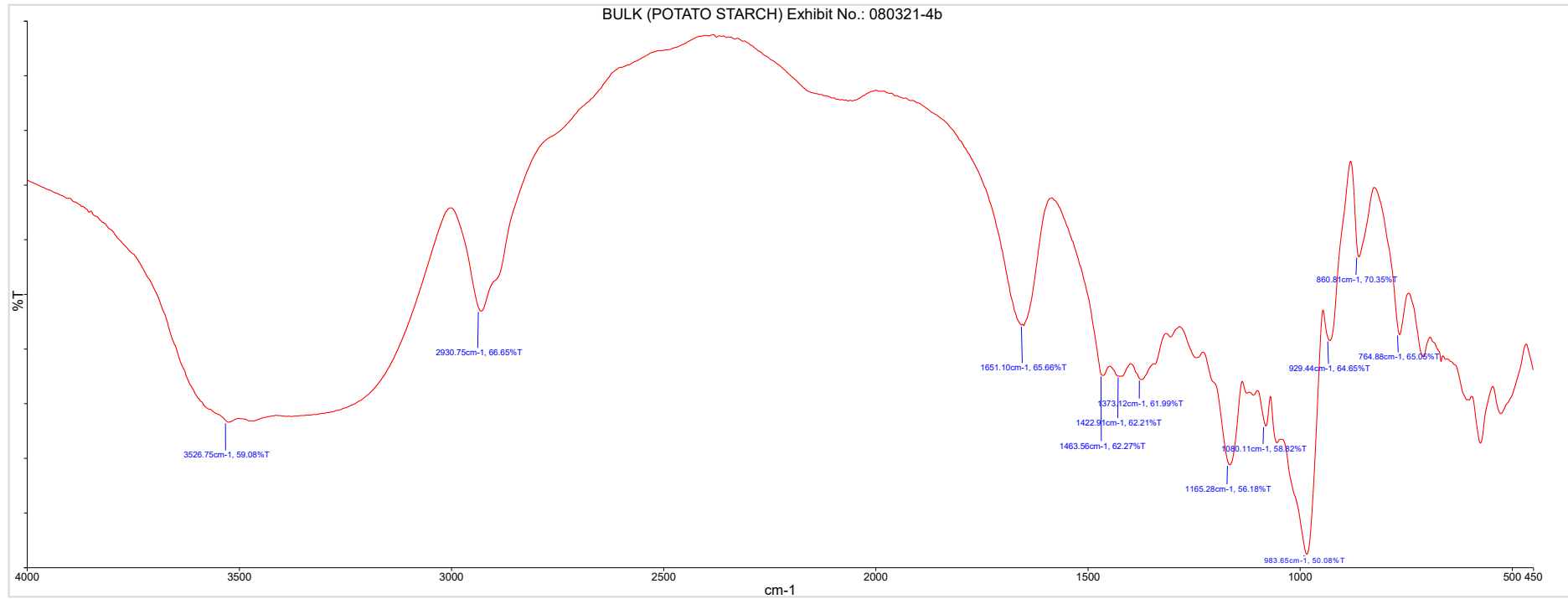


Figure 5 – FTIR spectrum of Specimen 5 - Bulk (Potato Starch), Exhibit No. 080321-4b

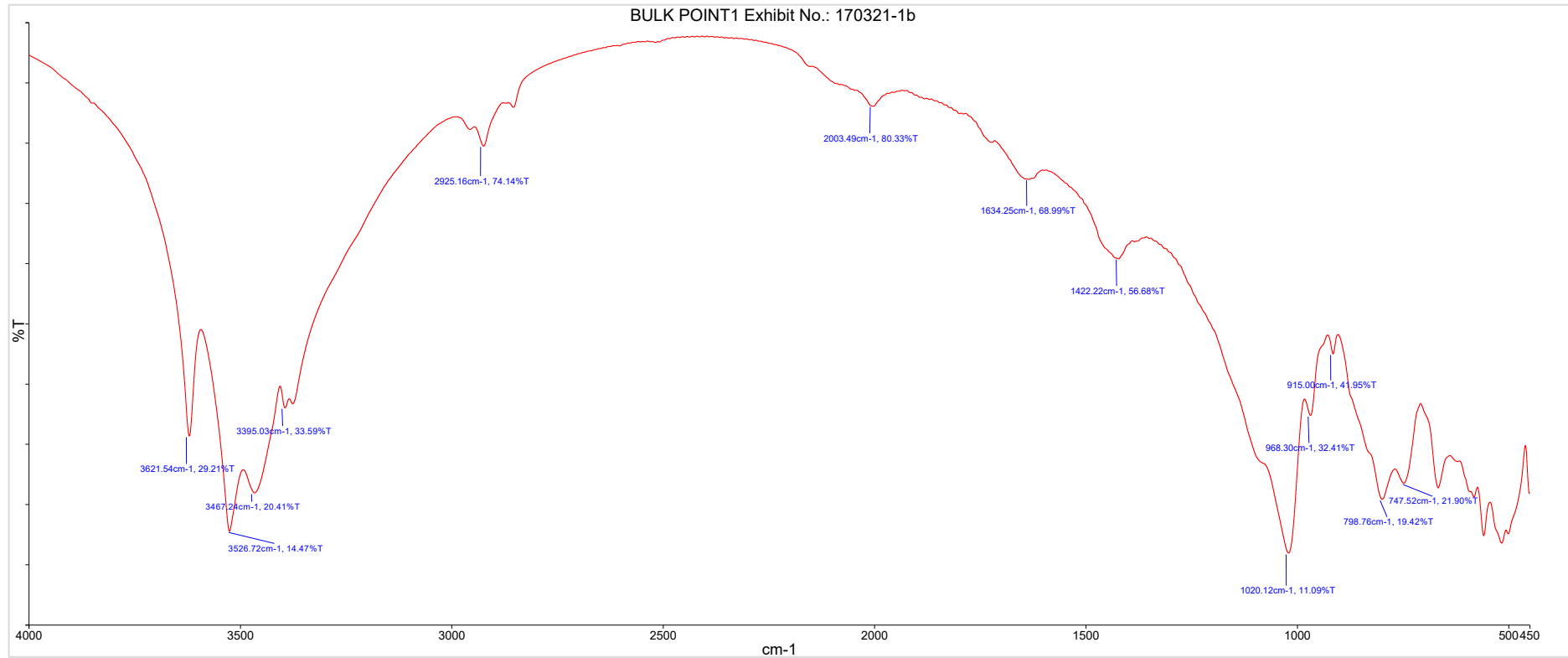


Figure 6 – FTIR spectrum of Specimen 6 - Bulk Point 1, Exhibit No. 170321-1b

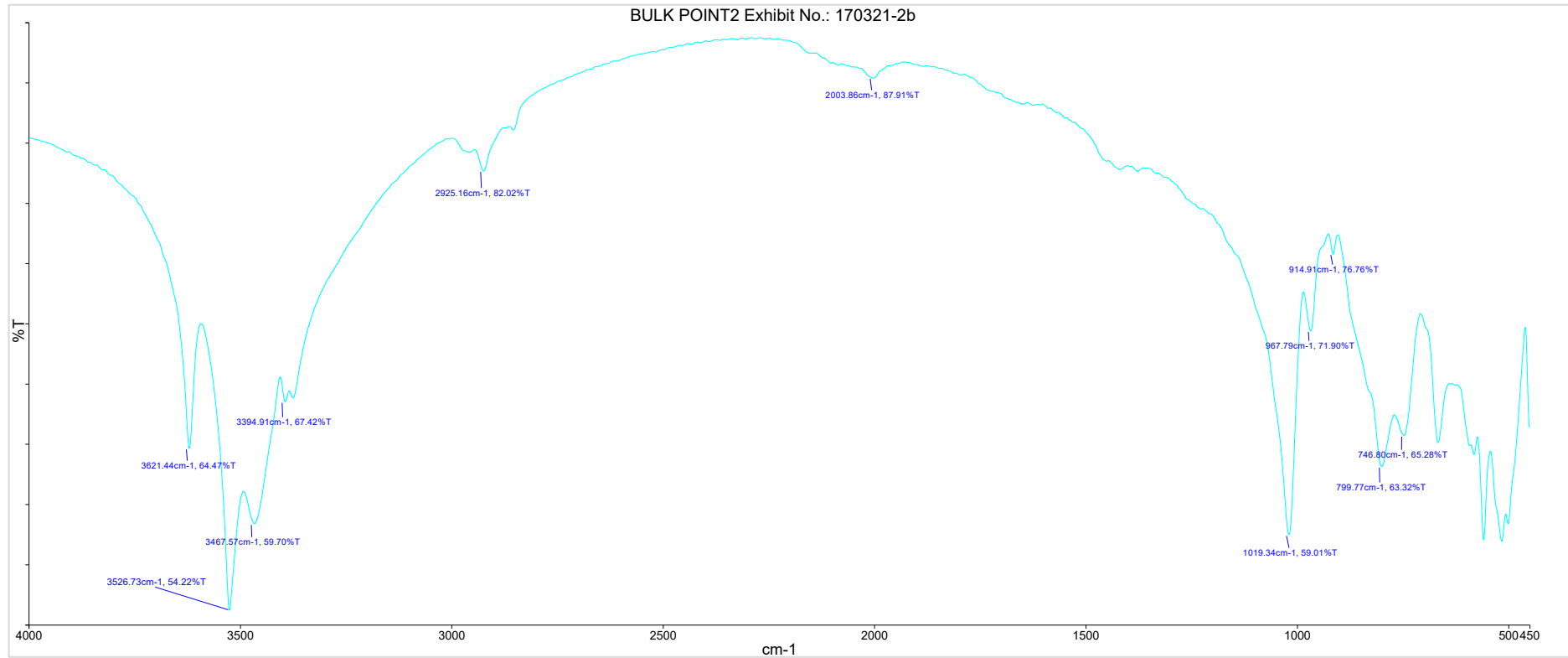


Figure 7 – FTIR spectrum of Specimen 7 - Bulk Point 2, Exhibit No. 170321-2b

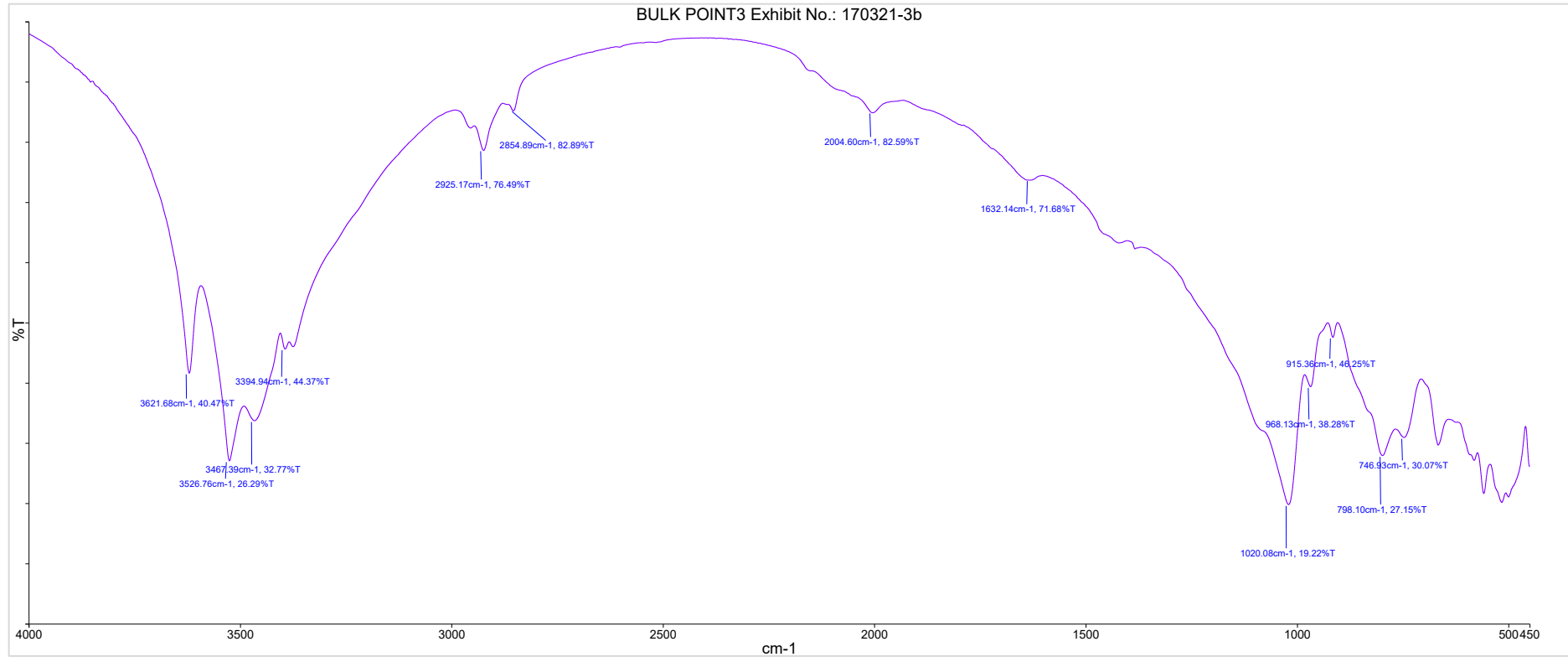


Figure 8 – FTIR spectrum of Specimen 8 - Bulk Point 3, Exhibit No. 170321-3b

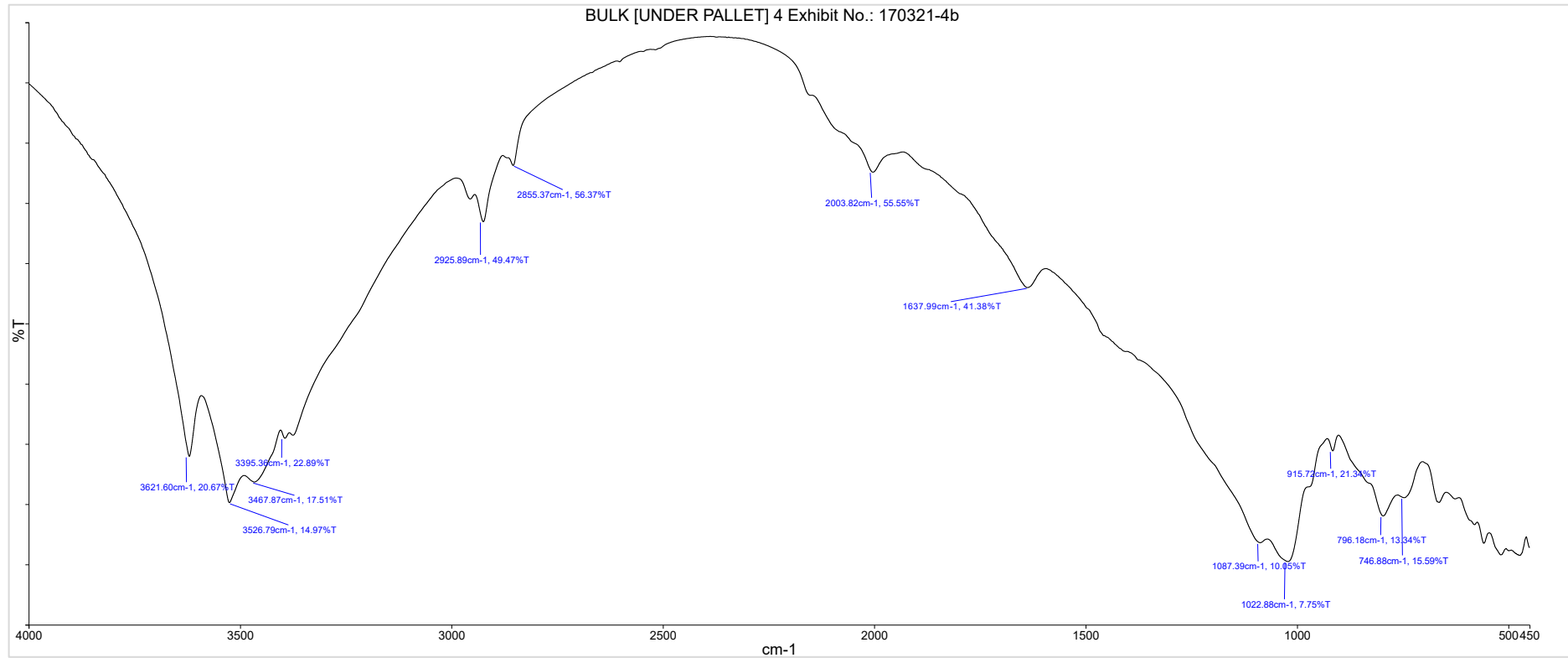


Figure 9 – FTIR spectrum of Specimen 9 - Bulk (Under Pallet) 4, Exhibit No. 170321-4b

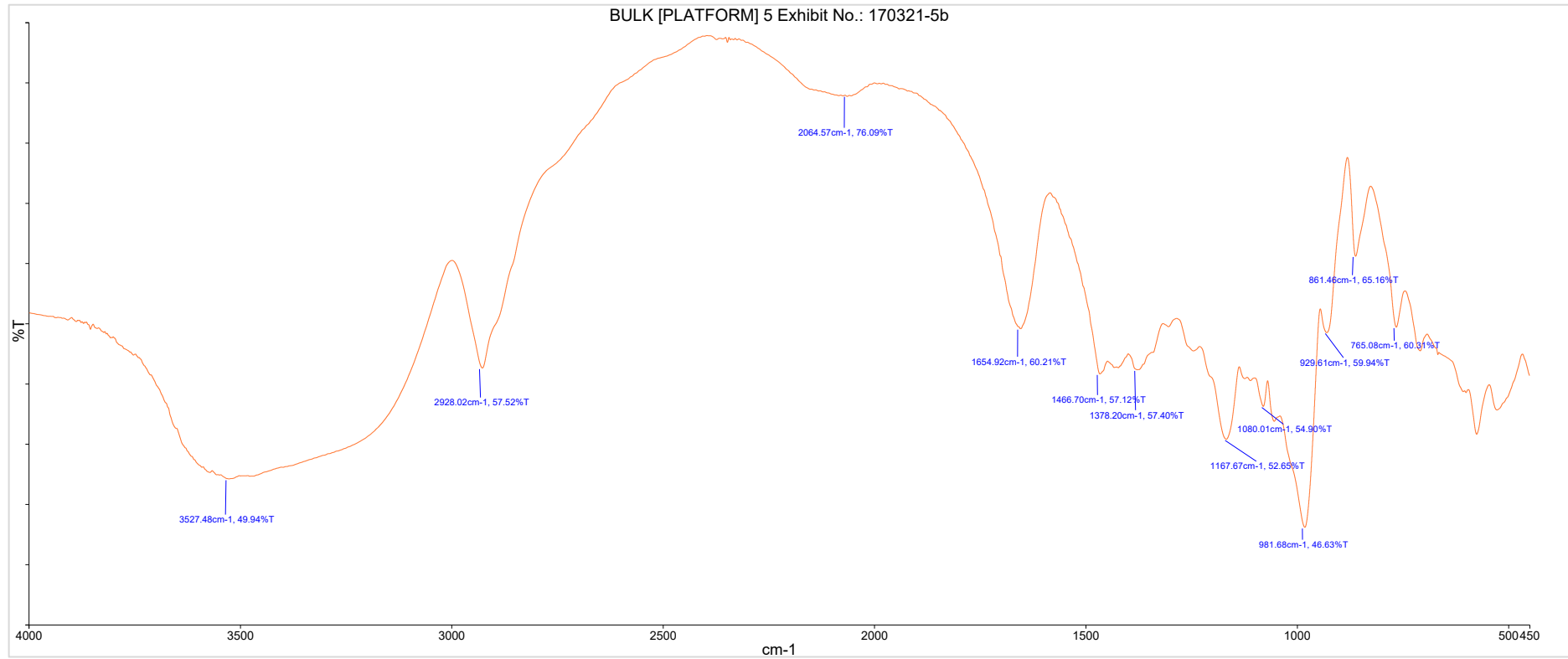


Figure 10 – FTIR spectrum of Specimen 10 - Bulk (Platform) 5, Exhibit No. 170321-5b

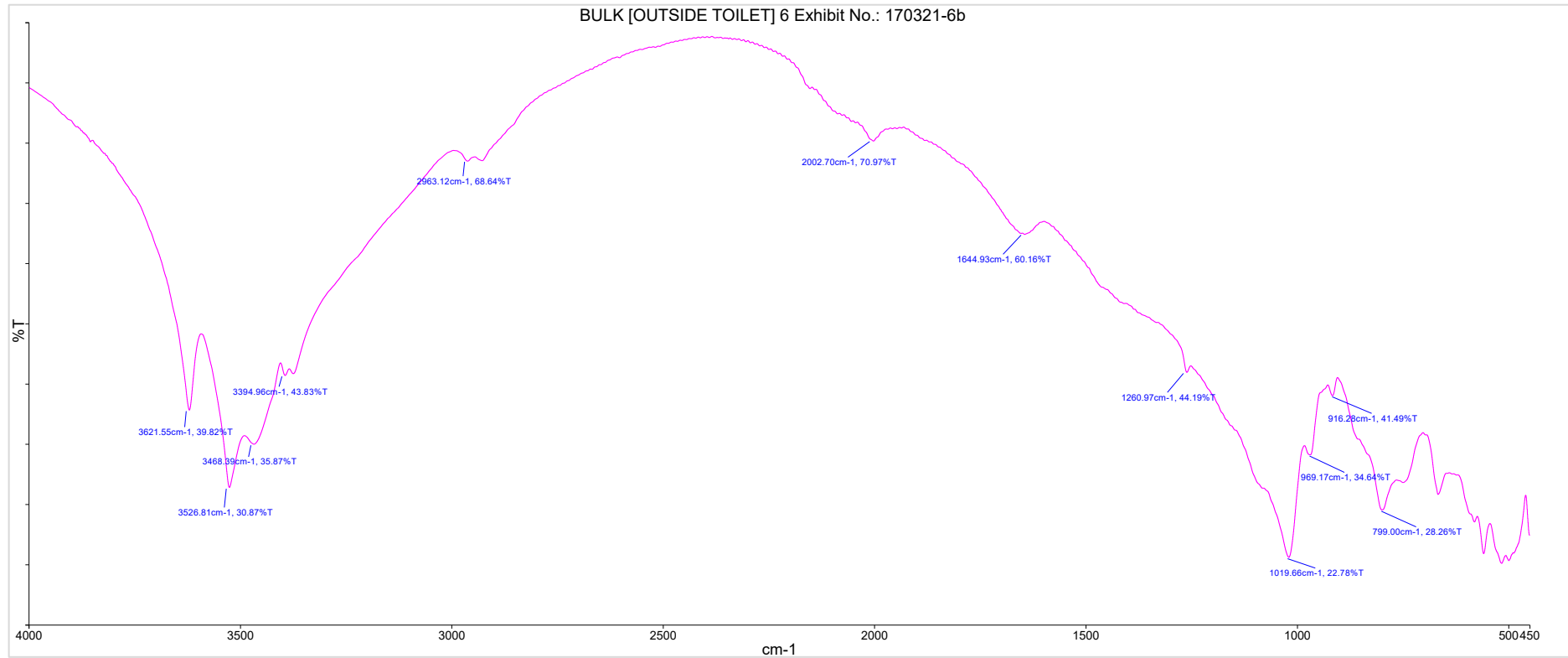


Figure 11 – FTIR spectrum of Specimen 11 - Bulk (Outside Toilet) 6, Exhibit No. 170321-6b

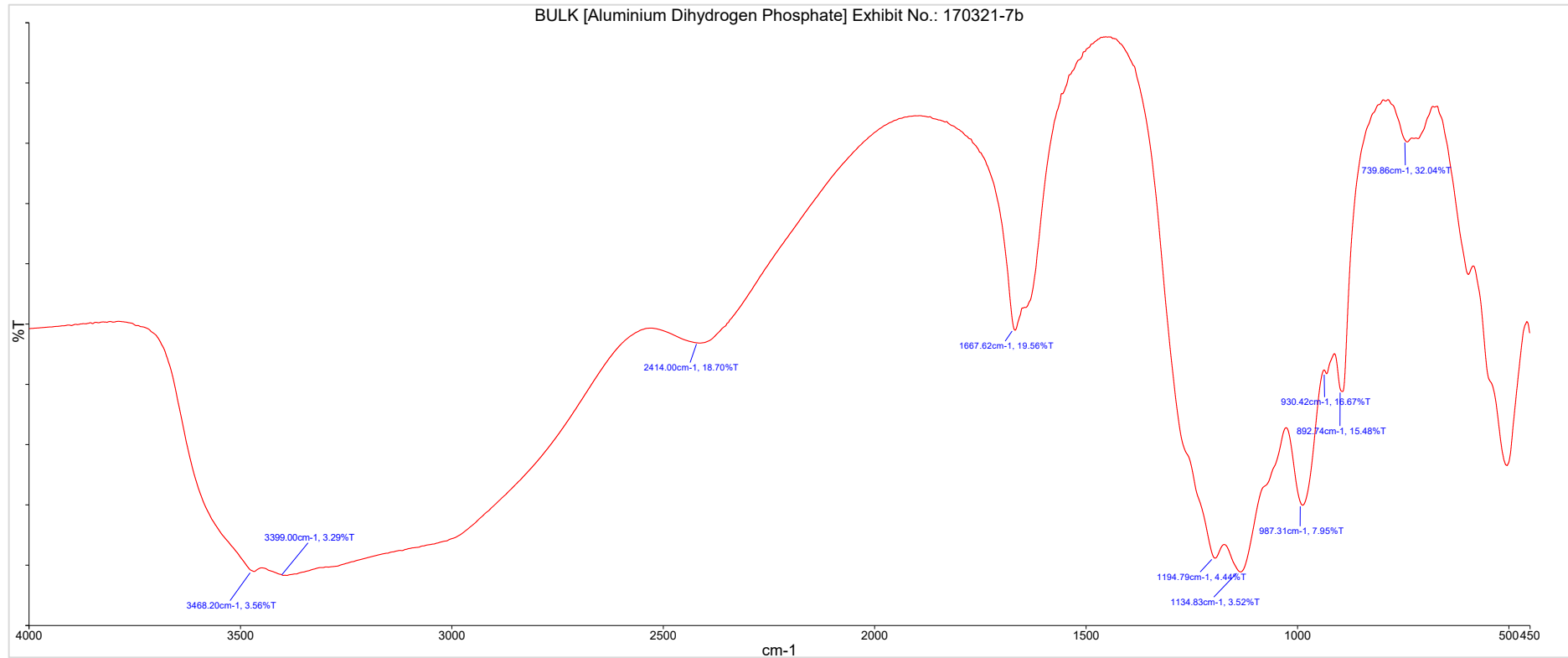


Figure 12 – FTIR spectrum of Specimen 12 - Bulk (Aluminium Dihydrogen Phosphate), Exhibit No. 170321-7b

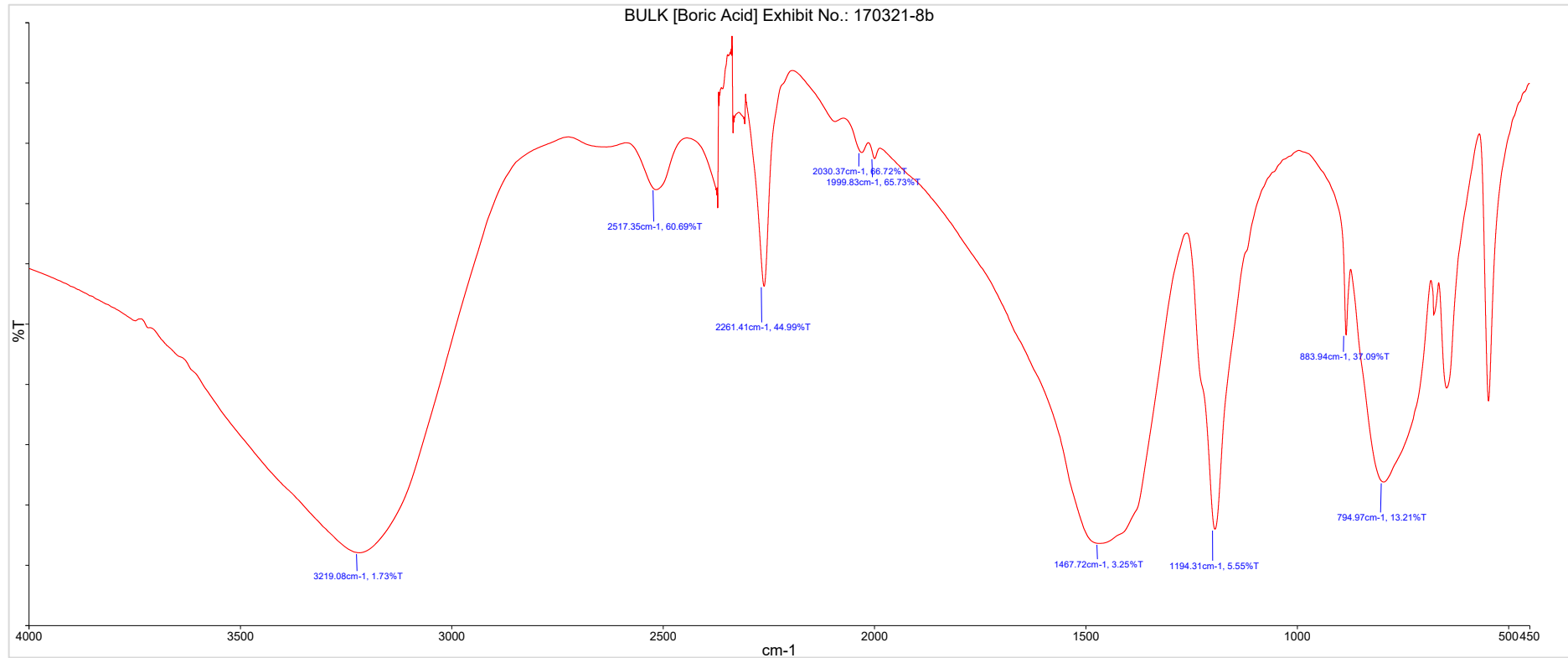


Figure 13 – FTIR spectrum of Specimen 13 - Bulk (Boric Acid), Exhibit No. 170321-8b

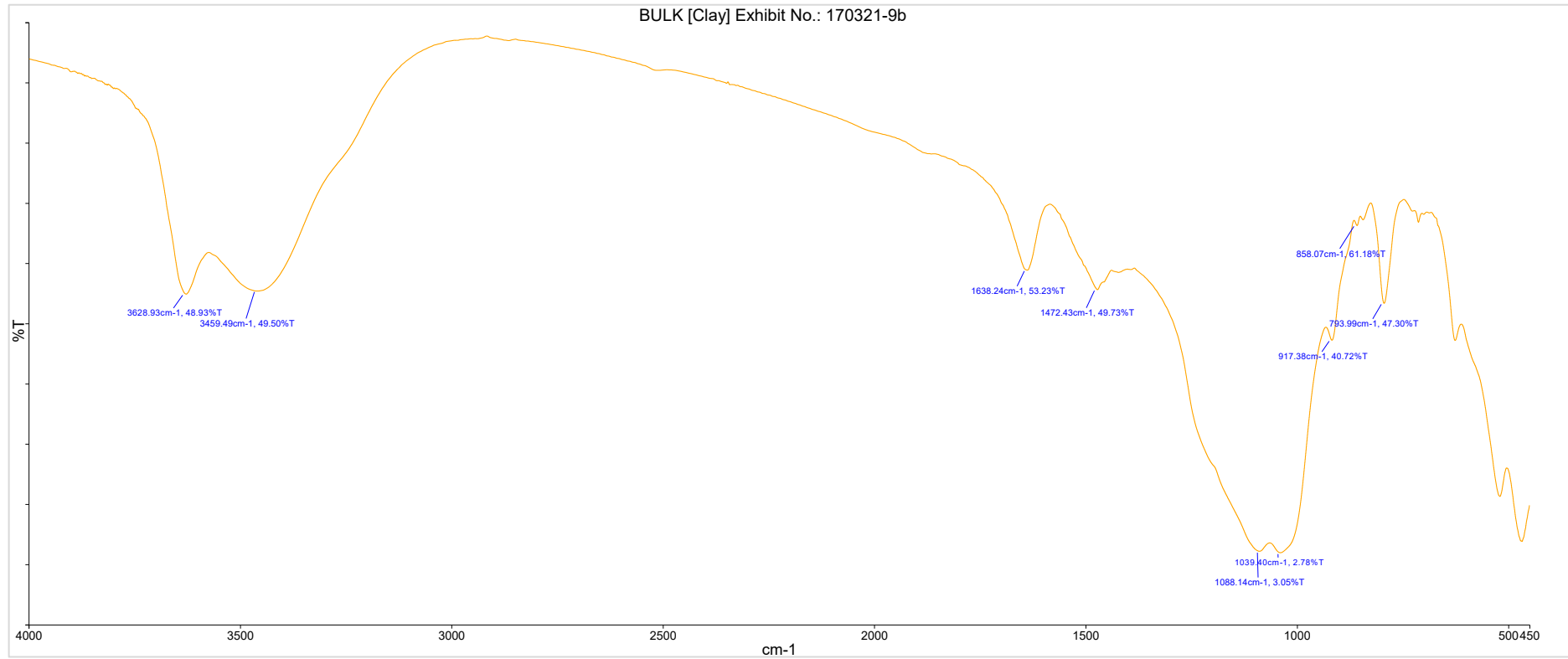


Figure 14 – FTIR spectrum of Specimen 14 - Bulk (Clay) Exhibit No. 170321-9b

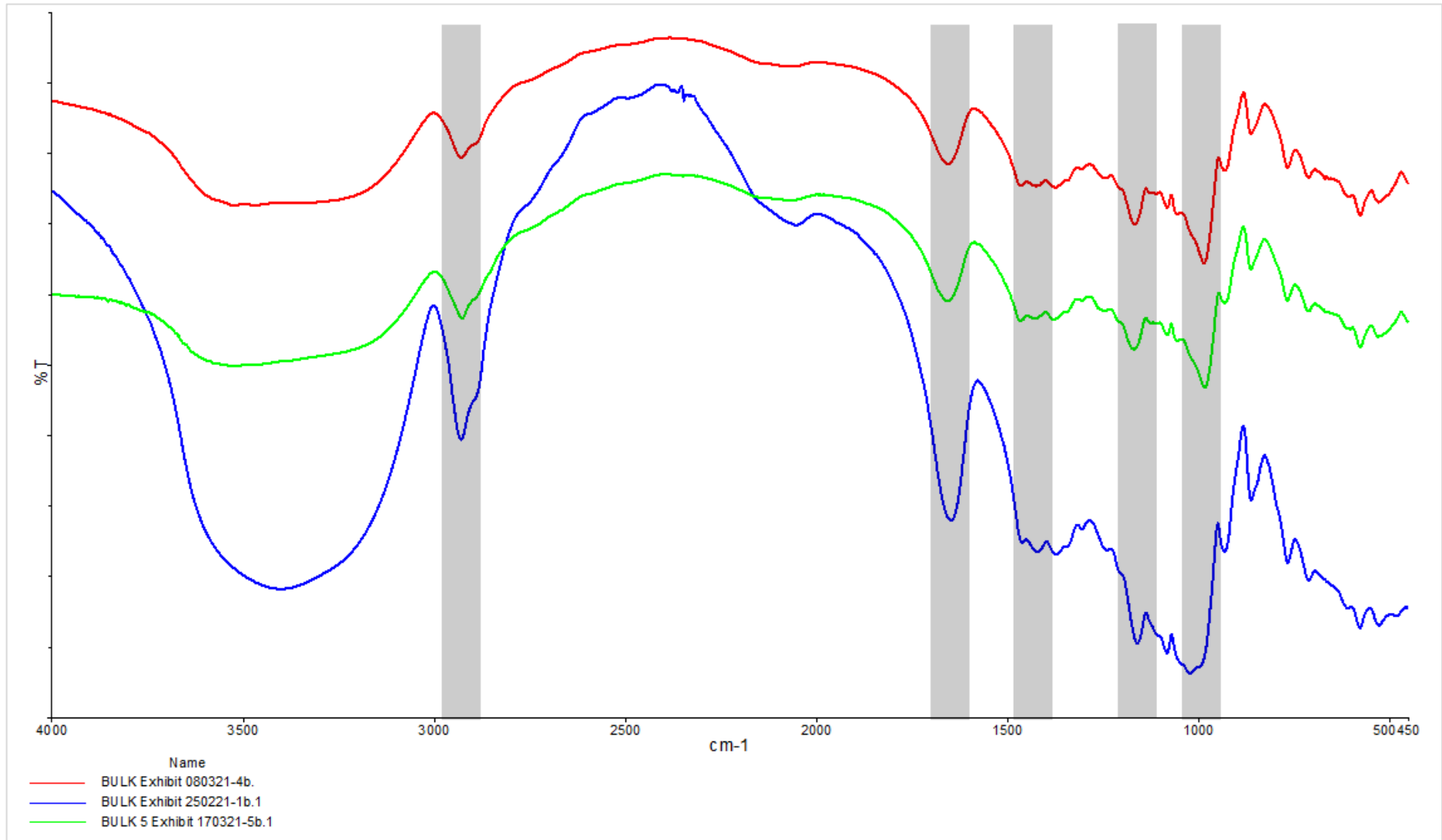


Figure 15 – FTIR spectrum comparison of Specimen 1, Specimen 5 and Specimen 10

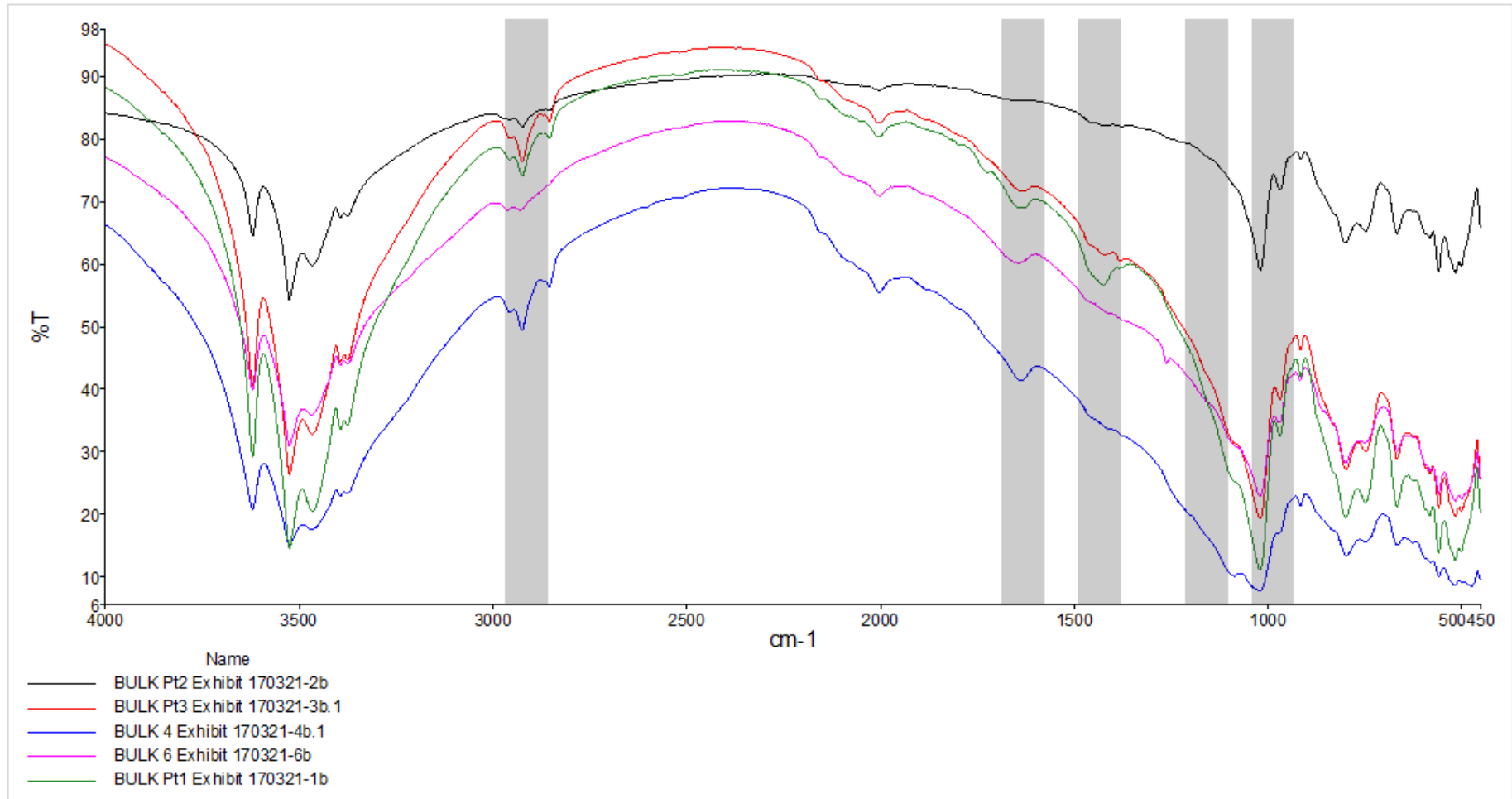


Figure 16a – FTIR spectrum comparison of Specimens 6, 7, 8, 9 and 11

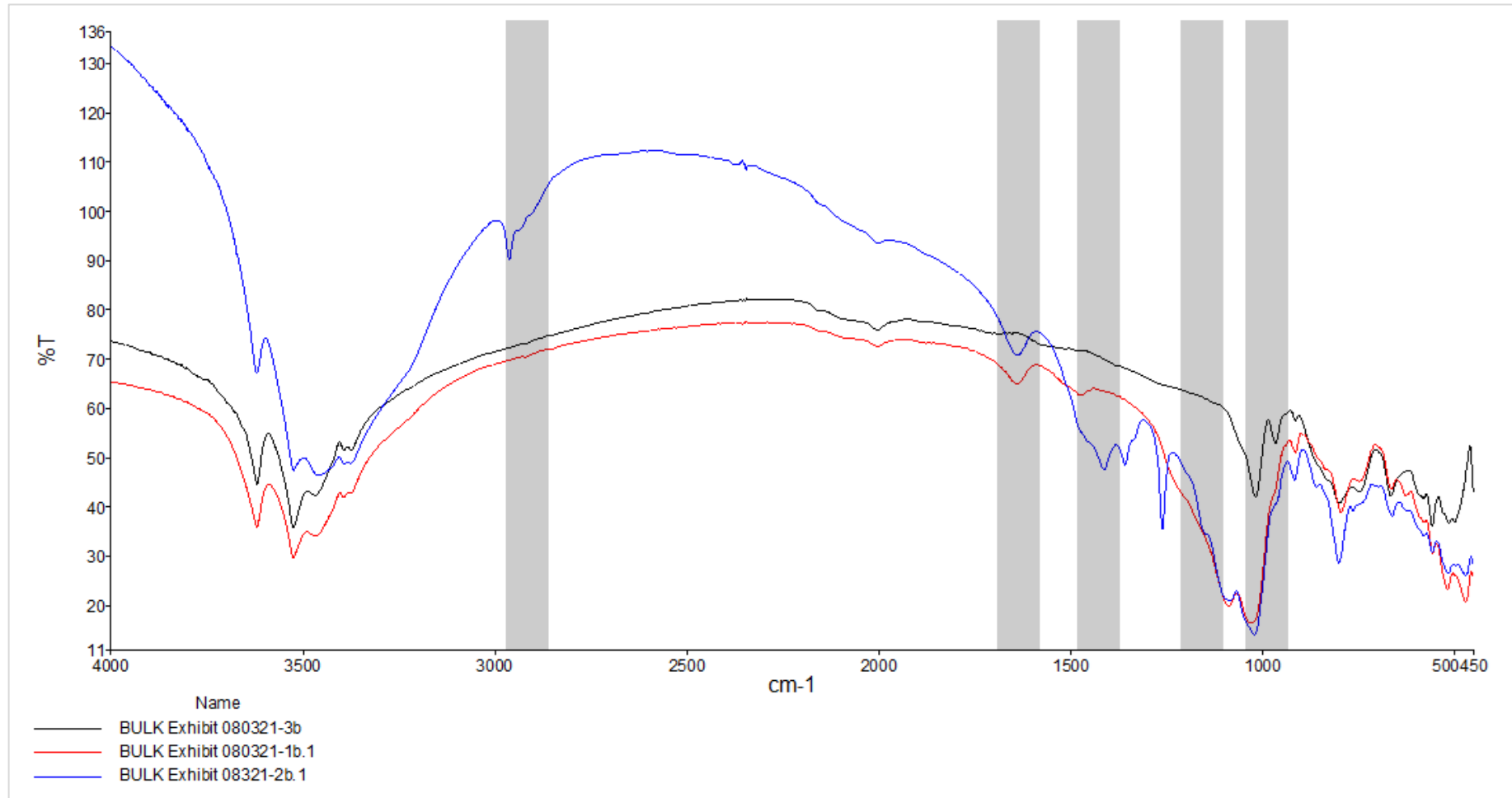


Figure 16b – FTIR spectrum comparison of Specimens 2, 3 and 4

TESTED BY:

Ms. Wang Zhan April
Senior Research Engineer II
Analytics & Characterisation



APPROVED BY:

Mr. Andrew Lim
Team Leader
Analytics & Characterisation
Scientific Infrastructure & Analytics



Note: This report shall not be reproduced except in full, without written approval from ICES. This report does not constitute an endorsement of any item or material tested and must not be used for any publicity materials, and/or for advertising purposes without approval from ICES. Test results relate only to sample(s) submitted by the client for technical studies and shall not be used for any purpose of technical litigation.

REPORT

REPORT REFERENCE: ICES/AC/21013_Part1b **DATE:** 6th May 2021

SUBJECT: UV-Vis analysis of powder specimens

COMPANY: ICES, A*STAR
1, Pesek Road, Jurong Island,
Singapore 627833

ATTENTION: Dr. Shaik Salim

DATE SAMPLE RECEIVED: 1st Apr 2021

DATE ANALYSED: 13th Apr 2021

DATE TEST COMPLETED: 3rd May 2021

DESCRIPTION OF SAMPLE(S):

Fourteen samples consisting of powder specimens (~5-10g each) were received.

S/N	Sample Description	Exhibit No.
1	Bulk	250221-1b
2	Bulk (Bulk Bag Left)	080321-1b
3	Bulk (Bulk Bag Right)	080321-2b
4	Bulk (Aluminium Hydroxide)	080321-3b
5	Bulk (Potato Starch)	080321-4b
6	Bulk Point 1	170321-1b
7	Bulk Point 2	170321-2b
8	Bulk Point 3	170321-3b
9	Bulk (Under Pallet) 4	170321-4b
10	Bulk (Platform) 5	170321-5b
11	Bulk (Outside Toilet) 6	170321-6b
12	Bulk (Aluminium Dihydrogen Phosphate)	170321-7b
13	Bulk (Boric Acid)	170321-8b
14	Bulk (Clay)	170321-9b

METHOD OF TEST:

The qualitative Spectroscopic (UV-Vis) analysis of powder specimens as received was prepared and conducted by PerkinElmer Lambda 950 UV/Vis/NIR Spectrophotometer.

1. Samples were prepared based on a 0.1% concentration in ultrapure water and heated to dissolve soluble starch. I₂-KI solution was added into cooled samples respectively to reveal blue complex, if any, after presence of amylose molecules from starch form an inclusion complex with polyiodide ions.
2. The prepared solutions were analyzed with UV/Vis/NIR Spectrophotometer to measure the absorbance of blue complex produced from 400 to 800 nm.
3. A reference standard curve was prepared from Specimen 5 - Bulk (Potato Starch), Exhibit No. 080321-4b, at concentration range between 0.01% to 0.10%.

RESULTS:

1. The sample images obtained after I₂-KI solution introduction are presented as Figure 1 and Table 1.

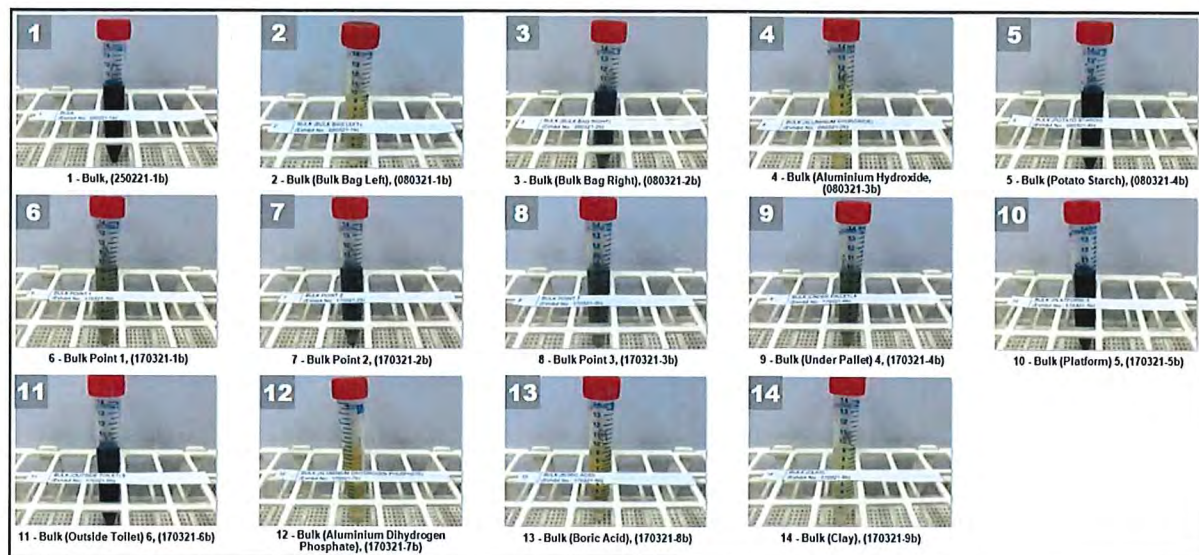


Figure 1 – Summary image of samples after I₂-KI solution introduction

S/N	Sample Description	Exhibit No.	Blue Coloration Appearance
1	Bulk	250221-1b	Yes
2	Bulk (Bulk Bag Left)	080321-1b	No
3	Bulk (Bulk Bag Right)	080321-2b	Yes
4	Bulk (Aluminium Hydroxide)	080321-3b	No
5	Bulk (Potato Starch)	080321-4b	Yes
6	Bulk Point 1	170321-1b	Faint
7	Bulk Point 2	170321-2b	Yes
8	Bulk Point 3	170321-3b	Faint
9	Bulk (Under Pallet) 4	170321-4b	Faint
10	Bulk (Platform) 5	170321-5b	Yes
11	Bulk (Outside Toilet) 6	170321-6b	Yes
12	Bulk (Aluminium Dihydrogen Phosphate)	170321-7b	No
13	Bulk (Boric Acid)	170321-8b	No
14	Bulk (Clay)	170321-9b	No

Table 1 – Qualitative indication as based on Blue Coloration appearance

2. The samples obtained after I₂-KI solution introduction were submitted to UV/Vis/NIR Spectrophotometer where an absorbance value as a function of blue complex was measured.

S/N	Sample Description	Exhibit No.	Absorbance (A)
1	Bulk	250221-1b	500.6
2	Bulk (Bulk Bag Left)	080321-1b	<20.0
3	Bulk (Bulk Bag Right)	080321-2b	34.1
4	Bulk (Aluminium Hydroxide)	080321-3b	ND
5	Bulk (Potato Starch)	080321-4b	592.0
6	Bulk Point 1	170321-1b	<20.0
7	Bulk Point 2	170321-2b	26.8
8	Bulk Point 3	170321-3b	<20.0
9	Bulk (Under Pallet) 4	170321-4b	<20.0
10	Bulk (Platform) 5	170321-5b	590.2
11	Bulk (Outside Toilet) 6	170321-6b	160.4
12	Bulk (Aluminium Dihydrogen Phosphate)	170321-7b	ND
13	Bulk (Boric Acid)	170321-8b	ND
14	Bulk (Clay)	170321-9b	ND

* ND refers to Not Detected

Table 2 – Absorbance values of samples after I₂-KI solution introduction

3. A reference standard curve plotted between 0.01% to 0.10% concentration range was generated with Specimen 5 - Bulk (Potato Starch), Exhibit No. 080321-4b.

S/N	Sample Description	Exhibit No.	Absorbance (A)	R ²
1	Bulk (Potato Starch) – 0.01%	080321-4b	20.0	0.9998
2	Bulk (Potato Starch)) – 0.02%		92.5	
3	Bulk (Potato Starch) – 0.05%		286.1	
4	Bulk (Potato Starch) – 0.10%		607.3	

Table 3 – Absorbance values of reference spectrum prepared from Specimen 5 - Bulk (Potato Starch), Exhibit No. 080321-4b.

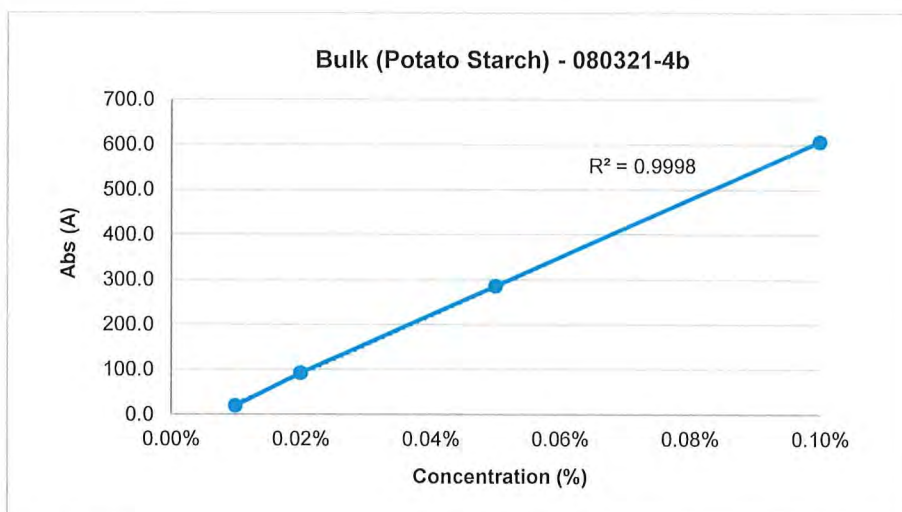


Figure 2 – Reference spectrum standard curve of Specimen 5 - Bulk (Potato Starch), Exhibit No. 080321-4b

TESTED BY:

Ms. Wang Zhan April
 Senior Research Engineer II
 Analytics & Characterisation

APPROVED BY:

Mr. Andrew Lim
 Team Leader
 Analytics & Characterisation
 Scientific Infrastructure & Analytics

Note: This report shall not be reproduced except in full, without written approval from ICES. This report does not constitute an endorsement of any item or material tested and must not be used for any publicity materials, and/or for advertising purposes without approval from ICES. Test results relate only to sample(s) submitted by the client for technical studies and shall not be used for any purpose of technical litigation.



ADDENDUM

ACCIDENT INVESTIGATION REPORT

FIRE AND EXPLOSION AT STARS ENGRG PTE LTD

(32E, TUAS AVENUE 11)

Prepared by

Shaik Mohamed Salim PhD, P.Eng.

Principal Specialist

Institute of Chemical and Engineering Sciences, A*STAR

A handwritten signature in black ink, appearing to read 'Shaik Mohamed Salim'.

Prepared for



4 October 2021

1 **Evaluation of whether there was sufficient oxygen available to support**
2 **combustion within heating jacket**

3

4 **1. Combustion requirements based on TNT equivalent**

5 Making a conservative assumption that the volume of air within the heating jacket is
6 approximately 300 L (0.3 m³)¹. This volume does not take into account the HTF fill volume that
7 was estimated to range from 40 to 160 L and would result in a corresponding reduction of air
8 available in the jacket to about 260 to 140 L.

9

10 With oxygen (O₂) comprising about 21 vol% of air, the number of moles of O₂ available to support
11 combustion within the heating jacket is calculated as follows:

- 12 i. Volume of O₂ within the heating jacket is = 0.21 x 0.3 m³ = 0.063 m³
13 ii. Taking O₂ density as 1.33 kg/m³ and molecular mass as 32 kg/kmol,
14 iii. Mass of O₂ available within the heating jacket is = 0.063 m³ x 1.33 kg/m³ = 0.08379 kg
15 iv. Hence, O₂ available within the heating jacket is = 0.08379 kg ÷ 32 kg/kmol = **0.0026 kmol.**

16

17 The heat transfer fluid (HTF) which acts as the fuel², is made up of highly refined hydrocracked
18 paraffinic base oil³. Hydrocracked base oils typically contains more than 90% saturated
19 hydrocarbons⁴. The hydrocarbons that makes up base oils are typically a complex mixture of
20 paraffins, isoparaffins, aromatic, and naphthenic (cycloparaffinic) molecules ranging in carbon
21 number from 20 to 40. In an analysis of lubricating oils, that are also made using base oils, Liang
22 et al. identified hydrocarbons in the range of C18 to C25⁵. Without proper formulation and

¹ The modelled capacity of the heating jacket is 300 L (0.3m³).

² Idemitsu Daphne Thermic 32-S oil

³ Lubricant Product Information, Daphne Thermic Oil Series – High Performance Heat Transfer Oil (Exhibit S-272 / CXD-53).

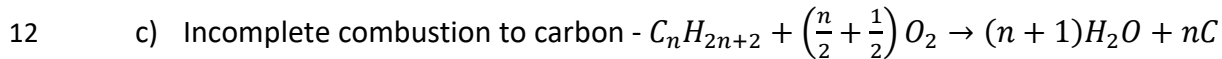
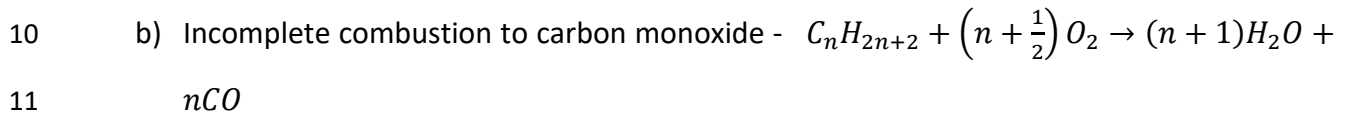
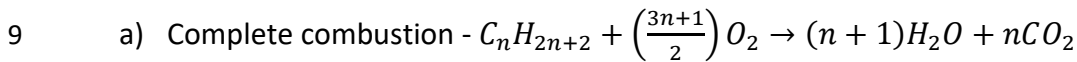
⁴ API 1509 (2021). Engine Oil Licensing and Certification System, American Petroleum Institute

⁵ Liang, Zhirong, et al. "Comprehensive chemical characterization of lubricating oils used in modern vehicular engines utilizing GC×GC-TOFMS." Fuel 220 (2018): 792-799.

1 blending, pure hydrocarbons C17 and above typically exists as a solid with liquid alkanes ranging
 2 from C5 (pentane) to C16 (hexadecane). It is therefore unlikely for base oils and therefore
 3 products such as heat transfer fluids to be primarily made of heavier hydrocarbons ranging from
 4 C17 to C40 as they would exist in a solid state at room temperature (i.e. melting points above 20
 5 °C). Nonetheless, in this evaluation, we will illustrate the oxygen needed for combustion of C5 to
 6 C40 alkanes to cover the wide range of hydrocarbons.

7

8 The general equations for combustion of alkanes are as follows:



13 Based on my first report dated 13 September 2021, the damage sustained at Stars Engrg factory
 14 unit correlates to overpressure from a chemical explosion involving a HTF volume of 40 L (0.04
 15 m³)⁶. In the calculation of this chemical explosion, the TNT equivalent energy released was based
 16 on the approximate heat of combustion of the HTF (40,000 kJ/kg)⁷ and explosion efficiency of
 17 1%⁸. The equation used to calculate the TNT equivalent of the explosion is given as:

18
$$m_{TNT} = \frac{\eta m \Delta H_c}{E_{TNT}} \text{ --- Equation 1}$$

19 Rearranging and expressing it in terms of HTF volume (V) and density (ρ) gives:

20
$$m_{TNT} = [\eta V] \left(\frac{\rho \Delta H_c}{E_{TNT}} \right) \text{ --- Equation 2}$$

21 From Equation 2, the term $[\eta V]$, denotes the effective amount of HTF that is converted
 22 (combusted) in the chemical explosion and is therefore = 0.01 x 0.04 m³ = 0.0004 m³. Based on
 23 the density obtained from the publicly available technical data sheets of Idemitsu Daphne

⁶ See pages 42-43 and Figure 24 of my report dated 13 September 2021.

⁷ See page 27 and Table 3 of my report dated 13 September 2021.

⁸ Typical efficiency value in TNT calculations range from 1 to 10% with 1% being used in a conservative calculation.

1 Thermic 32-S oil (i.e. 816 kg/m³ at 100 °C)⁹, the mass of HTF involved in the explosion is =
2 0.0004m³ x 816kg/m³ = 0.326 kg. The sample calculation¹⁰ for the O₂ needed to combust C5
3 alkanes is as follows:

- 4 • Complete combustion - $C_5H_{12} + 8O_2 \rightarrow 6H_2O + 5CO_2$
- 5 • 1 mole of C₅H₁₂ requires 8 moles of O₂ for complete combustion
- 6 • Assuming the HTF comprises 100% C₅H₁₂ (molar mass = 72 kg/kmol), the number of moles
7 of C₅H₁₂ involved in the explosion = $\frac{mass (kg)}{molar\ mass (\frac{kg}{kmol})} = \frac{0.326 (kg)}{72 (\frac{kg}{kmol})} = 0.00453\ kmol$
- 8 • Therefore the number of moles of O₂ required for complete combustion = 0.00453 x 8 =
9 **0.036 kmols.**

10

11 The graph in **Figure 1** shows the plotted values for the amount of O₂ required to combust 0.326
12 kg of HTF assuming it consists of hydrocarbon alkanes with carbon numbers ranging from C5 to
13 C40. The detailed results are listed in **Table 2**.

⁹ See page 27 and Table 3 of my report dated 13 September 2021.

¹⁰ Sample calculation values are rounded off.

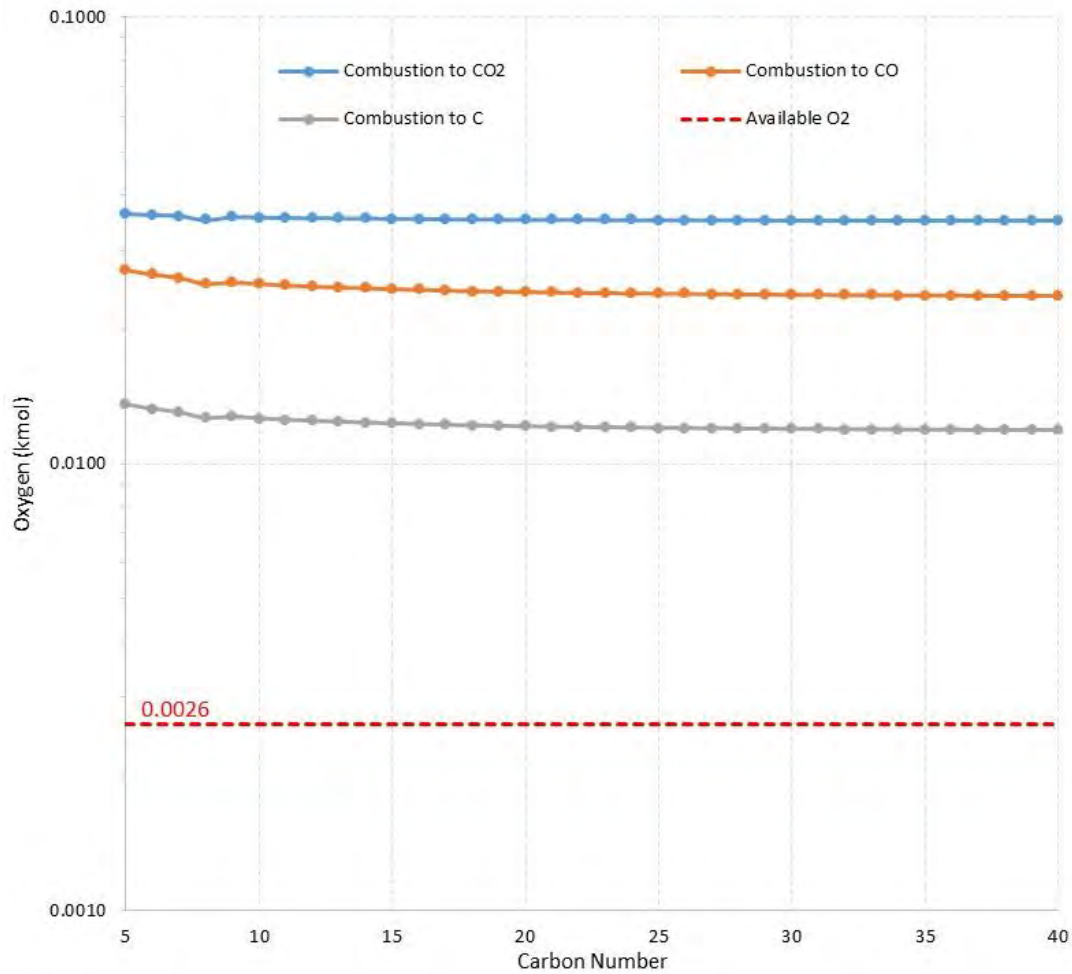


Figure 1. Plots of oxygen required for the complete and incomplete combustion of C5 to C40 alkanes based on the TNT equivalent approach.

From **Figure 1**, we can see that at all carbon numbers (i.e. C5 to C40), the amount of O₂ required for either complete or incomplete combustion exceeds that available in the heating jacket (i.e. 0.0026 kmol O₂). The lowest level of oxygen required is for the incomplete combustion of C40 (tetracontane) to carbon which needs 0.0119 kmol of O₂. Since it is practically impossible for the HTF to consist solely of C40 hydrocarbons (melting point 84 °C) and would actually consist of hydrocarbons with lower carbon numbers, such a mixture of alkanes would require more than 0.0119 kmol of O₂ for combustion.

1 **Table 1.** Overpressures corresponding to various oil (HTF) mist concentrations

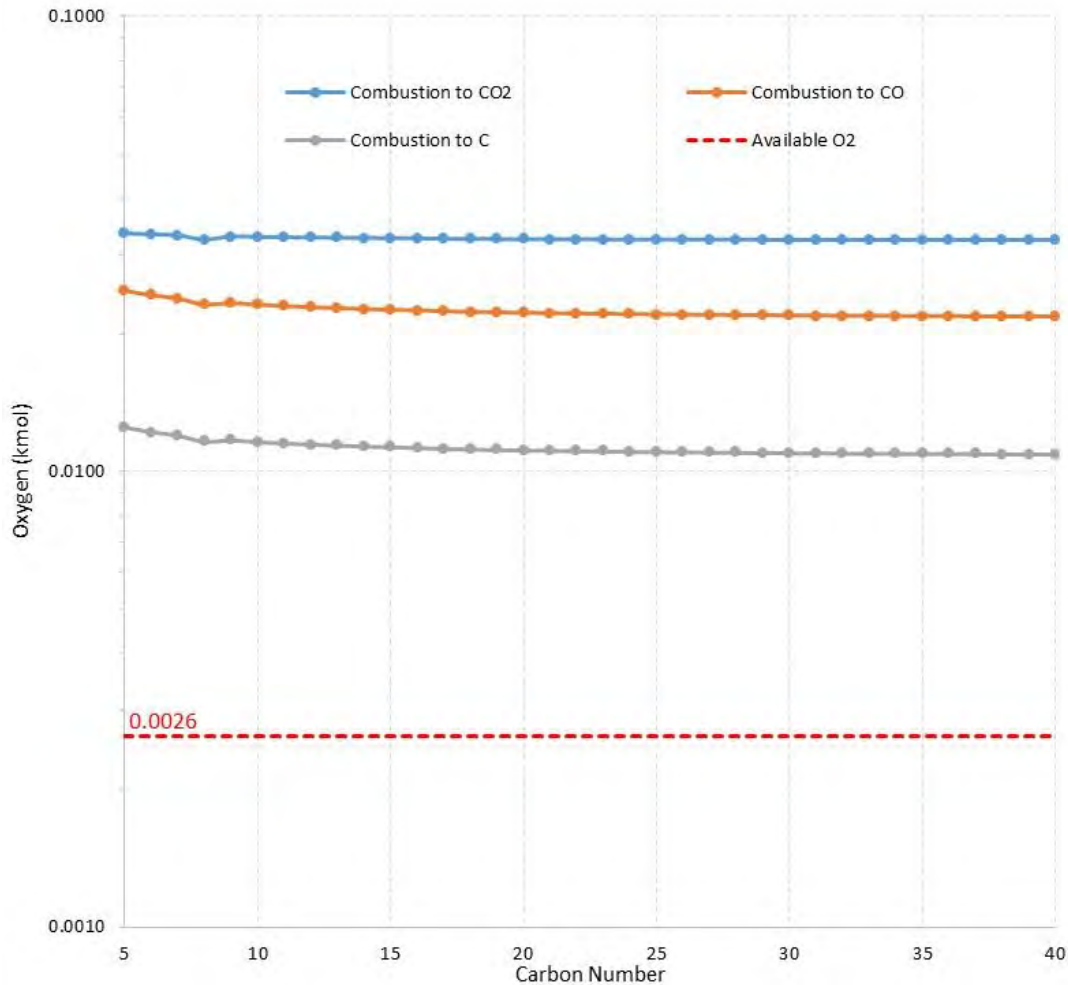
HTF mist concentration (mg/L)	Overpressure at 5 m (kPa)	Overpressure at 58 m (kPa)
48	9.9	0.7
50	10.0	0.7
100	13.9	0.9
200	19.9	1.2
300	25.0	1.3
400	29.7	1.5
500	34.1	1.6
600	38.3	1.7
700	42.3	1.8
800	46.3	1.9
900	50.1	1.9
1000	53.9	2.0

2
 3 As shown in Table 1, we can see that the oil (HTF) mist concentration should be about 1000 mg/L
 4 ($m' = 0.3 \text{ kg}$) in order to generate overpressures that are consistent with the physical damage
 5 seen at the Stars Engrg accident site. Based on this HTF mist concentration level of 1000 mg/L,
 6 the required amount of O_2 is again calculated in the same way as described above in Section 1.
 7 The sample calculation¹² for the O_2 needed to combust C5 alkanes is as follows:

- 8 • Complete combustion - $C_5H_{12} + 8O_2 \rightarrow 6H_2O + 5CO_2$
- 9 • 1 mole of C_5H_{12} requires 8 moles of O_2 for complete combustion
- 10 • Assuming the oil mist comprises 100% C_5H_{12} (molar mass = 72 kg/kmol), the number of
 11 moles of C_5H_{12} involved in the explosion = $\frac{\text{mass (kg)}}{\text{molar mass } (\frac{\text{kg}}{\text{kmol}})} = \frac{0.3 \text{ (kg)}}{72 (\frac{\text{kg}}{\text{kmol}})} = 0.00417 \text{ kmol}$
- 12 • Therefore the number of moles of O_2 required for complete combustion = $0.00417 \times 8 =$
 13 **0.033 kmols.**

14
 15 The resulting graph is shown in **Figure 2** below. The detailed results can be seen in **Table 3**.

¹² Sample calculation values are rounded off.



1 **Figure 2.** Plots of oxygen required for the complete and incomplete combustion of C5 to C40
 2 alkanes based on the oil mist concentration approach

3

4 From **Figure 2**, we can see that at all carbon numbers (i.e. C5 to C40), the amount of O₂ required
 5 for either complete or incomplete combustion exceeds the O₂ available in the heating jacket (i.e.
 6 0.0026 kmol O₂). The lowest level of oxygen required is for the incomplete combustion of C40
 7 (tetracontane) to carbon which needs 0.0109 kmol of O₂. Similarly, as deduced in Section 1, based
 8 on HTF mist concentrations, we would also expect that there is insufficient O₂ present within the
 9 heating jacket to result in an explosion that would generate sufficient overpressures that would
 10 correlate with the damage observed at the Stars Engrg accident site.

Table 2. Tabulated results for the required oxygen amounts for combustion based on TNT equivalent approach

Carbon Number	Molecular mass (kg/kmol)	O ₂ required (kmol)		
		Combustion to CO ₂	Combustion to CO	Combustion to C
5	72	0.0363	0.0272	0.0136
6	86	0.0361	0.0266	0.0133
7	100	0.0359	0.0261	0.0131
8	116	0.0352	0.0253	0.0127
9	128	0.0357	0.0255	0.0128
10	142	0.0356	0.0253	0.0126
11	156	0.0356	0.0251	0.0126
12	170	0.0355	0.0250	0.0125
13	184	0.0355	0.0248	0.0124
14	198	0.0354	0.0247	0.0124
15	212	0.0354	0.0246	0.0123
16	226	0.0354	0.0246	0.0123
17	240	0.0353	0.0244	0.0122
18	255	0.0353	0.0244	0.0122
19	269	0.0352	0.0243	0.0122
20	283	0.0352	0.0243	0.0121
21	297	0.0352	0.0242	0.0121
22	311	0.0352	0.0242	0.0121
23	325	0.0352	0.0241	0.0121
24	339	0.0352	0.0241	0.0120
25	353	0.0352	0.0241	0.0120
26	367	0.0352	0.0240	0.0120
27	381	0.0351	0.0240	0.0120
28	395	0.0351	0.0240	0.0120
29	409	0.0351	0.0240	0.0120
30	423	0.0351	0.0239	0.0120
31	437	0.0351	0.0239	0.0120
32	451	0.0351	0.0239	0.0119
33	465	0.0351	0.0239	0.0119
34	479	0.0351	0.0239	0.0119
35	493	0.0351	0.0238	0.0119
36	507	0.0351	0.0238	0.0119
37	521	0.0351	0.0238	0.0119
38	535	0.0351	0.0238	0.0119
39	549	0.0351	0.0238	0.0119
40	563	0.0351	0.0238	0.0119

Table 3. Tabulated results for the required oxygen amounts for combustion based on oil (HTF) mist concentration approach

Carbon Number	Molecular mass (kg/kmol)	O ₂ required (kmol)		
		Combustion to CO ₂	Combustion to CO	Combustion to C
5	72	0.0333	0.0250	0.0125
6	86	0.0331	0.0244	0.0122
7	100	0.0330	0.0240	0.0120
8	116	0.0323	0.0233	0.0116
9	128	0.0328	0.0234	0.0117
10	142	0.0327	0.0232	0.0116
11	156	0.0327	0.0231	0.0115
12	170	0.0326	0.0229	0.0115
13	184	0.0326	0.0228	0.0114
14	198	0.0326	0.0227	0.0114
15	212	0.0325	0.0226	0.0113
16	226	0.0325	0.0226	0.0113
17	240	0.0324	0.0225	0.0112
18	255	0.0324	0.0224	0.0112
19	269	0.0324	0.0223	0.0112
20	283	0.0324	0.0223	0.0111
21	297	0.0324	0.0223	0.0111
22	311	0.0324	0.0222	0.0111
23	325	0.0323	0.0222	0.0111
24	339	0.0323	0.0221	0.0111
25	353	0.0323	0.0221	0.0111
26	367	0.0323	0.0221	0.0110
27	381	0.0323	0.0221	0.0110
28	395	0.0323	0.0220	0.0110
29	409	0.0323	0.0220	0.0110
30	423	0.0323	0.0220	0.0110
31	437	0.0323	0.0220	0.0110
32	451	0.0323	0.0220	0.0110
33	465	0.0323	0.0219	0.0110
34	479	0.0323	0.0219	0.0110
35	493	0.0323	0.0219	0.0110
36	507	0.0322	0.0219	0.0109
37	521	0.0322	0.0219	0.0109
38	535	0.0322	0.0219	0.0109
39	549	0.0322	0.0219	0.0109
40	563	0.0322	0.0218	0.0109

[END]

EXPERT OPINION REPORT

A handwritten signature in blue ink, reading "Chew Yong Tian", is centered within a white rectangular box. The signature is written in a cursive style with a horizontal line underneath.

Authored by: Emeritus Prof. Chew Yong Tian

13 September 2021

Table of Contents

1	INTRODUCTION.....	1
1.1	Opinion sought.....	1
2	OVERVIEW OF THE MIXER MACHINE.....	1
2.1	Technical Details	1
2.2	A Commonly Used Machine.....	4
3	DESIGN ADEQUACY OF THE MIXER MACHINE	4
3.1	Safety Interlock System and RTD Mounting Position	4
3.2	Use of Heat Transfer Oil in Mixer Machine.....	6
3.3	Pressure Relief	7

Annex A – NH Sigma Kneader User’s Guide

Annex B – Mixer Machine Drawing, with Dimensions

Annex C – Electrical Line Diagram of the Mixer Machine

1 INTRODUCTION

1.1 Opinion sought

1.1.1 I have been asked by the Ministry of Manpower (“**MOM**”) to provide my opinion on the engineering design of the kneader/mixer machine used by Stars Engrg Pte Ltd (“**Stars**”) at its workplace at 32E Tuas Avenue 11, Singapore 636854 and which was involved in the fatal accident on 24 February 2021 (“**the Mixer Machine**”).

1.1.2 I have reviewed the following instructional materials which Stars had obtained from the manufacturer of the Mixer Machine, as provided by MOM to me:

(a) a 5-page “*NH Sigma Kneader User’s Guide*” (“**User Guide**”) (enclosed at Annex A);

(b) a drawing showing the dimensions of the Mixer Machine (enclosed at Annex B); and

(c) an electrical line diagram of the Mixer Machine (enclosed at Annex C).

1.1.3 I did not have the opportunity to physically inspect the Mixer Machine, but I was able to obtain relevant information regarding the Mixer Machine from my review of the technical report dated 10 September 2021 prepared by Matcor (the “**Matcor Report**”).

2 OVERVIEW OF THE MIXER MACHINE

2.1 Technical Details

2.1.1 I reproduce, with Matcor’s permission, the following 3-D drawings of the Mixer Machine from the Matcor Report:

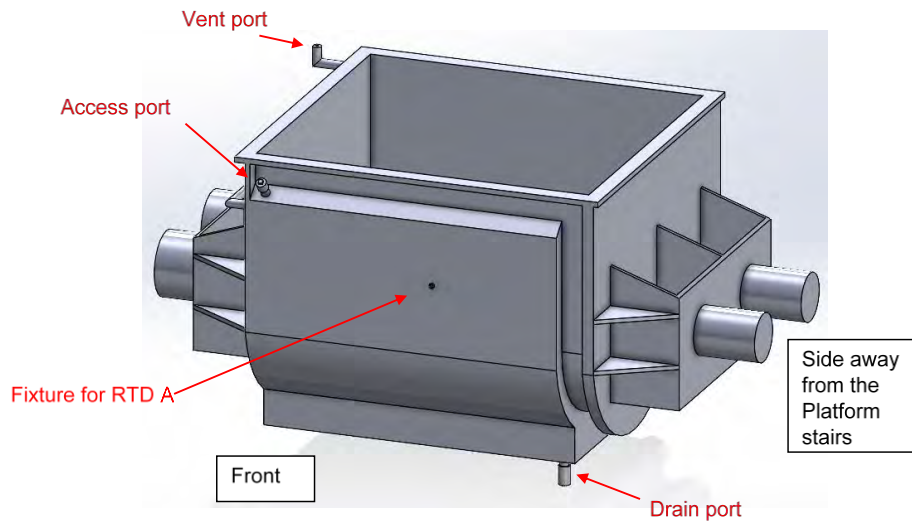


Fig. 1: Front view of Mixer Machine

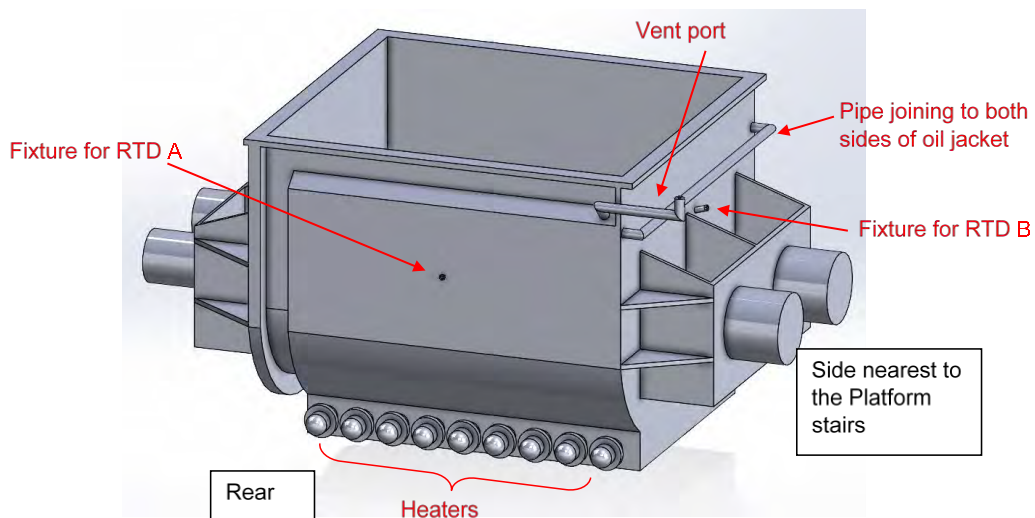


Fig. 2: Rear view of Mixer Machine

2.1.2 Briefly, the Mixer Machine was used to mix different high viscosity materials at a chosen temperature to produce a fire-retardant clay that can be used to make fire-retardant wrapping. The capacity of the Mixer Machine’s mixing chamber is 1000 litres and mixing is achieved through the counter-rotation of a pair of sigma-shaped blades at differential speed in two semi-cylindrical chambers with a horizontal dividing ridge in the middle at the bottom of the mixing chamber.

2.1.3 Heating of the materials within the mixing chamber is achieved through a heating jacket which encases the front, rear and bottom of the mixing chamber and which is to be filled with heat transfer oil. The heat transfer oil is heated by nine electrical

heaters rated at 5kW of power each at the bottom of the heating jacket. The heaters are connected to the electrical control panel and controlled by power switches (green knobs) at the bottom right hand corner of the electrical control panel (see Fig. 3).

2.1.4 The Mixer Machine's design temperature is 200°C, and the operating temperature range is 70°C to 160°C. The heating jacket temperature is measured by a resistance temperature detector/sensor (RTD A) mounted either on the front or the rear of the heating jacket. RTD A is connected to an electrical control panel as shown in Fig. 3 where the jacket temperature can be set. Based on the 'Electrical Report on Local Electric Panel' dated 25 July 2021, prepared by Yong Chun Hao, a licenced electrical worker with Yogo Engineering, and Vincent Char Poh Fang, a Switchboard Manufacturer of One Electric Pte Ltd (annexed to Matcor's Report), RTD A operates on an interlock system where, once the jacket temperature exceeds the value preset at the control panel, the interlock system will switch off power supply to the electrical heaters for safety.

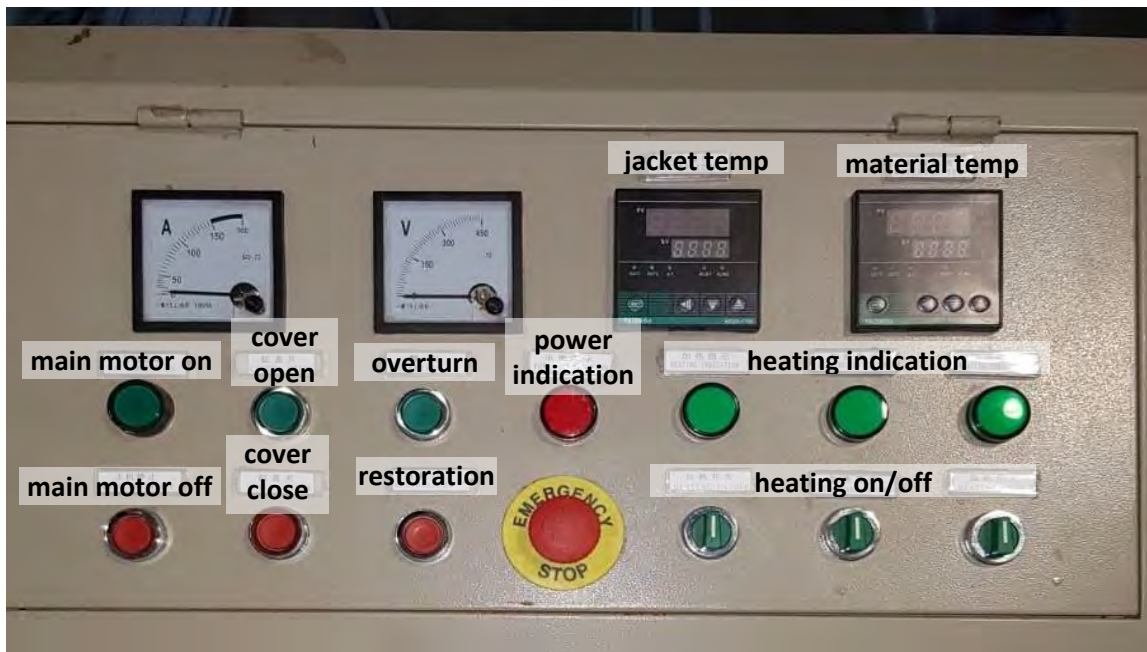


Fig. 3: Photograph of the control panel, with labels added (obtained from MOM)

2.1.5 The temperature in the mixing chamber is measured by a resistance temperature detector (RTD B) mounted on the side of the mixing chamber. RTD B is connected to the electrical control panel to indicate the material temperature in the mixing

chamber. There is no interlock system for this temperature input which only functions as an indicator.

2.2 A Commonly Used Machine

2.2.1 A kneader/mixer machine such as the Mixer Machine is a common machine used to mix contents of high viscosity. It has been used widely in the food industry for processing chewing gum, dough, toffee, and chemical industry for processing rubber, silicone, adhesives and resins.

2.2.2 The differential counter rotating blades apply shear force to the contents while mixing, similar to the function of manual kneading of flour and water together to form dough for making bread or noodles. The rotating blades can be vertical or horizontal and resemble the mathematical sign sigma (Σ), hence the name. It can also be designed for batch or continuous production.

2.2.3 The sigma kneader was invented by Heinz List, a German engineer in the 1940s. It is well tested over the years and safe to use if operated properly. The design of sigma kneaders can be with or without a heating jacket encasing the mixing chamber. In the former design, heat required in the production process would be added indirectly through heat transfer oil in the heating jacket (as in the case of the Mixer Machine). In the latter design, heat would be added directly to the contents in the mixing chamber via steam or hot water if water is required. Direct heating is the quickest way to achieve the desired temperature while indirect heating requires a lag time for the temperature to reach an equilibrium condition.

3 **DESIGN ADEQUACY OF THE MIXER MACHINE**

3.1 Safety Interlock System and RTD Mounting Position

3.1.1 In the case of the Mixer Machine, heat was added indirectly to the contents in the mixing chamber by increasing the temperature of the heat transfer oil via the heaters at the bottom of the heating jacket.

3.1.2 As electrical power was supplied to the heaters to increase the heat transfer oil temperature, there was a temperature interlock system to cut off the power supply

when the temperature exceeds the set point. This is an appropriate and important safety system to ensure that the heat transfer oil is not over-heated, maintaining jacket temperatures within the operating temperatures of 70°C to 160°C, as stated in the User Guide.

- 3.1.3 However, I note that there was no mention of the safety interlock feature of RTD A in the User Guide, or of how the RTDs were intended to be connected. For a safety interlock system as important as this, there should be clear explanation of how the temperature monitoring system operates, and instructions on how to connect the RTDs properly to ensure that the right temperature inputs are correctly received and processed by the control panel.
- 3.1.4 The temperature value that a user should preset for the heating jacket will depend on whether the desired material temperature in the mixing chamber can be achieved. This will involve a trial-and-error process. Thus, it is important for RTD A and RTD B to measure the heat transfer oil and material temperatures accurately so that the heating jacket temperature can be set accurately within the range of 70°C to 160°C to achieve the desired material temperature. To reduce lag time for a more responsive feedback temperature control system, RTD A and RTD B should be mounted close to the heat transfer oil level and the material level respectively. This will minimise the time required by the oil and material temperature to reach the RTD A and RTD B locations through conduction. However, this is not the case in the present Mixer Machine as it appears that the mounting positions for at least RTD A could have been lower. According to the Matcor Report, the heat transfer oil level of 245 litres (corresponding to half of the heating jacket cylinder height) is lower than the mounting positions for RTD A. In relation to the mounting position for RTD B, this would depend on the level of material used by the user and may vary. A less responsive feedback temperature control system means that it will take a longer time for the system to recognise that the desired equilibrium temperature has been reached. However, the trial-and-error process can be safe as long as the heating jacket is operated within the temperature range of 70°C to 160°C and sufficient heat transfer oil is used in the heating jacket.

3.2 Use of Heat Transfer Oil in Mixer Machine

3.2.1 Assuming that there was sufficient heat transfer oil in the heating jacket so that the heaters are fully immersed in the oil and the oil is in contact with most of the bottom surface area of the mixing chamber, there would be good heat transfer between the heat transfer oil and the materials inside the mixing chamber. Heat transfer within the heat transfer oil is achieved through the process of natural convection where oil is much hotter next to the heating elements. The temperature within the heat transfer oil will not be homogenous but can be kept within the stated design temperature of 200°C at any location through the use of RTD A with its safety interlock system. Heat is then transferred to the contents in the mixing chamber by conduction through the mixing chamber wall. The larger the area of the mixing chamber surface in contact with the heat transfer oil, the more efficient is this heat transfer process.

3.2.2 The User Guide specifically mentions the required heat transfer oil level in the heating jacket as shown in the extract at Fig. 4.

Equipment name	Oil grade	Oil quantity
Reducer	45 # engine oil	Add it to see the oil by the window.
Vacuum pump	special oil for vacuum pump	It has been added before leaving the factory
Kneader jacket	HD320-350 #	When refueling, you need to open one side vent hole and add it to half the height of the cylinder.
Remarks: Observe the oil window and add various oils regularly		

Fig. 4: Extract from page 5 of the User Guide

The User Guide which specifies adding oil to *“half the height of the cylinder”* is not very useful in a closed/opaque heating jacket where the height cannot be visualised. A closed/opaque heating jacket (such as that of the Mixer Machine) is common for design simplicity and strength consideration. In such a design, it is better to specify the volume of the heat transfer oil required instead of just describing the *“height” / level* which the oil should reach. Then users are able to top up the heating jacket with the right volume of oil, which would correspond to the minimum required level. Ideally, there should also be a safety margin in the minimum oil volume, to account for minor fluctuations and possible human errors. This could be presented as a

minimum volume with some additional buffer already included within. For example, if 200 litres is the minimum volume for safe operation of the heaters in the heat transfer oil, a 20% safety buffer could be included so that the user is instructed to use a minimum of 240 litres of heat transfer oil. Notwithstanding the above, it is common sense that minimally, the user should fill enough heat transfer oil to cover the heaters and have the oil contact a significant amount of the mixing chamber's surfaces. This can be checked, for example, with the use of a dipstick.

3.2.3 In this regard, in an opaque/closed heating jacket (such as that of the Mixer Machine) where oil level cannot be visualised, provision of a flexible dip stick similar to that for detecting the oil level in an automobile automatic transmission gear box should be provided with clear marking on the dip stick of the required oil level.

3.3 Pressure Relief

3.3.1 The User Guide stated that the heating jacket had a design temperature of 200°C and an operating temperature range of 70°C to 160°C, and was designed to operate at not more than 2 barg.

3.3.2 In my view, the design of Mixer Machine is clearly not meant for closed pressurised system operation (i.e. with all the openings of the heating jacket closed during operation). There are three openings in the heating jacket, namely access port, vent port, both at the top of the jacket, with the drain port at the bottom (see Fig. 1 and Fig 2 above).

3.3.3 The drain port is always closed unless draining of the heat transfer oil is required.

3.3.4 Either the vent port or the access port can be used for adding the heat transfer oil, during which time the other port must be opened to vent the displaced air.

3.3.5 During production, heat is introduced through the heating jacket. There will be some evaporation of the heat transfer oil inside which increases with increasing temperature. The vent port should be opened to allow the oil vapour to escape to prevent the building up of pressure in the jacket. The vent port is described in page 4 of the User Guide as "*an oil vapor vent... provided at the highest point behind the machine*".

- 3.3.6 After production, the mixing chamber has to be tilted towards the front by 90° to facilitate emptying of the contents in the mixing chamber. In this position, the access port is at the bottom and oil would leak out if not closed. Thus, according to information provided by MOM, a plug was provided by the manufacturer to close the access port.
- 3.3.7 When the mixing chamber is tilted forward, the heat transfer oil in the heating jacket would flow towards the front of the jacket. The connecting pipe between both front and rear of the heating jacket facilitates the equalisation of oil within the heating jacket. The vent port should be opened to allow the displaced gas to flow to the rear of the jacket. The vent port at the rear would now be at the top and allow venting of the gas, relieving the build-up of any pressure within the heating jacket.
- 3.3.8 In my view, the design of the Mixer Machine is sound when operating as an open system. A closed system will not enhance the heat transfer from the oil in the heating jacket to the contents of the mixing chamber, so there is no reason / benefit for the Mixer Machine to be designed with a closed pressurised system or for it to be operated as a closed system. I understand from MOM, however, that Stars had operated the Mixer Machine as a closed pressurised system by plugging both the access and vent ports during operation/production. If the vent port had been designed without a threaded screw connector, it absolutely cannot be plugged by a user.
- 3.3.9 If, contrary to my view, the heating jacket were to be operated as a closed pressurised system, I would expect there to be safety precautions given in the User Guide with a minimum requirement of a pressure gauge and a safety interlock system, to stop the heating when pressures are close to unsafe levels. Otherwise, the jacket could suffer mechanical stresses and over time, fatigue could lead to loss in strength of the metallic structure.

-End-

Annex A – NH Sigma Kneader User's Guide



NH Sigma Kneader

USER'S GUIDE

Laizhou Keda Chemical Machinery Co., Ltd.

Address: Xidingjia Village Shahe Town, Laizhou City, Shandong Province, China.

Tel: 0086-(0)535-2377668 Fax: 0086-(0)535-237767 Website: www.kedahuai.com

One. Product description

It is special used for mixing and kneading high-viscosity material. It has excellent effect for mixing, kneading, crushing and dispersing because of the intense shearing force which produced by two powerful rotary blades.

Kneader temperature adjustment can be done by using heat transfer oil circulation, electric heating, steam and water cooling. It can be made tank body jacket, wallboard jacket, stirrer passing cooling water, passing heat transfer oil and such structures for heating and cooling.

Two. Technical parameter

Discharge Way: hydraulic tilt, screw extruding, bottom valve.

Function: can be cooling or heating (electrical, cycle hot water/oil).

Type: normal type, pressure type, vacuum type.

Material: SS304, SS316 or carbon steel can be available.

Speed: controlled by inverter, or fixed

Blades & Chamber: can be fine polished

Three. Application

Widely used in high viscosity product

-----Chemicals Industry:

Resins, Sealant, silicon rubber, glue/ adhesive, paint, Clay, Dye, BMC/CMC, pigment, plastics, batteries.

-----Food Industry:

Bubble gum, dough, chewing gum, soft candy, cheese etc.

-----Pharmaceutical:

Some medicines & medical materials.

Four. Technical specification

Model	Motor Power (KW)	Heating Way	Steam Pressure (Mpa)	Vacuum Degree (Mpa)	Pressure (Mpa)	Dimensions (M)	Weight (KG)
2L	1.1-2.2	Electrical/Cycle Steam/Hot Oil/Hot Water in Jacket	Usually 0.3(can add as requirement)	- 0.09Mpa (Vacuum Type)	0.45 (Pressure Type)	1.1*0.4*0.5	150
5L	1.1-2.2					1.1*0.5*0.6	200
10L	1.1-2.2					1.2*0.5*0.6	300
50L	2.2-7.5					1.5*0.7*1.0	600
100L	4-11					1.6*0.7*1.3	1000
200L	5.5-15					2.0*1.2*1.5	1800
300L	5.5-22					2.3*1.2*1.8	2200
500L	11-22					2.6*1.2*1.8	3000
1000	15-37					2.8*1.2*1.8	4500

L							
1500 L	18.5- 45					3.3*1.9*1.9	5500
2000 L	37-75					3.5*2.2*2.2	6800
3000 L	45- 110					4.0*2.2*2.4	9500

Five. Structural characteristics and working principle

-The NH kneader is a horizontal double shaft parallel type, the stirring shaft is Σ type, the double paddles are horizontally arranged, rotate oppositely and have different speeds. When working, it is driven by the motor through the reducer to the active paddle, and the driven paddle is driven by the gear. So that the materials can be fully kneaded, blended, mixed, and sheared to accelerate physical and chemical reactions.

-Main feature:

1. Strong and powerful during mixing.
2. Large loading factor, and the charging is more at one time.
3. The diameter of the mixing blade is large and the spiral angle is excellent, the material has good axial flow during the kneading process.
4. Adopt chassis, easy to install and debug
5. Centralized electrical control, including the operation of the host, tilting cylinder and digital display temperature control, which is convenient for user operation and process control.

-Structure and working principle

The NH series kneader is mainly composed of the main body of the kneader, the transmission system, the tilting cylinder pouring system, the heating system, and the electrical control system.

The main body of the kneader is composed of a mixing cylinder, a mixing paddle, wall plates at both ends, a shaft seal, a bracket and a base. It is W-shaped, which is welded by two layers of steel plates. The inner layer is made of stainless steel. The bottom is composed of two semi-cylindrical columns. There is a horizontal dividing ridge in the middle. The jacket can be injected with cold and hot medium to carry out cold heat treatment on the material of the mixing tank.

The bottom of the electric heating mixing cylinder is provided with an electric heating tube. The jacket needs to be filled with heat conduction oil. The heat conduction oil is heated by the electric heating tube, and the heat conduction oil transfers the materials inside the mixing cylinder

After manually opening the cover, it is necessary to plug in the safety.

Six. Installation of the machine

1. Installation space
 - 1) The height is 90cm, which is necessary for tilting the cover.
 - 2) The minimum width space is reserved, 0.5m on the left and 0.8m behind the machine, which can be used for supporting pipelines and maintenance.
 - 3) The operating space in front of the machine shall be set aside according to the specific requirements of customers.

2. Foundation requirements

- 1) Concrete floor thickness is more than 20cm.
 - 2) Certificate cement base of specific level standard.
3. Installation and positioning

There are two positioning methods, one is welding, and the other is ground bolt.

- 1) For welding positioning, before and after the user purchases the machine, according to the foundation map provided by the supplier, six square irons can be directly welded when the foundation is poured.
- 2) Positioning of anchor bolt: The user reserves square holes for anchor bolts when pouring the foundation according to the foundation plan provided by the supplier. After the machine is purchased, it is moved to the foundation and the anchor bolts are fixed to the ground or pouring with cement.

Seven. Power

Power supply quality Voltage: 380V \pm 10V

Frequency: 50Hz \pm 5Hz

If regulated power supply can be used, the service life of motors and electrical components can be extended.

Eight. Electric heat source

Heating method: electric heating oil

1. Design of thermal jacket

- 1) Design temperature: 200 $^{\circ}$ C
- 2) Operating temperature: 70-160 $^{\circ}$ C
- 3) Working pressure: \leq 0.2Mpa

2. This system uses heat conduction oil electric heating tube for heating, which has high requirements for the quality and material of heat conduction oil. It is recommended to use HD series high temperature heat conduction oil. Generally, the heat conduction oil should be preheated before being injected into the jacket of the mixing tank to facilitate the evaporation of the moisture of the oil. An oil vapor vent is provided at the highest point behind the machine, and the oil vapor vent is directly connected to the vent Pool. Care should be taken in the heating process, and avoid using hands to detect whether the pipes and the outside of the mixing tank are heated. It's easy to get burned.

Nine. Maintenance

A good device needs daily maintenance, the specific matters are as follows:

1. Transmission system:

- 1) The V-belt is a wearing part. The elasticity of the V-belt should be suitable. After the extension, the motor base can be adjusted.
- 2) Cylindrical gear reducer uses gear oil, the first maintenance is 500h.
- 3) The drive gear of the kneader should be filled with lubricating oil regularly.
- 4) Lubricant should be refilled regularly at the bearing end of the main shaft.

2. Hydraulic system

The hydraulic system should periodically replace the hydraulic oil, and pay attention to whether the oil quality is discolored. The hydraulic oil should be replaced once a year. The maintenance of the hydraulic cylinder should be checked for oil leakage and keep the piston rod clean.

3. Heating system

In the heat conduction oil heating system, it is strictly forbidden to dry the electric heating tube, and pay attention to check that the heat conduction oil in the jacket is added in time with the loss of heat conduction oil. A heating power of 800w, a total of three.

4. Shaft seal part

Daily inspection of the shaft seal should not be too loose, and should be adjusted to a slightly compressed state, but it should not be pressed too strongly. The shaft seal part should be maintained every six months, remove the seal seat, and clean the shaft diameter and seal chamber with silicone oil, replace the V-ring or PTFE packing, oblique incision should be taken.

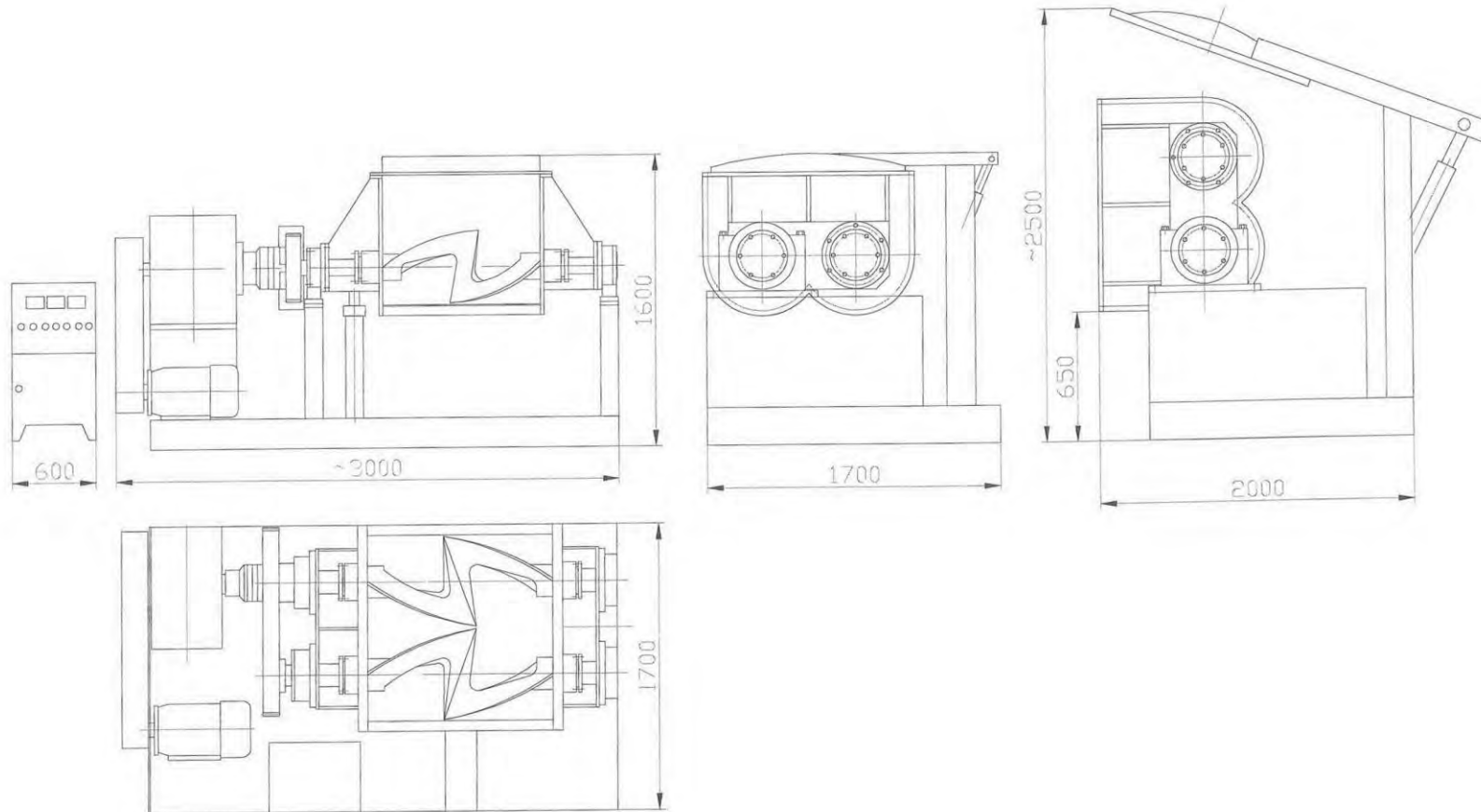
5. Clean

After each work, the opening of the mixing tank should be cleaned and the cover closed.

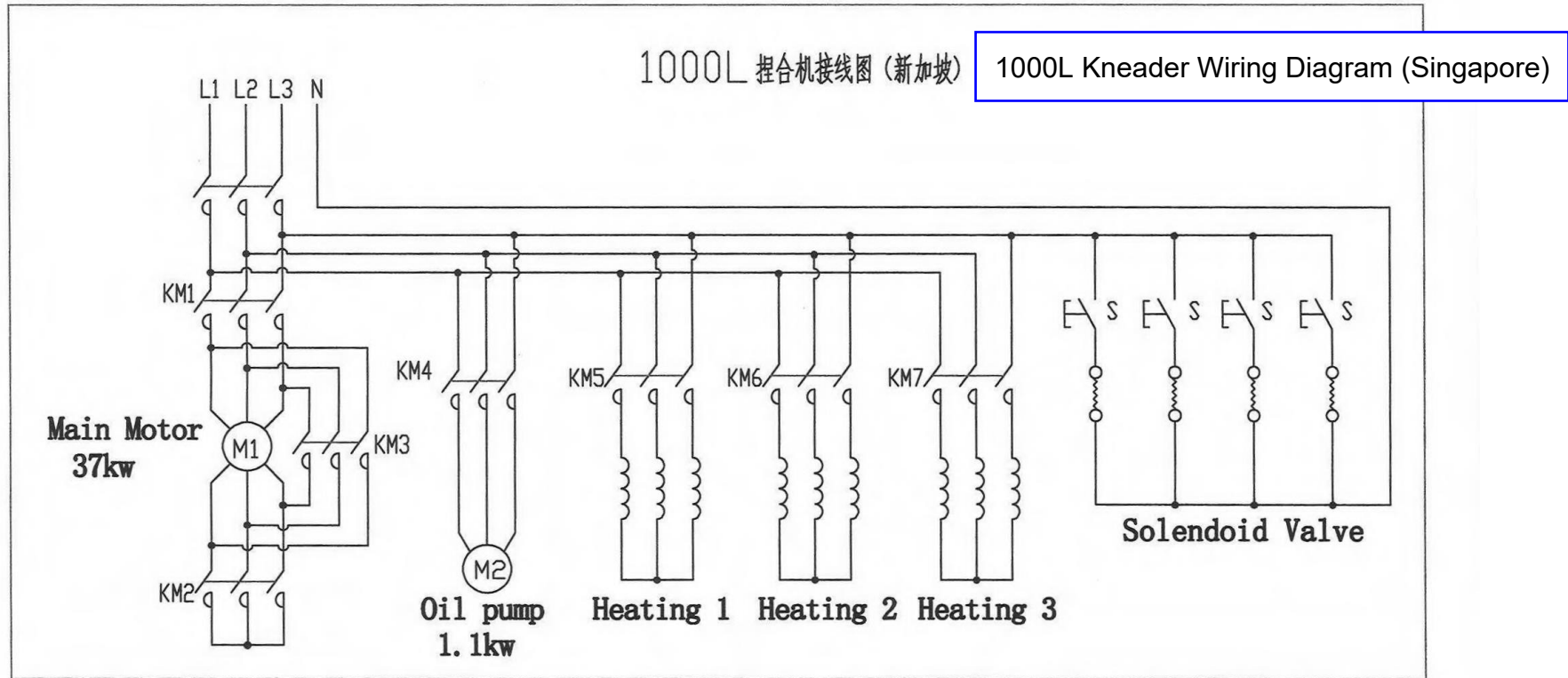
Ten. Attached sheet of the equipment needs oil grade and quantity

Equipment name	Oil grade	Oil quantity
Reducer	45 # engine oil	Add it to see the oil by the window.
Vacuum pump	special oil for vacuum pump	It has been added before leaving the factory
Kneader jacket	HD320-350 #	When refueling, you need to open one side vent hole and add it to half the height of the cylinder.
Remarks: Observe the oil window and add various oils regularly		

Annex B – Mixer Machine Drawing, with Dimensions



Annex C – Electrical Line Diagram of the Mixer Machine



**INVESTIGATION INTO THE CAUSE OF THE EXPLOSION
THAT OCCURRED AT 32 E TUAS AVENUE 11, SINGAPORE ON
24 FEBRUARY 2021**

**PREPARED ON THE INSTRUCTIONS OF
RAJAH AND TANN LLP**

D J Rose BSc PhD CChem FRSC
Singapore Office
15 September 2021

Our Ref: S36-543816
Your Ref: TCK/JCF/ZYG/TCW/352017/1

Hawkins

Leaders in forensic investigation
www.hawkins.biz

Offices at:

Cambridge	Tel	+ 44 (0)1223 420 400
Manchester	Tel	+ 44 (0)161 493 1860
Bristol	Tel	+ 44 (0)1454 273 402
London	Tel	+ 44 (0)20 7481 4897
Birmingham	Tel	+ 44 (0)121 705 3222
Leeds	Tel	+ 44 (0)113 260 0172
Reigate	Tel	+ 44 (0)1737 763 957
Glasgow	Tel	+ 44 (0)1355 228 103

Hawkins is the trading name of HAWKINS & ASSOCIATES (SINGAPORE) PTE LTD
Registered office: 1 Marina Boulevard, #28-00, One Marina Boulevard, Singapore (018989)
Registered in Singapore - Registration Number: 201622202E

International Offices:

Dubai	Tel	+ 971 4372 1260
Hong Kong	Tel	+ 852 2548 0577
Singapore	Tel	+ 65 6202 9280

CONTENTS

1. INTRODUCTION	1
2. BACKGROUND	4
2.1 Stars	4
2.2 The Purchase of the Machine	7
2.3 The Delivery and Installation of the Machine	10
2.4 Witness Information	11
a) Mr Chua	11
b) Messrs Rahad, Mehedi, Lizon, Molla and Jitu	16
2.5 Video Footage	18
3. THE MACHINE	20
4. INSPECTION OF THE SCENE	22
4.1 Overview	22
4.2 Unit 32F	22
4.3 Unit 32E	22
5. INSPECTIONS AT MATCOR	27
6. DISCUSSION	31
6.1 The Cause of The Explosion	31
6.2 Factors that Contributed to the Explosion	38
6.3 Should the oil reservoir have been vented?	41
6.4 The Effect of Repairs	43
7. PRELIMINARY CONCLUSIONS	45
8. EXPERT'S DECLARATION	47

TABLE 1 (Within Report)

1. Heating element resistances.

APPENDICES A - C

A. Summary of qualifications and experience of Dr D J Rose and Mr GA Cooper.

B. Documents and Information provided by Stars.

C. Summary of information provided by Messrs Rahad, Mehedi and Lizon.

PHOTOGRAPHS 1 - 54

1. INTRODUCTION

1.1 An explosion occurred in premises occupied by Stars Engrg Pte Ltd (Stars) at 32E Tuas Avenue 11 (the Site) at approximately 11:25 hours on 24 February 2021. Unfortunately, three people died as a result of their wounds and seven more suffered varying degrees of burn injuries. Stars instructed Hawkins & Associates (Singapore) Pte Ltd to provide independent technical advice, for the purposes of gathering evidence to assist an Inquiry Committee arising from the incident. Hawkins was instructed that the Terms of Reference to the Inquiry Committee should be:

(a) Inquire into and ascertain the causes and circumstances of the accident that led to an explosion at the premises of Stars located at 32E Tuas Ave 11 on 24 February 2021.

(b) Make recommendations to prevent the recurrence of such an accident at workplaces.

(c) Consider the evidence put before the Inquiry Committee as led by State Counsel from the Attorney-General's Chambers.

(d) Make and submit a report of its proceedings, findings, recommendations and any other relevant observations related to the cause of the accident to the Minister for Manpower.

(e) If the District Judge appointed to the Inquiry Committee is of the opinion that criminal proceedings ought to be instituted against any person in connection with the accident, he shall also forward a copy of the report to the Public Prosecutor.

1.2 On 12 August 2021 Hawkins was instructed by Rajah and Tann (Singapore) LLP, solicitors representing Stars that the scope of our work should include

“(a) Conducting assessments of the Site and/or conducting inspections of the evidence retrieved from the Site to review the evidence;

- (b) *Conducting interviews with the relevant persons including factual witnesses such as the surviving workers;*
- (c) *Preparing a forensic report on your findings (the "**Report**") to determine the cause of the accident and where appropriate, comment on other factors that may have caused and/or contributed to the accident;*
- (d) *Preparing supplemental reports where necessary, including report(s) commenting on the reports issued from experts appointed by other parties (including but not limited to the Ministry of Manpower); and*
- (e) *Testify as Stars' technical expert in the COI proceedings and any other court proceedings that may arise from the accident."*

1.3 Hawkins was instructed that the Report "should set out, inter alia, the following:

- (a) *A summary of your findings from assessing and reviewing the Site and the evidence, including the interviews conducted with all relevant persons;*
- (b) *Your technical opinion on the factors that contributed to and/or the cause of the explosion at the Site on 24 February 2021;*
- (c) *Your technical opinion on the cause of the explosion at the Site on 24 February 2021;*
- (d) *Any other matter that you deem relevant for the purposes of the Report and the COI in determining the cause of the accident."*

1.4 I have been responsible for Hawkins' work in connection with these instructions. I have been assisted by my colleague, Mr Graham Cooper. Copies of our respective curriculum vitae are provided in **Appendix A** of this report.

1.5 I attended the Site on 15 March 2021, to undertake a brief inspection of the scene under the supervision of the Ministry of Manpower (MoM), returning on 24 March 2021 to witness the removal of an industrial mixing machine known as a sigma blender (the machine), which forms the focus of this investigation. Mr Cooper attended the

premises of Matcor (consultants appointed by MoM to assist them with their enquiries) on 31 March 2021, to inspect fracture surfaces on the machine and the intended locations where Matcor was to cut the metal, prior to further inspections of features such as fracture surfaces. He returned to Matcor's facility on 12 April 2021, after the machine had been cut, to inspect the cut sections and the interior surfaces of the machine that had not been accessible previously. Mr Cooper and I attended an inspection of the machine and heating elements that were fitted to it on 3 June 2021. Unfortunately, we were unable to inspect one of the heating elements or any of the cut sections of the fracture surfaces. During our investigations, we took photographs of the damage, a selection of which is used to illustrate this report.

- 1.6 On 14 May 2021, I attended the MoM Services Centre to interview three witnesses, Mr Ahmmed Lizon, Mr Mehedi and Mr Rahad Asfaquzzaman, who were working in the affected premises at the time of the explosion and who were burned. I interviewed a fourth witness, Mr Molla Md Yousuf, and a fifth witness, Mr Hossain Jitu remotely (by Zoom video conference) on 10 and 29 June 2021 respectively.
- 1.7 This report is based on incomplete evidence, as Mr Cooper and I have been unable to inspect in detail all the components and fracture surfaces of the machine. I have not been provided the written statements of the factual witnesses to be called at the inquiry hearing as at the date of this report, and I understand that parties are in the process of confirming these witness statements to be submitted to the Inquiry Committee. I reserve my right to revise or supplement the findings of this report, if additional information becomes available.
- 1.8 I have been provided with some background information relating to Stars, including the purchase, installation and use of the machine by Mr Chua, the sole Director of Stars. A list of the information given to me is provided in **Appendix B**.

2. BACKGROUND

2.1 Stars

2.1.1 I was told by Mr Chua that Stars provided a variety of fire protection services to clients, including the installation of sprinkler systems and the manufacture of a propriety fire-resistant wrap using potato starch powder, water and other (commercially confidential) ingredients blended in stages within the machine that stood on the mezzanine at the rear of the premises.

2.1.2 The Stars website shows that the company was incorporated in 2010 and is involved in the design, manufacture, supply, installation, and maintenance of fire protection systems. The company achieved the BizSAFE Star and Occupational Health & Safety Assessment Series (OHSAS) 18001 accreditation in 2012. The Bizsafe Star certificate expiry date is 22 October 2021. OHSAS 18001 was superseded by ISO 45001; Stars was assessed and registered against the requirements of ISO 45001 in 2018, with that certificate also due to expire on 22 October 2021.

2.1.3 Mr Chua provided me with details of his staff training records. These include details of courses regulated by MoM (Construction Safety Orientation Course for Workers, Building Construction Supervisors' Safety Course, Apply Workplace Safety and Health in Construction Sites), in addition to further details of staff being sent on a welding course and being awarded certificates from different contractors / providers to Stars' staff, for excellence relating to Health and Safety. These documents indicate that the staff had received regular H&S training, including refresher courses, during their employment.

2.1.4 Mr Chua gave me documents to indicate the risk assessments and method statements used by Stars. They included a 'Fall Protection Plan' produced by Mr Chua and

countersigned by Mr Lwin (known by staff as Mr Moe) specifically written in relation to the operation of the machine on the platform. The document outlines the risk, the control measures and the responsibilities of the supervisors and workers. It states that the work area shall be kept clean and tidy, it shall be cleaned at the end of each day or at any time the supervisor deems necessary, and that the workers shall stop work if, for any reason, they consider that the task assigned to them has become unsafe and report this to their supervisor. Stars also provided a 'Fall Protection Plan' for staff working away from the premises, which was more comprehensive and which included sections relating to the use of harnesses, fall protection systems and training. I have been provided with risk assessments for staff working off site (installing sprinkler systems), working in stores and, most significantly, using the machine.

2.1.5 The risk assessment for using the machine was produced by Mr Chua and countersigned by Mr Lwin on 31 March 2020. The risk assessment covered all aspects of the production process, from delivery of the ingredients to the use of the machine. It considered hazards from staff being hit by moving vehicles, electrocuted, falling from height, falling into the machine, and fires and explosions; the inclusion of fire and explosion hazards is noteworthy, owing to the accident that occurred. The control measures for fire and explosion hazards comprised providing fire extinguishers and warning signs, daily housekeeping, no unauthorised people to be in the work area, close supervision with regular inspections and 'briefing safe working procedure (SWP)'.

2.1.6 Mr Chua provided me with a SWP for work away from the factory and one specifically for using the machine. The SWP for the use of the machine was signed by Mr Chua and Mr Lwin but was undated. The objective of the SWP was stated to be the safe procedure for the manufacture of Shield+ Fire-rated Wrap. The document states that before starting, all workers were required to attend in-house training for the manufacturing process, clear the work area (of obstacles and obstructions) and to

ensure that all personal protective equipment is in good condition. The operation of the machine was straightforward; although no details were provided of what individual controls on the control panel operated. The first task was to fill the mixing chamber (part of the 'hopper', which is the assembly containing the mixing vessel and oil reservoir below it) with water. The water should then be heated until it attained a temperature of 80°C, at which point the heaters should be turned off. Starch should then be added and the contents mixed for 15 minutes, after which boric acid (powder) should be added and the contents mixed for a further 15 minutes. Aluminium hydroxide (also known as Aluminium trihydrate – ATH) and clay are then added and the contents mixed for 15 minutes, before the product is removed from the mixing chamber and cut into blocks. The (predominantly) clay blocks are then rolled into sheets using two separate machines. Details of the stage relating to removing the product from the mixing chamber and transferring it to the rolling machine were omitted, as was a description for cleaning the mixing chamber after use.

2.1.7 Mr Chua provided me with material safety data sheets (MSDSs) for the ingredients used to make the fire-resistant wrap. The MSDS of the ingredients, except for the potato starch powder, indicate nothing to suggest that the ingredients are combustible.

2.1.8 The product specification sheet and MSDS for the potato starch that Mr Chua received before the explosion indicate nothing to suggest that the powder is potentially dangerous. The MSDS was provided by Sigma Aldrich. The Hazards Identification (Section 2) provided by the supplier states, "*not a hazardous substance or mixture*". No specific warnings are provided in Section 5 (fire-fighting measures) or Section 7 (handling and storage), although the information in Section 5 implies that the product is combustible.

2.1.9 Another MSDS for the potato starch, that I am told by Mr Chua was received after the incident, published by Birk Amidon records at Section 2 "*This substance is not classified as hazardous according to Regulation (EC) No. 1272/2008*". It makes no reference to the material being combustible in Section 5, but at Section 7, paragraph 7.1 titled '*Precautions for Safe Handling*' it states:

"Advice on safe handling

Avoid generation of dust.

Advice on protection against fire and explosion

Explosive dust-air mixtures may form. Dust explosive,

Dust explosion category: ST 1

Avoid dust deposits".

2.2 The Purchase of the Machine

2.2.1 The machine was purchased directly from the manufacturer (Laizhou Keda Chemical Machinery Co. Ltd) of Shandong Province, the People's Republic of China in 2019. Mr Chua sent me a copy of the quotation provided for a 1000L bentonite clay kneader, dated 13 May 2019, for a price of US \$13,500. A subsequent order document dated 28 August 2019 for a price of US \$11,700, provides detail in the order remarks section that the oil jacket was 6 mm thick, the heating system was electrical, and there was a temperature probe and sight glass fitted.

2.2.2 It was claimed that the machine was manufactured under the ISO 9001:2015 quality management system (certificate issued on 16 June 2020), but I do not know whether the production facility conformed to this system when the machine was built. More significantly, it was claimed that the machine was manufactured according to seven ISO standards. A certificate of conformity dated 30 September 2019 (after the

machine was manufactured) and issued by Shenzhen CCT Testing Technology Co Ltd states that the machine was found to comply with to following Standards:

1. ISO 12100: 2010 (titled "*Safety of machinery – General principles for design – Risk Assessment and risk reduction*"),
2. EN 60204-1: 2006+ A1:2009+ AC: 2010 (titled "*Safety of machinery – Electrical equipment of machines*"),
3. EN 60825-1:2014 (titled "*Safety of laser products. Equipment classification and requirements*"),
4. EN 61000-6-3:2007+ A1: 2011+AC:2012 (titled "*Electromagnetic compatibility (EMC) Generic standards. Emission standard for residential, commercial and light-industrial environments*"),
5. EN 61000-6-1: 2007 (titled "*Electromagnetic compatibility (EMC) Generic standards. Immunity for residential, commercial and light-industrial environments*"),
6. EN 61000-3-2:2014 (titled "*Electromagnetic compatibility (EMC) Limits. Limits for harmonic current emissions (equipment input current ≤ 16 A per phase*") and
7. EN 61000-3-3: 2003 (titled "*Electromagnetic compatibility (EMC) Limits. Limitation of voltage changes, voltage fluctuations and flicker in public low-voltage supply systems, for equipment with rated current ≤ 16 A per phase and not subject to conditional connection*")

2.2.3 ISO 12100 specifies basic terminology and methodology to achieve safety and will be discussed below. EN 60204 is relevant to the mixer as it covers electronic equipment of machines including switchgear and control systems (the applicability of the Standard is not relevant to the explosion, but does relate to wiring practices). The version of EN 60204 applicable when the equipment was manufactured is dated 2016. EN 60825 relates to products emitting laser radiation and as such is not relevant to a mixing machine. EN 61000-6-1 and EN 61000-6-3 relate to electromagnetic

compatibility (EMC immunity), whilst EN 61000-3-2 relates to harmonic current emissions and EN 61000-3-3 relates to voltage fluctuations caused by the equipment.

2.2.4 ISO 12100 is the only Standard that might be relevant to this case, in terms of the cause of the accident. According to the ISO website it: *"specifies basic terminology, principles and a methodology for achieving safety in the design of machinery. It specifies principles of risk assessment and risk reduction to help designers in achieving this objective. These principles are based on knowledge and experience of the design, use, incidents, accidents and risks associated with machinery. Procedures are described for identifying hazards and estimating and evaluating risks during relevant phases of the machine life cycle, and for the elimination of hazards or sufficient risk reduction. Guidance is given on the documentation and verification of the risk assessment and risk reduction process."* Annex B of the document provides examples of hazards, hazardous situations and hazardous events. Section 3 of Annex B covers thermal hazards (explosion, flame, objects or materials with a high temperature and radiation from heat sources).

2.2.5 The most relevant sections of the Standard to this case are included in Section 6, which relates to risk reduction:

- Section 6.2.12 includes the use of reliable parts and the duplication (redundancy) of safety related parts.
- Section 6.2.3 considers general technical knowledge of machine design, including mechanical stresses and stress limitation by overload prevention (bursting disks, pressure limiting valves, etc).
- Section 6.2.10 discusses pneumatic and hydraulic hazards, stating that the machine shall be designed so that the maximum rated pressure cannot be exceeded, no hazard results from pressure fluctuations or increases, no hazardous fluid jet results from leakage or component failure, the inclusion of warning labels relating to depressurization of equipment by exhaust devices. Clauses 6.2.11

(applying inherently safe design measures to control systems) and 6.2.12 (Minimizing probability of failure of safety functions) discuss safety devices.

- Section 6.2.11, for example, discusses inappropriate selection, design and location of control devices, machine action resulting from inhibition (defeating or failure) of protective devices and the clear display of faults.

2.3 The Delivery and Installation of the Machine

2.3.1 I was provided with a series of photographs by Mr Chua showing the delivery and installation of the machine at 32E Tuas Avenue 11. I have included copies of some of the images provided as **Photographs 1 to 4**. I do not have original copies of the photographs or documents relating to the delivery of the machine, so I cannot verify the delivery date. However, the information I have seen indicate that the machine was installed on the platform on 12 June 2020. The platform was designed by a specialist company (DP Engineers) on 15 April 2020 and subsequently approved by a Professional Engineer.

2.3.2 The photograph of the machine inside its packaging crate (Photograph 2) has been annotated to highlight some of the component parts. The notable features are the heating elements and what appears to be a filling funnel. The machine was fitted with nine heating elements with yellow covers over their heads and a funnel at the extreme right of the image. It is also apparent that there is no thermal lagging over the oil reservoir on the side of the machine facing the camera.

2.3.3 **Photograph 5**, also provided by Mr Chua, shows details of the control panel provided with the machine, although the quality of the image is not high enough to provide comment other than that it incorporates an emergency stop button. The control panel, in-situ on the mezzanine, is shown in **Photograph 6**. There was no thermal lagging on the oil reservoir of the machine at the time the image was taken in December 2020.

The other equipment in the unit had been installed by this time. A view of the other equipment, looking toward the roller shutter, is provided at **Photograph 7** to provide context for the following section of this report and to show the general level of housekeeping. There appears to be no visible accumulation of dust or debris in the premises.

2.3.4 An image of the machine taken prior to the fire (**Photograph 8**) shows the machine in-situ on the mezzanine after it had been in operation for several months. This image was taken at 19:55 hours on 13 February 2021 and shows the interior of the unit from the roller shutter. The machinery, floor and stock in the foreground are clean, or free of dust. There was no thermal lagging on the oil reservoir.

2.4 Witness Information

2.4.1 The following information has been provided by Mr Chua and Messrs Mehedi, Rahad, Molla, Lizon and Jitu, five of his staff.

a) Mr Chua

2.4.2 Nine electric heating elements immersed in heat transfer oil were used to heat the mixing chamber. The machine was connected to the electricity supply in accordance with information provided by the manufacturer. Messrs Chua, Imam, Meku and Moe then tested and commissioned the machine on 12 June 2020; after functional tests, a small batch of fire clay was manufactured. During these tests, the oil reservoir was filled with water, as Mr Chua was not aware that oil was a better medium (in terms of heat transfer and corrosion). It was after consultation with the manufacturer that he realised that heat transfer oil would be more appropriate and so he ordered 40 litres of oil on 16 June 2020. Subsequently more oil was ordered and an additional 60 litres of oil added to the oil reservoir on 8 August 2020.

- 2.4.3 Mr Chua was instructed by the manufacturer to follow the instructions of the User's Guide when operating the machine. He then taught Messrs Imam and Moe to use it and they subsequently taught some of their colleagues (Messrs Mehedi, Anis and Marimuthu). Mr Chua conducted routine maintenance monthly, which included checking the oil level in the oil reservoir and 'topping up the oil' as and when required. He measured the oil level using a dipstick, which owing to the shape of the reservoir would not touch the bottom.
- 2.4.4 The trial runs for the manufacturer of the fire clay took place between June and October 2020. No production took place in September 2020, as Mr Chua was in Malaysia. The trial runs were to perfect the manufacturing process, to ensure that the fire clay was made consistently and had the correct viscosity. Mr Chua said that the heaters were supposed to switch off automatically when the water (in the mixing chamber) reached about 80°C, but this did not always happen so he instructed the workers to switch them off at the control panel when the desired water temperature was attained. The heaters would not be used again until the next batch of fire clay was to be made.
- 2.4.5 The machine was operated initially with the oil reservoir in the vented configuration. A small batch of fire clay was manufactured overnight on 7 and 8 August 2020 and it was just after midnight on 8 August that it was established that there was insufficient oil in the oil reservoir. It was for this reason that more oil was purchased and the configuration of the oil jacket changed to a sealed system (to prevent a loss of oil through evaporation). At about the same time Mr Chua was told by Mr Imam that there was a problem with heater No. 1 (that closest to the control panel), which appeared to have been emitting smoke. Mr Chua told him to drain all the oil from the oil reservoir before replacing the heater with a new one. The oil reservoir was refilled after the new batch of oil was delivered to the site on 8 August 2020.

- 2.4.6 Regular production of the fire clay started in October 2020, but the output between October and December was limited by the supply of raw materials. It was at about this time that Mr Anis replaced Mr Imam as the supervisor of the Tuas site. Subsequently Mr Marimuthu became the site supervisor during January 2021. By this time the production target had been agreed to be 16 rolls of fire wrap a day (per assembly table), which allowed sufficient time for the workers to clean their workstations at the end of the day.
- 2.4.7 One problem associated with the machine during the early phases of production was a water leak from the mixing chamber onto the mezzanine. Mr Chua could not recall the date that this occurred, but it appears to have been resolved by tightening of the sigma blade shaft sealing glands and was not associated with the oil reservoir or heaters.
- 2.4.8 A small crack in a weld of the oil reservoir was discovered during late September 2020, when oil was found to have leaked. It was initially thought that the presence of oil on the mezzanine might have been due to spillages that occurred when the oil reservoir was topped-up. Consequently, nothing was done about this until 12 October 2020, when the amount of oil became more pronounced. Mr Chua thinks he instructed Mr Molla, a certified welder in the company, to repair the crack by re-welding the defective joint.
- 2.4.9 On 8 January 2021, Mr Lwin contacted Mr Chua to inform him of smoke coming from the machine. It transpired upon investigation that the smoke was steam caused when the fire clay being made spilled over the sides of the hopper.
- 2.4.10 At the beginning of February 2021, Mr Chua had been told by the workers that the surface of the machine was hot during use. As such, he instructed Mr Marimuthu to

use welding pins to attach insulation material to the outside of the hopper. The insulation material was fitted on 6 February 2021.

2.4.11 A small fire occurred at the unit on 12 February 2021. Mr Chua was informed of the fire by Mr Marimuthu, who said it occurred at one side of the machine and that the fire had been extinguished. Mr Mehedi sent Mr Chua photographs of the premises filled with smoke and as such he realised that the extraction fan was not working properly (the fan was then repaired on 15 or 16 February 2021). Initially, Mr Chua thought that the fire was caused by another escape of oil, so he instructed his staff (amongst other things) to take off the insulation material, drain the oil to find the leak and repair any cracks they found. However, it was subsequently established that the fire was not caused by an escape of oil, but the ignition of tape used to seal and secure the edges of the insulation material attached to the machine.

2.4.12 Mr Chua had thought initially that the fire on 12 February had been caused by the oil reservoir leaking because of cracked welds (as had occurred in October 2020), so he instructed Mr Murugan to inform Mr Molla to re-weld the seams and add a plate to the bottom of the reservoir. This was to catch any potential oil leak and enable the oil to drain from a hole in the plate. He also instructed Murugan to have plates added to the corners of the reservoir to reinforce the structure. The leaks were repaired between 13 and 15 February 2021 and new insulation material fitted once the repairs had been made. On 17 February 2021, Mr Chua went to the site to inspect the work and make a batch of fire clay; the machine then worked without fault until the day of the incident.

2.4.13 Mr Chua told me that the oil was 'topped up' most recently after the repairs in February 2021. The practice followed when replacing or replenishing the oil was that the oil was heated to its operating temperature, so that any dissolved water could boil off, after which the sealing cap was fitted. In that way, the system operated at, or

close to ambient pressure and was under a slight vacuum when the oil cooled to room temperature.

2.4.14 The temperature of the machine's mixing chamber was controlled by a thermocouple inserted into the water in the mixing chamber when a new batch of fire clay was to be produced. The set temperature was about 80°C; he said that the metal jacket of the machine would be at about 150°C when the set temperature was reached (i.e. the oil-filled jacket was considerably hotter than the contents of the mixing chamber).

2.4.15 Mr Chua provided me with the machinery maintenance check list for the equipment in the premises (the machine, a compressor, and a roller machine) spanning the period June 2020 to January 2021. The check list comprised a tick box sheet that could be used to record whether certain features or parameters were acceptable or not. In addition, there was a remarks column. The sheets were signed by Mr Chua and record that the machine and a roller machine were commissioned and tested on 12 June 2020. The sheets dated July and September 2020 indicate that no work was conducted on them in those months. The other inspection sheets indicated that all was satisfactory and that the heating oil had been topped up. It seems therefore that the heat transfer oil was topped up monthly, but no record of a leak was made on the maintenance sheets and no indication was given as to how much oil was added.

2.4.16 Mr Chua was not in the factory on the day of the incident, but at 09.09 hours he received a WhatsApp message from Mr Marimuthu saying that a heater of the machine had caught fire. I was given a copy of a photograph he was subsequently sent by Mr Lwin, showing the machine on fire (**Photograph 9**) and others taken subsequently. Photograph 9 shows clearly that the fire is centred on the second heater from the right. It also shows that thermal insulation had been fitted to the external surfaces of the oil reservoir of the machine and the surfaces below the mezzanine are free of obvious dust.

2.4.17 **Photographs 10 to 12** show the machine after the fire had been extinguished. The fire had been extinguished using a foam fire extinguisher and the thermal insulation was still in-situ. The cover of the fire-damaged heater had been removed and a heater cable was detached. Photograph 11 shows that the machine's hopper had been tilted at some time before being returned to its normal operating position. Photograph 12 shows that the fire damage was centred on an electrical connection.

2.4.18 Mr Chua told me that Mr Lwin had sent him a message saying that 'Muthu' was changing the damaged heater. Mr Chua exchanged some messages with Mr Marimuthu and spoke with him by telephone. During one conversation he asked him if he knew how to change a heater. Mr Marimuthu said no, so Mr Chua instructed him to drain the oil, unscrew the nuts securing the heater to the reservoir and pull out the heater then wait until he arrived in site. He did not instruct anyone to repair the damaged wires, or reconnect them to the heater, or to resume production. It seems that his instructions were not followed, as the explosion and a fire occurred before Mr Chua returned to the factory.

b) Messrs Rahad, Mehedi, Lizon, Molla and Jitu

2.4.19 The five men were all employed as general workers and gave similar accounts of events leading up to and including the explosion. I have included a more detailed account of the information provided by the men in **Appendix C**.

2.4.20 The men all received safety briefings when they collected their pay cheque each month. The briefings were given by Mr Sarkar Shibu and in general the briefings covered topics such as wearing the appropriate personal protective equipment and working safely. They were told to report to Mr Chua anything they considered to be

unsafe. The men all received the instructions for their daily tasks verbally, however on occasion Mr Mehedi would receive them by text.

2.4.21 The men were familiar, to varying degrees, with the machine, although none had been trained to operate it. They said that the machine was delivered to site already assembled and lifted onto the mezzanine before being commissioned by Mr Chua. Mr Mehedi recalled that Mr Chua taught Mr Marimuthu and Mr Imam how to use it. They did not know who was taught how to repair the machine or by whom. Mr Mehedi said that the person using the equipment was instructed to contact Mr Lwin or Mr Chua if there was a problem.

2.4.22 The men said that raw materials were kept in a store on the level 2 of the building and were taken onto the mezzanine as and when required. The workstations were cleaned daily and any rubbish taken outside. They recalled that the factory was clean, although some surfaces had a light coating of dust, including those of the mezzanine.

2.4.23 None of the men was aware of any problem with the machine prior to February 2021. The men were all aware of a fire involving the machine on 12 February 2021, but only Messrs Mehedi and Molla saw the fire, which they helped to extinguish. They said it was caused by oil leaking from the oil reservoir. After the fire, Mr Molla welded plates and repaired joints to rectify the problem at the request of Mr Chua. Mr Mehedi thought that there had been a fire, which involved a heater prior to 12 February 2021. The damaged heater was replaced by Mr Chua and Mr Imam without problem.

2.4.24 On 24 February 2021, the men arrived for work at 08:00 hours and were given their tasks for that day. Messrs Mehedi, Rahad, Molla and Jitu were wrapping product. Mr Lizon was making sheets of clay.

2.4.25 Only Mr Mehedhi was aware of a fire involving a heater on the machine on that day prior to the explosion (Mr Molla recalled a fire, but he was not certain of the date, whilst Mr Jitu recalled a small fire, but no other detail). He was asked by Mr Marimuthu, who was using the machine, for help and then if he could buy another heating element locally, but Mr Mehedi told him that there were spares in the store on level 2. Mr Mehedi told Mr Marimuthu to contact Mr Chua or Mr Lwin to inform them of the fire and follow their instructions. Mr Molla recalled seeing Mr Marimuthu speak by telephone with someone, but he did not know who it was. He assumed it was Mr Lwin or Mr Chua owing to the seriousness of the problem.

2.4.26 Mr Mehedi saw that Mr Marimuthu had retrieved a spare heater and that he (and Mr Shohel) returned to the mezzanine. He then saw Mr Marimuthu and Mr Shohel 'checking or changing' the damaged heater, but he was not sure what they were doing or how long they did this for. He was aware that they resumed production as he heard the motors of the machine running.

2.4.27 The explosion occurred after 11:00 hours, but none of the men was certain when exactly. None of the men saw the explosion occur or described what those using the machine were doing at the time, as they were concentrating on their own tasks.

2.5 Video Footage

2.5.1 I was provided with two video clips attached to an email received from Rajah and Tann on 5 August 2021. The videos were taken after the two incidents on 8 January and 12 February 2021.

2.5.2 The video footage recorded on 8 January 2021 seems to have been taken at about 14:00 hours and is about 12 seconds long. The hopper of the machine is in the vertical orientation and there is no lagging on the external surfaces. The footage starts with

the camera pointing towards the rear of the unit (opposite to that with the heaters) and shows that the paint at the bottom of the heating jacket is discoloured. It also shows that product appears to have spilt out of the reactor and is dripping onto the mezzanine floor. Steam can be seen coming from the surface of the heating jacket. The camera is then panned around the machine to show the side with the heaters fitted. Steam is seen coming from the side of the heating jacket on the heater side also. The footage also shows that there was a fire extinguisher next to the machine by the heaters. The extinguisher had not been discharged, as the pin was still inserted in the handle.

2.5.3 The video footage recorded on 12 February was a WhatsApp video recorded at about 18:40 hours and is about 19 seconds long. It shows some fire-damaged foil-lined thermal insulation. It appears from the footage that the damage was localised and centred on the edges of the sheets of insulation and possibly at taped joints. It is not clear from the footage what caused the damage, but the localised nature might suggest that the fire was caused by some form of localised oil leak or ignition of combustible tape/adhesive.

3. THE MACHINE

- 3.1 The machine was manufactured by the Laizhou Keda Chemical Machinery Co Ltd in Shandong Province, People's Republic of China. It is described by the manufacturer as a 'Sigma Blade Kneader'. Its identification plate indicated that it was a 1000 litre unit, it was rated at 37 kW (by which I assume it means the rating of the drive motors), had an operating voltage of 400 V and it was made in September 2019.
- 3.2 The User's Guide confirmed some of the information provided by Mr Chua. It recorded at section 8 that it utilised an electric heat source, had a design temperature of 200°C, an operating temperature of 70 to 160°C and a working pressure of less than or equal to 0.2 MPa.
- 3.3 The manual stated, also at section 8, that the thermal conduction oil (normally called heat transfer oil) should be heated to evaporate the moisture in the oil and that oil vapour would vent from the highest point of the machine.
- 3.4 At section 9, titled Maintenance, the manual states "*it is strictly forbidden to dry the heating tube*", so the oil must be topped up 'in time'. The heating power is declared as $800W \times 3 \text{ elements} = 2400W$, which is inconsistent with other information provided by the manufacturer, such as the quotation that stated the heating power is 36 kW (despite the heating power actually being 45 kW). The heat transfer oil specification is HD 320-350.
- 3.5 Mr Chua sent me details of the heat transfer oil used in the machine in the form of delivery orders and data sheets. The delivery orders from Ming Hup Trading Pte Ltd are dated 16 June 2020, 8 August 2020, and 5 February 2021. They refer to deliveries of 40 litres, 80 litres and 80 litres respectively of Exxon Mobil / Idemitsu branded Daphne Thermic 32-S oil.

- 3.6 The data sheets for that oil state that it is formulated using a highly refined hydrocracked paraffinic base oil, with additives selected to provide oxidation resistance and thermal stability. The oil is suitable for use in open and closed systems at operating temperatures up to 200°C and 300°C respectively. The lower maximum operating temperature for oil used in an open system is a consequence of the greater risk of oxidation.
- 3.7 The data sheet provides information on the flash point of the oils, but not the autoignition temperature, which will be notably higher. The flash point for the 32-S oil is given as 226°C, which is inconsistent with the claimed maximum operating temperature in a closed system. Given the claimed operating temperatures, it is likely that the flash point and AIT are both well in excess of 300°C.
- 3.8 The hopper of the machine can be rotated by about 90° from the horizontal to aid the discharge of the mixed product from the mixing chamber of the machine.
- 3.9 The CVS 200 gasket material specification (this is used to form an oil-tight seal between the heaters and the oil reservoir) indicates that its rated maximum continuous temperature is 250°C.

4. INSPECTION OF THE SCENE

4.1 Overview

4.1.1 Number 32E Tuas Avenue 11 forms part of a three-storey multiple occupancy building with a mixture of industrial units on the first floor and storage units and dormitories occupying the floors above (**Photograph 13**). The first-floor units were formed from what appeared to be a mixture of a steel frame, concrete and blockwork. The front of the units had roller shutters and pedestrian access doors, whilst the rear had windows and a pedestrian fire escape door that led into an alleyway. The damage caused by the explosion and fire was limited to the first floor of Units 32E (Stars) and 32F (next door).

4.2 Unit 32F

4.2.1 The damage to Unit 32F was slight, as the explosion had displaced the partition wall between it and 32E into Unit 32F at high level. The lower edge of the roller shutter of Unit 32F had been forced outwards and the front wall was cracked. The unit had sustained some smoke damage at high level only (**Photograph 14**).

4.3 Unit 32E

4.3.1 The covered area outside the front of Unit 32E has damaged by smoke in a manner consistent with that caused by smoke venting through the raised roller shutter, which was mis-aligned. The area had sustained slight fire damage consistent with that caused by a short duration fire and localised flash burning or scorching. Plastic and cardboard packaging materials in the covered loading area and in the front of the unit had melted or charred slightly (**Photograph 15**).

- 4.3.2 The stock, packaging materials, equipment, and items such as the plastic diffusers fitted to fluorescent light fittings inside the unit were burnt slightly or melted by heat. I saw nothing to indicate that a significant sustained fire had burnt inside the premises despite the sprinklers having operated (**Photographs 16 to 19**).
- 4.3.3 The electrical panels at the front of the unit adjacent to the roller shutter were still energised (Photograph 16). I saw no evidence that any circuit breakers had operated because of the fire.
- 4.3.4 The rear wall and windows had been displaced outwards into the alleyway (**Photographs 20 and 21**) and the fire escape door pushed outwards. The contents at the rear of Unit 32E had sustained more severe damage than those at the front; however, none was fire damaged significantly.
- 4.3.5 I saw no evidence to suggest that there had been an accumulation of dust inside the unit. Horizontal surfaces and inaccessible areas / corners throughout the unit were free of significant deposits.
- 4.3.6 I saw that fire hoses and fire extinguishers were displayed prominently and accessible within the unit. One fire hose had been unfurled and routed towards the mezzanine at the rear of the unit (**Photograph 22**). Three portable fire extinguishers had been left adjacent to the steps leading up to the mezzanine. Two had been discharged.
- 4.3.7 There was no evidence to indicate that a fire had been seated on the floor below the mezzanine (**Photograph 23**); however, the plastic packaging of some bags of raw materials next to it had melted and there were what appeared to be witness marks on the party wall (between units 32E and 32F) consistent with those caused by burning liquid.

- 4.3.8 The mezzanine was 3.5 m deep x 4.5 m wide. It had a safety railing around its perimeter that had sustained damage consistent with that caused by burning liquid impinging on it. Three portable fire extinguishers were on the mezzanine (**Photograph 24**); all had their safety pins in-situ and all were full. The fire extinguishers stood next to an intermediate bulk container (IBC) of water and a water pump that was plugged into a wall socket nearby. The nozzle of the water pump was in the stowed position; the pump's wall socket switch was in the conventional 'on' position. Next to this were some burnt bags that appeared to include potato starch (**Photograph 25**).
- 4.3.9 The machine stood in the centre of and occupied most of the footprint of the mezzanine (**Photograph 26**). The machine was connected to a control panel that was in one corner of the mezzanine; the control panel had sustained localised fire damage, consistent with that caused by a fire spreading to it from the machine (**Photograph 27**). The main switch inside the control panel cabinet was in the 'off' position, as were the three heater switches.
- 4.3.10 The control panel was connected to a three-phase electricity supply which was isolated at a switch under the mezzanine. The isolator was in the 'off' position at the time of my inspection.
- 4.3.11 One thermocouple wire was routed from the control panel into the mixing chamber of the machine (**Photograph 28**). The inside of the mixing chamber appeared to be undamaged. The potato starch and water paste within were unburnt and the two kneader mechanisms were exposed. The lid of the hopper was in the partly raised position (Photograph 26). A second thermocouple appeared to have been routed into the casing of the machine, but was no longer in-situ (**Photograph 29**).

4.3.12 A spare heating element lay on the mezzanine next to the machine. There were also some tools on the mezzanine and on horizontal surfaces of the machine. These included a spanner, a screwdriver, cable crimps, a socket and ratchet (**Photograph 30**).

4.3.13 The oil reservoir of the machine had what appeared to be two filling points, one at each side of the hopper, connected by a pipe routed between them around the outside of the machine (to equalise the pressure as the top of the reservoir was a nominal 'W' shape when viewed in cross section). The two filling points, which are shown in **Photographs 31** and **32**, had been capped off. I saw no sign of a pressure relief system, nor a dip stick or a sight glass to determine the oil level.

4.3.14 The lower half of the external surfaces of the machine had been covered in an insulation material. It was mostly missing from the side facing the rear of the unit (Photograph 26); whereas that covering the side fitted with the heating elements was mostly still in-situ (**Photograph 33**). The underside and some of the end mineral wool insulation material was still fitted as can be seen in **Photograph 34**.

4.3.15 The exposed steel of the machine's oil reservoir was blackened on the side fitted with the heating elements, but it was rusty on the opposite side (**Photograph 35**). The weld repairs to the casing on this side of the machine can be seen clearly. The damage to the steel appeared to be greatest at low level, consistent with a fire burning below the machine, although the thermal insulation was mostly undamaged (Photograph 33). By contrast, the frame on which the machine stood was only fire damaged on the upper surface of the cross member below the failed joint of the oil reservoir (**Photograph 36**).

4.3.16 The front corner of the oil reservoir at the end of the machine closest to the drive motors was torn open slightly along a weld (**Photograph 37**). The opposite end,

closest to the control panel, was also torn open along a weld line, but to a much greater extent (**Photograph 38**). The opening exposed the nine heating elements inside the oil reservoir (**Photographs 39** and **40**); the elements closest to the control panel were distorted and some appeared to be discoloured.

4.3.17 The nine heating elements were still connected to the control panel. Each element had a gasket fitted between the exposed head of the element and the body of the machine. The heating element that was reportedly damaged by fire earlier in the day (the second from the end closest to the control panel) had what appeared to be PTFE insulation tape around the two conductors attached to the element terminals (**Photograph 41**). The protective cover of the heating element was not fitted as the bolt securing it and those of the elements either side of it had been removed (see bottom left image of Photograph 30). Interestingly, two of the six nuts securing the heating element next to it had been removed (they are also apparent in Photograph 30). They had been removed after Photograph 11 had been taken.

4.3.18 There was a small amount of oil residue on the mezzanine below the machine.

4.3.19 I inspected some of the unused spare heating elements for the machine. They had a resistance of 9.9, 10.1 and 10.3 ohms. These figures were consistent with the stated rating of the elements, which were declared to be 5 kW (**Photograph 42**). None of the heating elements installed in the machine or kept as spares, was fitted with an integral thermostat to control the oil temperature.

5. INSPECTIONS AT MATCOR

- 5.1 The inspection on 31 March 2021 was to observe where Matcor intended to cut-out the fracture surfaces of the oil reservoir (**Photographs 43** and **44**). At this time, Mr Cooper was able to make a close inspection of the welds used to construct the machine and the subsequent repairs.
- 5.2 Matcor told Mr Cooper that their intention was to cut-out (by grinding) a section of the oil reservoir to remove the heating elements, which would remain in-situ during cutting. He saw that the oil reservoir's welds had been repaired at the lower quarters of the oil reservoir and that the repair welds were of a poor quality. Despite this, the oil reservoir had ruptured along original weld lines forming the structure (i.e. not those of the repairs) and the surrounding metal had sustained plastic deformation. The distortion was greatest at the heating element side of the machine.
- 5.3 **Photograph 45** shows the tear along the weld between the end of the oil reservoir at the drive-motor end and the side wall where the heaters had been fitted, whereas **Photograph 46** shows the end closest to the control panel. The two ends had not been repaired by the application of a patch; however, the bottom of the reservoir, which had been fitted with a patch, was also distorted outwards (**Photograph 47**).
- 5.4 Mr Cooper confirmed that the oil reservoir was not fitted with a pressure relief system, any means of determining the oil level, or any direct means to control the oil temperature. The oil reservoir was fitted with a simple drain cock at the lowest point of the jacket; this was in the 'closed' position. The oil level would nominally be about 300 mm above the base of the mixing chamber. As such, the heaters would be fully submerged under normal conditions.

- 5.5 During Mr Cooper's second attendance at the Matcor facility on 12 April 2021, he was able to see the inside of the oil reservoir clearly and found that it was free of wet residues of oil. The internal surfaces appeared to be covered in a fine covering of soot (**Photographs 48 to 52**), with no evidence of a tide mark to indicate the oil level in the reservoir at the time of the explosion. He saw that the interior of the oil jacket appeared to be intact and saw no evidence of a leak from the mixing chamber into the oil reservoir.
- 5.6 The three heating elements at the end closest to the control panel were bent in towards the centre of the oil reservoir (**Photographs 53 and 54**). Mr Cooper saw no sign of arcing damage to the element sheaths; however, he was not able to touch them, so as to turn them over and inspect their underside.
- 5.7 Mr Cooper inspected the fracture surfaces of the welds and saw no evidence of fatigue. The features he saw were consistent with failure by ductile overload.
- 5.8 Mr Cooper and I visited Matcor on 3 June 2021 to measure the resistances of the heating elements, inspect the heating element gaskets, study the wiring arrangements, and inspect the micro-sections of the fracture surfaces of the machine. Unfortunately, the micro-sections and the heating element that had caught fire were not available for inspection and two other heating elements had been cut.
- 5.9 I measured the conductivity of the two thermocouples retained from the scene to be 26 Ohms and 36 Ohms. One of the thermocouple assemblies had been disconnected from the temperature controller by unscrewing the terminals (that inserted into the metal jacket), whereas the second thermocouple cable (that for the product) had been pulled from the terminals attached to the controller.

- 5.10 I inspected the heating element assemblies and saw no sign of arcing damage on the elements, the terminals, or the cables attached to them. Elements 1, 3, 4, 8 and 9 (counting from the end of the machine that had been closest to the control panel) were discoloured in a manner consistent with that caused by oxidation. The heating element gaskets available for inspection had been damaged severely by fire; however, those that I was able to inspect bore witness marks that indicated that they were still imperforate.
- 5.11 The thickness of the steel of the machine varied according to the panel and the load it was required to bear. The oil reservoir outer shell was 4 mm thick on the sides and underside. One end panel was 8 mm thick and the other was 16 mm thick. The repair panels were 3.2 mm (1/8") thick.
- 5.12 I inspected the control panel and measured the continuity of the switches. The Emergency Stop button was electrically continuous (it had not been depressed). The left-hand heating element switch was open circuit, whereas the centre and the right-hand switches were electrically continuous. All three heating element switches were in the 'on' position. Other switches on the control panel would only operate whilst pressed. All these switches operated when a small pressure was applied to them and the mechanisms then became electrically continuous. The two temperature controllers were burnt on their exposed surfaces, but their bodies within the control panel were unaffected. Their wiring was linked, but there were no manually configured 'bridges' to indicate their mode of operation. An internal 16 A fuse within the control panel was electrically continuous.
- 5.13 After our inspection Ms Lim (MoM) sent Rajah and Tann an email with the heating element resistances prior to them being removed and some of them cut into sections. This email detailed that the resistances of the elements was as provided in **Table 1** below.

Heating Element Number	Resistance in Ohms	
	Determined by Hawkins	Determined by Matcor
1	17	26.6
2	Missing	207.0
3	17	13.7
4	11	10.3
5	Cut	9.1
6	15	14.0
7	22	17.0
8	Cut	10.0
9	11	11.4
Spare on mezzanine	10	-
Spare from store	10	-

Table 1: Heating element resistances. The numbering is denoted as from the end closest to the control panel, when the machine stood on the mezzanine.

5.14 On 17 August 2021, Ms Lim (MoM) sent Rajah and Tann an email detailing some measurements made by Matcor. In it, Ms Lim explained that Matcor had taken continuity measurements between the heating element terminals and the body of the machine. Heaters 1, 5 and 6 had short-circuited. Additionally, the gaskets were found to be in a brittle condition; so, they were unable to determine if any had failed before the explosion. There were no signs of electric arcing between the heating elements and the body of machine. The only arcing found was on the "lug" of heating element number 2.

6. DISCUSSION

6.1 The Cause of The Explosion

6.1.1 The seat and cause of the explosion is in little doubt. The damage to the machine was consistent with that caused by a build-up of pressure within the oil reservoir. Had the cause of the incident been an explosion outside the machine, then the fabric of the machine would have been concave (bent inwards) rather than convex (bulging outwards). This therefore eliminates ignition and fuel sources outside the machine, such as a spark igniting an accumulation of potato starch, as has been reported in the press. Dust explosions also, in my experience, tend to result in more post-blast burning than I observed and, as the blast tends to be slower than a vapour/gas/oil mist explosion, there are also normally dust accumulations on surfaces remote from the epicentre after the incident. In the event of an incident being caused by accumulations of dust, a dust explosion often comprises a series of explosions that increase in intensity with each event. I saw no evidence that there had been multiple explosions.

6.1.2 The distortion of the oil reservoir could have been caused by a build-up of pressure resulting from:

- The air inside it heating up and expanding,
- The reservoir being over-filled and the oil expanding when heated and exerting hydraulic pressure on the metal,
- An explosion or fire fuelled by oil inside the reservoir, because the oil level was too low to immerse the heaters.

6.1.3 I shall discuss the possible causes and likelihood of each.

6.1.4 The possibility that the incident was caused by air heating up and causing the oil reservoir of the machine to rupture is one worth considering only briefly for three reasons. Firstly, the air would have to be heated by the oil, which in turn would have to be at a higher temperature and which would preferentially heat up the steel of the oil reservoir and the mixing chamber above. The reservoir had a nominal working pressure of 2 bar, which consequently means that the air temperature would have to attain about 333°C. This is because air pressure is directly related to the temperature of the system. It is 1 bar at about 30°C or 303K, so it will be 2 bar at 606K or 333°C. Clearly the metal of the machine would be extremely hot and the water in the mixing chamber would boil (at 100°C). This would leave dry potato starch inside the mixing chamber, which might be expected to ignite at about 250°C. The thermostat inside the mixing chamber was connected to a controller that should isolate power to the heaters before this temperature was attained (this aspect is discussed below). More significantly there was no sign of fire damage within the mixing chamber.

6.1.5 The second reason I do not think an overpressure of air caused this incident is that the rupture of the reservoir owing to an increase in air pressure would not result in the types of fire damage I observed. The damage I saw was consistent with that caused by a spray of oil burning as it was ejected from the oil reservoir. I would expect any oil ejected from the machine because of an increase in air pressure to be hot and mostly in the form of a large 'body of liquid', but with some as a spray. Hot oil as a large body would be difficult to ignite but might be ignited subsequently if it impinged on a suitable ignition source and cause a liquid pool fire (of which there was no evidence). However, I would not expect any fire damage to extend far because there was not much oil in the reservoir and because any oil released as a spray would cool dramatically on contact with air at ambient temperatures and so be less likely to be ignited also.

- 6.1.6 The third reason is that I would not expect to see explosion damage beyond the confines of the mezzanine. The damage to the building is consistent with that caused by an explosion involving burning oil vapour or mist rather than the sudden release of pressure from a chamber that was about 100 litres in volume. This would only cause a small increase in pressure within the unit owing to the relative sizes of the unit and the reservoir.
- 6.1.7 I do not think the incident was caused by the oil reservoir being over-filled, the oil expanding when heated and exerting hydraulic pressure on the metal until it failed. This type of failure results in the instantaneous release of pressure and, as such, I would not expect to see damage to the fabric of the building. An over-filled oil reservoir would also be very unlikely to result in fire damage as the oil would not attain a temperature high enough to ignite before the metal failed and the oil was released. The oil ejected from the oil reservoir would not be in the form of finely divided droplets and as such would not be readily ignited as it would be more likely to quench any flame that might notionally exist.
- 6.1.8 Despite the presence of soot on the internal surfaces of the reservoir, and the absence of a tide mark (which are both likely to have resulted from the oil residues in the reservoir burning to completion after the explosion), it is clear that the reservoir had contained some oil prior to the explosion. Had it not, then the explosion and fire damage would not have occurred.
- 6.1.9 I saw no evidence to suggest that any of the heating elements had failed catastrophically. If the heaters had been submerged, the oil would potentially have quenched the flash-over. If the elements were exposed, then the catastrophic failure of an element might have been sufficient to ignite oil vapours inside the reservoir. If the heaters were exposed or not any catastrophic failure would have been readily

apparent. As such, it remains that the incident was the result of the ignition oil, in whatever form owing to uncontrolled heating.

6.1.10 Oil vapour in the atmosphere above and around the heaters (as opposed to a localised area at the oil surface) is extremely difficult to ignite as it requires the oil to be heated to a very high temperature before sufficient oil vapour is generated (the auto-ignition temperature of the oil is not quoted in the MSDS or any literature I have seen, but it will be considerably more than the 226°C flash point quoted and in my experience it is likely to be between 350 and 400°C). If the oil had been heated to its flash point (let alone the auto-ignition temperature), the water inside the mixing chamber would have boiled and the starch would have ignited. As such, we can exclude the uncontrolled heating of the bulk oil followed by the ignition of vapours.

6.1.11 A fire inside the oil reservoir would occur only if the oil level were low and the heating elements exposed (even partly) to the air. The heating elements would no longer be cooled by the oil and would glow red-hot. The elements would attain a temperature that would boil the surface of the oil if it were close enough to the heaters and the heat input were sufficient, it is possible that vapours close to the oil surface ignited. The ensuing fire would heat up the air inside the oil reservoir, but also deplete the oxygen. The fire would liberate a considerable amount of smoke during the stages that it was limited by the oxygen available and I saw nothing to suggest that was the case. As such, I think it is unlikely that a fire inside the reservoir was the root cause of this incident. A fire might also boil the water and ignite the starch inside the mixing chamber, but this would depend on the duration of the fire. It could cause the paint to burn off the metal surfaces of the reservoir, but it would not do so from only on the bottom of the side wall.

6.1.12 It is, in my opinion, more likely that the incident was the result of the accumulation and subsequent ignition of an oil mist inside the reservoir. The ignition of an oil mist

would generate sufficient pressure to rupture the oil reservoir, project burning droplets of oil around the unit and result in a pressure wave sufficient to displace the internal walls, windows, doors, and roller shutters of units 32E and 32F. If oil inside the reservoir was heated to create vapours, the air temperature would be noticeably cooler than the oil, so some vapours would condense to form a mist (in the same way a cloud is formed). The oil mist thus formed is very stable as the droplets are very small (ranging in size between about 0.6 and 10 microns in diameter) and so continual heating would result in a proportional increase in oil mist concentration. The oil mist has a similar ignition energy and lower flammable limit to the vapour but can be formed with a lower heat input. An oil mist explosion could occur once an oil concentration of 48 mg/l in air is attained. As the concentration rises, the chance of ignition increases as the minimum ignition energy of the mist reduces. This scenario would also need a heating element to be (at least partly) exposed as the oil mist would not be ignited by the temperature of boiling oil.

6.1.13 The evidence I have seen suggests that the heating element that caught fire (number 2 in Table 1) was potentially the ignition source. The elements should have had a resistance of 10 Ohm and most of them were nominally in the range of 10-20 Ohm after the incident. Those with a higher resistance were probably corroded rather than faulty. Element number 2 had a resistance of over 200 Ohm, as determined by Matcor. I do not know why this was the case, but it was recorded to be the only element with a high resistance. This could be consistent with it overheating and its internal insulation failing, resulting in a short circuit to the external sheath (the final conduction path along the element is thus via the sheath or through a thin damaged heater wire hence the higher resistance). A short circuit, if one occurred, would provide a potent ignition source.

6.1.14 It follows that the explosion was ultimately caused because there had to be exposed heating elements and no thermal control to prevent the oil that was present

overheating. The exposure of the heating elements was possibly because of the fire earlier that morning. The image I have seen shows a fire burning at the head of a heating element and it follows that the gasket between the head of the fire-damaged heating element and the body of the oil reservoir was possibly damaged by the heat of the fire (the gaskets were rated at 250°C and a fire is significantly hotter than that). If so, this could have resulted in the loss of sufficient oil to cause the oil level to drop sufficiently to expose an element and it might explain why the hopper was tilted after the fire (see Photograph 11). There would be no evidence of an oil leak visible on the thermal insulation as the flange between the heating element and the oil reservoir protruded beyond the insulation material and thus oil would have fallen onto the mezzanine.

6.1.15 Another possible cause of an oil leak is that the staff appear to have removed two of the six nuts that had secured the heating element at the end of the reservoir and next to that which had been affected by the fire. Removing these nuts would loosen the clamping force imposed on the gasket and might have enabled oil to escape from the reservoir. Ms Lim in her email to Rajah & Tann explained that Matcor had taken continuity measurements between the heating element terminals and the body of the machine. Heaters 1, 5 and 6 had short-circuited, which indicates that their gaskets were compromised electrically. There was no evidence of arcing damage between the heaters and the oil reservoir, so the continuity measurements suggest that the three gaskets were damaged after the explosion and during the fire. The gaskets were found to be in a brittle condition; so, it was not possible to confirm whether, or not, that was the case. However, the gaskets were rated to 250°C, which was below the temperature that would be attained by the metal of the oil reservoir during a fire and so I think failure of the gaskets of Heaters 1, 5 and 6 was an effect of and not related to the cause of the incident.

6.1.16 The staff would not have known that the oil level had dropped unless they "dipped the oil", since the equipment was not fitted with an oil level sensor or a sight glass as claimed by the manufacturer in the contract of sale dated 28 August 2019. This shortcoming would not, under normal circumstances be a problem as the system was sealed. My findings, and the account given to me by Mr Chua, were that the oil reservoir was operated as a pressurised and not a vented system. This means that once filled, there would be no loss of oil because of evaporation of the light (low molecular weight) fractions and so the oil level would only need checking (by dipping) when it was changed, if there were no leaks.

6.1.17 The main cause of the incident, apart from the poor design of the system, which I discuss below, was that the staff operating the machine did not follow the instructions from management and replace the damaged heater. I determined that the switches for all heating elements were in the 'on' position after the explosion. The continuity of the switch controlling heaters 1 to 3 was open circuit when I tested it after Matcor had dismantled the equipment, so whilst this might have been switched off and only heaters 4 to 9 energised at the time of the explosion, the arcing damage on heating element 2 suggests that was not the case. If it were then heaters 1 to 3 might have been switched 'off' to resume production without replacing the heating element. It is not clear to me why this might have been the case since a replacement heating element was bought to the mezzanine (Matcor should have determined the switch's continuity before disassembly of the equipment and so I will await sight of their report to determine the condition of the switch). Had the operators of the machine replaced the damaged heating element, the oil would have been drained and replaced to the correct level. Then, if they had followed the standard operating procedures for the machine, they would have waited to have their work inspected by management before production resumed. These steps would have prevented the explosion occurring.

6.2 Factors that Contributed to the Explosion

6.2.1 The temperature of the oil was not controlled directly in any way that I could see. My observations, and the account of Mr Chua, are that the temperature of the metal jacket of the hopper was merely monitored, whilst the thermocouple in the mixing chamber was used for temperature regulation of the contents (when the contents were only water) by switching the oil heater elements on/off. This has two limitations. Firstly, there is no temperature control of the oil whatsoever if the mixing chamber thermocouple is not immersed in the product or if it breaks (either scenario is entirely foreseeable) and there is potentially no control of the oil temperature during the early stages of the heating process before the mixing chamber's contents reach their target temperature. The thermocouple was connected to a RKC Instruments REXD-C700 controller¹, which is normally connected to a computer. This device has the option to set the temperature regulation settings; there are two, the default being proportional, derivative, integral control (PID) and the optional being 'automatic tuning'. I do not know what settings were used or whether the PID settings (if used) were appropriate. PID settings can be time consuming to set-up correctly. The account of Mr Chua is that Stars had to switch off the heaters manually as the temperature control was unreliable, which suggest that the temperature control had not been set-up correctly.

6.2.2 The requirement for control over the heating process is well known as (in this case) there will inevitably be a time lag between the temperatures of the oil, the metal of the oil reservoir, the metal of the mixing chamber and the product inside it reaching any set value. What will happen with no, or inadequate control, is that the oil heats up to a temperature beyond that required to heat the product in the mixing chamber to 80°C and power to the heaters is cut off only once the product is warmed beyond the set point. The oil then cools sufficiently that the material in the mixing chamber

¹ Download RKC INSTRUMENT REX-D Series Instruction Manual | ManualsLib

cools to just below the set point. The heaters will then be re-energised and heat up again. The resulting temperature-time curve of the oil (and to a lesser extent the material in the mixing chamber) will be sinusoidal, with a decreasing amplitude as the temperature of the product starts to stabilise around its target temperature / set point, but with no direct control of the initial peak oil temperature. Mr Chua's comment that he instructed the workers to turn off the heaters manually once the water attained the set temperature suggests that the temperature control was poor.

6.2.3 I saw no evidence of any over-temperature protection device being fitted which would have prevented the oil being heated beyond a factory pre-set temperature in the event of any of the conditions in the paragraphs described above prevailing. Since it is entirely foreseeable that failure of a thermostat or the temperature control / regulation system could occur, it would be prudent for the manufacturer to have installed a safety cut-out to prevent the oil being heated so much that the design pressure of the oil reservoir was exceeded. A safety cut-out, fitted directly in the oil reservoir, could have been set at 250°C and thus ensured that there was a margin of safety in the system. The safety cut-out ideally should not be self-resetting (and it should not be easily accessible) so that it forces operators to switch off the machine, allow it to cool down then determine the root cause of the temperature control failure and rectify the problem before resetting the cut-out. Had a safety cut-out been installed then the explosion would potentially not have occurred. They have limitations, like all devices and can only react if immersed in the oil and if the oil was heated beyond the set temperature.

6.2.4 Another means of controlling the oil temperature and ensuring safety would be to have installed a thermostat in the oil reservoir connected to the temperature control equipment of the control panel. That way the oil temperature could have been controlled separately from the contents of the mixing chamber and this would have resulted not only in finer control of the apparatus, but would have prevented the

explosion from occurring. Alternatively, the manufacturer could have installed heating elements with integral thermostats fitted (as those of a water heater) so that they cut power to the heating element at a set temperature and then re-energise them when the element (and therefore oil around the element) has cooled slightly. This would also prevent the heaters becoming hot enough to ignite oil mist or smoke particles. If each heater was fitted with an integral thermostat, then it would require multiple failures (three or four) before the oil might be heated uncontrollably. Either system would make thermal runaway of the oil statistically unlikely. In this case, it is likely that the explosion would not have occurred if such devices had been fitted as the heating elements could not have got hot enough to vapourise and ignite the oil.

6.2.5 The final way to ensure that the oil was not over-heated would have been to use fewer and less powerful heating elements. I note that the machine was fitted with nine 5 kW rated heaters, providing a heat input of 45 kW into the oil reservoir. The User's Guide states in one section that the heating power was 2.4kW, which is approximately 5% of that fitted, but also that was nominally 36kW (80% of that fitted). It can be seen from the photographs provided by Mr Chua that the heaters installed were those supplied by the manufacturers, so it is not clear to me why this discrepancy existed.

6.2.6 The text above also shows that the explosion could have been prevented if a means of determining the oil level was installed in the oil reservoir. The oil used in the reservoir was, according to documentation I have seen, almost new and of a high quality that was entirely appropriate for use in the machine. The use of the oil of the type documented would have reduced the likelihood of the incident occurring as it was less likely to boil or be ignited, but it would, or could, not have prevented it. The next question worth considering was whether the design of the oil reservoir as a sealed system had any bearing on the incident.

6.3 Should the oil reservoir have been vented?

- 6.3.1 I consider that the explosion would have most probably occurred and the consequences potentially been the same whether, or not, the system was sealed or vented. The configuration of the oil reservoir as a sealed system would have reduced the degradation of the oil, but configuration as an open system might have alerted the workers to there being something untoward.
- 6.3.2 If the system were open to atmosphere, heat transfer oil vapours would have been lost to atmosphere and the oil within the reservoir would be exposed to fresh air. The reservoir would draw in fresh air every time the oil cooled and the oxygen in this 'fresh' air would accelerate the degradation of the heat transfer oil and thus the likelihood of it igniting (its flash point and auto-ignition temperatures will reduce). If there was no means to limit or control the oil temperature during the early stages of the heating cycle (or the control was inadequate) the oil could potentially have been heated beyond its specified operating temperature (for an open system).
- 6.3.3 When the oil was heated (whether in a sealed system or not) it would generate vapours and if heated sufficiently it would start to liberate smoke also. Operation of the equipment in an open configuration would have enabled vapours and smoke to escape from the 'vent' or filling port (there were two openings, but that on the opposite side to the heaters has to be sealed if the hopper is to be tilted – otherwise oil would be lost every time the hopper was tilted to discharge the product), but it would only be the liberation of smoke that might have alerted anyone to the unusual operating conditions unless the vapours were so dense that they condensed to form a noticeable mist outside the machine. It is unlikely that the power would or could have been switched off early enough to prevent the ignition of the smoke or mist and vapours inside the oil reservoir and thus the explosion occurring as any exposed heaters would glow red hot, which is enough to ignite the atmosphere inside the oil reservoir (if the

lower flammable limit of the vapours and / or oil mist is attained); however, I accept there is a very small chance that the incident might have been averted if the system were not sealed and the operators attentive.

6.3.4 If ignition were to occur with the system being used in the open configuration, then the outcome would have been almost the same as that which occurred. This is because the pressure wave of an oil mist/vapour/smoke explosion is so slow that it, in effect, acts as a static pressure on all internal surfaces of an object simultaneously and because any pressure rise might only be vented from a single small orifice. The internal pressure of the explosion inside the oil reservoir would cause it to fail at its weakest point. The oil reservoir would have failed at a welded seam between panels as it did (albeit there would also have been a jet of flame from the filling port, which is where I see the main difference in the two scenarios). The fabric of the building would have sustained the same level of damage as the energy input from the explosion would have been the same. This is because the energy content of the oil would be the same (whether the system was sealed or not) and once the explosion occurred, small droplets would burn rapidly and cause a rise in pressure within the building. The walls, doors, roller shutter and windows all fail at a relatively low pressure (about 0.02MPa or 0.2 bar) and allow the excess pressure to vent before the nominal peak pressure is attained.

6.3.5 I have investigated and seen reports of many diesel engine crankcase explosions; these are all vented to atmosphere and the large engines are mostly fitted with pressure relief equipment. The engines are regularly damaged severely by an explosion involving oil mist and vapour within the crankcase. It is often the case that jets of flames and burning oil are ejected from the crankcase and set fire to the surrounding area. The result is often considerable structural damage and unfortunately the injury to people that happen to be nearby. The explosion also often results in the crankcase pressure relief equipment breaking and debris / shrapnel

being thrown throughout the space. It follows that the explosion would likely have caused the same extent of damage even if pressure relief equipment had been fitted to the oil reservoir.

6.3.6 I note with interest that the contract of sale dated 28 August 2019 states that the thickness of the jacket would be 6 mm. I measured it to be 4 mm, thus the strength of the oil reservoir was considerably lower than claimed by the manufacturer. This will have made failure more likely as the machine would not be able to withstand the 0.2MPa claimed; it would be closer to 0.17MPa.

6.4 The Effect of Repairs

6.4.1 I have considered whether the repairs to the oil reservoir made any difference to the severity of the explosion and the outcome in terms of the injuries and the loss of life, in addition to the damage to the building. Repairs were made to welds along the sides and bottom of the oil reservoir in the form of new welds and patches. The patches had no material effect other than to increase the thickness of the walls of the reservoir in discrete areas and increase their resistance to buckling. The weakest points of the structure were (before and after the repairs) the original weld lines and so the addition of the patches only resulted in the walls and floor of the oil reservoir deforming slightly less. The oil reservoir failed at the original welded joints and would have done so had no repairs been made. The ignition of oil/mist/vapours will generate a pressure well in excess of the 0.2Mpa (2 bar) rated pressure of the reservoir and so failure of welds was inevitable.

6.4.2 I note that the repairs included the addition of some thermal lagging. This was to protect the workers from burns as it was noted that the walls of the hopper became hot during use. The lagging would enable the oil in the reservoir (and thus the product in the mixing chamber) to heat up faster, it but would have had little effect on the

highest temperature attained (the initial peak oil temperature might have been higher, but I expect the effect would probably have been small) if the temperature control equipment was functioning correctly.

6.4.3 Fatal or severe injuries can be sustained by being exposed to quite low pressures, shrapnel or burning oil. It is likely that those injured in this incident were exposed at the very least to blast injuries and burning oil and whilst I am not a medical expert it seems unlikely to me that the outcome would have been any different in terms of human casualties. The explosion would likewise always have created a greater pressure than can be resisted by structural parts that failed.

7. PRELIMINARY CONCLUSIONS

- 7.1 The explosion at Stars that resulted in many casualties was caused by the ignition of oil vapour / mist / smoke inside the oil reservoir of a mixing machine.
- 7.2 The most likely ignition source was a heating element that had become exposed to the atmosphere above the oil level.
- 7.3 It is my opinion that the level of oil in the reservoir was lower than normal (required for safe operation) as oil had leaked through a heating element gasket as a consequence of damage sustained by fire earlier that day and that oil had not been replenished.
- 7.4 Staff operating the machine were instructed to replace the heating element that had caught fire, then wait for the machine to be inspected by management before putting it back into service. For an unknown reason they failed to do so. Had they followed their instructions and the SOP for the machine, they would have waited for management to inspect their work before switching the machine back on and the explosion would not have happened.
- 7.5 I saw that there were deficiencies in the temperature control equipment for the machine that could result in the uncontrolled heating of the oil and any exposed heating elements remaining energised. Had basic control devices been fitted then the explosion would not have occurred.
- 7.6 I consider that the operation of the oil reservoir as a sealed system made no difference to the outcome of the explosion. The machine's User's Guide indicates that the oil reservoir was designed to be operated as a sealed system.

- 7.7 I consider that the repairs to the outside of the oil reservoir, to prevent oil leaking from defective welds, had no effect on the explosion.
- 7.8 It is my opinion that the machine, as designed, did not meet the safety standards claimed by the manufacturer. Some of the EN standards claimed to be met did not apply to this type of equipment. The ISO design standard claimed was not met as no safety equipment was installed in the machine.
- 7.9 The machine, as supplied, to not meet the standard claimed in the document of sale. No sight glass was fitted in the oil reservoir and the thickness of the steel wall of the reservoir was 4 mm rather than the 6 mm claimed.

8. EXPERT'S DECLARATION

I confirm that insofar as the facts stated in my report are within my own knowledge, I have made clear they are and I believe them to be correct; and that the opinions I have expressed represent my accurate and complete professional opinion.

I also confirm that in preparing this report, I am aware that my primary duty is to the Court and/or the Inquiry Committee, not the person(s) from whom I have received my instructions or by whom I am paid.

A handwritten signature in black ink that reads "David Rose". The signature is written in a cursive style with a large initial 'D' and 'R'.

David Jonathan Rose

Dated: 15 September 2021

APPENDIX A

Summary of qualifications and experience

David Rose

3 Pickering Street
#01-66
Singapore
048660
Tel: + 65 6202 9284
Mob: + 65 9117 2143
Email: david.rose@hawkins.biz

Academic and Professional Qualifications

PhD	Physical Chemistry – Leeds University 1988 to 1990
BSc Hons	Applied Chemistry – Portsmouth Polytechnic 1983 to 1987
CChem FRSC	Chartered Chemist – Fellow of the Royal Society of Chemistry

Career Summary

2016 - date	Regional Director - Hawkins & Associates (Singapore) Pte Limited
2014 - 2016	International & Shipping Manager - Hawkins & Associates Limited
2011 - 2014	Principal Associate – Hawkins & Associates Limited
2001 - 2010	Senior Associate – Hawkins & Associates Limited

Consultant Scientist involved with the forensic investigation of scientific and technical matters of interest to the insurance and legal professions in both the UK and abroad. Travelled globally to investigate large losses and provide risk management advice to clients.

Provided expert witness evidence in Magistrates' Court, Crown Court, High Court (Queen's Bench Division) in the UK, Supreme Court (Singapore) and Arbitration and Mediation in the UK.

Ongoing CPD including attending training on managing Hazmat incidents, the IMDG Code and The DeHaan Fire and Explosion Course.

Specialising in petrochemical incidents (fires and contamination), fire and explosion investigation in marine, industrial, commercial, and domestic premises, including:

- Arson
- Hot work
- Cooking and heating appliances
- Self-heating in stored materials
- Electricity supply and distribution equipment
- Electric apparatus

Specialising in the investigation of vehicle and ship fires including:

- Engine room fires
- Hot works
- General cargo fires
- Mis-declared cargo fires
- IMDG fires
- Self-heating of bulk cargos

- 1993 - 2001 **Senior Scientist with DERA**
Managing the Fire Hazards & Fuel Handling Groups. Consultant to the Armed Forces concerning the fire hazards associated with fuels and lubricants. DERA TWA 800 air accident investigation team member, responsible for the composition of the fuel air mixture and the vapour monitoring in the test aircraft centre wing fuel tank prior to ignition of the combustible vapours. Manager for projects concerning the flammability hazards of fuels and lubricants; preventing diesel engine and gearbox explosions; the compression ignition of fire-resistant hydraulic fluids; novel fuel treatment systems; fuel reformation for fuel cells. Gas Analysis, Confined space entry and Approved Person POL (Petroleum, Oil, Lubricant) qualified. As such qualified to issue permits to work and supervise maintenance works in fuel farms.
- 1991 - 1993 **Post Doctoral Research Fellow**
Studying the spontaneous ignition kinetics of hydrocarbons under rapid compression conditions, performing experiments and computer simulation to support the practical results.
- 1988 - 1990 **Research Student (PhD)**
Analysing antioxidant behaviour in lubricating oils, using pressurised differential thermal analysis and cyclic voltammetry. Developing the test method for the electrochemical technique. Sat on the Institute of Petroleum thermal analysis panel STG-9, for the study of oils and greases.
- 1987 **Graduate Chemist - BP Chemicals Hythe, Fawley**
Compiling a computer database of the company produce whilst working in the Technical Services and Development Laboratories.
- 1985 - 1986 **Sandwich Student - BP Chemicals Hythe, Fawley**
Working in the Technical Services and Development Laboratories. Running the company's 10 litre pilot plant, manufacturing polyalkylene glycols; preparing the starters, producing the product, neutralising the product and then performing the physical and chemical tests required.

Graham Cooper

3 Pickering Street
#01-66
Singapore
048660
Tel: + 65 6202 9280
Mob: + 65 9138 4789
Email: graham.cooper@hawkins.biz

Academic and Professional Qualifications

BSc (Hons)	Materials Technology - Coventry Polytechnic - 1985
MSc	Advanced Materials Technology - University of Surrey - 1991
CEng	Chartered Engineer
MIMMM	Professional Member of the Institute of Materials, Minerals and Mining

Career Summary

2014 - Date	Principal Associate - Hawkins & Associates (Singapore) Pte. Ltd.
1998 – 2014	Principal Member/Consultant - Dr J H Burgoyne and Partners LLP
1995 - 1998	Team Leader, Materials and Processes Group - British Airways Plc.
1987 - 1995	Senior Section Leader/Specialist - British Aerospace Defence, Military Aircraft Ltd.
1985 - 1987	Graduate Apprentice - British Aerospace Civil Aircraft Division

- Specialist in Materials, Metallurgy and Mechanical Engineering based in Singapore having previously worked in UK. Investigation of over 800 mechanical and material related failures including aviation, marine, road traffic and rail accident investigation; personal injuries; and industrial process plant incidents on behalf of legal, insurance and corporate clients.
- Extensive experience of acting as an Expert Witness and Single Joint Expert in litigation cases, having given written and oral evidence in civil court cases, criminal court cases, arbitrations and mediations in UK, Switzerland and Singapore
- Major cases include: Passenger aircraft crash landing, UK, 1998; Passenger train derailment, UK, 1998; Passenger train derailment, UK, 2000 (7 fatalities); Oil exploration drill ship corrosion failures, Gulf of Mexico, 2000; Rail collision, UK, 2001 (10 fatalities); Cargo loss, North Pacific, 2001; Passenger helicopter crash, North Sea, 2002 (15 fatalities); Military helicopter crash, USA, 2002 (3 fatalities); 600MW steam turbine failure, South Africa, 2003; Sub-sea gas transportation pipeline failure, Irish Sea,

2004; Oil drilling platform collapse, Middle East, 2005; Power generation gas turbine failures, UK, 2006; Gold ore processing plant failure, China, 2007; Oil transportation pipeline failure, Myanmar, 2008; Sub-sea gas transportation pipeline failure, Australia, 2008; Oil refinery equipment failures, Vietnam, 2009; Rudder damage to newbuild oil tankers, China, 2010; Sub-sea oil transportation pipeline failures, South China Sea, 2010; Aircraft fuselage corrosion, Philippines, 2011; Bulk storage tank collapse, Indonesia, 2011; Cargo crane collapse, Belgium, 2011; Power generation steam Turbine failure, Middle East, 2011; Cargo crane collapse, Middle East, 2012; Gas transportation pipeline valve failures, UK and China, 2013; Power generation gas turbine failure, Middle East, 2014; Bulk storage tank collapse, Denmark, 2015; Power generation steam Turbine failure, Middle East, 2015; Water desalination plant equipment failure, Middle East, 2015; Oil refinery equipment failure, Middle East, 2016; Oil transportation pipeline failure, Middle East, 2016; Oil transportation pipeline failure, Middle East, 2017, Oil refinery equipment failure, Middle East, 2017.

APPENDIX B

Documents and Information provided by Stars.

Appendix B - List of documents and Information provided.

1. CAD drawings of the layout of the premises.
2. Details of the CVS 200 gaskets used between the heaters and the oil body of the machine.
3. Data Sheet of the heat transfer oil.
4. Photographs provided by Mr Chua that were taken during the investigation.
5. Jacket and material temperature - thermocouple controller specifications.
6. Maintenance checklist.
7. Mixer manufacturer details including ISO and CE certificates.
8. Platform design documents.
9. Powder MSDS.
10. Pre-incident photographs.
11. Sigma mixer documents.
12. Stars Risk Assessment and Safe working Procedures.
13. Workers Certificates and Safety Awards.
14. Draft of Appendix A to Matcor report M21091 (date 28 May 2021).
15. Email from Ms Jamie Lim of MoM to Ms Josephine Chee of Rajah & Tann, dated 6 June 2021.
16. Bentonite Clay Kneader Quotation from Laizhou Keda Chemical Machinery Co. Ltd. to Mr XD Chua, dated 13 May 2019.
17. Contract for the supply of a Bentonite Clay Kneader from Laizhou Keda Chemical Machinery Co. Ltd. to Stars Engrg Pte Ltd, dated 28 August 2019.
18. Video footage of the machine recorded at about 13:57:39 hours on 8 January 2021.
19. WhatsApp video footage of fire damaged insulation material, recorded at about 18:40:06 hours on 12 February 2021.
20. Email from Ms Jamie Lim of MoM to Ms Josephine Chee of Rajah & Tann, dated 17 August 2021.

APPENDIX C

Summary of information provided by Messrs Rahad, Mehedi and Lizon

Report 543816 Appendix C – Witness Information

Messrs Rahad, Mehedi, Lizon, Molla and Jitu

- C.1 The five men gave similar accounts of events leading up to and including the explosion. As such, I shall only discuss key difference in the accounts provided by Messrs Mehedi, Lizon, Molla and Jitu (from that provided by Mr Rahad). Mr Rahad had worked for Stars for about 18 months. Mr Mehedi had worked for Stars since May 2019, Mr Lizon since June 2018, Mr Molla since November 2019 and Mr Jitu for about three and a half years. All four were employed as a general worker, although their normal tasks varied for most of their employment.
- C.2 The men told me that their general working hours were 08:00 – 20:00 hours, with an hour for lunch. They worked 7-day a week. The men all said that they received safety briefings when they collected their pay cheque each month. The briefings were given by Mr Sarkar Shibu and in general the briefings covered topics such as wearing the appropriate personal protective equipment and working safely. They were told to report to Mr Chua if they were asked to do anything they considered to be unsafe.
- C.3 The men were familiar, to varying degrees with the machine. Messrs Rahad, Molla and Jitu worked mostly on building sites and had only worked at the factory for a week prior to the explosion. The three men lived above the factory. Mr Rahad and knew that the mezzanine was built by Mr Molla, with the assistance of others who lived on site, and the machine lifted onto it during the lockdown period. Mr Rahad saw that the machine was delivered to site already assembled and he knew it was used to make clay as he was tasked with wrapping the product when he worked at the factory.

- C.4 Rahad said that he did not know how the machine worked, or what the component parts did, so he never operated the machine. He only knew that it was commissioned by Mr Chua and he did not know who was trained to use it or how they were trained.
- C.5 Rahad's only association with the machine was that had been asked to collect chemicals from the store on level 2 of the building. Rahad was trained to wrap the clay product by colleagues. He worked with a colleague at a table below the mezzanine. As far as he was aware, two people operated the machine. The clay produced was dropped to the floor, pressed and cut up by two more people and then two teams (of two) wrapped the blocks thus produced.
- C.6 Rahad was not aware of any problem or safety issues with the machine prior to February 2021. He did not know that the oil needed to be replenished as he concentrated on his own work. He did recall that the machine often operated when he was wrapping product.
- C.7 Rahad said that he did not clean his work area during his time at the factory as that was done by others. He was aware that the workstations were cleaned daily and the rubbish taken outside. He described the factory as clean. He noted that some surfaces had a slight coating of dust, including those of the mezzanine when he went there to have a look (out of curiosity). He noted at that time there was a water tank, a pump, the machine and some 25 kg bags of ingredients there. The bags were closed.
- C.8 Rahad said that if he was aware of a problem with a machine, or process, he would inform Mehedi for help.

- C.9 Regarding the fire on 12 February 2021, Mr Rahad was in the canteen, so did not see it, although he did see the smoke afterwards and he was told what had happened and that there had been a fault with the machine.
- C.10 On 24 February 2021, Mr Rahad arrived for work at 08:00 hours and all eight workers were present. He was assigned his tasks (wrapping product) just after he arrived. He took the previous day's product outside (to the store in front of the roller shutter) to make space and then started wrapping clay. The explosion occurred when he was just outside the roller shutters placing stock on a rack. He described that he felt a push from behind that knocked him over. He then saw that his shirt was on fire and that his colleague was next to him. He ran for help and saw some of the other workers come out of the factory before the sprinklers activated. He noted that Mr Shohel was still inside for a further 4-5 minutes. The Singapore Civil Defence Force (SCDF) arrived on site within 3-5 minutes and he was taken to hospital 20-40 minutes later.
- C.11 Mr Rahad was not aware that there had been a problem with the machine (the small fire involving a heater) in the morning until he was recovering in hospital after the explosion.
- C.12 Mr Mehedi had worked in the factory since the circuit breaker. His task of wrapping the product was assigned to him by Mr Imam, Mr Marimuthu or Mr Lwin. He mostly received his instructions verbally, however on occasion he would receive them by text.
- C.13 Mr Mehedi recalled that the machine was supplied with a control panel and spare heaters as he helped erect the mezzanine on which it stood. He recalled that Mr Chua and the company electrician connected the control panel and then the

machine tested by Mr Chua. Mr Chua then taught Mr Marimuthu and Mr Imam how to use it.

- C.14 Mr Mehedi said that the mezzanine would be cleaned daily with rags, or more frequently if necessary. Two people used the machine, including Messrs Imam and Marimuthu. Mr Marimuthu had asked him to help open the lid of the reactor by pressing a button or by adding chemicals. He knew that water was added to the reaction vessel and heated before chemicals were added and that the machine came with a temperature sensor connected to the control panel. That was the extent of his use and knowledge of the machine. Not much was stored on the mezzanine as the chemicals were stored on level 2. They would be brought to the mezzanine when needed.
- C.15 Mr Mehedi did not know who undertook maintenance or servicing. He did not know who was taught how to repair the machine or by whom, but he knew that the person using the equipment was instructed to contact Mr Lwin or Mr Chua if there was a problem.
- C.16 Mr Mehedi was not aware of any problem with the machine prior to February 2021, although he knew that the oil needed topping up. He was aware of the fire on 12 February and he thought one before that, which involved a heater. The damaged heater was replaced by Mr Chua and Imam without problem. Mr Mehedi was present when the fire occurred on 12 February 2021. He helped extinguish the fire and said it was caused by oil leaking from the oil reservoir, on the opposite side of the machine to the heaters. After the fire, Mr Molla welded plates and repaired joints to rectify the problem at the request of Mr Chua.
- C.17 On 24 February 2021, Mr Mehedi was working with Mr Jitu wrapping product. He was aware of a fire involving a heater on the machine at about 09:00 hours as

Mr Marimuthu called him for help and he got a fire extinguisher for him. Mr Marimuthu also asked Mr Mehedi if he could buy another heating element locally, but Mr Mehedi told him that there were spares in the store on level 2. Mr Mehedi also told Mr Marimuthu to contact Mr Chua to inform him of the fire and follow his instructions. He then saw that Mr Marimuthu had retrieved a spare heater and that he (and Mr Shohel) returned to the mezzanine.

- C.18 Mehedi saw Messrs Marimuthu and Shohel 'checking or changing' the damaged heater, but was not sure what they did as he was busy with his own work. He was not certain when this was or how long they did this for. He was aware that they resumed production as he heard the motors of the machine running. The explosion occurred after 11:00 hours, but he was not certain when exactly. He heard a loud noise, felt hot air and pressure hit him from behind and he fell over. He started to crawl out of the building as it was full of smoke and upon seeing daylight, he stood up and ran outside. It was then that he realised he was burnt. Once outside he saw Messrs Rahad and Yousef already there.
- C.19 Mr Mehedi was approached by a worker from another company who told him that there was a tap nearby so that he could cool his burns.
- C.20 Mr Mehedi said that there was a WhatsApp group including Mr Chua, Mr Lwin and workers that was used to discuss work.
- C.21 Mr Lizon had been employed by Stars since June 2018, but only started working at the Tuas Avenue 11 site on 22 February 2021 and as such he was the least familiar with operations. He was given his tasks by Mr Marimuthu and his role was to carry clay down from the mezzanine and cut it into blocks, before placing it into a machine that pressed it into 10 mm thick panels.

- C.22 Mr Lizon lived in a dormitory at 32 Tuas Avenue 11. The machine was already in-situ on the mezzanine when he first saw it during June 2020. He only knew that it was used to make clay. Other than cutting up clay was to bring ingredients from the store on level 2, which he would leave on the floor below the mezzanine. He would also on occasion carry bags of potato starch onto the mezzanine.
- C.23 Mr Lizon was not aware of any previous problem with the machine prior to the explosion and he was not aware of the fire that occurred on 24 February 2021. He was aware that a fire occurred on 12 February 2021 but did not know it involved the machine.
- C.24 Mr Lizon was first aware of the explosion when a ball of fire landed on him. He ran outside and tore off his shirt when he realised that it was on fire. He then went to a unit next door and poured water on himself to cool his burns.
- C.25 Mr Lizon said that the clay produced by the machine was extremely hot and he would leave it to cool for about 30 - 60 minutes before he could cut it up.
- C.26 Mr Molla's main role was installing sprinkler systems in new buildings, but he had been working at 32 Tuas Avenue 11 for 6 or 7 days before the explosion. He lived in the dormitory at Tuas Avenue 11 and so would often receive WhatsApp messages with general instructions to report to a particular site and once there he would receive his instructions verbally each day.
- C.27 Mr Molla's supervisor at Tuas Avenue 11 was Mr Marimuthu, who had shown him how to do the different jobs he might be required to perform. In his short time working at that site, he wrapped the finished product with Mr Rahad, although he did at times help carry clay from the cutting table. He did not collect any raw

ingredients for the machine from the store on level 2, but he did go there to retrieve fibre that he needed for his work.

C.28 Mr Molla knew that the machine on the mezzanine was used to make clay, but he did not know anything about the production process other than it was used to make two batches of clay a day and that it was operated mostly by Messrs Marimuthu and Shohel; Mr Lizon only helped for a few days. Ingredients for the manufacture of the clay were brought down from the store on level 2, but he did not know what they were. The only knowledge he had regarding the machine was that it was delivered to site fully assembled.

C.29 Mr Molla was aware of the fire on 12 February 2021 as he was at the dormitory when it occurred. He was walking to a vending machine when he saw the fire and he then helped his colleagues extinguish it. He said that it was a small fire at the back of the machine. He added that the machine was inspected by the supervisor and the incident was reported to Mr Chua, who then instructed him to repair the cracked weld. He did not know if any other repairs or checks were carried out.

C.30 On 24 February 2021, Mr Molla was wrapping product at a table by the entrance. He heard the machine start operating just after 08:00 hours, but he did not know who was helping Mr Marimuthu operate it that day. His recollection of the events on the day of the fire was confused as he knew that there had been a fire one morning when he worked at the Tuas Avenue 11 site, but he did not know which day it was. It was only since he returned to the dormitory that he learnt that it was on the same day as the explosion. Nonetheless, Mr Molla stated that he saw a small fire burning at the heating elements on the end closest to the control panel. He did not know who extinguished the fire and after it was extinguished, he returned to his work, so he did not know what was done or by whom.

- C.31 Mr Molla said that after the fire on 24 February 2021, the machine was switched off for a while. He saw Mr Marimuthu speak to someone by telephone, so assumes that he was discussing the matter with Mr Chua or Mr Lwin owing to the serious nature of the incident as only they would know what to do.
- C.32 Mr Molla heard the machine re-start, but does not recall what time it was, although he remembered that Messrs Marimuthu and Shohel were on the mezzanine. He only recalled hearing a very loud sound, feeling his back burning, and falling to the floor. He remembered seeing Mr Rahad on the floor and that the room was dark inside. His shirt was on fire so he ran outside with Mr Rahad, followed closely by Messrs Mehedi and Jitu.
- C.33 Mr Molla cleaned his work area every as everyone did. He described that the factory was generally clean, with very little dust. He added that he went onto the mezzanine on only one occasion (to retrieve clay) and he described the mezzanine area as clean.
- C.34 Mr Jitu's main role had been sprinkler system and piping installation on building sites, but he had worked at the Tuas Avenue 11 site for a week prior to the explosion. During that time he reported to Mr Marimuthu and his role was to wrap product with Mr Mehedi.
- C.35 Mr Jitu had seen the machine on the mezzanine and knew that it was used to make the product, but he had not operated it and did not know how it worked. He said that Messrs Marimuthu and Shohel operated the machine and cleaned their work area; but did not know how or when they did so as he was concentrating on his task. He knew that raw ingredients were collected from Level 2 and taken to the machine daily as the machine was operated but switched off at the end of each day.

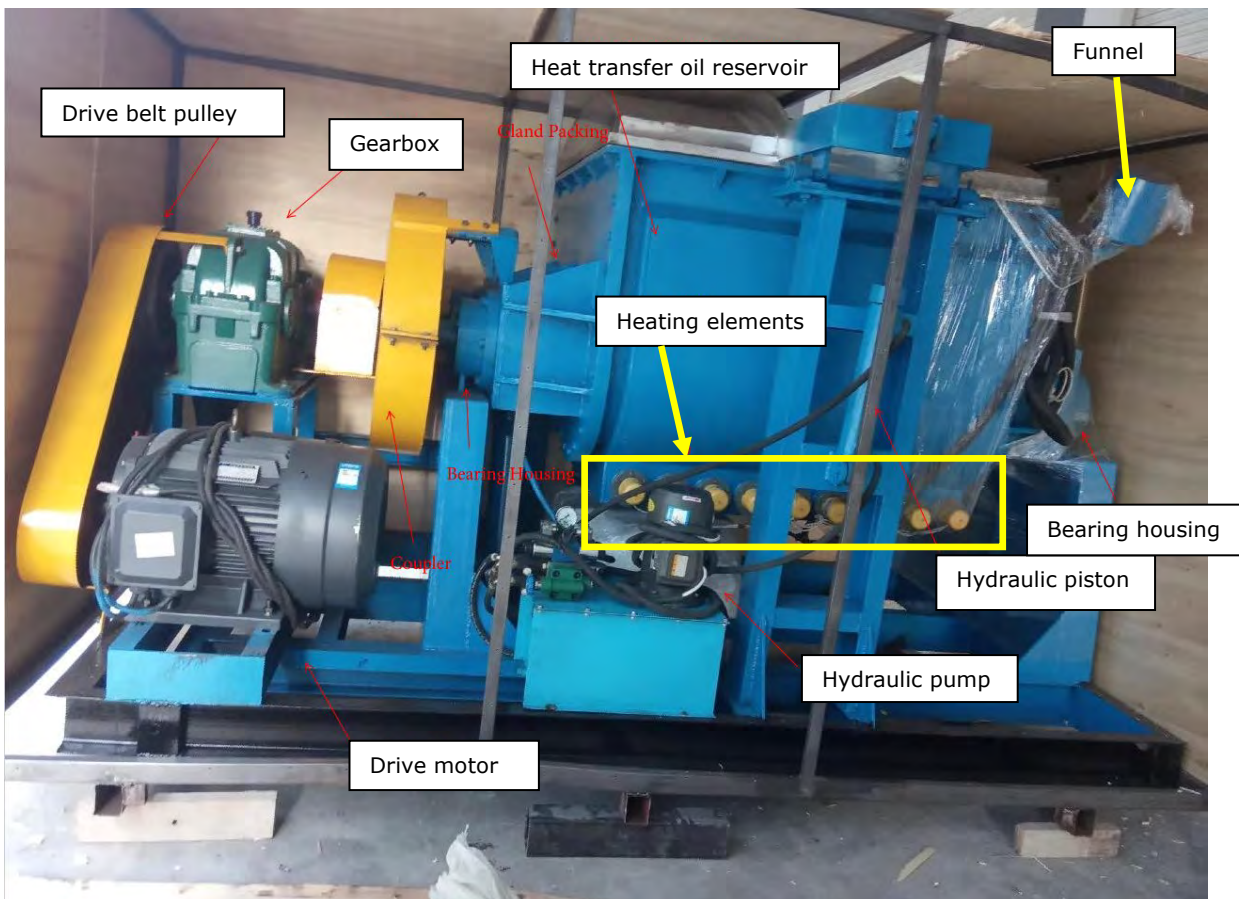
- C.36 Mr Jitu said that there had been no problems with the machine in the time he worked at Tuas Avenue 11 and no safety concerns. He was aware of the fire on 12 February 2021 as he was in his room asleep when it occurred. He woke up and left the building to join his colleagues, so he saw smoke in Level 1, but he did not talk to his colleagues so did not know what had happened. He did not know the fire had involved the machine and as such did not know if it had been repaired afterwards.
- C.37 Mr Jitu's recollection of the events of 24 February 2021 was not clear; however, he recalled reporting for work at 08:00 hours, preparing his work-space and starting to wrap product on the table adjacent to the roller shutter and by the electricity intake. He was concentrating on his own work so was originally not aware that there had been a fire involving the machine that morning. He knew that the machine had been operating that morning as he heard the noise of the drive motors. He recalled that at about 09:30 hours a lorry arrived at the site and he and his colleagues loaded wrapped product onto it before returning to their own tasks.
- C.38 Later, after discussing the loading of the lorry, Mr Jitu recalled that there had been a small fire involving the machine, but no other detail regarding fire-fighting or anyone's actions after that. Initially, he could not recall when the fire occurred, but on reflection he considered it most likely that the fire occurred before the lorry arrived on site.
- C.39 Mr Jitu's recollection of the explosion was limited to him hearing a very loud sound and seeing that the whole room was on fire. He said that he jumped over his work-table and left the building to join his colleagues.

C.40 Mr Jitu had never been on the mezzanine so could not comment on how clean it was. He said that he cleaned his work area every day and that the whole production area was clean and tidy, with only a small amount of dust on surfaces.

PHOTOGRAPHS 1-54



Photograph 1: The machine being delivered in a crate.



Photograph 2: The machine in its crate with key parts annotated. The locations of the filling funnel and heating elements are highlighted.



Photographs 3 and 4:
The installation of the machine on the mezzanine on 12 June 2020.





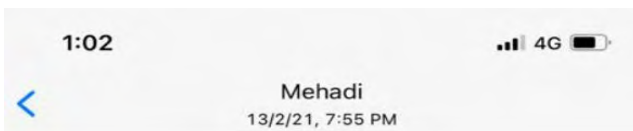
Photograph 5:
The control panel of the machine incorporated an emergency stop button (arrowed).



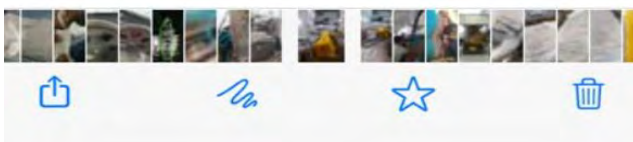
Photograph 6: The machine and control panel (highlighted by the arrow) on the mezzanine. Image taken on 18 December 2020.



Photograph 7: The tables and product adjacent to the roller shutter. Image taken on 23 January 2021.



Photograph 8: Image taken on 13 February 2021, looking toward the machine on the mezzanine at the end of that working day and after stock had been placed between tables.





Photograph 9: Photograph sent to me by Mr Chua. The red arrow is pointing to the fire involving the machine. The fire is centred on the second heater from the right. The image shows that the thermal insulation of the machine is intact and below the mezzanine the surfaces appear free of dust.



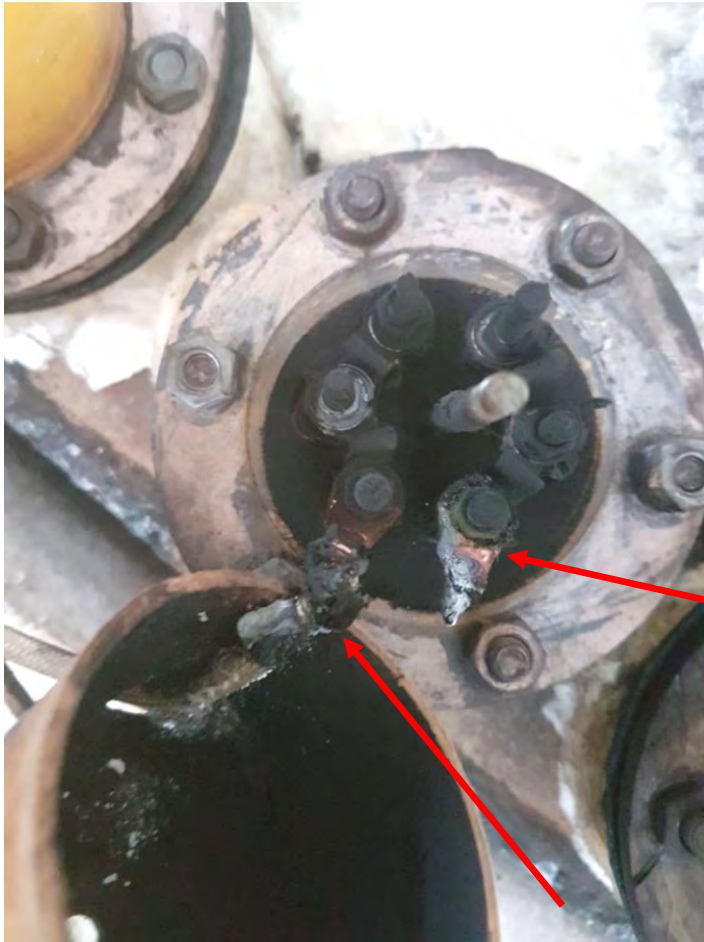
Photograph 10:

Taken after the fire had been extinguished. Smoke is still visible and (white) foam fire-fighting medium is apparent.



Photograph 11:

Taken after the fire. The yellow cover of the fire damaged heater has been removed. The red arrow is pointing to the heater cover and a detached heater cable. Note that the 'body' of the machine has been rotated from the normal operating orientation, shown in Photograph 10.



Photograph 12:
Taken after the fire. Note the fire damage to the heating element connection and cables.



©Hawkins 2021

Photograph 13: 32 Tuas Avenue 11 (on the left) looking towards Unit 32E, which is within the cordon.



©Hawkins 2021

Photograph 14: Overview of the damage to Unit 32F. Note the hole and cracks in the party wall, the displaced roller shutter and the sprinkler wash on the ceiling.



©Hawkins 2021

Photograph 15: Looking into Unit 32E. Note the slight fire damage to packaging materials.



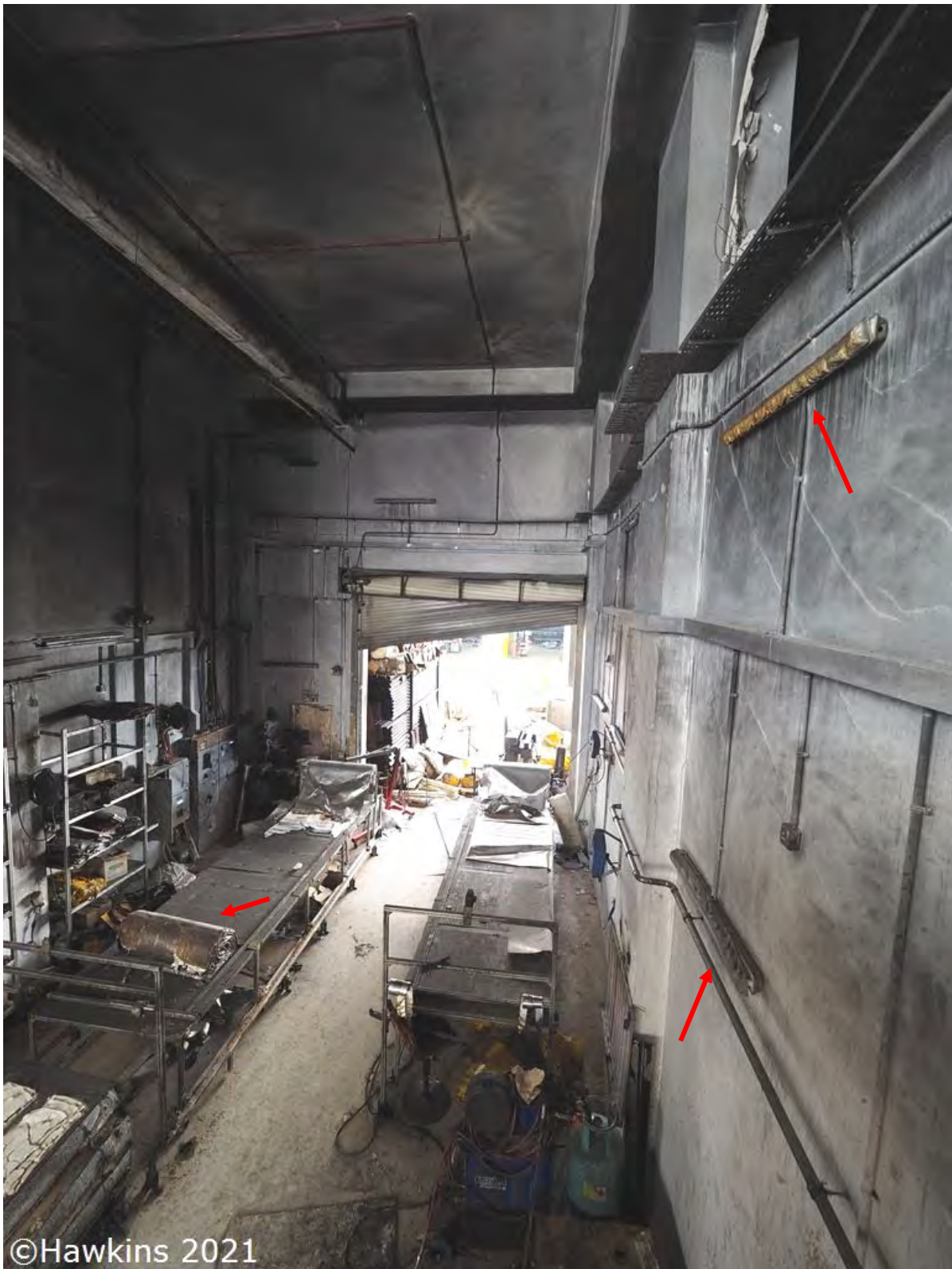
©Hawkins 2021

Photograph 16: Just inside the roller shutter, looking towards the electricity intake equipment. The items are heat damaged. Note the unburnt items on the shelving and the indicator lights of the electrical intake are illuminated.



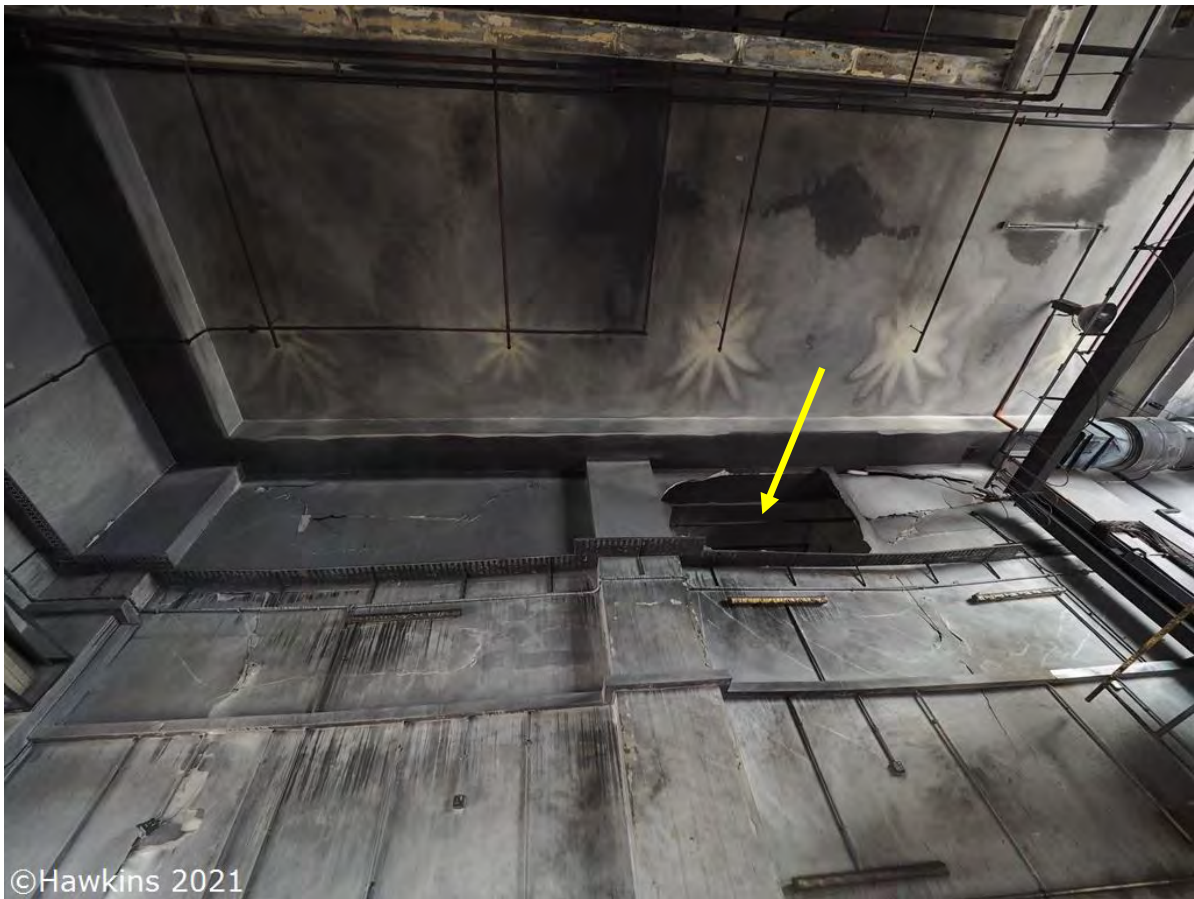
©Hawkins 2021

Photograph 17: Just inside the roller shutter looking away from electricity intake equipment. The items are heat damaged. Note the unburnt cardboard.



©Hawkins 2021

Photograph 18: Looking from the mezzanine to the roller shutter. Note there is no evidence of sustained fire damage, only scorching, blistering and superficial melting of papers, plastics etc.



©Hawkins 2021

Photograph 19: Soot wash marks showing that the sprinklers had activated. Note the hole in the party wall between units 32E and 32F.



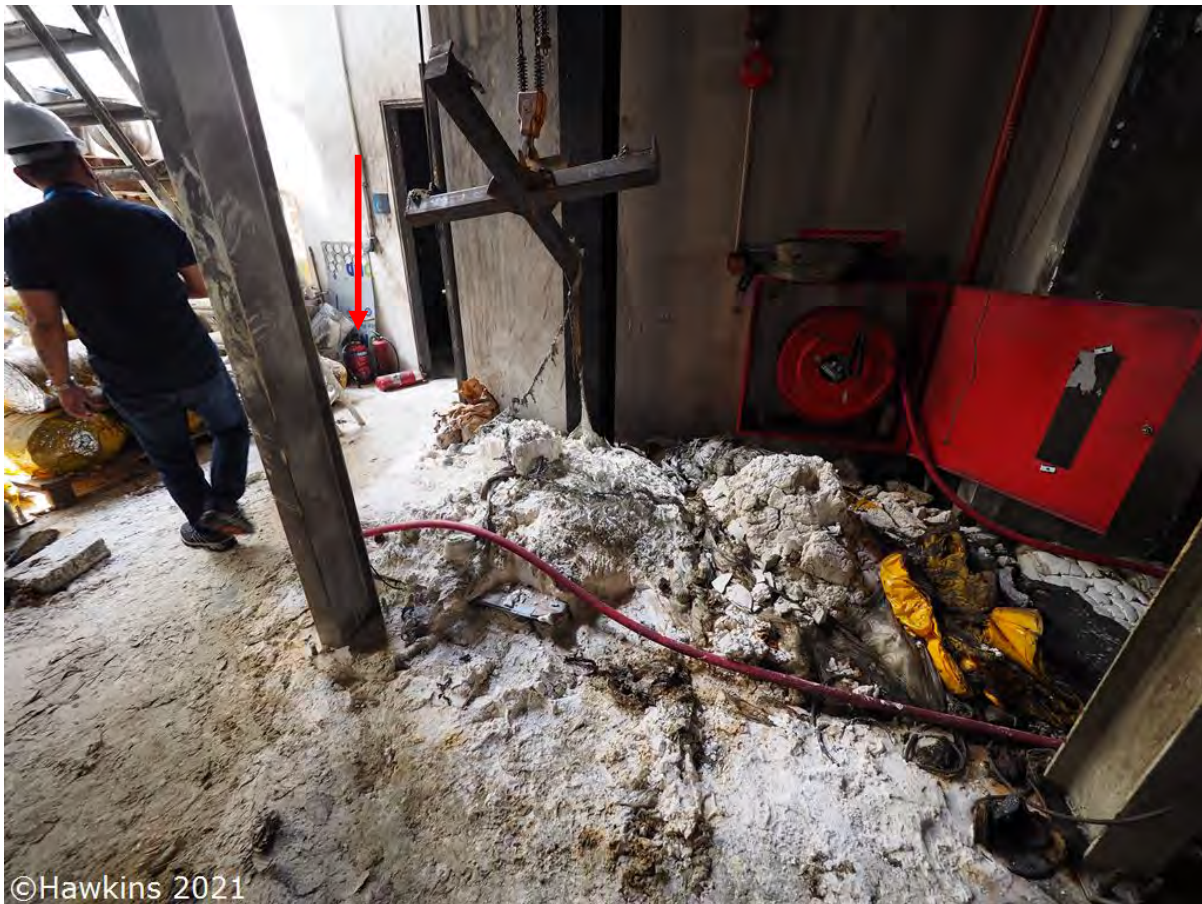
©Hawkins 2021

Photograph 20: The rear wall of 32E, as viewed from the alleyway.



©Hawkins 2021

Photograph 21: The rear wall of the unit as viewed from the mezzanine.



©Hawkins 2021

Photograph 22: The rear of the unit adjacent to the mezzanine. An unfurled fire hose can be seen along with some fire-extinguishers, two of which had been discharged.



©Hawkins 2021

Photograph 23: The work area under the mezzanine.



©Hawkins 2021

Photograph 24: The IBC, water pump (red arrow) and fire extinguishers (yellow arrows) on the mezzanine.



©Hawkins 2021

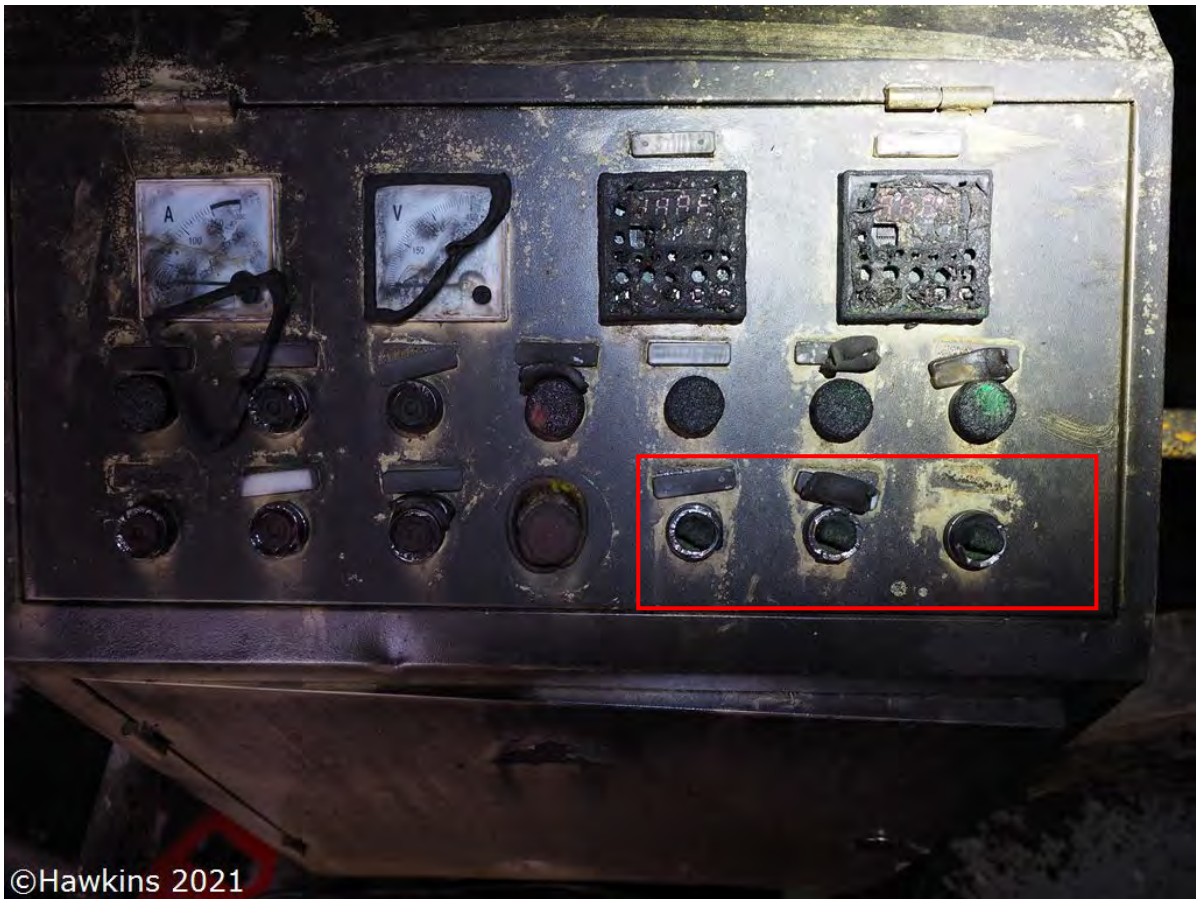
Photograph 25: Bags of potato starch on the mezzanine.



©Hawkins 2021

Photograph 26:

The machine stood at the centre of the mezzanine. The heaters were on the opposite side. Note the thermal lagging had been displaced.



©Hawkins 2021

Photograph 27: The damage to the control panel. The heater switches are highlighted.



©Hawkins 2021

Photograph 28: The mixing chamber of the machine. The thermocouple wire is highlighted.



©Hawkins 2021

Photograph 29: What appeared to be a port for a second thermocouple. No thermocouple was in-situ.



Photograph 30: Montage of the spare heater with a socket and ratchet (top left) and the selection of tools left on the machine and mezzanine. They included spanners, a screwdriver and cable crimps. Note the two nuts on the machine next to the spanners (bottom left image).



©Hawkins 2021

Photograph 31: One of the oil reservoir filling points. Note that it is capped. The pipe connecting the two halves of the reservoir is highlighted by the arrow.



©Hawkins 2021

Photograph 32: One of the oil reservoir filling points. Note that it is capped.



©Hawkins 2021

Photograph 33: The thermal insulation on the side of the machine fitted with the heating elements was mostly in-situ.



©Hawkins 2021

Photograph 34: The thermal insulation remained attached to one end and the underside of the machine.



©Hawkins 2021

Photograph 35: The casing of the machine was rusty at low level on one side of the oil reservoir.



©Hawkins 2021

Photograph 36: The localised fire damage to the frame that supported the machine. The opposite side of the steel frame was hardly affected.



©Hawkins 2021

Photograph 37: The tear in the oil reservoir casing relative to the heating elements.



©Hawkins 2021

Photograph 38: The end of the machine that had been closest to the control panel. Note the insulation material is still in-situ and the tear in the oil reservoir casing by the heaters.



Photograph 39:

Looking past the tear into the oil reservoir. The row of nine heating elements can be seen.



Photograph 40: The distortion of the heating elements closest to the control panel.



©Hawkins 2021

Photograph 41: The heads of the heating elements. Note the insulation tape wrapped around the cables of the element that had caught fire earlier in the day. Also note the two missing nuts (arrowed) of the heating element next to it (see Photograph 30).



©Hawkins 2021

Photograph 42: The heating elements were each rated at 5kW.



©Hawkins 2021

Photograph 43: The machine as seen at Matcor. Note the orange chalk marks indicate the intended cut-lines.



Photograph 44: The machine as seen at Matcor. Note the orange chalk marks indicate the intended cut-lines.



@Hawkins

Photograph 45: A closer view of the tear at the drive-motor end. Note how the end wall of the oil reservoir had distorted outwards.



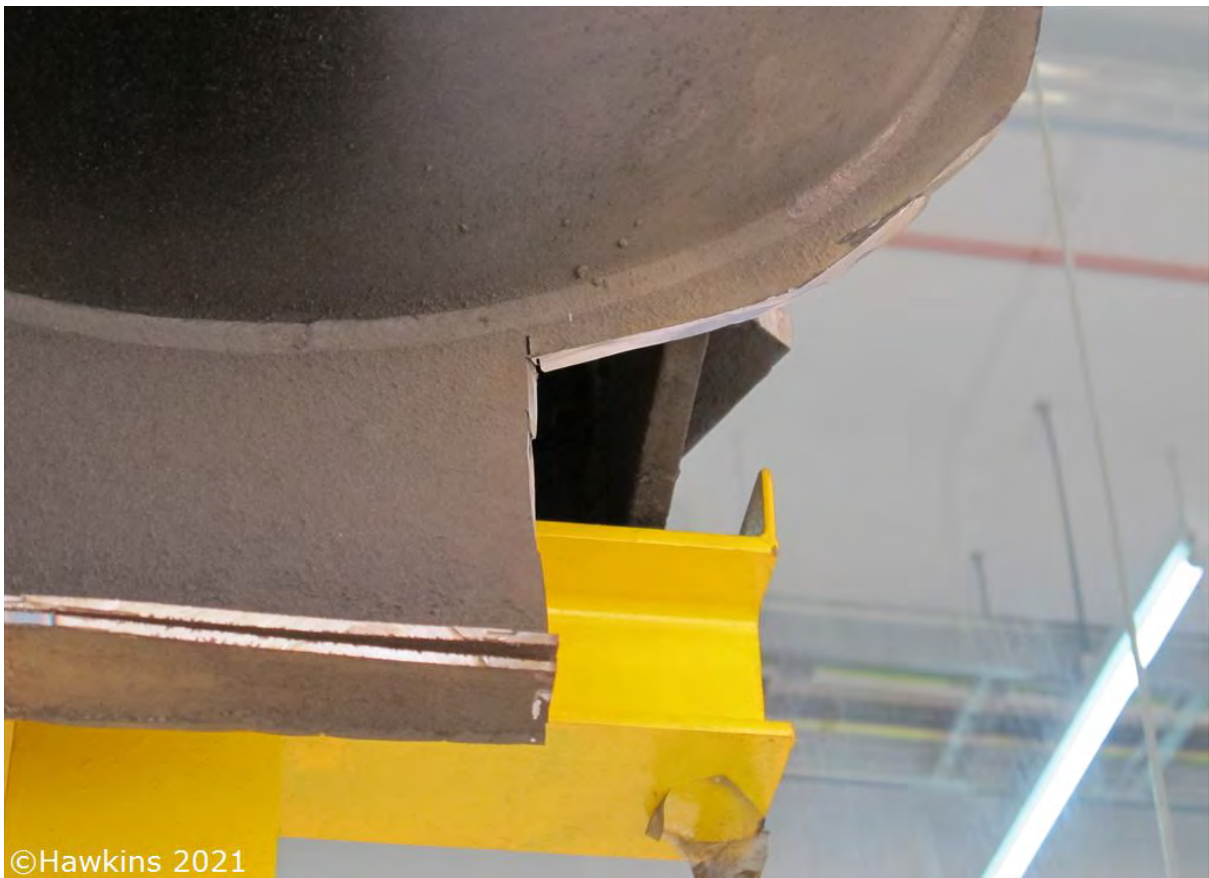
Hawkins 2021

Photograph 46: A closer view of the tear at the end adjacent to the control panel. Note how the side wall of the oil reservoir had distorted outwards.



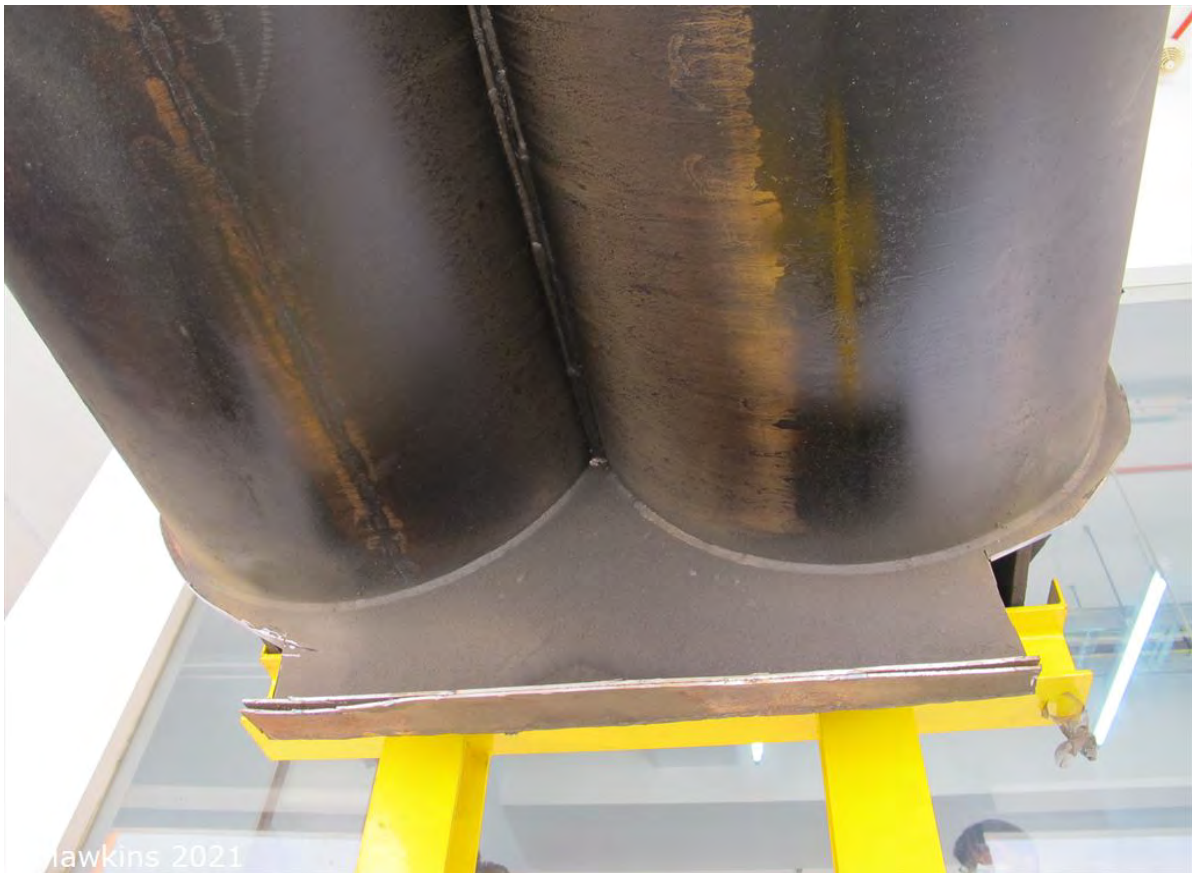
©Hawkins 2021

Photograph 47: The bottom of the oil reservoir was distorted downwards.



©Hawkins 2021

Photograph 48: The inside of the oil reservoir looking upwards to the underside of the reaction vessel at the location of the corner closest to the control panel. The soot deposits and the 'double skin' repair can be seen.



©Hawkins 2021

Photograph 49: Photograph 48 in context. Note there is no evidence of a tidemark on the end wall of the reservoir to indicate the oil level before the explosion.



©Hawkins 2021

Photograph 50: The inside of the oil reservoir looking across the underside of the reaction vessel from the location of the corner closest to the control panel. What appears to be a 'spray' mark is apparent.



Photograph 51:
The drive motor end of the oil reservoir looking up to the underside of the reaction vessel.



Hawkins 2021

Photograph 52: The bottom and one side of the oil reservoir. Note the soot marks.



©Hawkins 2021

Photograph 53: The oil reservoir heating elements.



©Hawkins 2021

Photograph 54: The oil reservoir heating elements. The three elements on the left (this end had been closest to the control panel) had been bent in towards the centre of the reservoir.